

Phenomenological analysis of the Two Higgs
Doublet Model.
Ph.D. Thesis

Rodolfo Alexander Diaz Sanchez
Universidad Nacional de Colombia.
Bogotá, Colombia.

List of Figures

4.1	Leading order diagrams for the processes: $(g - 2)_\mu$ (top left), $L \rightarrow l\gamma$ (top right), $L \rightarrow \bar{l}l$ (bottom left), and $\mu^- \rightarrow \vartheta_e \bar{\vartheta}_\mu e^-$ (bottom right). In the two former, we have neglected the contribution of the charged Higgs and a neutrino into the loop.	76
4.2	Contourplots in the $\xi_{\tau\tau} - m_{A^0}$ plane for each of the five cases cited in the text. On left: case 1 corresponds to the long-dashed line, case 4 to the short-dashed line, and case 5 to the solid line. On right: case 2 corresponds to dashed line, and case 3 is solid line.	79
4.3	Contourplots in the $\xi_{\mu\mu} - m_{A^0}$ plane for each of the five cases cited in the text. On left: case 1 corresponds to the long-dashed line, case 4 to the short-dashed line, and case 5 to the solid line. On right: case 2 corresponds to dashed line, and case 3 is solid line.	79
4.4	Lower and upper bounds for $\tilde{\eta}_{\mu\tau} \left(\tilde{\xi}_{\mu\tau} \right)$ vs $\tan\beta$, for parametrizations I and II using $m_{h^0} = m_{H^0} = 150$ GeV and $m_{A^0} \rightarrow \infty$. . .	86
4.5	Lower and upper bounds for $\tilde{\xi}_{\mu\tau}$ vs m_{H^0} , for parametrization of type II, taking $m_{h^0} = m_{H^0}$ and $m_{A^0} \rightarrow \infty$, the pair of dotted lines correspond to $\tan\beta = 0.1$, the dashed lines are for $\tan\beta = 1$, and the solid lines are for $\tan\beta = 30$	88
4.6	Contourplot of m_{A^0} vs $\tan\beta$ using parametrization type II and assuming $m_{h^0} = m_{H^0}$. From left to right: (1) $m_{h^0} = 115$ GeV, $\xi_{\mu\tau} = 2.5 \times 10^{-2}$ (2) $m_{h^0} = 300$ GeV, $\xi_{\mu\tau} = 2.5 \times 10^{-2}$ (3) $m_{h^0} = 115$ GeV, $\xi_{\mu\tau} = 2.5 \times 10^{-3}$ (4) 300 GeV, $\xi_{\mu\tau} = 2.5 \times 10^{-3}$	90
4.7	Contourplot of m_{A^0} vs m_{H^0} setting $\tan\beta = 2$, the line above correspond to $\tilde{\xi}_{\mu\tau} = 2.5 \times 10^{-2}$ and $m_{h^0} = m_{H^0}$, while the line below correspond to $\tilde{\xi}_{\mu\tau} = 2.5 \times 10^{-2}$ for $m_{h^0} = 115$ GeV.	92

4.8 (top) Contourplot of m_{A^0} vs α' , for parametrization type II, with $m_{h^0} = 115$ GeV, $m_{H^0} = 300$ GeV and $\tan \beta = 20$. Line above corresponds to $\tilde{\xi}_{\mu\tau} = 2.5 \times 10^{-3}$, and line below corresponds to $\tilde{\xi}_{\mu\tau} = 2.5 \times 10^{-2}$. (bottom) Contourplot of m_{A^0} vs $\tan \beta$ for $m_{h^0} = 115$ GeV, $m_{H^0} = 300$ GeV, $\alpha = \pi/6$, and for parametrization type II. Line above corresponds to $\tilde{\xi}_{\mu\tau} = 2.5 \times 10^{-3}$, and line below corresponds to $\tilde{\xi}_{\mu\tau} = 2.5 \times 10^{-2}$	93
5.1 LO (dashed) and NLO (solid) cross sections for stop pair production in $p\bar{p}$ collisions at Tevatron Run I (1.8 TeV) and Run II (2.0 TeV), from PROSPINO [150, 149]. Cross sections are evaluated at the scale $\mu = m_{\tilde{t}}$	110
5.2 Branching ratio for the decay of the lightest neutralino into a photon and a gravitino as a function of the neutralino mass. Shown are the branching ratio if the neutralino is a pure bino (solid line) and for 20% and 50% Higgsino admixtures (long and short dashed lines, respectively) assuming that $m_{h^0} = 120$ GeV and that the other MSSM Higgs bosons are very heavy. For the Higgsino admixture in the lightest neutralino, we choose the \tilde{H}_1 – \tilde{H}_2 mixing so that the field content is aligned with that of h^0 and the longitudinal component of the Z boson in order to minimize the branching ratio to photons.	114
5.3 Cross sections in fb for stop pair production in Run II with $\tilde{t} \rightarrow c\gamma\tilde{G}$, after cuts. No efficiencies have yet been applied. The black area is excluded by non-observation of $jj\gamma\gamma \not{E}_T$ events in Run I.	118
5.4 Cross section in fb for stop pair production with $\tilde{t} \rightarrow bW\gamma\tilde{G}$, after cuts. Both W bosons are assumed to decay hadronically. The black area is excluded by non-observation of $jjWW\gamma\gamma \not{E}_T$ events in Run I.	125

5.5	95% confidence level exclusion limits for top quark decays to stops from Run I for various signal efficiencies, in the case that $\tilde{t}_1 = \tilde{t}_R$, which gives the largest event rates. The area to the left of the curves is excluded. The case $\tilde{t}_1 = \tilde{t}_L$ gives no exclusion for the signal efficiencies considered and is not shown here. The solid line from upper left to lower right is the kinematic limit for $m_t = 175$ GeV. The solid line from upper right to lower left separates the regions in which the 2-body FC decay and the 3-body decay of the stop dominate.	128
5.6	5σ discovery contours for top quark decays to stops at Run II with 4 fb^{-1} for various signal efficiencies, in the case that $\tilde{t}_1 = \tilde{t}_L$, which gives the smallest event rates. The case $\tilde{t}_1 = \tilde{t}_R$ would be discovered virtually up to the kinematic limit even with 10% signal efficiency, and is not shown here. The solid lines are as in Fig. 5.5.	129
5.7	Gluino mass dependence of the NLO cross section for production of ten degenerate squarks in 2 TeV $p\bar{p}$ collisions, from PROSPINO [150]. Shown are the cross sections for $\tilde{q}\tilde{q}^*$ production normalized to the value at large $m_{\tilde{q}}$, for common squark masses of 200, 300, 400 and 500 GeV. Production of $\tilde{q}\tilde{q}$ is small at a $p\bar{p}$ collider and is neglected here; it yields an additional 3-15% increase in the total cross section at low $m_{\tilde{q}}$ for this range of squark masses. Cross sections are evaluated at the scale $\mu = m_{\tilde{q}}$	131
5.8	LO (dashed) and NLO (solid) cross sections for the production of ten degenerate squarks in the heavy gluino limit in $p\bar{p}$ collisions at Tevatron Run I (1.8 TeV) and Run II (2.0 TeV), from PROSPINO [150]. Cross sections are evaluated at the scale $\mu = m_{\tilde{q}}$	132
5.9	Cross section in fb for production of 10 degenerate squarks in Run II in the heavy gluino limit with $\tilde{q} \rightarrow q\gamma\tilde{G}$, after cuts. The black area is excluded by non-observation of $jj\gamma\gamma$ E_T events in Run I.	133

Contents

1	Introduction	1
1.1	Local gauge invariance	1
1.2	Spontaneous symmetry breaking and Higgs mechanism	3
1.3	The Higgs mechanism in the Standard Model	6
1.3.1	The Higgs Potential	8
1.3.2	The kinetic term	8
1.3.3	The Yukawa Lagrangian	9
2	The Two Higgs Doublet Model	11
2.1	Motivation	11
2.2	The contribution of the Higgs sector in the 2HDM	13
2.2.1	The Higgs potential	13
2.2.2	The kinetic sector	20
2.2.3	The Yukawa Lagrangian	26
3	Present Status of the general Two Higgs Doublet Models	43
3.1	Theoretical constraints	43
3.2	Phenomenological constraints	48
3.2.1	The fermiophobic limit	56
3.2.2	The decoupling limit	59
3.2.3	Scenarios with a light Higgs boson	62
3.2.4	The 2HDM with FCNC	64
4	Flavor Changing Neutral Currents in the Lepton Sector of the 2HDM (III)	71
4.1	Brief survey on $(g - 2)_\mu$	72
4.2	The $(g - 2)_\mu$ factor in the 2HDM type III	74
4.3	Lepton Flavor Violating decays	75

4.4	Obtaining the bounds for the flavor changing vertices	76
4.5	Bounds on the Higgs boson masses	83
5	Addendum: Top-squark searches at the Fermilab Tevatron in models of low-energy supersymmetry breaking	95
5.1	General framework	95
5.1.1	The MSSM	96
5.1.2	SUSY breaking schemes	99
5.2	Introduction	101
5.3	Light Stop in Low Energy Supersymmetry Breaking Models .	105
5.4	Top squark production at Tevatron Run II	109
5.5	Previous studies of stops at Run II	110
5.6	Top squark decay branching ratios	112
5.7	Top squark signals in low-energy SUSY breaking	114
5.7.1	Two-body FC decay: $\tilde{t} \rightarrow c\gamma\tilde{G}$	115
5.7.2	Three-body decay: $\tilde{t} \rightarrow bW^+\gamma\tilde{G}$	120
5.7.3	Stop production in top quark decays	125
5.8	Ten degenerate squarks	129
5.8.1	Production at Tevatron Run II	130
5.8.2	Signals in low-energy SUSY breaking	131
6	Concluding remarks	137
A	Determination of the minima of the potential and the mass eigenstates	143
A.1	Minimum condition for the potential	143
A.1.1	The potential with C -invariance	147
A.1.2	The potential with a Z_2 invariance	151
A.1.3	The potential with the global $U(1)$ symmetry	154
B	Rotation of the Yukawa Lagrangian in the 2HDM (III)	157
C	Rotation in the Higgs potential	167
C.1	Transformation of the parameters in the potential	167
C.1.1	Tadpoles	171
C.1.2	Higgs boson masses	172

Acknowledgments

I am strongly indebted to my advisor Dr. Roberto Martinez M. for his academical, personal and financial support throughout my Ph. D. program. I am also especially indebted to Drs. Marcela Carena for giving me the opportunity to interact and work with her and some other colleagues at the Fermi National Accelerator Laboratory.

I thank to Alexis Rodriguez for his important contributions in many topics of this work. I also acknowledge to my thesis examiners: Marcela Carena, and Marek Nowakowski for their useful comments and suggestions to improve this work. I also acknowledge to Gabriel López Castro and Enrico Nardi for their comments about the thesis proposal.

Further, I am grateful to all members of the group of “Física Teórica de Altas Energías” of the Universidad Nacional de Colombia, especially to Diego Torres for helping me with the edition of the manuscript, and John Idárraga for his useful support in some computational issues. Finally, I am very grateful to Debajyoti Choudhury, Heather Logan and Carlos Wagner for helping me to understand several topics developed at Fermilab, especial acknowledgment to Heather for her patience and unconditional collaboration.

On the other hand, I thank to Universidad Nacional de Colombia for accepting me in its Ph.D. program, and for providing me with many of the necessary resources. I also thank to Colciencias, DIB, DINAIN, and Banco de la República for the financial support to carry out the Ph.D. program. I am indebted to the CLAF for the financial support to assist at the Third Latin American Symposium of High Energy Physics (SILAFAE III) held at Cartagena (Colombia). I also acknowledge as well to Sociedad Mexicana de Física for its invitation and financial support to participate at the IX Mexican School of Particles and Fields, and at the Workshop on Ultrahigh Energy Cosmic Rays, realized at Puebla (Mexico). I am grateful to CERN and CLAF for the financial support to participate at the First CERN-CLAF School of High Energy Physics held in itacuruca (Brazil), and to the ICTP for the financial support to participate in the Summer School on Particle Physics 2001, held at Trieste (Italy). I am besides indebted to Fermilab (USA), for its kind hospitality and financial support.

Abstract

The Two Higgs Doublet model and its phenomenological implications are discussed. A brief survey on the present status of this model is given. In particular,

we concentrate on the Two Higgs Doublet Model with Flavor Changing Neutral Currents. First, we develop some new parametrizations of the 2HDM type III, in such a way that the relation of it with models type I and type II become apparent, based on two of these parametrizations we get some bounds on the mixing vertex involving the second and third lepton generations, as well as some lower bounds on the mass of the pseudoscalar Higgs boson; such bounds are obtained from the $g - 2$ muon factor.

Further, by using a parametrization in which one of the vacuum expectation values vanishes, we constrain some lepton flavor violating vertices, assuming that the lightest scalar Higgs mass m_{h^0} is about 115 GeV and that the pseudoscalar Higgs is heavier than h^0 . Specifically, based on the $g - 2$ muon factor and the decay width of $\mu \rightarrow e\gamma$, the following quite general bounds are obtained: $7.62 \times 10^{-4} \lesssim \xi_{\mu\tau}^2 \lesssim 4.44 \times 10^{-2}$, $\xi_{e\tau}^2 \lesssim 2.77 \times 10^{-14}$. Additionally, based on the processes $\tau \rightarrow \mu\gamma$, and $\tau \rightarrow \mu\mu\mu$, bounds on $\xi_{\tau\tau}$ and $\xi_{\mu\mu}$ are also gotten, such constraints on these parameters still give enough room for either a strong suppression or strong enhancement on the coupling of any Higgs boson to a pair of tau leptons or a pair of muons. Moreover, upper limits on the decay widths of the leptonic decays $\tau \rightarrow e\gamma$, and $\tau \rightarrow eee$ are calculated, finding them to stay far from the reach of near future experiments.

Finally, the Flavor Changing Charged Current decay $\mu \rightarrow \nu_e e \bar{\nu}_\mu$ is considered in the framework of the 2HDM type III as well. Since FCNC generates in turn flavor changing charged currents in the lepton sector, this process appears at tree level mediated by a charged Higgs boson exchange. From the experimental upper limit for this decay, we obtain the bound $|\xi_{\mu e}/m_{H^\pm}| \leq 3.8 \times 10^{-3}$ where m_{H^\pm} denotes the mass of the charged Higgs boson. This bound is independent on the other free parameters of the model.

On the other hand, as an addendum to this work, we study the production and decays of top squarks (stops) at the Tevatron collider in models of low-energy supersymmetry breaking. We consider the case where the lightest Standard Model (SM) superpartner is a light neutralino that predominantly decays into a photon and a light gravitino. Considering the lighter stop to be the next-to-lightest Standard Model superpartner, we analyze stop signatures associated with jets, photons and missing energy, which lead to signals naturally larger than the associated SM backgrounds. We consider both 2-body and 3-body decays of the top squarks and show that the reach of the Tevatron can be significantly larger than that expected within either the standard supergravity models or models of low-energy supersymmetry breaking in which the stop is the lightest SM superpartner. For a modest projection of the final Tevatron luminosity, $L \simeq 4 \text{ fb}^{-1}$, stop masses of order

300 GeV are accessible at the Tevatron collider in both 2-body and 3-body decay modes. We also consider the production and decay of ten degenerate squarks that are the supersymmetric partners of the five light quarks. In this case we find that common squark masses up to 360 GeV are easily accessible at the Tevatron collider, and that the reach increases further if the gluino is light.

Chapter 1

Introduction

The Standard Model (SM) of particle physics has been very successful in describing most of the smallest scale phenomenology known so far. However, it possesses some problems whose solution could imply physics beyond its scope. In order to motivate the study of the two Higgs doublet model (2HDM) which is one of the simplest extensions of the SM, it is necessary to discuss two important issues. Perhaps the two most fundamental ideas from which the success of the SM comes are, (1) the extension of the gauge invariance principle as a local concept (inspired in classical electrodynamics) and (2) the implementation of the Spontaneous Symmetry Breaking (SSB) phenomenon.

The introduction of local gauge invariance generates the so called *gauge bosons* as well as the interactions of these gauge bosons with matter (fermions), and also among the gauge bosons themselves (the latter only when the gauge group is non abelian). On the other hand, the combination of local gauge invariance with SSB leads naturally to the *Higgs mechanism* which in turn generates the masses of weak vector bosons and fermions. I shall give a brief survey of both ideas emphasizing in the Higgs mechanism, since the Two Higgs Doublet Model (2HDM) is an extension on the symmetry breaking sector.

1.1 Local gauge invariance

It is well known from classical electrodynamics that Maxwell's equations are invariant under a “*local*” *gauge transformation* of the form: $A_\mu \rightarrow A_\mu +$

$\partial_\mu \lambda(x)$ where A_μ is the four-vector potential. On the other hand, taking the free Dirac Lagrangian

$$\mathcal{L}_{free} = \overline{\Psi}(i\gamma^\mu \partial_\mu - m)\Psi \quad (1.1)$$

We can see that such Lagrangian is invariant under the global phase shift $\Psi \rightarrow e^{i\theta}\Psi$. Nevertheless, inspired in the local gauge symmetry in electrodynamics explained above, we could ask the following question, is it possible to extend the global symmetry and demand it to be local? if yes, what are the physical consequences?. It is straightforward to check that such locality could be accomplished by replacing the “normal” derivative ∂_μ by the “covariant derivative” $D_\mu \equiv \partial_\mu + iqA_\mu$, where A_μ is a four vector field that transforms as $A_\mu \rightarrow A_\mu + \partial_\mu \lambda(x)$ when the local transformation of $\Psi \rightarrow \exp(-iq\lambda(x))\Psi$ is realized. The Lagrangian (1.1) becomes

$$\mathcal{L} = \overline{\Psi}(i\gamma^\mu D_\mu - m)\Psi = \overline{\Psi}(i\gamma^\mu \partial_\mu - m)\Psi - qA_\mu \overline{\Psi}\gamma^\mu \Psi = \mathcal{L}_{free} - J^\mu A_\mu$$

it is easy to see that this new Lagrangian is invariant under the combined transformations $\Psi \rightarrow e^{-iq\lambda(x)}\Psi$, $A_\mu \rightarrow A_\mu + \partial_\mu \lambda(x)$. Now, if we interpret A_μ as the four vector electromagnetic potential, then J^μ is the four-vector electromagnetic current. To complete the Lagrangian of Quantum Electrodynamics (QED) we just add the kinetic term that describe the propagation of free photons

$$\begin{aligned} \mathcal{L}_{QED} &= \mathcal{L}_{free} - J^\mu A_\mu - \frac{1}{4}F^{\mu\nu}F_{\mu\nu} \\ F_{\mu\nu} &\equiv \partial_\mu A_\nu - \partial_\nu A_\mu \end{aligned}$$

And the kinetic term for the free photons (which leads to the Maxwell’s equations) is also local gauge invariant. Therefore, the matter-radiation coupling has been generated from the imposition of “locality” to the gauge principle. Additionally, to preserve locality we have introduced into the covariant derivative a four-vector field (the four-vector potential A_μ), which is called a *gauge field*, and also a parameter q which acts as the generator for the local group transformations $\widehat{U}(x) = \exp(-iq\lambda(x))$. In this case, to analize the symmetries we have used the unidimensional rotation group in the complex

space, this group is called $U(1)$, the group of unitary complex matrices 1×1 . In the electroweak SM we use besides, the group of unitary matrices 2×2 of determinant one (known as $SU(2)$), the latter is a non abelian group whose generators obey the Lie algebra of the rotation group in three dimensions $SO(3)$ (i.e. they are isomorphic). After applying local gauge invariance to the whole electroweak group $SU(2) \times U(1)$, four gauge fields appear and they in turn generate after some additional transformations the three weak vector bosons and the photon.

1.2 Spontaneous symmetry breaking and Higgs mechanism

Using local gauge invariance as a dynamical principle is not enough to predict particle physics phenomenology since it leads to massless gauge bosons that do not correspond to physical reality. SM predicts that these vector bosons acquire their masses from a Spontaneous Symmetry Breaking (SSB) phenomenon explained below.

Sometimes when the vacuum (minimum of the potential) of a system is degenerate, after choosing a particular one¹, this minimum is not invariant under the symmetry of the Lagrangian, when the vacuum does not have the symmetry of the Lagrangian we say that the symmetry has been spontaneously broken. When this phenomenon occurs some other massless particles called Goldstone bosons arise in the spectrum. However, if the Lagrangian possesses a local gauge symmetry an interrelation among gauge and Goldstone bosons endows the former with a physical mass, while the latter disappear from the spectrum, this phenomenon is called the *Higgs mechanism* [1]. To explain the mechanism we shall use a toy model describing a couple of self interacting complex scalar fields (ϕ and ϕ^*) whose Lagrangian is local gauge invariant

$$\mathcal{L} = \frac{1}{2} |D^\mu \phi|^2 - V(\phi^* \phi) - \frac{1}{4} F_{\mu\nu} F^{\mu\nu}; \quad V(\phi) \equiv -\frac{1}{2} \mu^2 |\phi|^2 + \frac{1}{4} \lambda^2 (\phi^* \phi)^2 \quad (1.2)$$

where

¹Quantum field theory demands the vacuum to be unique such that perturbation expansions are calculated around that point

$$\phi = \phi_1 + i\phi_2,$$

is a complex field and

$$D_\mu \equiv \partial_\mu + iqA_\mu \quad ; \quad F_{\mu\nu} \equiv \partial_\mu A_\nu - \partial_\nu A_\mu$$

This Lagrangian has already the local gauge invariance described by the simultaneous transformations

$$\phi(x) \rightarrow e^{-iq\lambda(x)}\phi(x), \quad A_\mu(x) \rightarrow A_\mu(x) + \partial_\mu\lambda(x) \quad (1.3)$$

Observe that the imposition of locality generates the interaction of the complex scalar fields with a four vector field. If $\mu^2 < 0$, The potential $V(\phi)$ posseses a unique minimum at $\phi = 0$ which preserves the symmetry of the Lagrangian. However, if $\mu^2 > 0$, the Lagrangian has a continuum degenerate set of vacua (minima) lying on a circle of radius μ/λ

$$\langle|\phi|^2\rangle = \langle\phi_1\rangle^2 + \langle\phi_2\rangle^2 = \frac{\mu^2}{\lambda^2} \equiv \nu^2$$

any of them might be chosen as the fundamental state, but no one of them is invariant under a local phase rotation². According to the definition made above, the symmetry of the Lagrangian has been spontaneously broken. Choosing a particular minimum:

$$\langle\phi_1\rangle = \frac{\mu}{\lambda} \equiv \nu \quad ; \quad \langle\phi_2\rangle = 0$$

we say that the field ϕ_1 has acquired a Vacuum Expectation Value (VEV) $\langle\phi_1\rangle$. It is convenient to introduce new fields

$$\eta \equiv \phi_1 - v \quad ; \quad \xi \equiv \phi_2$$

and expanding the Lagrangian in terms of these new fields we obtain:

²The set of all ground states is invariant under the symmetry but the obligation to choose (in order to set up a perturbation formalism) only one of the vacua, leads us to the breaking of the symmetry.

$$\mathcal{L} = \left[\frac{1}{2}(\partial_\mu \eta)(\partial^\mu \eta) - \mu^2 \eta^2 \right] + \frac{1}{2}[(\partial_\mu \xi)(\partial^\mu \xi)] + \left[-\frac{1}{4}F_{\mu\nu}F^{\mu\nu} + \frac{q^2 v^2}{2}A_\mu A^\mu \right] \\ - 2iqv(\partial_\mu \xi)A^\mu + \left\{ q[\eta(\partial_\mu \xi) - \xi(\partial_\mu \eta)]A^\mu + vq^2(\eta A_\mu A^\mu) \right. \\ \left. + \frac{q^2}{2}(\xi^2 + \eta^2)A_\mu A^\mu - \lambda\mu(\eta^3 + \eta\xi^2) - \frac{\lambda^2}{4}(\eta^4 + 2\eta^2\xi^2 + \xi^4) \right\} + \frac{\mu^2 v^2}{4}$$

The particle spectrum consists of

1. A field η with mass $\sqrt{2}\mu$.
2. A vector boson A_μ that has acquired a mass $q\nu > 0$ by means of the VEV.
3. A massless field ξ called a Goldstone boson.

However, the Lagrangian above looks disappointing because of a term of the form $(\partial_\mu \xi)A^\mu$ which does not have a clear interpretation in the Feynman formalism. Fortunately, we are able to remove the unwanted would be Goldstone field out, by exploiting the local gauge invariance of the Lagrangian. Writing Eq. (1.3) in terms of ϕ_1 and ϕ_2

$$\phi \rightarrow \phi' = e^{i\theta(x)}\phi = [\phi_1 \cos \theta(x) - \phi_2 \sin \theta(x)] + i[\phi_1 \sin \theta(x) + \phi_2 \cos \theta(x)]$$

where $\theta(x) \equiv -q\lambda(x)$, and using

$$\theta(x) = -\arctan\left(\frac{\phi_2(x)}{\phi_1(x)}\right) \quad (1.4)$$

we get ϕ' to be real³. The gauge field transforms as $A'_\mu(x) = A_\mu(x) + \partial_\mu \lambda(x)$. However, this gauge transformation does not affect the physical content of $A_\mu(x)$ so we drop the prime notation out from it. Using the local

³Observe that the invariance under a phase rotation of the complex field $\phi \rightarrow e^{i\theta}\phi$ is equivalent to the invariance under an SO(2) rotation of the real and imaginary parts $\phi_1 \rightarrow \phi_1 \cos \theta - \phi_2 \sin \theta$; $\phi_2 \rightarrow \phi_1 \sin \theta + \phi_2 \cos \theta$

transformations defined by (1.3) and (1.4), (i.e. this particular *gauge*), the Lagrangian reads

$$\begin{aligned}\mathcal{L} = & \left[\frac{1}{2}(\partial_\mu \eta)(\partial^\mu \eta) - \mu^2 \eta^2 \right] + \left[-\frac{1}{4}F_{\mu\nu}F^{\mu\nu} + \frac{q^2 v^2}{2}A_\mu A^\mu \right] \\ & + \left\{ q^2 v (\eta A_\mu A^\mu) + \frac{q^2}{2} \eta^2 A_\mu A^\mu - \lambda \mu \eta^3 - \frac{\lambda^2}{4} \eta^4 \right\} + \frac{\mu^2 v^2}{4}\end{aligned}$$

so we have got rid of the massless field ξ and all its interactions, especially the “disgusting” term $(\partial_\mu \xi) A^\mu$. On the other hand, we are left with a massive scalar field η (a Higgs particle) and a massive four vector field A_μ (a massive “photon”).

By making a counting of degrees of freedom we realize that one degree of freedom has dissapeared (a massless would be Goldstone boson) while another one has arisen (a longitudinal polarization for the four vector boson i.e. its mass). Therefore, it is generically said that the photon has “eaten” the would be Goldstone boson ξ in order to acquire mass. This result is known as the *Higgs mechanism*. Notwithstanding, it worths to emphasize that as well as the massive vector boson, the Higgs mechanism has provided us with an additional physical degree of freedom that corresponds to a scalar field describing the so-called “Higgs particle”.

We can note that the Higgs mechanism is possible because of the conjugation of both the local gauge invariance principle and the SSB. For instance, if we implement a SSB with a global symmetry, what we obtain is a certain number of (physical) massless Goldstone bosons, it is because with a global symmetry we do not generate vector bosons that “eat” such extra degrees of freedom. Technically, the number of Goldstone bosons generated after the symmetry breaking is equal to the number of broken generators (Goldstone theorem [2]).

In SM, the Higgs mechanism creates three massive vector bosons (W^\pm, Z) and one massless vector boson (the photon), as well as a Higgs particle which has not been discovered hitherto.

1.3 The Higgs mechanism in the Standard Model

The SM of particle physics [3], picks up the ideas of local gauge invariance and SSB to implement a Higgs mechanism. The local gauge symmetry

is $SU(2)_L \times U(1)_Y$ and the SSB obeys the scheme $SU(2)_L \times U(1)_Y \rightarrow U(1)_Q$ where the subscript L means that $SU(2)$ only acts on left-handed doublets (in the case of fermions), Y is the generator of the original $U(1)$ group, and Q correspond to an unbroken generator (the electromagnetic charge). Specifically, the symmetry breaking is implemented by introducing a scalar doublet

$$\Phi = \begin{pmatrix} \phi^+ \\ \phi^0 \end{pmatrix} = \begin{pmatrix} \phi_1 + i\phi_2 \\ \phi_3 + i\phi_4 \end{pmatrix}$$

It transforms as an $SU(2)_L$ doublet, thus its weak hypercharge is $Y = 1$. In order to induce the SSB the doublet should acquire a VEV different from zero

$$\langle \Phi \rangle = \begin{pmatrix} 0 \\ v/\sqrt{2} \end{pmatrix} \quad (1.5)$$

What is new respect to the toy model above, is that the original local symmetry $SU(2)_L \times U(1)_Y$ is non abelian⁴. Its generators are τ_i , Y corresponding to $SU(2)_L$ and $U(1)_Y$ respectively, the generators τ_i are defined as

$$\tau_i \equiv \frac{\sigma_i}{2}$$

where σ_i are the Pauli matrices. Therefore, such four generators obey the following lie algebra

$$[\tau_i, \tau_j] = i\epsilon_{ij}^k \tau_k \quad ; \quad [\tau_i, Y] = 0$$

When the symmetry is spontaneously broken in the potential (see below) the doublet acquire a VEV, we can see easily that all generators of the $SU(2)_L \times U(1)_Y$ are broken generators

$$\begin{aligned} \tau_1 \langle \Phi \rangle &= \frac{1}{2} \begin{pmatrix} v/\sqrt{2} \\ 0 \end{pmatrix} \neq 0 \quad ; \quad \tau_2 \langle \Phi \rangle = \frac{1}{2} \begin{pmatrix} -iv/\sqrt{2} \\ 0 \end{pmatrix} \neq 0 \\ \tau_3 \langle \Phi \rangle &= \frac{1}{2} \begin{pmatrix} 0 \\ -v/\sqrt{2} \end{pmatrix} \neq 0 \quad ; \quad Y \langle \Phi \rangle = \begin{pmatrix} 0 \\ v/\sqrt{2} \end{pmatrix} \neq 0 \end{aligned}$$

⁴A very important consequence of the non-abelianity of the gauge group is the generation of self interactions among the associated gauge bosons, they appear when the kinetic term for the gauge bosons (Yang-Mills Lagrangian) is introduced.

However, we can define an unbroken generator by the Gellman-Nijishima relation

$$Q = \left(\tau_3 + \frac{Y}{2} \right) ; \quad Q\langle\Phi\rangle = 0$$

In such a way that the scheme of SSB is given by $SU(2)_L \times U(1)_Y \rightarrow U(1)_Q$. According to the Goldstone theorem, the number of would be Goldstone bosons generated after the symmetry breaking is equal to the number of broken generators (which in turn is equal to the number of massive gauge bosons in the case of local symmetries). Therefore, instead of working with four broken generators we shall work with three broken generators and one unbroken generator Q . This scheme ensures for the photon to remain massless, while the other three gauge bosons acquire masses.

Let us examine the contributions that the doublet Φ introduces in the SM.

1.3.1 The Higgs Potential

The Higgs potential generates the SSB as well as the self interaction terms of the scalar boson, the most general renormalizable potential invariant under $SU(2)_L \times U(1)_Y$ is given by

$$V(\Phi^+\Phi) = \mu^2(\Phi^+\Phi) + \lambda(\Phi^+\Phi)^2 \quad (1.6)$$

where μ^2 and λ are free parameters of the theory. Since λ should be positive for the potential to be bounded from below, the minimization of the potential (1.6) leads to a SSB when $\mu^2 < 0$ with the following scheme $SU(2)_L \times U(1)_Y \rightarrow U(1)_Q$ where Q is the electromagnetic charge. After the SSB the Higgs doublet acquires a VEV as in Eq. (1.5) from which the Higgs doublet gives mass to the Higgs particle and is able to endow the vector bosons and fermions with masses (see below).

1.3.2 The kinetic term

The kinetic term describes the interactions between scalar particles and vector bosons, and provides the masses for the latter when the Higgs doublet acquires a VEV. The kinetic Lagrangian reads

$$\mathcal{L}_{kin} = (D_\mu\Phi)(D^\mu\Phi)^\dagger ; \quad D_\mu \equiv \partial_\mu - \frac{ig'}{2}YW_\mu^4 - ig\tau_iW_\mu^i \quad (1.7)$$

where W_μ^i with $i = 1, 2, 3$ are the four-vector fields (gauge eigenstates), associated to the three generators τ_i i.e. the $SU(2)_L$ symmetry. On the other hand, W_μ^4 is the four-vector field associated to the Y generator i.e. the $U(1)_Y$ symmetry. g and g' are coupling strengths associated to W_μ^i and W_μ^4 respectively. After diagonalizing the mass matrix of the gauge bosons we obtain the following mass eigenstates

$$W_\mu^\pm = \frac{W_\mu^1 \mp iW_\mu^2}{\sqrt{2}} ; \quad M_{W^\pm}^2 = \frac{1}{4}g^2v^2 \quad (1.8)$$

$$M_Z^2 = \frac{1}{4}v^2(g'^2 + g^2) = \frac{M_W^2}{\cos^2 \theta_W} \quad (1.9)$$

$$\begin{pmatrix} Z_\mu \\ A_\mu \end{pmatrix} = \begin{pmatrix} \cos \theta_W & -\sin \theta_W \\ \sin \theta_W & \cos \theta_W \end{pmatrix} \begin{pmatrix} W_\mu^3 \\ W_\mu^4 \end{pmatrix} \quad (1.10)$$

and the gauge boson A_μ (the photon) remains massless, it owes to the fact that this gauge boson is associated to the unbroken generator Q (the electromagnetic charge) i.e. to the remnant symmetry $U(1)_Q$.

1.3.3 The Yukawa Lagrangian

Finally, we build up a Lagrangian that describes the interaction among the Higgs bosons and fermions, the resultant $SU(2)_L \times U(1)_Y$ invariant Lagrangian is called the Yukawa Lagrangian

$$-\mathcal{L}_Y = \eta_{ij}^U \bar{\Psi}_L \tilde{\Phi} U_R + \eta_{ij}^D \bar{\Psi}_L \Phi D_R + h.c. \quad (1.11)$$

where $\bar{\Psi}_L$ are left-handed fermion doublets, U_R, D_R are the right-handed singlets of the up and down sectors of quarks⁵. $\eta_{ij}^{U,D}$ are free parameters that define the vertices and consequently, the Feynman rules of the Lagrangian where i, j are family indices. The Yukawa Lagrangian yields masses to the fermions when the Higgs doublet acquire VEV.

So in brief, Eqs. (1.6,1.7,1.11) describe the contribution that the Higgs sector gives to the SM.

⁵For leptons we have the same structure except that we do not have right handed singlets of neutrinos (corresponding to the up sector of leptons).

Chapter 2

The Two Higgs Doublet Model

2.1 Motivation

Despite the SM has been very sucessful in describing most of the Elementary Particles phenomenology, the Higgs sector of the theory remains unknown so far, and there is not any fundamental reason to assume that the Higgs sector must be minimal (i.e. only one Higgs doublet). Therefore, we could wonder to know whether the Higgs sector is not minimal. Of course, evocating arguments of simplicity we may consider the *next to minimal* extension as the best candidate. The simplest extension compatible with the gauge invariance is the so called Two Higgs Doublet Model (2HDM), which consists of adding a second Higgs doublet with the same quantum numbers as the first one.

Another motivation to introduce the second doublet comes from the hierarchy of Yukawa couplings in the third generation of quarks, the ratio between the masses of the top and bottom quarks is of the order of $m_t/m_b \approx 174/5 \approx 35$. In SM, the masses of both quarks come from the same Higgs doublet, consequently, it implies a non natural hierarchy between their corresponding Yukawa couplings. However, if the bottom received its mass from one doublet (say Φ_1) and the top from another doublet (say Φ_2), then the hierarchy of their Yukawa couplings could be more natural if the free parameters of the theory acquired the appropiate values.

On the other hand, the 2HDM could induce CP violation either explicitly or spontaneously in the Higgs potential (see section 2.2.1). However, we shall restrict our discussion on a CP conserving framework. A recent comprehensive overview of the conditions for the 2HDM to be CP invariant (or

violated) can be found in Ref. [46].

An extra motivation lies on the study of some rare processes called Flavor Changing Neutral Currents (FCNC). It is well known that these kind of processes are severely suppressed by experimental data, despite they seem not to violate any fundamental law of nature. On the other hand, Standard Model (SM) issues are compatible with experimental constraints on FCNC so far [4, 5], with the remarkable exception of neutrino oscillations [8]. In the case of the lepton sector this fact is “explained” by the implementation of the Lepton Number Conservation (LFC), a new symmetry that protects phenomenology from these dangerous processes. However, if we believe that this new symmetry is not exact and we expect to find out FCNC in near future experiments, SM provides a hopeless framework since predictions from it, are by far out of the scope of next generation colliders [7]. This is because in the SM, FCNC are absent in the lepton sector, and in the quark sector they are prohibited at tree level and further suppressed at one loop by the GIM mechanism [6]. So detection of these kind of events would imply the presence of new Physics effects. Perhaps the simplest (but not the unique) framework to look for these rare processes is the Two Higgs Doublet Model (2HDM). Owing to the addition of the second doublet, the Yukawa interactions lead naturally to tree level FCNC unless we make additional assumptions. On the other hand, because of the increasing evidence about neutrino oscillations, especial attention has been addressed to the Lepton Flavor Violation (LFV) in the neutral leptonic sector by experiments with atmospheric neutrinos [8]. Further, since neutrino oscillations imply LFV in the neutral lepton sector, it is generally expected to find out LFV processes involving the charged lepton sector as well, such fact encourage us to study the 2HDM as a possible source for these FCNC. More details in section 3.2.4 and in chapter 4.

Finally, another motivation to study the 2HDM is the fact that some models have a low energy limit with a non minimal Higgs sector. For instance, at least two Higgs doublets are necessary in supersymmetric models and the so called 2HDM type II has the same Yukawa couplings as the Minimal Supersymmetric Standard Model (MSSM). In particular, if the supersymmetric particles are heavy enough, the Higgs sector of the MSSM becomes a constrained 2HDM type II at low energies. SUSY models with two Higgs doublets could provide solutions to some problems of the SM such as the Higgs mass behavior at very high scales, the Planck and Electroweak scale hierarchy, the mass hierarchy among fermion families and the existence of masses for neutrinos and neutrino oscillations.

With these motivations in mind, let us go to see in what way the terms in the Higgs sector are modified by the introduction of a new Higgs doublet

2.2 The contribution of the Higgs sector in the 2HDM

As explained above, we introduce a new Higgs doublet that is a replication of the first one, so the Higgs sector includes two Higgs doublets with the same quantum numbers

$$\Phi_1 = \begin{pmatrix} \phi_1^+ \\ \phi_1^0 \end{pmatrix} ; \quad \Phi_2 = \begin{pmatrix} \phi_2^+ \\ \phi_2^0 \end{pmatrix} \quad (2.1)$$

with hypercharges $Y_1 = Y_2 = 1$, in general, both doublets could acquire VEV

$$\langle \Phi_1 \rangle = \frac{v_1}{\sqrt{2}} \quad ; \quad \langle \Phi_2 \rangle = \frac{v_2}{\sqrt{2}} e^{i\theta}$$

so it is more convenient to parametrize the doublets in the following way

$$\Phi_1 = \begin{pmatrix} \phi_1^+ \\ \frac{h_1 + v_1 + ig_1}{\sqrt{2}} \end{pmatrix} ; \quad \Phi_2 = \begin{pmatrix} \phi_2^+ \\ \frac{h_2 + v_2 e^{i\theta} + ig_2}{\sqrt{2}} \end{pmatrix} \quad (2.2)$$

Now, we examine each part of the Lagrangian that couples to the Higgs doublets

2.2.1 The Higgs potential

Since the Higgs potential is the sector that determines the SSB structure as well as the Higgs masses, Higgs mass eigenstates and Higgs self-interactions, we start examining this part of the Higgs sector. Unlike the SM case, the Higgs potential corresponding to the 2HDM is not unique, and each potential leads to different Feynman rules, details below.

In order to write the most general renormalizable Higgs potential compatible with gauge invariance, it is convenient to introduce a basis of hermitian, gauge invariant operators

$$\begin{aligned}\widehat{A} &\equiv \Phi_1^\dagger \Phi_1, \quad \widehat{B} \equiv \Phi_2^\dagger \Phi_2, \quad \widehat{C} \equiv \frac{1}{2} \left(\Phi_1^\dagger \Phi_2 + \Phi_2^\dagger \Phi_1 \right) = \text{Re} \left(\Phi_1^\dagger \Phi_2 \right), \\ \widehat{D} &\equiv -\frac{i}{2} \left(\Phi_1^\dagger \Phi_2 - \Phi_2^\dagger \Phi_1 \right) = \text{Im} \left(\Phi_1^\dagger \Phi_2 \right)\end{aligned}$$

and write down all possible hermitian bilinear and quartic interactions compatible with gauge invariance

$$\begin{aligned}V_g(\Phi_1, \Phi_2) = & -\mu_1^2 \widehat{A} - \mu_2^2 \widehat{B} - \mu_3^2 \widehat{C} - \mu_4^2 \widehat{D} + \lambda_1 \widehat{A}^2 + \lambda_2 \widehat{B}^2 + \lambda_3 \widehat{C}^2 + \lambda_4 \widehat{D}^2 \\ & + \lambda_5 \widehat{A} \widehat{B} + \lambda_6 \widehat{A} \widehat{C} + \lambda_8 \widehat{A} \widehat{D} + \lambda_7 \widehat{B} \widehat{C} + \lambda_9 \widehat{B} \widehat{D} + \lambda_{10} \widehat{C} \widehat{D} \quad (2.3)\end{aligned}$$

This Lagrangian is much more complex than the SM one given by Eq. (1.6), since in the potential (2.3) we have fourteen free parameters. As we shall see below, four new Higgses will be generated from it. The most general 2HDM potential (2.3), contains interaction vertices that are independent on the mass matrix and the VEV's. Nevertheless, these interactions vanish if we assume that the Higgs potential holds a charge conjugation invariance (C -invariance), and the number of parameters reduces to ten

$$\begin{aligned}V(\Phi_1, \Phi_2) = & -\mu_1^2 \widehat{A} - \mu_2^2 \widehat{B} - \mu_3^2 \widehat{C} + \lambda_1 \widehat{A}^2 + \lambda_2 \widehat{B}^2 + \lambda_3 \widehat{C}^2 + \lambda_4 \widehat{D}^2 \\ & + \lambda_5 \widehat{A} \widehat{B} + \lambda_6 \widehat{A} \widehat{C} + \lambda_7 \widehat{B} \widehat{C} \quad (2.4)\end{aligned}$$

It is important to say that at this step, charge conjugation invariance is equivalent to CP invariance since all fields are scalars¹. Under charge conjugation, a Higgs doublet Φ_i of hypercharge 1, transforms as $\Phi_i \rightarrow e^{i\alpha_i} \Phi_i^*$ where the parameters α_i are arbitrary. Consequently, under charge conjugation we obtain $\Phi_i^\dagger \Phi_j \rightarrow e^{i(\alpha_j - \alpha_i)} \Phi_j^\dagger \Phi_i$. In particular, if we choose $\alpha_i = \alpha_j$ the operator \widehat{D} reverse sign under C -conjugation, while the other ones are invariant², leading to the Lagrangian (2.4).

¹The appearing of pseudoscalar couplings come from the introduction of parity violation in the theory. It is carried out by introducing left-handed fermion doublets and right handed fermion singlets which in turn produces scalar and pseudoscalar couplings, the latter are proportional to γ_5 and are responsible for parity violation. Since the Higgs doublets do not have chirality, their self couplings respect parity and therefore they behave as scalars. However as we shall see in section (2.2.3) when the Higgs doublets couple to fermions some pseudoscalar couplings arise and one Higgs boson behaves as a pseudoscalar.

²Of course, we could have chosen $\alpha_i - \alpha_j = \pm\pi$, in whose case the operator $\widehat{C} =$

However, Lagrangian (2.4) could induce spontaneous CP violation [9]. There are two ways of naturally imposing for the minimum of the potential to be CP invariant [10]. The first one consists of demanding invariance under a Z_2 symmetry where $\Phi_1 \rightarrow \Phi_1$, $\Phi_2 \rightarrow -\Phi_2$. The resulting potential, that will be denoted V'_A is

$$V'_A = -\mu_1^2 \hat{A} - \mu_2^2 \hat{B} + \lambda_1 \hat{A}^2 + \lambda_2 \hat{B}^2 + \lambda_3 \hat{C}^2 + \lambda_4 \hat{D}^2 + \lambda_5 \hat{A} \hat{B} \quad (2.5)$$

and correspond to setting $\mu_3^2 = \lambda_6 = \lambda_7 = 0$ in Eq. (2.4). If we permit a soft breaking term of the form $-\mu_3^2 \hat{C}$, spontaneous CP violation occurs [29], in that case the potential reads

$$V_A = V'_A - \mu_3^2 \hat{C} \quad (2.6)$$

The other potential without spontaneous CP violation, results from imposing the global symmetry $\Phi_2 \rightarrow e^{i\varphi} \Phi_2$. This potential (called V'_B) reads

$$V'_B = -\mu_1^2 \hat{A} - \mu_2^2 \hat{B} + \lambda_1 \hat{A}^2 + \lambda_2 \hat{B}^2 + \lambda_3 (\hat{C}^2 + \hat{D}^2) + \lambda_5 \hat{A} \hat{B} \quad (2.7)$$

and is obtained by using $\mu_3^2 = \lambda_6 = \lambda_7 = 0$ and $\lambda_3 = \lambda_4$ in Eq. (2.4). Since we have a global broken symmetry for the potential V'_B , there is an extra Goldstone boson in the theory.

Additionally, it is customary to allow a soft breaking term $-\mu_3^2 \hat{C}$ in Lagrangian (2.7), obtaining

$$V_B = V'_B - \mu_3^2 \hat{C} \quad (2.8)$$

Neither V'_A or V_B have spontaneous CP violation. In the case of V_B , we end up in the CP conserving case of the scalar potential considered in the Higgs Hunter's guide (see appendix A), which in turn is the one of the MSSM. Both of them contain seven parameters and lead to different phenomenology, however the kinetic sector and the Yukawa sector are identical for both potentials. The soft breaking term in V_B is a quadratic term and consequently

$\text{Re}(\Phi_1^\dagger \Phi_2)$ is the one that violates charge conservation. Additionally, any other choice for $\alpha_i - \alpha_j$ is possible, and in general none parameter vanishes. However, taking into account that these phases must be fixed (though arbitrary), C -invariance would impose relations among the coefficients so that the number of free parameters is always the same (for instance μ_3 and μ_4 would not be independent any more).

it does not affect the renormalizability of the model, the complete renormalization scheme for the potential V_A has been accomplished in Ref. [11], the results for V_B are similar but changing appropriately the cubic and quartic scalar vertices.

The Higgs masses and Higgs eigenstates are defined in terms of the parameters μ_i, λ_i from the potential, and consequently depend on the potential chosen (see appendix A). When the mass matrix described in appendix A is properly diagonalized, we get the Higgs masses and Higgs mass eigenstates. From now on, we will consider the CP conserving case for which both VEV can be taken real, in that case the Higgs sector consists of the following spectrum, two Higgs CP-even scalars (H^0, h^0), one CP-odd scalar (A^0), two charged Higgs bosons (H^\pm), and the Goldstone bosons (G^\pm, G^0) corresponding to W^\pm, Z respectively. The mass eigenstates described above are obtained from the gauge eigenstates defined in (2.2) by the following transformations

$$\begin{aligned} \begin{pmatrix} \cos \beta & \sin \beta \\ -\sin \beta & \cos \beta \end{pmatrix} \begin{pmatrix} \phi_1^+ \\ \phi_2^+ \end{pmatrix} &= \begin{pmatrix} G^+ \\ H^+ \end{pmatrix} \\ \begin{pmatrix} \cos \alpha & \sin \alpha \\ -\sin \alpha & \cos \alpha \end{pmatrix} \begin{pmatrix} h_1 \\ h_2 \end{pmatrix} &= \begin{pmatrix} H^0 \\ h^0 \end{pmatrix} \\ \begin{pmatrix} \cos \beta & \sin \beta \\ -\sin \beta & \cos \beta \end{pmatrix} \begin{pmatrix} g_1 \\ g_2 \end{pmatrix} &= \begin{pmatrix} G^0 \\ A^0 \end{pmatrix} \end{aligned} \quad (2.9)$$

where

$$\tan \beta = \frac{v_2}{v_1}, \quad \sin \beta = \frac{v_2}{\sqrt{v_1^2 + v_2^2}}$$

and α is the mixing angle for the CP -even Higgs bosons, which is different for each potential (see below). $\tan \beta$ is a new parameter that clearly arises from the fact that both Higgs doublets could acquire VEV. In most of the 2HDM's we shall see that new physics contributions are very sensitive to it.

In the following we summarize the results obtained in appendix A, which are in agreement with [12, 17].

For the potential V in Eq. (2.4) the minimum conditions (Tadpoles at tree level) are

$$\begin{aligned} 0 &= T_a = -\mu_1^2 + \lambda_1 v_1^2 \\ 0 &= T_b = -\mu_3^2 + \frac{\lambda_6 v_1^2}{2} \end{aligned}$$

the Higgs masses and the mixing angle α , are written as

$$\begin{aligned} m_{H^+}^2 &= -\mu_2^2 + \frac{1}{2} \lambda_5 v_1^2 ; \quad m_{A^0} = -\mu_2^2 + \frac{1}{2} (\lambda_4 + \lambda_5) v_1^2 \\ m_{H^0,h^0} &= \left(\lambda_1 + \frac{1}{2} \lambda_+ \right) v_1^2 - \frac{1}{2} \mu_2^2 \pm k_1 \\ k_1 &= \sqrt{4\lambda_1 v_1^2 (\lambda_1 v_1^2 + \mu_2^2 - v_1^2 \lambda_+) + (\lambda_+^2 v_1^2 + \lambda_6^2 v_1^2 - 2\mu_2^2 \lambda_+) v_1^2 + \mu_2^4} \\ \tan 2\alpha &= \frac{\lambda_6 v_1^2}{(2\lambda_1 - \lambda_+) v_1^2 + \mu_2^2} \end{aligned}$$

For the potential V'_A Eq. (2.5), the minimum conditions are

$$\begin{aligned} 0 &= T_1 = v_1 (-\mu_1^2 + \lambda_1 v_1^2 + \lambda_+ v_2^2) \\ 0 &= T_2 = v_2 (-\mu_2^2 + \lambda_2 v_2^2 + \lambda_+ v_1^2) \end{aligned} \quad (2.10)$$

where $\lambda_+ = \frac{1}{2} (\lambda_3 + \lambda_5)$. Relations (2.10) lead to the following solutions
i)

$$v_1^2 = \frac{\lambda_2 \mu_1^2 - \lambda_+ \mu_2^2}{\lambda_1 \lambda_2 - \lambda_+^2} ; \quad v_2^2 = \frac{\lambda_1 \mu_2^2 - \lambda_+ \mu_1^2}{\lambda_1 \lambda_2 - \lambda_+^2}$$

or ii)

$$v_2^2 = 0 ; \quad v_1^2 = \frac{\mu_1^2}{\lambda_1}$$

for i) the masses of the Higgs bosons and the mixing angle α are given by

$$\begin{aligned} m_{H^\pm} &= -\lambda_3 (v_1^2 + v_2^2) ; \quad m_{A^0}^2 = \frac{1}{2} (\lambda_4 - \lambda_3) (v_1^2 + v_2^2) \\ m_{H^0,h^0}^2 &= \lambda_1 v_1^2 + \lambda_2 v_2^2 \pm \sqrt{(\lambda_1 v_1^2 - \lambda_2 v_2^2)^2 + 4v_1^2 v_2^2 \lambda_+^2} \\ \tan 2\alpha &= \frac{2v_1 v_2 \lambda_+}{\lambda_1 v_1^2 - \lambda_2 v_2^2} \end{aligned} \quad (2.11)$$

and for ii) they are

$$\begin{aligned} m_{H^\pm}^2 &= -\mu_2^2 + \frac{1}{2}\lambda_5 v_1^2 ; \quad m_{A^0}^2 = -\mu_2^2 + \frac{1}{2}(\lambda_4 + \lambda_5) v_1^2 ; \quad m_{H^0}^2 = 2\lambda_1(\frac{3}{4}12) \\ m_{h^0}^2 &= -\mu_2^2 + \frac{1}{2}(\lambda_3 + \lambda_5) v_1^2 ; \quad \tan 2\alpha = 0 \end{aligned} \quad (2.13)$$

Finally, for the potential V_B Eq. (2.8), the minimum conditions are

$$0 = T_1 - \frac{\mu_3^2}{2}v_2 \quad ; \quad 0 = T_2 - \frac{\mu_3^2}{2}v_1 \quad (2.14)$$

whose solutions are

$$\begin{aligned} v_1^2 &= \frac{\lambda_1 - \lambda_2 \pm Z_1}{2(\lambda_1 - \lambda_+)(\lambda_2 - \lambda_+)} \\ v_2^2 &= \frac{\lambda_2 - \lambda_1 \pm Z_2}{2(\lambda_1 - \lambda_+)(\lambda_2 - \lambda_+)} \\ Z_1 &= \sqrt{(\lambda_1 - \lambda_2)^2 - 4(\lambda_1 - \lambda_+)(\lambda_2 - \lambda_+) \left[(\lambda_+ v^2 - \mu_1^2)(\lambda_+ v^2 - \mu_2^2) - \frac{1}{4}\mu_3^4 \right]} \\ Z_2 &= \sqrt{(\lambda_1 - \lambda_2)^2 - 4(\lambda_2 - \lambda_+)(\lambda_1 - \lambda_+) \left[(\lambda_+ v^2 - \mu_2^2)(\lambda_1 v^2 - \mu_1^2) - \frac{1}{4}\mu_3^4 \right]} \end{aligned}$$

The masses and the mixing angle α are given by

$$\begin{aligned} m_{H^\pm} &= -\lambda_3(v_1^2 + v_2^2) + \mu_3^2 \frac{v_1^2 + v_2^2}{v_1 v_2} ; \quad m_{A^0}^2 = \frac{1}{2}\mu_3^2 \frac{v_1^2 + v_2^2}{v_1 v_2} \\ m_{H^0, h^0}^2 &= \lambda_1 v_1^2 + \lambda_2 v_2^2 + \frac{1}{4}\mu_3^2 (\tan \beta + \cot \beta) \\ &\quad \pm \sqrt{\left[\lambda_1 v_1^2 - \lambda_2 v_2^2 + \frac{1}{4}\mu_3^2 (\tan \beta - \cot \beta) \right]^2 + \left(2v_1 v_2 \lambda_+ - \frac{1}{2}\mu_3^2 \right)^2} \\ \tan 2\alpha &= \frac{2v_1 v_2 \lambda_+ - \frac{1}{2}\mu_3^2}{\lambda_1 v_1^2 - \lambda_2 v_2^2 + \frac{1}{4}\mu_3^2 (\tan \beta - \cot \beta)} \end{aligned} \quad (2.15)$$

Observe that a solution with one of the VEV's equal to zero is not possible for the potential V_B . As explained before, each potential has different Feynman rules and consequently, leads to different phenomenology [25], a

complete set of Feynman rules for these potentials could be found in Refs. [25, 46].

The potentials V'_A and V_B are different because they differ in some cubic and quartic interactions. For example, the coupling $h^0 H^+ H^-$ reveals some subtle aspects of the phenomenology of the potential; in terms of the λ 's it is given by

$$\begin{aligned} g_{h^0 H^+ H^-} = & 2v_2\lambda_2 \cos^2 \beta \cos \alpha + v_2\lambda_3 \sin \alpha \cos \beta \sin \beta - v_1\lambda_5 \cos^2 \beta \sin \alpha \\ & - 2v_1\lambda_1 \sin^2 \beta \sin \alpha + v_2\lambda_5 \sin^2 \beta \cos \alpha - v_1\lambda_3 \cos \alpha \cos \beta \sin \beta \end{aligned}$$

and coincides for both potentials V'_A and V_B ; it is because this interaction does not involve λ_4 nor μ_3 which are the factors that make the difference between them. However, by writing the coupling in terms of the Higgs boson masses the result is different for each potential

$$\begin{aligned} (g_{h^0 H^+ H^-})_A &= \frac{g}{m_W} \left[m_{h^0}^2 \frac{\cos(\alpha + \beta)}{\sin 2\beta} - \left(m_{H^+}^2 - \frac{1}{2}m_{h^0}^2 \right) \sin(\alpha - \beta) \right] \\ (g_{h^0 H^+ H^-})_B &= \frac{g}{m_W} \left[(m_{h^0}^2 - m_{A^0}^2) \frac{\cos(\alpha + \beta)}{\sin 2\beta} \right. \\ &\quad \left. - \left(m_{H^+}^2 - \frac{1}{2}m_{h^0}^2 \right) \sin(\alpha - \beta) \right] \end{aligned}$$

we can resolve the puzzle by remembering that what really matters in perturbative calculations is the position of the minimum of the potential and the values of the derivatives at that point. Now, the position of the vacuum (minimum) is different for each potential and the generation of masses come from the second derivative of the potential evaluated at this minimum, so the relation among the λ 's and the masses are different for V'_A and V_B , thus the coupling $h^0 H^+ H^-$ in terms of physical quantities differs for each potential. It should be pointed out that even before being able to test the Higgs bosons self-couplings in order to discriminate among the potentials, we might see a signature of them in processes with Higgs boson loops, for example, the decay $h^0 \rightarrow \gamma\gamma$ could be very sensitive to the difference among the self couplings of V'_A and V_B .

Finally, it is also important to notice that the symmetry of the potential ought to be extended to the other Higgs sectors, this fact is particularly important to write the Yukawa Lagrangian to be discussed in section 2.2.3.

2.2.2 The kinetic sector

The kinetic Lagrangian (1.7) of the SM is extended to become

$$\mathcal{L}_{kin} = (D_\mu \Phi_1)^+ (D^\mu \Phi_1) + (D_\mu \Phi_2)^+ (D^\mu \Phi_2) \quad (2.16)$$

where the covariant derivative is defined by Eq. (1.7). This Lagrangian endows the gauge bosons with mass and provides the interactions among gauge and Higgs bosons. In contrast to the Higgs potential and the Yukawa Lagrangian (see sections 2.2.1, 2.2.3), the kinetic sector is basically unique because of the gauge invariance³. Indeed, we can easily check that the kinetic Lagrangian described by Eq. (2.16) is already invariant under charge conjugation as well as under the discrete and global symmetries described in Sec. (2.2.1), therefore the imposition of these symmetries does not produce any difference in the kinetic sector unlike the case of the potential.

In order to expand the Lagrangian, it is convenient to work on a real representation for the generators, for which we make the assignment $L_a = -i\tau_a$ and double the dimension of the representation by means of the definition

$$\Phi_k = \begin{pmatrix} Re\phi_k^+ + iIm\phi_k^+ \\ Re\phi_k^0 + iIm\phi_k^0 \end{pmatrix} \rightarrow \begin{pmatrix} Re\phi_k^+ \\ Im\phi_k^+ \\ Re\phi_k^0 \\ Im\phi_k^0 \end{pmatrix} \quad k = 1, 2 \quad (2.17)$$

From which we find the real representation by looking at the action of the initial generators (multiplied by $-i$), over the two dimensional representation of the doublet Φ_k defined in Eq. (2.17). For example, for τ_1

$$L_1 \Phi_1 = -i\tau_1 \Phi_1 = \frac{-i\sigma_1}{2} \Phi_1 = \frac{1}{2} \begin{pmatrix} Im\phi_1^0 - iRe\phi_1^0 \\ Im\phi_1^+ - iRe\phi_1^+ \end{pmatrix} \quad (2.18)$$

And we extend $L_1 \Phi_1$ with the same correspondence rule

$$L_1 \Phi_1 \rightarrow \frac{1}{2} \begin{pmatrix} Im\phi_1^0 \\ -Re\phi_1^0 \\ Im\phi_1^+ \\ -Re\phi_1^+ \end{pmatrix} \quad (2.19)$$

³However, for some potentials and Yukawa Lagrangians it is possible to rotate the Doublets such that only one of them acquire VEV, as we will see later. In that case the kinetic term is basically the same but taking (say) $v_2 = 0$ i.e. $\tan \beta = 0$.

Finally, we look for a matrix L_1 that acting on (2.17) reproduces (2.19), we get

$$L_1 = \frac{1}{2} \begin{pmatrix} 0 & 0 & 0 & 1 \\ 0 & 0 & -1 & 0 \\ 0 & 1 & 0 & 0 \\ -1 & 0 & 0 & 0 \end{pmatrix} \quad (2.20)$$

Similarly we obtain for the other generators

$$\begin{aligned} L_2 &= \frac{1}{2} \begin{pmatrix} 0 & 0 & -1 & 0 \\ 0 & 0 & 0 & -1 \\ 1 & 0 & 0 & 0 \\ 0 & 1 & 0 & 0 \end{pmatrix}, \quad L_3 = \frac{1}{2} \begin{pmatrix} 0 & 1 & 0 & 0 \\ -1 & 0 & 0 & 0 \\ 0 & 0 & 0 & -1 \\ 0 & 0 & 1 & 0 \end{pmatrix} \\ L_4 &= \frac{1}{2} \begin{pmatrix} 0 & 1 & 0 & 0 \\ -1 & 0 & 0 & 0 \\ 0 & 0 & 0 & 1 \\ 0 & 0 & -1 & 0 \end{pmatrix} \end{aligned} \quad (2.21)$$

From which the covariant derivative in (1.7) reads

$$D_\mu = \partial_\mu + g L_i W_\mu^i + g' L_4 W_\mu^4 \quad (2.22)$$

Thus, we can expand the Lagrangian (2.16) by using the four dimensional representation for each doublet Eq. (2.17), and the four dimensional representation of the generators Eqs. (2.20), (2.21).

Gauge fields

The mass terms are obtained from the VEV's, the resulting mass matrix is given by

$$\frac{1}{2} M_{ab}^2 W_\mu^a W_\mu^b ; \quad M_{ab}^2 = 2 \sum_{k=1}^2 (g_a L_a v_k)^\dagger (g_b L_b v_k) \quad (2.23)$$

Where $a, b = 1, 2, 3, 4$ indicates the gauge bosons (gauge eigenstates) corresponding to the generators τ^i, Y respectively. After the diagonalization of (2.23) the mass terms and eigenstates for the Gauge bosons read

$$W_\mu^\pm = \frac{W_\mu^1 \mp iW_\mu^2}{\sqrt{2}} ; \quad M_{W^\pm}^2 = \frac{1}{4}g^2(v_1^2 + v_2^2) \quad (2.24)$$

$$M_Z^2 = \frac{1}{4}(v_1^2 + v_2^2)(g'^2 + g^2) = \frac{M_W^2}{\cos^2 \theta_W} \quad (2.25)$$

$$\begin{pmatrix} Z_\mu \\ A_\mu \end{pmatrix} = \begin{pmatrix} \cos \theta_W & -\sin \theta_W \\ \sin \theta_W & \cos \theta_W \end{pmatrix} \begin{pmatrix} W_\mu^3 \\ W_\mu^4 \end{pmatrix} \quad (2.26)$$

where θ_W is the Weinberg mixing angle. We can realize that the expressions for the vector bosons masses coincide with the ones in SM if $v_1^2 + v_2^2 = v^2$ (where v is the VEV of the Higgs doublet of the SM), and since $v^2 = 4M_W^2/g^2$ is a known parameter, we have at tree level the constraint $v_1^2 + v_2^2 = v^2$.

Since the kinetic sector provides the interactions of Higgs bosons with gauge bosons, let us discuss some interesting features of these interactions.

Interactions in the kinetic sector

We can obtain the interactions in the kinetic sector by expanding the Lagrangian (2.16) in terms of the mass eigenstates of Higgs bosons and Vector bosons Eqs. (2.24, 2.26, 2.9). On the other hand, it worths to note that some interactions that at first glance should appear, are absent in this expansion as is the case of $A^0 W^+ W^-$, and $A^0 Z Z$. Let us discuss shortly the origin of these missings. First of all we should emphasize that *in the SM, the discrete symmetries C and P are preserved separately when fermions are absent*. Then, we can assign a unique set of quantum numbers J^{PC} to all the bosons of the theory when fermions are ignored. The same argument holds for the two Higgs doublet model. These facts dictate the presence or missing of some interactions [17].

First of all, let us examine the assignment of these quantum numbers for the scalar and vector bosons in the table (2.1).

The existence of the vertex $Z H^+ H^-$ indicates that $J^{PC}(Z) = 1^{+-}$, the existence of $H^0 h^0 h^0$ in the Higgs potential says that $J^{PC}(H^0) = 0^{++}$; symmetrically the existence of $h^0 H^0 H^0$ tells us that $J^{PC}(h^0) = 0^{++}$. From

	J^{PC}		J^P
γ	1^{--}	W^\pm	1^+
Z	1^{+-}	H^\pm	0^+
H^0	0^{++}		
h^0	0^{++}		
A^0	0^{+-}		

Table 2.1: Assignments to the parity (P) and charge conjugation (C), quantum numbers for the Higgs and vector bosons before the introduction of fermions. When fermions are absent, P and C are conserved separately, (i.e. in the Higgs potential and kinetic Lagrangian).

these quantum number assignments we deduce from the vertex ZH^0A^0 that $J^{PC}(A^0) = 0^{+-}$.

Furthermore, in the 2HDM the imaginary parts combine to produce A^0 and G^0 so both must have the same quantum numbers, consequently A^0 and G^0 have the quantum numbers 0^{+-} . Owing to the assignment $J^{PC}(A^0) = 0^{+-}$ the vertices $A^0W^+W^-$ and A^0ZZ are forbidden. We should remark that despite the Higgs A^0 is usually called a *pseudoscalar Higgs*, at this step A^0 is a *scalar* particle. However, we shall see later that A^0 behaves as a pseudoscalar when it couples to matter (fermions), see section (2.2.3). Thus, the term pseudoscalar is not so proper for the Higgs A^0 and the denomination as a *CP*-odd Higgs is more appropriate.

Another way to explain the absence of vertices $A^0W^+W^-$ and A^0ZZ is the following: These interactions come from the kinetic term $(D_\mu\Phi)(D^\mu\Phi)^\dagger$ after replacing one of the ϕ_i^0 fields in Eq. (2.1) by its VEV, but in a CP conserving model the VEV is real while A^0 comes from the imaginary parts of the ϕ_i^0 fields as we can see from Eqs. (2.2) and (2.9). Therefore A^0 cannot be coupled to any massive vector boson. By the same token, the couplings $(H^0, h^0)\gamma\gamma$ are forbidden at tree level, since H^0, h^0 cannot be coupled at tree level to massless vector bosons. Finally, another interesting argument is that $A^0W^+W^-$ and A^0ZZ are prohibited by C -invariance, however, when fermions are introduced (by means of loops) C -invariance is no longer valid (though CP -invariance still holds in good approximation). Consequently, these vertices can appear at one loop level by inserting fermions into the

loops.

So in general, vertices with neutral particles only and one or two photons clearly vanish at tree level but can be generated at one loop. And same for a pair of gluons coupled to any of the neutral Higgs bosons. Gluon gluon fusion generated by one loop couplings $(A^0, H^0, h^0) gg$, is a very important source for Higgs production in Hadron colliders.

Additionally, there are other couplings whose absence can be explained by the quantum number assignments in table (2.1). For instance, the coupling of Z to non identical Higgs bosons is allowed only if such scalars have opposite CP numbers. Consequently, the couplings ZA^0H^0 , ZA^0h^0 are allowed while ZH^0h^0 is forbidden. On the other hand, the couplings of Z to identical Higgs bosons are forbidden by *Bose-Einstein symmetry*. Moreover, $H^\pm W^\mp \gamma$ is prohibited by conservation of electromagnetic current.

As for the vertices $H^\pm W^\mp Z$, they do not appear at tree level in the 2HDM. We should note however, that they are not forbidden by these quantum numbers (they appear in some triplet representations). In the case of multi-Higgs doublet models (including the 2HDM) they are prohibited at tree level because of the isospin symmetry. Notwithstanding, such couplings are allowed at loop levels owing to the breaking of the isospin symmetry by the loop particles. One loop contributions to the H^+W^-Z vertex are studied in [18, 19, 20] and will be discussed in section (3.2).

Finally, we should emphasize that when CP is violated, many of the missing vertices described above appear, though they are expected to be quite suppressed.

Furthermore, it is interesting to notice that the couplings of the kinetic sector satisfy automatically some tree level unitarity bounds. Since partial amplitudes cannot grow with energy, cancellations to avoid violation of unitarity are necessary. For example, in the case of $V_L V_L \rightarrow V_L V_L$ scattering, cancellation is possible in SM because the vertex is of the form $g_{\phi^0 WW} = gm_W$. When we have more than one doublet, this work does not have to be done by only one Higgs boson, instead we have the sum rule

$$\sum_i g_{h_i^0 VV}^2 = g_{\phi^0 VV}^2 \quad (2.27)$$

where i labels all the neutral Higgs bosons of the extended Higgs sector, and ϕ^0 denotes the SM Higgs. The sum rule (2.27) ensures the unitarity

of $V_L V_L \rightarrow V_L V_L$. Moreover, to ensure $f\bar{f} \rightarrow V_L V_L$ unitarity we ought to demand

$$\sum_i g_{h_i^0 VV} g_{h_i^0 f\bar{f}} = g_{\phi^0 VV} g_{\phi^0 f\bar{f}} \quad (2.28)$$

in such a way that only the contribution of all Higgs bosons cancels the effect.

In the particular case of the 2HDM, Eq. (2.27) becomes

$$g_{h^0 VV}^2 + g_{H^0 VV}^2 = g_{\phi^0 VV}^2 \quad (2.29)$$

where $\phi^0 VV$ denotes the coupling of the SM Higgs with two vector bosons⁴. We can check that in terms of the mixing angles α and β we get

$$\frac{g_{h^0 VV}}{g_{\phi^0 VV}} = \sin(\beta - \alpha) \quad ; \quad \frac{g_{H^0 VV}}{g_{\phi^0 VV}} = \cos(\beta - \alpha) \quad (2.30)$$

from which the constraint (2.29) is obviously accomplished.

A very important phenomenological consequence of (2.29) is that the couplings of h^0, H^0 to VV are suppressed respect to SM ones. In particular, if one of the scalar Higgs bosons decouples at tree level from VV then the Higgs coupling at tree level of the other scalar Higgs is SM-like. In that case we say that one of the Higgs bosons “exhausts” or “saturates” the sum rule, this is a natural scenario in the Minimal Supersymmetric Standard Model (MSSM) in which $\cos(\beta - \alpha) \sim 0$ is expected, so the coupling $h^0 VV$ almost saturates the sum rule and is SM like, while the coupling $H^0 VV$ is highly suppressed.

It is worthwhile to point out that the existence of V–Higgs–Higgs couplings is a new feature of the 2HDM respect to SM. As we shall discuss in section (3.1), tree level unitarity constraints involving those kind of couplings are also satisfied.

As for the sum rule (2.28), it involves also the couplings of the Higgs bosons to fermions, which are model dependent, we shall see in next section that such rule is also automatically accomplished at tree level by some sets of Yukawa couplings.

⁴Remember that the coupling $A^0 VV$ does not appear at tree level.

2.2.3 The Yukawa Lagrangian

The Most general gauge invariant Lagrangian that couples the Higgs fields to fermions reads

$$-\mathcal{L}_Y = \eta_{ij}^{U,0} \overline{Q}_{iL}^0 \tilde{\Phi}_1 U_{jR}^0 + \eta_{ij}^{D,0} \overline{Q}_{iL}^0 \Phi_1 D_{jR}^0 + \xi_{ij}^{U,0} \overline{Q}_{iL}^0 \tilde{\Phi}_2 U_{jR}^0 + \xi_{ij}^{D,0} \overline{Q}_{iL}^0 \Phi_2 D_{jR}^0 + \eta_{ij}^{E,0} \overline{l}_{iL}^0 \Phi_1 E_{jR}^0 + \xi_{ij}^{E,0} \overline{l}_{iL}^0 \Phi_2 E_{jR}^0 + h.c., \quad (2.31)$$

where $\Phi_{1,2}$ represent the Higgs doublets, $\tilde{\Phi}_{1,2} \equiv i\sigma_2 \Phi_{1,2}$, η_{ij}^0 and ξ_{ij}^0 are non diagonal 3×3 matrices and i, j denote family indices. D_R^0 refers to the three down-type weak isospin quark singlets $D_R^0 \equiv (d_R^0, s_R^0, b_R^0)^T$, U refers to the three up-type weak isospin quark singlets $U_R^0 \equiv (u_R^0, c_R^0, t_R^0)^T$ and E_R^0 to the three charged leptons. Finally, \overline{Q}_{iL}^0 , \overline{l}_{iL}^0 denote the quark and lepton weak isospin left-handed doublets respectively. The superscript “0” indicates that the fields are not mass eigenstates yet.

From now on, I shall restrict the discussion to the quark sector only, since the extension of the arguments to the lepton sector is straightforward. What we can see from the model described by Eq. (2.31) is that in the most general case, both Higgs bosons couple (and consequently give masses) to the up and down sectors simultaneously. However, this general case leads to processes with Flavor Changing Neutral Currents (FCNC) at tree level. This is basically because by rotating the fermion gauge eigenstates of the down sector to get the mass eigenstates we are not able to diagonalize both coupling matrices $\eta^{D,0}, \xi^{D,0}$ simultaneously⁵, the situation is similar for the up and lepton sectors.

Now, since processes containing FCNC are very strongly suppressed experimentally, especially due to the small $K_L - K_S$ mass difference, these processes were considered dangerous. Consequently, several mechanisms to avoid them at the tree level were proposed, for instance one possibility is to consider the exchange of heavy scalar or pseudoscalar Higgs Fields [4] or by cancellation of large contributions with opposite sign. Perhaps the most “elegant” or “natural” suppression mechanism is the one suggested by Glashow and Weinberg [30], who implemented a discrete symmetry that automatically forbids the couplings that generate such rare decays. Another

⁵Of course, we still have the possibility of a fine tuning that allows us to diagonalize both matrices with the same transformation. Although it is not a very natural assumption, it leads to a model without FCNC different from the ones obtained from arguments of symmetry.

mechanism was proposed by Cheng and Sher arguing that a natural value for the FC couplings from different families ought to be of the order of the geometric average of their Yukawa couplings [5], this assumption has been tested by Ref. [31] in the quark sector. Remarkably, absence of FCNC at tree level is possible even with both Higgs doublets coupled simultaneously to the up and down sectors; Ref. [22] studies the possibility of suppressing FCNC in a general 2HDM, by demanding a S_3 permutation symmetry among the three fermion families, this S_3 permutation symmetry would be broken spontaneously when the SSB of the gauge symmetry occurs, more details in section 3.1. On the other hand, Ref. [46] shows that the decoupling limit (to be discussed later on) is a natural scenario to get rid of tree level FCNC in the general 2HDM.

Let us first discuss the mechanism proposed by Weinberg and Glashow. We have said that the matrices $\eta^{U,0}, \xi^{U,0}$ cannot be diagonalized simultaneously, and the same applies to the couple of matrices $\eta^{D,0}, \xi^{D,0}$. So it is immediate to realize that we can suppress the FCNC at tree level in Lagrangian (2.31), if we manage to get rid of one of the pair of matrices $(\eta^{U,0}, \xi^{U,0})$ that couples the up sector to the Higgs doublets, and same for the down sector. We can achieve that, by implementing the following discrete symmetry

$$\begin{aligned}\Phi_1 &\rightarrow \Phi_1 \text{ and } \Phi_2 \rightarrow -\Phi_2 \\ D_{jR} &\rightarrow \mp D_{jR} \text{ and } U_{jR} \rightarrow -U_{jR}\end{aligned}$$

so by demanding invariance under this discrete symmetry we have two cases

- When we use $D_{jR} \rightarrow -D_{jR}$ we should drop out $\eta_{ij}^{U,0}$ and $\eta_{ij}^{D,0}$. So, Φ_1 decouples from the Yukawa sector and only Φ_2 couples and gives masses to the up and down sectors. This case is known as the 2HDM type I
- When we use $D_{jR} \rightarrow D_{jR}$ then $\eta_{ij}^{U,0}$ and $\xi_{ij}^{D,0}$ vanish and therefore Φ_1 couples and gives masses to the down sector while Φ_2 couples and gives masses to the up sector. In this case we call it, the 2HDM type II.

In the most general framework of multi-Higgs doublet models, this suppression mechanism acquires the character of a theorem [30], the theorem of Glashow and Weinberg says that the FCNC processes mediated by Higgs exchange are absent at tree level in a general multi-Higgs doublet model if

all fermions of a given electric charge couple to no more than one Higgs doublet. The Lagrangians type I and II discussed above clearly accomplish the theorem. It is important to say that we can use the same type of couplings for both the quark and lepton sectors or on the other hand, we can treat them asymmetrically giving a total of four different Lagrangians⁶.

Furthermore, the Yukawa Lagrangians type I and II can also be generated from a continuous global symmetry. The set of transformations

$$\begin{aligned}\Phi_1 &\rightarrow \Phi_1 \text{ and } \Phi_2 \rightarrow e^{i\varphi}\Phi_2 \\ D_{jR} &\rightarrow e^{-i\omega}D_{jR} \text{ and } U_{jR} \rightarrow e^{-i\varphi}U_{jR}\end{aligned}$$

with $\omega \equiv \varphi, 0$; leads to the models type I and type II, respectively.

The discrete symmetry arises as a special case of this continuous symmetry when we fix $\varphi = \pi$. Nevertheless, we should remember that the discrete symmetry leads to a Higgs potential which is phenomenologically different from the one generated by the continuous global symmetry as we saw in Sec. (2.2.1). Consequently, we should be careful in choosing the symmetry. For instance, as we saw in Sec. (2.2.1), the potential V_B in Eq. (2.8) that coincides with the potential of the Higgs Hunter's Guide and the MSSM, comes from the imposition of the continuous global symmetry (plus a soft breaking term) and not from the discrete symmetry⁷, while the potential V'_A in Eq. (2.5) comes from the discrete symmetry.

However, the discrete (or global) symmetry is not compulsory and we should explore the possibility of having the whole model Eq. (2.31) including the FCNC, and look for the constraints that the experimental measurements impose on the region of parameters of the model. When we take into account all terms in (2.31), the two Higgs doublets couple and yield masses to both up-type and down-type fermions, in that case we call it the 2HDM type III.

From the discussion above, we conclude that the Feynman rules of the Yukawa Lagrangian are highly model dependent, and could be enhanced or suppressed respect to SM in contrast to the kinetic couplings which are always

⁶For instance, Ref. [11] classified these Yukawa Lagrangians as models I, II, III, and IV. I prefer to use the most common notation taking into account that for instance, the leptonic sector could be of type I and the quark sector of type II.

⁷We could argue that the potential V_B i.e. the potential in the Higgs Hunter's Guide and the MSSM, comes from the discrete symmetry but adding a fine tuning such that $\lambda_3 = \lambda_4$. Notwithstanding, the global continuous symmetry generates this potential without the necessity of any fine tuning.

particle	J^{PC}	particle	J^P
γ	1^{--}	W^\pm	$1^+, 1^-$
Z	$1^{+-}, 1^{--}$	H^\pm	$0^+, 0^-$
H^0	$0^{++}, 0^{--}$		
h^0	$0^{++}, 0^{--}$		
A^0	$0^{+-}, 0^{-+}$		

Table 2.2: Assignments to the parity (P) and charge conjugation (C), quantum numbers for the Higgs and vector bosons when fermions are introduced. After the introduction of fermions, P and C are not conserved separately anymore. However, in good approximation CP is still a good quantum number.

suppressed. Consequently, the phenomenology is very sensitive to the choice in the Yukawa sector.

There are however, some general characteristics related to the quantum spectrum J^{PC} for the particles involved in the Yukawa interactions. When we introduce fermions, C and P are not conserved separately any more, however CP is still a good symmetry (but not exact). If we assume CP conservation, the Higgs bosons and vectors that were considered above could be thought as admixtures of two states with well defined C and P (appropriate linear combinations of them are CP eigenstates, and even we can introduce a CP deviation ϵ), we show in table (2.2) the J^{PC} quantum numbers for Higgs and vector bosons when fermions are introduced i.e. when C and P are not conserved separately but CP is.

On the other hand, it is well known that for a $f\bar{f}$ system, the quantum C and P numbers are $P = (-1)^{L+1}$, $C = (-1)^{L+S}$; where L , S denote the total orbital angular momentum and the total spin of the $f\bar{f}$ system, respectively. Then, $f\bar{f}$ cannot be coupled to states of the type $0^{--}, 0^{+-}$. Therefore, in the couplings $f\bar{f}(H^0, h^0)$ the Higgs bosons behave as purely 0^{++} , while in $f\bar{f}A^0$ the Higgs behaves as purely 0^{-+} . Hence, H^0, h^0 couples with parity $+1$ to matter (fermions) while A^0 couples with parity -1 to fermions, it is because of this fact that the Higgs boson A^0 is usually called a pseudoscalar boson. Obviously, H^0, h^0 continue being CP -even and A^0 continues being CP -odd as long as CP invariance is demanded.

Additionally, there are two interesting gauge frameworks to generate the

Yukawa couplings, the U -gauge and the R -gauge. Though calculations in the unitary gauge are simpler because the would be Goldstone bosons are removed, the usage of the R -gauge in which the would be Goldstone bosons appears explicitly, could be useful if we are interested in calculations involving longitudinal vector bosons at high energies, since the equivalence theorem could be applied.

Now we shall examine the most interesting choices for the Yukawa Lagrangian and their features. Once again, for the sake of simplicity, I will restrict the equations and discussions to the quark sector, nevertheless most of the results hold for the leptonic sector too, with the proper changes.

The 2HDM type I

In the 2HDM type I, only one Higgs doublet (say Φ_2), couples to the fermions, so the Yukawa Lagrangian becomes

$$\begin{aligned} -\mathcal{L}_Y \text{ (type I)} = & \xi_{ij}^{U,0} \bar{Q}_{iL}^0 \tilde{\Phi}_2 U_{jR}^0 + \xi_{ij}^{D,0} \bar{Q}_{iL}^0 \Phi_2 D_{jR}^0 \\ & + \text{leptonic sector} + h.c., \end{aligned} \quad (2.32)$$

When we expand in terms of mass eigenstates the Lagrangian reads

$$\begin{aligned} -\mathcal{L}_Y \text{ (type I)} = & \frac{g}{2M_W \sin \beta} \bar{D} M_D^{diag} D (\sin \alpha H^0 + \cos \alpha h^0) \\ & + \frac{ig \cot \beta}{2M_W} \bar{D} M_D^{diag} \gamma_5 D A^0 \\ & + \frac{g}{2M_W \sin \beta} \bar{U} M_U^{diag} U (\sin \alpha H^0 + \cos \alpha h^0) \\ & - \frac{ig \cot \beta}{2M_W} \bar{U} M_U^{diag} \gamma_5 U A^0 \\ & + \frac{g \cot \beta}{\sqrt{2}M_W} \bar{U} (K M_D^{diag} P_R - M_U^{diag} K P_L) D H^+ \\ & - \frac{ig}{2M_W} \bar{U} M_U^{diag} \gamma_5 U G_Z^0 + \frac{ig}{2M_W} \bar{D} M_D^{diag} \gamma_5 D G_Z^0 \\ & + \frac{g}{\sqrt{2}M_W} \bar{U} (K M_D^{diag} P_R - M_U^{diag} K P_L) D G_W^+ \\ & + \text{leptonic sector} + h.c. \end{aligned} \quad (2.33)$$

The interactions involving would be Goldstone bosons given above, appears in the R -gauge and are identical in all Yukawa Lagrangians, however they vanish in the unitary gauge.

Note that since only one Higgs doublet couples to the fermions, the Lagrangian (2.32) is SM-like. However, it does not mean that the Higgs fermion interactions are SM-like, in Eq. (2.33) we see that all five Higgs bosons and the mixing angles from the 2HDM appears. It is because when we replace the scalar gauge eigenstates contained in the doublet by the corresponding mass eigenstates, we are taking into account the mixing of both doublets coming from the potential to obtain such mass eigenstates.

On the other hand, the Yukawa couplings in SM are given by

$$g_{\phi^0 f \bar{f}} = \frac{m_f}{v} = \frac{g m_f}{2 M_W}$$

in both the up and down sectors (f denotes any quark or charged lepton). It is interesting to analyze the deviations of these couplings respect to the ones in SM. In order to do it, we calculate the **relative couplings** (the quotient between the Yukawa couplings of the new physics and the SM Yukawa couplings). I will follow the notation defined in [72] for the relative couplings i.e. $\chi_i^h \equiv g_i^h / \left(g_i^{\phi^0} \right)_{SM}$ with “ i ” denoting a fermion antifermion (or VV) pair and “ h ” represents a generic Higgs boson. For the Lagrangian type I we get in third family notation

$$\begin{aligned} \chi_t^{H^0} &: \frac{\sin \alpha}{\sin \beta} = \cos(\beta - \alpha) - \cot \beta \sin(\beta - \alpha) \\ \chi_b^{H^0} &: \frac{\sin \alpha}{\sin \beta} = \cos(\beta - \alpha) - \cot \beta \sin(\beta - \alpha) \\ \chi_t^{h^0} &: \frac{\cos \alpha}{\sin \beta} = \sin(\beta - \alpha) + \cot \beta \cos(\beta - \alpha) \\ \chi_b^{h^0} &: \frac{\cos \alpha}{\sin \beta} = \sin(\beta - \alpha) + \cot \beta \cos(\beta - \alpha) \\ \chi_t^{A^0} &: -i\gamma_5 \cot \beta \quad ; \quad \chi_b^{A^0} : i\gamma_5 \cot \beta \end{aligned} \quad (2.34)$$

There are several interesting features that could be seen above. First, the relative couplings of a certain Higgs boson to the down-type quarks are equal to the ones to the up type quarks, only the A^0 couplings to the up and down type quarks differs from a relative sign. Second, from Eqs. (2.30) and (2.34)

we see that the model type I satisfies the tree level unitarity bound given in Eq. (2.28). In the case of minimal mixing in the CP even sector i.e. $\alpha = 0$, H^0 is decoupled from the Yukawa sector while the couplings of h^0 are maximal (for a given value of $\tan\beta$). In the case of $\alpha = \pi/2$, the behavior is the same but interchanging the roles of both CP even Higgses. Additionally, the Yukawa couplings for a certain Higgs can be enhanced or suppressed depending on the values of the mixing angles α, β .

On the other hand, from (2.34) we can realize that in model I the heaviest (lightest) CP even Higgs becomes totally fermiophobic (i.e. all $H^0(h^0) f\bar{f}$ couplings vanish) if $\alpha = 0(\pi/2)$. We should bear in mind however, that decays of $H^0(h^0)$ to fermions are still possible via $H^0(h^0) \rightarrow W^*W(Z^*Z) \rightarrow 2f\bar{f}$ or $H^0(h^0) \rightarrow W^*W^*(Z^*Z^*) \rightarrow 2f\bar{f}$. If the fermiophobic scenario were accomplished it would be a signature for physics beyond the SM, and the 2HDM type I would be an interesting candidate. In addition, we see that if we further assume that $\beta - \alpha = \pi/2(0)$ then $H^0(h^0)$ becomes also bosophobic (respect to vector bosons, see Eq. (2.30) and ghostphobic, while $h^0(H^0)$ acquires SM-like couplings to fermions and vector bosons. In the latter case, $H^0(h^0)$ always needs another scalar particle to decay into fermions or vector bosons.

The 2HDM type II

In this case, one Higgs doublet (e.g. Φ_1) couples to the down sector of fermions while the other Higgs doublet (e.g. Φ_2) couples to the up sector.

$$-\mathcal{L}_Y \text{ (type II)} = \eta_{ij}^{D,0} \overline{Q}_{iL}^0 \Phi_1 D_{jR}^0 + \xi_{ij}^{U,0} \overline{Q}_{iL}^0 \tilde{\Phi}_2 U_{jR}^0 + \text{leptonic sector} + h.c. \quad (2.35)$$

In this case the expanded Lagrangian becomes

$$\begin{aligned}
-\mathcal{L}_Y \text{ (type II)} = & \frac{g}{2M_W \cos \beta} \overline{D} M_D^{diag} D (\cos \alpha H^0 - \sin \alpha h^0) \\
& - \frac{ig \tan \beta}{2M_W} \overline{D} M_D^{diag} \gamma_5 D A^0 \\
& + \frac{g}{2M_W \sin \beta} \overline{U} M_U^{diag} U (\sin \alpha H^0 + \cos \alpha h^0) \\
& - \frac{ig \cot \beta}{2M_W} \overline{U} M_U^{diag} \gamma_5 U A^0 \\
& - \frac{g}{\sqrt{2}M_W} \overline{U} \left[(\cot \beta M_U^{diag} K P_L + \tan \beta K M_D^{diag} P_R) \right] D H^+ \\
& - \frac{ig}{2M_W} \overline{U} M_U^{diag} \gamma_5 U G^0 + \frac{ig}{2M_W} \overline{D} M_D^{diag} \gamma_5 D G^0 \\
& + \frac{g}{\sqrt{2}M_W} \overline{U} \left[(K M_D^{diag} P_R - M_U^{diag} K P_L) \right] D G_W^+ \\
& + \text{leptonic sector} + h.c.
\end{aligned} \tag{2.36}$$

this is the Lagrangian that is required in the MSSM. Notice that since the down fermion sector receives its masses on the first Higgs doublet while the up sector receives its masses from the second one; the hierarchy of the Yukawa couplings between the top and bottom quarks of the third generation becomes more natural if $\tan \beta \sim 35$ and $\tan \alpha \sim 1$. On the other hand, we can see that the couplings of up type fermions to Higgs bosons are the same for both models type I and II. It is because in both lagrangians (2.32) and (2.35) the up sector couples to the same Higgs doublet while the down sector couples to different ones⁸.

Once again, comparison with SM is useful, calculating the relative couplings in the third generation notation, we get

⁸If we had chosen in the model type II to couple the doublet Φ_1 to the up sector and Φ_2 to the down sector, the couplings of the down type fermions would had been the ones that coincide for models type I and II. It is a fact of convention.

$$\begin{aligned}
\chi_t^{H^0} &: \frac{\sin \alpha}{\sin \beta} = \cos(\beta - \alpha) - \cot \beta \sin(\beta - \alpha) \\
\chi_b^{H^0} &: \frac{\cos \alpha}{\cos \beta} = \cos(\beta - \alpha) + \tan \beta \sin(\beta - \alpha) \\
\chi_t^{h^0} &: \frac{\cos \alpha}{\sin \beta} = \sin(\beta - \alpha) + \cot \beta \cos(\beta - \alpha) \\
\chi_b^{h^0} &: -\frac{\sin \alpha}{\cos \beta} = \sin(\beta - \alpha) - \tan \beta \cos(\beta - \alpha) \\
\chi_t^{A^0} &: -i\gamma_5 \cot \beta ; \quad \chi_b^{A^0} : -i\gamma_5 \tan \beta
\end{aligned} \tag{2.37}$$

from this results and Eqs. (2.30), we can see the following interesting relations among the relative couplings in the 2HDM type II

$$\begin{aligned}
\left(\chi_V^{h^0}\right)^2 + \left(\chi_V^{H^0}\right)^2 &= 1 \\
\left(\chi_u^{h^0, H^0} - \chi_V^{h^0, H^0}\right) \left(\chi_V^{h^0, H^0} - \chi_d^{h^0, H^0}\right) &= 1 - \left(\chi_V^{h^0, H^0}\right)^2 \\
\left(\chi_u^{h^0, H^0} + \chi_d^{h^0, H^0}\right) \chi_V^{h^0, H^0} &= 1 + \chi_u^{h^0, H^0} \chi_d^{h^0, H^0} \\
\left(1 - \frac{m_{h^0}^2}{2m_{H^+}}\right) \chi_V^{h^0} + \frac{m_{h^0}^2 - \mu_3^2}{2m_{H^+}^2} \left(\chi_d^{h^0} + \chi_u^{h^0}\right) &= \chi_{H^+}^{h^0}
\end{aligned}$$

From Eqs. (2.30) and (2.37) we see that the model type II satisfies the tree level unitarity bound given in Eq. (2.28). The relative couplings of a certain Higgs to the down-type quarks are different from the ones to the up type quarks unlike the case of Lagrangian type I .

On the other hand, if $\cos(\beta - \alpha) \simeq 0$, the couplings of the lightest CP even Higgs boson h^0 are almost identical to the SM Higgs couplings not only in the Yukawa potential but in the kinetic sector as well, if we additionally take H^0, A^0, H^\pm sufficiently heavy while keeping the quartic Higgs self couplings $\lesssim O(1)$, we obtain the decoupling limit in which the low energy effective theory is the SM [46]. In general, if one saturates the sum rules for VV with one scalar, the unitarity sum rules can be achieved by assuming SM-like couplings of the same Higgs with fermions. This is a natural scenario in the MSSM. However, it is not the only way to satisfy the sum rules, for instance the other Higgs (that is obviously weakly coupled to VV) could be strongly coupled to fermions so that the product $g_{hVV} g_{h\bar{f}f}$ is still significant.

It is worthwhile to point out that there is a very strong difference between models I and II, in model II when $\tan\beta > 1$ some couplings (like $A t \bar{t}$) are suppressed, and others like $A b \bar{b}$ are enhanced, for instance in $H^+ \bar{t} b$ the contributions of the top (bottom) are suppressed (enhanced). In contrast, model I gives a uniform suppression or enhancement pattern (for fixed α).

Moreover, from (2.37) we can check that model type II does not exhibit a totally fermiophobic limit for any Higgs boson, unlike the model type I. For instance, if $\alpha = \pi/2$ then $h^0 (H^0)$ become fermiophobic to fermions of up(down)-type, while couplings to the down(up)-type fermions are maximal, the opposite occurs when $\alpha = 0$. This partially fermiophobic behavior of the model type II is another important difference with model type I and with SM.

The 2HDM type III

The model type III consists of taking into account all terms in Lagrangian (2.31)

$$\begin{aligned} -\mathcal{L}_Y = & \eta_{ij}^{U,0} \bar{Q}_{iL}^0 \tilde{\Phi}_1 U_{jR}^0 + \eta_{ij}^{D,0} \bar{Q}_{iL}^0 \Phi_1 D_{jR}^0 + \xi_{ij}^{U,0} \bar{Q}_{iL}^0 \tilde{\Phi}_2 U_{jR}^0 + \xi_{ij}^{D,0} \bar{Q}_{iL}^0 \Phi_2 D_{jR}^0 \\ & + \text{lepton sector} + h.c. \end{aligned} \quad (2.38)$$

in the case of the model type III, we are able to make a rotation of the doublets in such a way that only one of the doublets acquire VEV. Therefore, we can assume without any loss of generality that $\langle \Phi_1 \rangle = v/\sqrt{2}$, $\langle \Phi_2 \rangle = 0$ (see appendices B,C). After expanding the Lagrangian (2.38) we obtain

$$\begin{aligned} -\mathcal{L}_Y (\text{type III}) = & \frac{g}{2M_W} \bar{D} M_D^{diag} D (\cos \alpha H^0 - \sin \alpha h^0) \\ & + \frac{1}{\sqrt{2}} \bar{D} \xi^D D (\sin \alpha H^0 + \cos \alpha h^0) \\ & + \frac{i}{\sqrt{2}} \bar{D} \xi^D \gamma_5 D A^0 + \frac{g}{2M_W} \bar{U} M_U^{diag} U (\cos \alpha H^0 - \sin \alpha h^0) \\ & + \frac{1}{\sqrt{2}} \bar{U} \xi^U U [\sin \alpha H^0 + \cos \alpha h^0] - \frac{i}{\sqrt{2}} \bar{U} \xi^U \gamma_5 U A^0 \\ & + \bar{U} (K \xi^D P_R - \xi^U K P_L) D H^+ \\ & + \text{Goldstone interactions} + \text{leptonic sector} + h.c. \end{aligned} \quad (2.39)$$

where the Goldstone interactions are the same as in the case of (2.33) and (2.36).

There are several interesting characteristics: the diagonal couplings of the pseudoscalar Higgs boson and the charged Higgs bosons to fermions are not proportional to the fermion mass as is the case of models type I and II; they are proportional to ξ_{ff} i.e. the diagonal elements of the mixing matrix ξ . Additionally, the diagonal couplings involving CP –even Higgs bosons have one term proportional to the fermion mass and other term proportional to ξ_{ff} . Once again we shall calculate the relative couplings of the model

$$\begin{aligned}
\chi_t^{H^0} &: \cos \alpha + \frac{\xi_{tt} \sin \alpha}{\sqrt{2}m_t} v \\
\chi_b^{H^0} &: \cos \alpha + \frac{\xi_{bb} \sin \alpha}{\sqrt{2}m_b} v \\
\chi_t^{h^0} &: -\sin \alpha + \frac{\xi_{tt} \cos \alpha}{\sqrt{2}m_t} v \\
\chi_b^{h^0} &: -\sin \alpha + \frac{\xi_{bb} \cos \alpha}{\sqrt{2}m_b} v \\
\chi_t^{A^0} &: -\frac{i\xi_{tt}}{\sqrt{2}m_t} v ; \quad \chi_b^{A^0} : \frac{i\xi_{bb}}{\sqrt{2}m_b} v
\end{aligned} \tag{2.40}$$

The presence of diagonal mixing vertices could play a crucial role in looking for FCNC. At this respect, it is worthwhile to point out that the *relative couplings* in model type III are *not universal* because of the contribution of the factor ξ_{ff}/m_f , as a manner of example the relative couplings $\chi_t^{H^0}$, $\chi_c^{H^0}$, $\chi_u^{H^0}$ are in general different⁹, a deviation from the universal behavior could be a clear signature of FCNC at the tree level; even if only diagonal processes are observed. In particular, we cannot obtain a totally fermiophobic limit of (say) the Higgs h^0 unless that a very precise pattern of the quotient ξ_{ff}/m_f is demanded, we can have for instance the possibility of h^0 to be top-phobic¹⁰ but not charm-phobic or up-phobic, this is due to the

⁹As we can easily see from Eqs. (2.34, 2.37) in model type I, the relative couplings χ_f^h for a certain Higgs h , are the same for all fermions. In model type II, these relative couplings are equal for all up type fermions and for all down type fermions. In contrast, in the model type III all these relative couplings are in general, different each other. This breaking of the universality of the relative couplings in the model type III owes to the presence of the flavor diagonal contributions ξ_{ii}/m_i , unless we assume them to be universal as well.

¹⁰With the top-phobic limit for certain Higgs, we mean that the coupling of that Higgs to a pair of top quarks vanishes. Nevertheless, the couplings of such Higgs to a top and any other quark could exist.

lack of universality discussed previously [38]. In contrast, model type I, can only be fermiophobic to all fermions simultaneously [11], while model type II can only be fermiophobic to all down-type or all up-type fermions simultaneously. Moreover, as it was explained above, A^0 couples to a pair of fermions $f\bar{f}$ through the matrix element ξ_{ff} . Therefore in model III, if $\xi_{ff} = 0$ for a certain specific fermion, then A^0 becomes fermiophobic to it (and only to it). It is also interesting to see that the matrix elements ξ_{ij} modify the charged Higgs couplings as well: $g_{H^+ f_i f_j} = (K_{ik}\xi_{kj}^D P_R - \xi_{ik}^U K_{kj} P_L)$, where K is the Kobayashi Maskawa matrix and $P_{L(R)}$ are the left(right) projection operators. At this respect there are two features to point out i) the flavor changing charged currents (FCCC) in the quark sector are modified by the same matrix that produces FCNC, ii) in the lepton sector FCCC are generated by the same matrix that generates FCNC [39].

Finally, we can see that the tree level unitarity constraints (2.28) impose a condition on the diagonal elements ξ_{ff} of the mixing matrix, preventing them to be arbitrarily large.

Since in model III we can find a basis in which we are able to get rid of one of the VEV's, the mass eigenstates become simpler. By using say $\langle\Phi_2\rangle = 0$, we obtain the mass eigenstates by setting $\beta = 0$ in Eq. (2.9). We shall call it the **“fundamental parametrization”**. In that case, only the doublet Φ_1 generates the spontaneous symmetry breaking, thus it is the only one that provides masses for the fermions and vector bosons. The second doublet Φ_2 only provides interactions with them.

Additionally, taking $\langle\Phi_2\rangle = 0$ and using the basis of states (h_1, h_2, g_2, H^\pm) we can see that Φ_1 corresponds to the SM doublet and h_1 to the SM Higgs field since it has the same couplings and no interactions with h_2, g_2 [32]. Consequently, all the new scalar fields belong to the second doublet Φ_2 . Moreover, h_2, g_2 do not have couplings to gauge bosons of the form $h_2(g_2)ZZ$ or $h_2(g_2)W^+W^-$. Nevertheless, we ought to remember that h_1, h_2 are not mass eigenstates, they mix through the angle α (see Eq. (2.9)). However, as soon as we consider a scenario with $\alpha \approx 0$ these features become important since the set (h_1, h_2, g_2, H^\pm) becomes a mass eigenstates basis. As we will see later on, when $\alpha = 0$ in the fundamental parametrization, we arrive to the decoupling limit of the 2HDM.

On the other hand, we can parametrize the Yukawa Lagrangian type III by preserving both VEV's different from zero, we shall see below that the relation between the model type III with the models type I or type II is clearer with this parametrization[36]. In order to distinguish between the

parametrization with only one VEV Eq. (2.38) from the parametrization with two VEV, we write down the latter in the following way

$$\begin{aligned} -\mathcal{L}_Y = & \tilde{\eta}_{ij}^{U,0} \overline{Q}_{iL}^0 \tilde{\Phi}'_1 U_{jR}^0 + \tilde{\eta}_{ij}^{D,0} \overline{Q}_{iL}^0 \Phi'_1 D_{jR}^0 + \tilde{\xi}_{ij}^{U,0} \overline{Q}_{iL}^0 \tilde{\Phi}'_2 U_{jR}^0 + \tilde{\xi}_{ij}^{D,0} \overline{Q}_{iL}^0 \Phi'_2 D_{jR}^0 \\ & + \text{lepton sector} + h.c. \end{aligned} \quad (2.41)$$

where $\langle \Phi'_1 \rangle = v_1$, $\langle \Phi'_2 \rangle = v_2$. The relations among $(\tilde{\eta}_{ij}^{U,D}, \tilde{\xi}_{ij}^{U,D})$ and $(\eta_{ij}^{U,D}, \xi_{ij}^{U,D})$ are calculated in appendix (B). First we split the Lagrangian (2.41) in two parts

$$\begin{aligned} -\mathcal{L}_{Y(U)} &= \tilde{\eta}_{ij}^{U,0} \overline{Q}_{iL}^0 \tilde{\Phi}_1 U_{jR}^0 + \tilde{\xi}_{ij}^{U,0} \overline{Q}_{iL}^0 \tilde{\Phi}_2 U_{jR}^0 + h.c. \\ -\mathcal{L}_{Y(D)} &= \tilde{\eta}_{ij}^{D,0} \overline{Q}_{iL}^0 \Phi_1 D_{jR}^0 + \tilde{\xi}_{ij}^{D,0} \overline{Q}_{iL}^0 \Phi_2 D_{jR}^0 + \text{lepton sector} + h.c. \\ -\mathcal{L}_Y (\text{type III}) &= -\mathcal{L}_{Y(U)} - \mathcal{L}_{Y(D)} \end{aligned}$$

In order to convert this lagrangian into mass eigenstates we make the unitary transformations

$$\begin{aligned} D_{L,R} &= (V_{L,R}) D_{L,R}^0, \\ U_{L,R} &= (T_{L,R}) U_{L,R}^0 \end{aligned} \quad (2.42)$$

from which we obtain the mass matrices. In the parametrization with both VEV different from zero we get

$$\begin{aligned} M_D^{diag} &= V_L \left[\frac{v_1}{\sqrt{2}} \tilde{\eta}^{D,0} + \frac{v_2}{\sqrt{2}} \tilde{\xi}^{D,0} \right] V_R^\dagger, \\ M_U^{diag} &= T_L \left[\frac{v_1}{\sqrt{2}} \tilde{\eta}^{U,0} + \frac{v_2}{\sqrt{2}} \tilde{\xi}^{U,0} \right] T_R^\dagger. \end{aligned} \quad (2.43)$$

We can solve for $\tilde{\xi}^{D,0}, \tilde{\xi}^{U,0}$ obtaining

$$\begin{aligned} \tilde{\xi}^{D,0} &= \frac{\sqrt{2}}{v_2} V_L^\dagger M_D^{diag} V_R - \frac{v_1}{v_2} \tilde{\eta}^{D,0} \\ \tilde{\xi}^{U,0} &= \frac{\sqrt{2}}{v_2} T_L^\dagger M_U^{diag} T_R - \frac{v_1}{v_2} \tilde{\eta}^{U,0} \end{aligned} \quad (2.44)$$

Let us call the Eqs. (2.44), parametrization of type I. Replacing them into (2.41) the expanded Lagrangians for up and down sectors are [36]

$$\begin{aligned}
-\mathcal{L}_{Y(U)}^{(I)} \text{ (type III)} = & \frac{g}{2M_W \sin \beta} \overline{U} M_U^{diag} U (\sin \alpha' H^0 + \cos \alpha' h^0) \\
& - \frac{1}{\sqrt{2} \sin \beta} \overline{U} \tilde{\eta}^U U [\sin (\alpha' - \beta) H^0 + \cos (\alpha' - \beta) h^0] \\
& - \frac{ig \cot \beta}{2M_W} \overline{U} M_U^{diag} \gamma_5 U A^0 + \frac{i}{\sqrt{2} \sin \beta} \overline{U} \tilde{\eta}^U \gamma_5 U A^0 \\
& - \frac{g \cot \beta}{\sqrt{2} M_W} \overline{U} M_U^{diag} K P_L D H^+ + \frac{1}{\sin \beta} \overline{U} \tilde{\eta}^U K P_L D H^+ \\
& - \frac{ig}{2M_W} \overline{U} M_U^{diag} \gamma_5 U G^0 - \frac{g}{\sqrt{2} M_W} \overline{U} M_U^{diag} K P_L D G_W^+ \\
& + h.c. \tag{2.45}
\end{aligned}$$

$$\begin{aligned}
-\mathcal{L}_{Y(D)}^{(I)} \text{ (type III)} = & \frac{g}{2M_W \sin \beta} \overline{D} M_D^{diag} D (\sin \alpha' H^0 + \cos \alpha' h^0) \\
& - \frac{1}{\sqrt{2} \sin \beta} \overline{D} \tilde{\eta}^D D [\sin (\alpha' - \beta) H^0 + \cos (\alpha' - \beta) h^0] \\
& + \frac{ig \cot \beta}{2M_W} \overline{D} M_D^{diag} \gamma_5 D A^0 - \frac{i}{\sqrt{2} \sin \beta} \overline{D} \tilde{\eta}^D \gamma_5 D A^0 \\
& + \frac{g \cot \beta}{\sqrt{2} M_W} \overline{U} K M_D^{diag} P_R D H^+ - \frac{1}{\sin \beta} \overline{U} K \tilde{\eta}^D P_R D H^+ \\
& + \frac{ig}{2M_W} \overline{D} M_D^{diag} \gamma_5 D G^0 + \frac{g}{\sqrt{2} M_W} \overline{U} K M_D^{diag} P_R D G_W^+ \\
& + \text{leptonic sector} + h.c. \tag{2.46}
\end{aligned}$$

where K is the CKM matrix, $\tilde{\eta}^{U(D)} = T_L(V_L) \tilde{\eta}^{U(D),0} T_R^\dagger(V_R)^\dagger$ and similarly for $\tilde{\xi}^{U(D)}$. The superindex (I) refers to the parametrization type I. In order to make the expansion above, we have used the Eqs. (2.9) but replacing $\alpha \rightarrow \alpha'$ since the notation α will be reserved for the mixing angle between CP even scalars in the fundamental parametrization (see appendix B). The leptonic sector is obtained from the equation (2.46) replacing the down-type (up-type) quarks by the charged leptons (neutrinos).

It is easy to check that if we add (2.45) and (2.46) we obtain a Lagrangian consisting of the one in the 2HDM type I [17], plus some FC interactions,

i.e., $-\mathcal{L}_{Y(U)}^{(I)} - \mathcal{L}_{Y(D)}^{(I)}$. Therefore, we obtain the Lagrangian of type I from Eqs. (2.45) and (2.46) by setting $\tilde{\eta}^D = \tilde{\eta}^U = 0$.

On the other hand, from (2.43), we can also solve for $\tilde{\eta}^{D,0}, \tilde{\eta}^{U,0}$ instead of $\tilde{\xi}^{D,0}, \tilde{\xi}^{U,0}$, to get

$$\begin{aligned}\tilde{\eta}^{D,0} &= \frac{\sqrt{2}}{v_1} V_L^\dagger M_D^{diag} V_R - \frac{v_2}{v_1} \tilde{\xi}^{D,0} \\ \tilde{\eta}^{U,0} &= \frac{\sqrt{2}}{v_1} T_L^\dagger M_U^{diag} T_R - \frac{v_2}{v_1} \tilde{\xi}^{U,0}\end{aligned}\quad (2.47)$$

which we call parametrization of type II. Replacing them into (2.41) the expanded Lagrangians for up and down sectors become [36]

$$\begin{aligned}-\mathcal{L}_{Y(U)}^{(II)} \text{ (type III)} &= \frac{g}{2M_W \cos \beta} \overline{U} M_U^{diag} U (\cos \alpha' H^0 - \sin \alpha' h^0) \\ &+ \frac{1}{\sqrt{2} \cos \beta} \overline{U} \tilde{\xi}^U U [\sin (\alpha' - \beta) H^0 + \cos (\alpha' - \beta) h^0] \\ &+ \frac{ig \tan \beta}{2M_W} \overline{U} M_U^{diag} \gamma_5 U A^0 - \frac{i}{\sqrt{2} \cos \beta} \overline{U} \tilde{\xi}^U \gamma_5 U A^0 \\ &+ \frac{g \tan \beta}{\sqrt{2} M_W} \overline{U} M_U^{diag} K P_L D H^+ - \frac{1}{\cos \beta} \overline{U} \tilde{\xi}^U K P_L D H^+ \\ &- \frac{ig}{2M_W} \overline{U} M_U^{diag} \gamma_5 U G^0 - \frac{g}{\sqrt{2} M_W} \overline{U} M_U^{diag} K P_L D G_W^+ \\ &+ h.c.\end{aligned}\quad (2.48)$$

$$\begin{aligned}-\mathcal{L}_{Y(D)}^{(II)} \text{ (type III)} &= \frac{g}{2M_W \cos \beta} \overline{D} M_D^{diag} D (\cos \alpha' H^0 - \sin \alpha' h^0) \\ &+ \frac{1}{\sqrt{2} \cos \beta} \overline{D} \tilde{\xi}^D D [\sin (\alpha' - \beta) H^0 + \cos (\alpha' - \beta) h^0] \\ &- \frac{ig \tan \beta}{2M_W} \overline{D} M_D^{diag} \gamma_5 D A^0 + \frac{i}{\sqrt{2} \cos \beta} \overline{D} \tilde{\xi}^D \gamma_5 D A^0 \\ &- \frac{g \tan \beta}{\sqrt{2} M_W} \overline{D} K M_D^{diag} P_R D H^+ + \frac{1}{\cos \beta} \overline{D} K \tilde{\xi}^D P_R D H^+ \\ &+ \frac{ig}{2M_W} \overline{D} M_D^{diag} \gamma_5 D G^0 + \frac{g}{\sqrt{2} M_W} \overline{D} K M_D^{diag} P_R D G_W^+ \\ &+ \text{leptonic sector} + h.c.\end{aligned}\quad (2.49)$$

The superindex (II) refers to the parametrization type II. Moreover, if we add the Lagrangians (2.45) and (2.49) we find the Lagrangian of the 2HDM type II [17] plus some FC interactions, $-\mathcal{L}_{Y(U)}^{(I)} - \mathcal{L}_{Y(D)}^{(II)}$. Similarly like before, Lagrangian type II is obtained setting $\tilde{\xi}^D = \tilde{\eta}^U = 0$, in the total Lagrangian $-\mathcal{L}_{Y(U)}^{(I)} - \mathcal{L}_{Y(D)}^{(II)}$. Therefore, Lagrangian type III can be written as the model type II plus FC interactions if we use the parametrization type I in the up sector and the parametrization type II in the down sector, it is valid since $\tilde{\xi}^U$ and $\tilde{\xi}^D$ are independent each other and same to $\tilde{\eta}^{U,D}$.

Moreover, we can build two additional parametrizations by adding $-\mathcal{L}_{Y(U)}^{(II)} - \mathcal{L}_{Y(D)}^{(II)}$ and $-\mathcal{L}_{Y(U)}^{(II)} - \mathcal{L}_{Y(D)}^{(I)}$. The former corresponds to a model type I plus FC interactions but interchanging the role of the doublets $\Phi_1 \leftrightarrow \Phi_2$; the latter gives a model type II plus FC interactions with the same interchange. On the other hand, terms involving would-be Goldstone bosons are the same in all parametrizations in the R-gauge, while in the unitary gauge they vanish [17, 36].

Finally, as it is demonstrated in appendix (B) the FC matrices $\tilde{\eta}^{U,D}, \tilde{\xi}^{U,D}$ are related to the FC matrices $\eta^{U,D}, \xi^{U,D}$ in the fundamental parametrization Eq. (2.39) through the following formulae (see Eqs. (B.14)), here we shall write them in terms of $\tan \beta$

$$\begin{aligned}
\tilde{\eta}^{U,D} &= \frac{M_{U,D}}{v} \sqrt{\frac{2}{1 + \tan^2 \beta}} - \frac{\tan \beta}{\sqrt{1 + \tan^2 \beta}} \xi^{U,D} \\
\tilde{\xi}^{U,D} &= \left(\sqrt{\frac{2}{1 + \tan^2 \beta}} \right) \frac{M_{U,D}}{v} \tan \beta + \frac{1}{\sqrt{1 + \tan^2 \beta}} \xi^{U,D} \\
\eta^{U,D} &= \frac{\sqrt{2}}{v} M_{U,D} \\
\xi^{U,D} &= \left(\sqrt{1 + \tan^2 \beta} \right) \tilde{\xi}^{U,D} - \frac{\sqrt{2} \tan \beta}{v} M_{U,D}
\end{aligned} \tag{2.50}$$

The development of these new parametrizations of the 2HDM type III, facilitates the comparison of it with the models type I and type II. In addition, one of these parametrizations has been used by Haber and Gunion [46] to study the decoupling limit of the general two Higgs doublet model. Further, in Sec. (4.5) we shall obtain some limits on the free parameters of the model in the framework of one of these parametrizations.

Chapter 3

Present Status of the general Two Higgs Doublet Models

3.1 Theoretical constraints

The most important theoretical constraints come from the ρ parameter and the unitarity limits. In SM, $\rho = 1$ at tree level. On the other hand, in models beyond the standard model values around $\rho \simeq 1$ are expected too. In arbitrary Higgs multiplet representations the value of ρ at tree level is given by[17]

$$\rho \equiv \frac{M_W^2}{M_Z^2 \cos^2 \theta_W} = \frac{\sum_{T_i, Y_i} [4T_i(T_i + 1) - Y_i^2] |V_{T_i Y_i}|^2 C_{T_i Y_i}}{\sum_{T_i, Y_i} 2Y_i^2 |V_{T_i Y_i}|^2} ,$$

where $V_{T_i Y_i} = \langle \Phi(T_i Y_i) \rangle_0$ defines the VEV of the neutral Higgses, Y_i is the hypercharge value of the multiplet number i . T_i is the $SU(2)_L$ isospin i.e. $T_i(T_i + 1)$ are the eigenvalues of the generators: $\sum_{j=1}^3 (T_i)_{jL}^2$. Finally, the coefficients $C_{T_i Y_i}$ are defined as

$$C_{T_i Y_i} = \begin{cases} 1, & \text{if } Y_i \neq 0 \\ \frac{1}{2}, & \text{if } T_i \text{ is integer and } Y_i = 0. \end{cases}$$

in the case of the 2HDM, we have $Y_1 = Y_2 = 1$, $C_{T_1 Y_1} = C_{T_2 Y_2} = 1$, $T_1 = T_2 = 1/2$. From which we can see that the relation $\rho = 1$ is maintained at tree level.

In SM the one loop correction to the ρ parameter [33] is dominated by the top quark loop

$$\Delta\rho = \frac{3G_F m_t^2}{8\sqrt{2}\pi^2}$$

by contrast, the contributions coming from the first family are given by mild logarithmic terms. This fact is related to the breaking of a global $SU(2)_V$ symmetry [34]. This isospin symmetry “protects” the relation $\rho = 1$ at next to leading order. The first generation of quarks preserves in good approximation such “custodial symmetry”. In contrast, the third generation of quarks breaks the symmetry strongly producing a very sizeable one loop contribution [34]. Constraints coming from radiative corrections to ρ in the 2HDM will be discussed later on.

Other important theoretical constraints come from unitarity. As it was mentioned in section (2.2.2), the unitarity bound coming from $V_L V_L \rightarrow V_L V_L$ scatterings is accomplished if

$$\sum_i g_{h_i^0 VV}^2 = g_{\phi^0 VV}^2 \quad (3.1)$$

where i labels all the neutral Higgs bosons of the 2HDM and ϕ^0 refers to the SM Higgs. Additionally, we saw that the requirement of unitarity for the $f\bar{f} \rightarrow V_L V_L$ scattering leads to

$$\sum_i g_{h_i^0 VV} g_{h_i^0 f\bar{f}} = g_{\phi^0 VV} g_{\phi^0 f\bar{f}} \quad (3.2)$$

As we saw in Sec. (2.2.2), the condition (3.1) is accomplished for the general 2HDM since the couplings of any Higgs to VV are universal. In contrast, the second condition (3.2) is accomplished automatically by the 2HDM type I and II, but not by the type III one, in the latter case this condition provides a constraint for the diagonal terms of the mixing matrix as it was already mentioned.

On the other hand, unitarity bounds of processes involving $V - Higgs - Higgs$ couplings determines the form of such couplings. For instance, unitarity constraints in $H^+ W^- \rightarrow H^+ W^-$ and $A^0 Z \rightarrow A^0 Z$ leads to the following sum rule [17].

$$g_{H^+W-h^0}^2 + g_{H^+W-H^0}^2 = (g_{h^0A^0Z}^2 + g_{H^0A^0Z}^2) \cos^2 \theta_W = \frac{g^2}{4} \quad (3.3)$$

Moreover, unitarity of $A^0Z \rightarrow W^+W^-$ requires a precise ratio between $g_{H^0A^0Z}$ and $g_{h^0A^0Z}^2$ [17]. Similarly, unitarity of $H^+W^- \rightarrow W^+W^-$ determines a relation among the couplings $g_{H^+W-h^0}$ and $g_{H^+W-H^0}$. Combining the sum rule (3.3) with the unitarity bounds from $A^0Z \rightarrow W^+W^-$ and $H^+W^- \rightarrow W^+W^-$, the following values for the $V - Higgs - Higgs$ couplings are obtained

$$\begin{aligned} g_{h^0A^0Z} &= \frac{g}{2 \cos \theta_W} \cos(\beta - \alpha) \quad ; \quad g_{H^+W-h^0} = \frac{g}{2} \cos(\beta - \alpha) \\ g_{H^0A^0Z} &= \frac{g}{2 \cos \theta_W} \cos(\beta - \alpha) \end{aligned}$$

They coincide with the values gotten by direct expansion of the kinetic Lagrangian, and tree level unitarity is also automatically satisfied by $V - Higgs - Higgs$ couplings.

On the other hand, tree level unitarity bounds in the Higgs potential can also be derived from the two body scattering of scalars $S_1S_2 \rightarrow S_3S_4$. Tree level unitarity constraints for the potential V'_A in Eq. (2.5) have been calculated [43] obtaining strong upper limits on some free parameters of the Higgs potential with exact Z_2 invariance. For instance, Ref. [43] obtains the following useful bound

$$m_{h^0} \leq \sqrt{\frac{16\pi\sqrt{2}}{3G_F} \cos^2 \beta - m_{H^0}^2 \cot^2 \beta}$$

Notwithstanding, Akeroyd *et. al.* [44] showed that by introducing the soft breaking term μ_3^2 (from which we arrive to the potential V_A Eq.(2.6)) such bounds are weaken considerably. Additionally, Ref. [44] also shows that the inclusion of charged states not included in [43] changes significantly the bounds on m_{H^\pm} and m_{A^0} . In the absence of the soft breaking term, general unitarity bounds are $m_{H^\pm} \lesssim 691$ GeV, $m_{A^0} \lesssim 695$ GeV, $m_{h^0} \lesssim 435$ GeV, $m_{H^0} \lesssim 638$ GeV. These bounds are obtained for relatively small values of $\tan \beta$ ($\tan \beta \approx 0.5$). For large values of it the upper bound is smaller, but only h^0 is very sensitive to the variation in $\tan \beta$, especially for small values

of the soft breaking term. For $\mu_3^2 = 0$, the sensitivity is very strong, but for large values of μ_3^2 e.g. $\mu_3^2 = 15$, the plot m_{h^0} vs $\tan\beta$ becomes a horizontal line predicting $m_{h^0} \lesssim 670$ GeV. The relaxation of the strong correlation between m_{h^0} and $\tan\beta$ could be a mechanism to distinguish between the potential with the exact symmetry and with the softly broken symmetry.

Unfortunately, no general unitarity bounds have been calculated for the potentials V Eq. (2.4) and V_B Eq. (2.8). However in the fermiophobic limit of model I, a tree level unitarity bound can be easily obtained for V_B [25]

$$m_{h^0}^2 = m_{A^0}^2 - 2(\lambda_+ - \lambda_1)v^2 \cos^2\beta \quad (3.4)$$

we see that if we assume $\beta \approx \pi/2$ then $m_{h^0}^2 \approx m_{A^0}^2$. As for the potential V , Ref. [46] estimates that in the decoupling limit the introduction of unitarity implies for the heavy Higgs bosons to be nearly degenerate.

However, it should be pointed out that tree level unitarity is only a guide, its violation could imply a strongly interacting Higgs sector. Nevertheless, in that case perturbative arguments become suspect.

It has also been mentioned that flavor changing neutral currents impose strong constraints on the 2HDM, since the introduction of the second doublet produces them automatically. These rare processes can be suppressed on either theoretical or phenomenological grounds. The most common theoretical mechanism consists of the imposition of a Z_2 symmetry (or a global $U(1)$ symmetry) as discussed in section (2.2.3) generating the models type I and II. Nevertheless, there are also some theoretical considerations that permits us to avoid FCNC in the type III model. Two interesting scenarios for a flavor conserving type III model deserves special attention. 1) A model type III with a permutation symmetry among the fermion families [22], and 2) the decoupling limit of the 2HDM type III [46]. Let us discuss them briefly.

The motivation for introducing the S_3 permutation symmetry, comes from the similarity among the fermion families. Since there are not fermion masses before the SSB of the gauge symmetry, it is logical to assume that before the SSB the three generations of fermions are indistinguishable i.e. they hold an S_3 symmetry. After the SSB of the gauge symmetry, fermions acquire masses i.e. distinguishability, thus the S_3 symmetry should be spontaneously broken as well. The implementation of such permutation symmetry conduces automatically to the suppression of FCNC at tree level [22], but also leads to a 3×3 unit CKM matrix. Notwithstanding, Ref. [22] showed that by introducing an appropriate soft breaking term, we could still get a flavor conserving type III model while obtaining a reasonable CKM matrix.

As for the decoupling limit, Ref. [46] shows that this particular scenario automatically suppress both FCNC and CP violating couplings in the 2HDM type III. More details about the decoupling limit will be discussed in Sec. (3.2.2).

Furthermore, renormalization group equations could be utilized to obtain some useful constraints. For instance, we can demand that the self interacting parameters in the Higgs potential remain perturbative up to a large scale (typically the grand unification scale i.e. $\Lambda_{GUT} \sim 10^{16}$ GeV), and also that the vacuum of the potential remains stable up to such large scale. In SM such bounds have been studied at first by Cabibbo *et. al.* [13] and Lindner [14]. The criterium of perturbativity provides an upper limit of the SM Higgs mass of about 180 GeV when the cut-off scale is taken to be $\Lambda_{GUT} \sim 10^{16}$ GeV. Meanwhile, vacuum stability provides a lower limit of about 130 GeV [15], for the same cut-off. On the other hand, if the cut-off scale is extended up to the Planck scale $\Lambda_{Planck} \sim 10^{19}$ GeV, the allowed interval becomes $145 \text{ GeV} \lesssim m_h \lesssim 175 \text{ GeV}$ [16], therefore perturbativity and vacuum stability requirements gives a rather strong allowed interval for the Higgs mass in SM. As for the 2HDM, Ref. [15] has examined the constraints coming from perturbativity and vacuum stability up to the grand unification scale in the type II version without the soft breaking term in the potential. Such reference found that these criteria impose an upper limit for the charged Higgs of $m_{H^\pm} \lesssim 150$ GeV which is in conflict with the lower bound for it $m_{H^\pm} \gtrsim 500$ GeV¹. Consequently, the 2HDM type II (without the soft breaking term) cannot be valid up to the unification scale. In contrast, model I is not excluded by these criteria, since the experimental lower limit for m_{H^\pm} is significantly milder.

We should remark however that bounds from perturbativity and vacuum stability from the electroweak (EW) scale up to any cut-off scale is only a guidance, if they are not accomplished it merely means that the model is only valid up to a lower scale (or that it belongs to a non-perturbative regime). Indeed, we can reverse the problem and check until what scale might our model be valid. For instance, Ref. [16] have calculated lower and upper bounds of m_{h^0} in the context of the 2HDM types I and II but including the soft breaking term in the potential. These bounds are estimated as a function of the cutoff scale and also of the soft breaking term of the discrete

¹At the time of ref [15], the lower bound was significantly smaller $m_{H^+} \gtrsim 165$ GeV, but enough for the conflict to arise.

symmetry, requiring that the running coupling constants neither blow up nor fall down below Λ . Comparing with the corresponding SM constraints, the upper bound does not change so much but the lower bound is substantially reduced. In particular, in the decoupling limit with a large soft breaking term, the upper bound for the 2HDM for $\Lambda_{Planck} = 10^{19}$ GeV, and $m_t = 175$ GeV, is about 175 GeV, which is basically the same as the corresponding SM upper bound. By contrast, the corresponding lower bound for the 2HDM is about 100 GeV while the SM bound is about 145 GeV. In the region of small soft breaking term the lower and upper bounds depend on the soft-breaking mass and when the soft breaking term vanishes, the lower bound no longer appears [16].

Finally, perturbativity could be also examined at a fixed scale (typically the electroweak one) to bound the free parameters of the model at that scale. For example, perturbative constraints at the EW scale [45] on the λ_i restrict the allowed values of $\tan \beta$, from these grounds it is found that $\tan \beta \geq 30$ is strongly disfavoured [44].

3.2 Phenomenological constraints

Let us discuss radiative corrections to ρ first. There are different renormalization schemes, Marciano and Sirlin [48] maintain the relation $m_W = m_Z \cos \theta_W$ and radiative corrections appear in the relation between G_F and m_W . In the Veltman scheme [49], the free parameters of the electroweak theory are g , $\sin \theta_W$ and m_W . The effective one loop value for m_Z^2 is extracted from $\bar{\vartheta}_\mu e$ and $\vartheta_\mu \bar{e}$ at one loop, and writing them in the tree level form with a corrected m_Z value. From the Veltman scheme the one loop correction $\Delta \rho$ is written as

$$m_W^2 \Delta \rho = A_{WW} (k^2 = 0) - \cos^2 \theta_W A_{ZZ} (k^2 = 0) \quad (3.5)$$

A_{VV} are the propagator corrections at zero momentum transfer.

In the R -gauge, the terms that could be quadratically dependent on the Higgs boson masses come from diagrams with either two Higgs bosons or a Higgs boson and a Goldstone boson, as well as associated tadpole type diagrams.

The contribution of the Higgs sector in the R -gauge in the 2HDM type

II is given by [17]

$$\begin{aligned}
A_{WW}^{HH}(0) - \cos^2 \theta_W A_{ZZ}^{HH}(0) &= \frac{g^2}{64\pi^2} \left\{ F_{\Delta\rho}(m_{H^+}^2, m_{A^0}^2) + [F_{\Delta\rho}(m_{H^+}^2, m_{H^0}^2) \right. \\
&\quad \left. - F_{\Delta\rho}(m_{A^0}^2, m_{H^0}^2)] \sin^2(\beta - \alpha) \right. \\
&\quad \left. + [F_{\Delta\rho}(m_{H^+}^2, m_{h^0}^2) \right. \\
&\quad \left. - F_{\Delta\rho}(m_{A^0}^2, m_{h^0}^2)] \cos^2(\beta - \alpha) \right\} \\
A_{WW}^{HG}(0) - \cos^2 \theta_W A_{ZZ}^{HG}(0) &= \frac{g^2}{64\pi^2} \cos^2(\beta - \alpha) \left[F_{\Delta\rho}(m_W^2, m_{H^0}^2) \right. \\
&\quad \left. - F_{\Delta\rho}(m_W^2, m_{h^0}^2) - F_{\Delta\rho}(m_Z^2, m_{H^0}^2) \right. \\
&\quad \left. - F_{\Delta\rho}(m_Z^2, m_{h^0}^2) + F_{\Delta\rho}(m_Z^2, m_{h^0}^2) \right] \quad (3.6)
\end{aligned}$$

where $F_{\Delta\rho}(m_1^2, m_2^2)$ is defined as

$$F_{\Delta\rho}(m_1^2, m_2^2) \equiv \frac{1}{2} (m_1^2 + m_2^2) - \frac{m_1^2 m_2^2}{m_1^2 - m_2^2} \ln \frac{m_1^2}{m_2^2} \quad (3.7)$$

Notwithstanding, we should be careful in removing the contribution from the SM Higgs, a natural approach could be to take h^0 as the SM Higgs with modified couplings, and extract the contribution of h^0 with SM couplings.

Since $m_W \sim m_Z$ the HG (Higgs-Goldstone) contribution is very small. While the HH contribution could be large depending upon the mixing angles and masses. From expressions (3.5-3.7) it is easy to check that $\Delta\rho$ depends basically on the splitting between m_{H^+} and m_{A^0} as well as from the splitting of m_{H^+} with the CP even Higgses. Combined experimental measurements on neutral currents of $\sin^2 \theta_W$, m_Z and m_W , imply that the charged Higgs mass cannot be much larger than the neutral Higgs mass (except if the Higgs is SM like). There are some bounds about the splitting between m_{H^0} and m_{H^+} . In SUSY a very natural scenario consists of $m_{H^0} \sim m_{A^0} \sim m_{H^+}$ with a SM like h^0 Higgs. The term $F_{\Delta\rho}(m_{H^+}^2, m_{A^0}^2)$ vanishes in this case and the other terms tend to be cancelled by the small splitting of $m_W \sim m_Z$, then these contributions are expected to be small in SUSY scenarios. Notice that $A_{ZZ}(0)$ tends to cancel the otherwise large $A_{WW}(0)$ contribution.

For the model type I, the contribution to $\Delta\rho$ has been estimated in the

unitary gauge [50]

$$\begin{aligned}\Delta\rho &= \frac{1}{16\pi^2 v^2} [\sin^2(\beta - \alpha) F(m_{H^\pm}, m_{A^0}^2, m_{H^0}^2) \\ &\quad + \cos^2(\beta - \alpha) F(m_{H^\pm}, m_{A^0}^2, m_{h^0}^2)] \\ F(a, b, c) &\equiv a + \frac{bc}{b-c} \ln \frac{b}{c} - \frac{ab}{a-b} \ln \frac{a}{b} - \frac{ac}{a-c} \ln \frac{a}{c}\end{aligned}$$

In the case of model type I, if a light h^0 Higgs still exists, the variation of $\Delta\rho$ with h^0 is soft, but it depends on m_{A^0} and $m_{A^0} - m_{H^\pm}$ (or m_{H^\pm} and $m_{A^0} - m_{H^\pm}$). Once again, $\Delta\rho$ can be used to restrict the splitting between the charged Higgs and neutral Higgs bosons. Ref [51] shows that in the general 2HDM when m_{A^0} is small, the contribution to $\Delta\rho$ can grow quadratically with the other Higgs masses, so in order to keep $\Delta\rho$ small, a correlation among the Higgs boson masses to cancel this large loop contributions should be assumed. Ref [52] presents constraints in the framework of the general 2HDM with a very light CP-odd scalar, these bounds are shown in a $m_H - m_{H^+}$ plane for three different values of $\sin^2(\beta - \alpha)$, constraining strongly the splitting between such scalars.

Other observables useful to constrain the 2HDM are $Br(b \rightarrow s\gamma)$, the $Z \rightarrow b\bar{b}$ hadronic decay branchig ratio (R_b), the forward backward asymmetry of the bottom quark in Z decays (A_b); and the muon anomalous magnetic moment of the muon, a_μ . The effectiveness of each observable to constrain the model depend on the specific scenario, for instance, when $\tan\beta$ is of the order of 1 the asymmetry A_b is less effective to constrain in the $m_{H^+} - \tan\beta$ plane than R_b [52]. The anomalous magnetic moment of the muon a_μ is a very important parameter to restrict any physics beyond the SM, in particular the 2HDM. Since much of our analysis is based on this observable, we shall revise its present status in section 4.1. For now, I just say that its present world average experimental value is given by [68]

$$a_\mu^{\text{exp}} \equiv \frac{(g-2)_\mu^{\text{exp}}}{2} = 11\,659\,203\,(8) \times 10^{-10}$$

and the SM estimation has been calculated recently by a variety of authors [70], though their estimations are rather different, all of them coincide in the fact that the SM value based on $e^+e^- \rightarrow \text{hadrons}$ data, is roughly 3σ below the present world average measurement (see details in section 4.1). Thus, the theoretical and experimental current estimations seem to show the necessity

of new physics. The fact that Δa_μ should be positive at 95% CL, impose strong restrictions to any physics beyond the SM.

On the other hand, bounds on the 2HDM might also be extracted from the non-observation of direct Higgs production and/or decays. For instance, in scenarios with a very light CP odd Higgs boson constraints can be derived from $Br(\Upsilon \rightarrow A^0\gamma)$, $Z \rightarrow AAA$, $f(f')\bar{f} \rightarrow Z(W^\pm)AA \rightarrow Z(W^\pm) + \gamma\gamma$ and $f\bar{f} \rightarrow H^+H^- \rightarrow Z(W^+W^-) + \gamma\gamma$ [52]. Similar decays with A^0 replaced by h^0 can be used to bound scenarios with a very light CP even Higgs boson. For intermediate Higgs bosons, limits could be derived from the non observations of processes like $e^+e^- \rightarrow Z^* \rightarrow Zh^0$, and in the heavy regime from processes like $h^0 \rightarrow ZZ \rightarrow \text{leptons}$.

Further, as well as constraining the model it is necessary to explore the possibility to produce the Higgs bosons from colliders. The expected observed production rate is usually very model dependent and, of course depend also on the experimental luminosity and detector efficiency.

At e^+e^- machines production mechanisms depend upon substantial VV couplings. The most advantageous scenario for these machines would be a roughly equally VV couplings for both scalars, if one of the Higgses tend to saturate these couplings (as in MSSM) then the discovery of the weak coupled Higgs would be problematical in e^+e^- machines. A^0 is particularly problematical in these colliders since it is not coupled to VV , the main production mode that is available is $e^+e^- \rightarrow Z^* \rightarrow A^0h^0$ or A^0H^0 . The cross sections of these processes are proportional to $\cos^2(\beta - \alpha)$, $\sin^2(\beta - \alpha)$ for h^0, H^0 respectively. Detection might be possible if $m_{A^0} + m_{h^0}$ (or $m_{A^0} + m_{H^0}$) is not too large compared to the machine energy, and the vertex $Z A^0(h^0) H^0$ is a saturating coupling. Further, if h^0, A^0 are sufficiently light, they may be produced with a Z on shell and the production rate would be higher. With sufficiently high energy, the heavy states can be produced via $e^+e^- \rightarrow H^+H^-$ or $e^+e^- \rightarrow H^0A^0$. We should notice that modes in which one or both Higgses go to ee are difficult to detect because of the QED background. Prospects for detection of a single Higgs in e^+e^- colliders are $e^+e^- \rightarrow Z \rightarrow Zh^0(A^0)$ where one of the Z 's is off shell. If $m_{h^0} > 2m_Z$ “the gold-plated” detection mode is $h^0 \rightarrow ZZ \rightarrow \text{leptons}$ (for $m_{h^0} \gtrsim 130$ GeV, $h^0 \rightarrow ZZ^*$ could be a signature). In the intermediate mass Higgs regimes other decays are required [66]. With increasing center of mass energy, W^+W^- fusion begins to be the dominant mechanism.

In hadron colliders, the dominant mechanism for Higgs production is the gg fusion through a top quark loop. Important prospects for single Higgs

production are $gg \rightarrow A^0, h^0, H^0$ and $gb \rightarrow H^-t$. An interesting method could be from $gg \rightarrow Q\bar{Q}'(H^0, A^0, H^\pm)$ where Q is a heavy quark (b or t) and the Higgs decays into a Heavy quark pair. Another interesting source is the quarkonium decay to $h\gamma$ which could be enhanced or suppressed according to the model. Indirect signatures could be given by ${}^3S_1(t\bar{t}) \rightarrow b\bar{b}$, the SM contributions come from W exchange, but in two doublets a H^+ could be placed wherever the W^+ is. So alterations of the rate could be detected especially if $\tan\beta < 1$ so that the $t\bar{b}H^+$ coupling is enhanced. Many other quarkonium decays can be a direct source for Higgs boson pairs. Some of them take into account exotic quarks with new CKM elements.

Another possibility is the $\gamma\gamma$ collider mode via $\gamma\gamma$ fusion (dominated by ρW^- or $t\bar{t}$ loop), depending on the mass of the Higgs in the final state decay.

On the other hand, muon muon colliders offer interesting perspectives for Higgs discovery, because Higgs bosons s -channels are enhanced respect to e^+e^- colliders, though still weak (proportional to the muon mass) but production can be significant if the collider is run on the Higgs resonance $\sqrt{s} = m_H$. Further, they could be made feasible to reach energy in the multi-TeV regime. Many references have address the perspective of looking for the Higgs bosons in this kind of machines [21]. In particular, the fourth of Refs. [21] shows that in the large $\tan\beta$ regime, production of a single charged or pseudoscalar Higgs in association with a gauge boson is possible in muon colliders (i.e. $\mu^+\mu^- \rightarrow H^\pm W^\mp, A^0 Z$) with sizeable cross sections whose analogies at e^+e^- would be very small.

As for e^+e^- machines, LEP have obtained limits on the charged Higgs mass from $e^+e^- \rightarrow \gamma^*, Z^* \rightarrow H^+H^-$. It worths to point out that far from the Z mass shell electromagnetic interaction become dominant, thus the bound on m_{H^+} obtained from this process is nearly model independent, LEP excludes a region of $2m_\tau \lesssim m_{H^+} \lesssim 80.5\text{GeV}$. The region $m_{H^+} \lesssim 2m_\tau$ is excluded by the non observation of $B \rightarrow H^+ X_c$. In this region they look for $H^+ \rightarrow \tau\vartheta_\tau$ when $m_{H^+} > m_\tau$.

Some other limits are gotten from some rare decays like $b \rightarrow s\gamma$, $b \rightarrow sg$, $K \rightarrow \pi\vartheta\bar{\vartheta}$. In particular, for the model type II a lower bound of $m_{H^+} \geq 500\text{ GeV}$ at 95% CL is reported based on NLO analysis of the $b \rightarrow s\gamma$ data [67]. Further, as it was mentioned above constraints on the $m_H - m_{H^+}$ plane are obtained based on $\Delta\rho$ and on the $m_{H^+} - \tan\beta$ plane from R_b and A_b [51, 52].

The top and charged Higgs phenomenologies are intimately related. Since the present upper bound of $m_{H^+} \geq 500\text{GeV}$ for model II seems to show

that $m_{H^+} > m_t + m_b$ we shall examine this assumption first. In that case two important scenarios emerge. In the first, $m_{H^+} < m_W + m_{h^0}$ so that $H^+ \rightarrow W^+ h^0$ is forbidden, thus $H^+ \rightarrow t\bar{b}$ dominates fermion modes. But if $H^+ \rightarrow W^+ h^0$ is allowed there is a competition. We get

$$\frac{BR(H^+ \rightarrow W^+ h^0)}{BR(H^+ \rightarrow t\bar{b})} = \frac{2 \cos^2(\beta - \alpha) p_W^2 m_{H^+}^2}{3p_{\bar{b}} M}$$

$$M \equiv [(m_t^2 \cot^2 \beta + m_b^2 \tan^2 \beta) (m_{H^+}^2 - m_t^2 - m_b^2) - 4m_t^2 m_b^2]$$

for H^0 we replace $\cos(\beta - \alpha) \rightarrow \sin(\beta - \alpha)$. So for large m_{H^+} , $H^+ \rightarrow W^+ h^0$ could be important or even dominant for $\cos(\beta - \alpha)$ not too small, because of the availability of longitudinal W 's, if we assume saturation of h^0 i.e. $\cos^2(\beta - \alpha) = 1$, we see that for large m_{H^+} the mechanism $H^+ \rightarrow W^+ h^0$ would be dominant. However for masses accessible to the LEP II $H^+ \rightarrow W^+ h^0$ is smaller than $H^+ \rightarrow t\bar{b}$. Additionally, since the condition $m_t < m_{H^+} + m_b$, is obviously accomplished and taking into account that $t \rightarrow W^+ b$ is the dominant top decay, the off shell contribution of the charged Higgs is very small even for light Higgses; in that case it could be interesting to examine branchings of the type $BR(t \rightarrow H^{*+} b \rightarrow \tau^+ \vartheta_\tau b)$. On the other hand, if $m_{H^+} < m_t + m_b$ and $m_{H^+} < m_W + m_{h^0}$ (as it is still possible in models I and III) only $H^+ \rightarrow \tau^+ \vartheta_\tau$ and $H^+ \rightarrow c\bar{s}$ are relevant. So we examine the ratio of their branchings, in model I this ratio is independent of $\tan \beta$, while in model type II it yields

$$\frac{BR(H^+ \rightarrow \tau^+ \vartheta_\tau)}{BR(H^+ \rightarrow c\bar{s})} = \frac{p_\tau}{3p_c} \frac{m_\tau^2 \tan^2 \beta \cos^2 \theta_c (m_{H^+}^2 - m_\tau^2)}{K}$$

$$K \equiv (m_s^2 \tan^2 \beta + m_c^2 \cot^2 \beta) + (m_{H^+}^2 - m_c^2 - m_s^2) - 4m_c^2 m_s^2 \tan \beta \cot \beta$$

in model I it is $\sim 30\%$ and independent of $\tan \beta$. We should remember that small values of $\tan \beta$ with small values of m_{H^+} are probably excluded by $B_d^0 - \overline{B}_d^0$ mixing. Now, if $t \rightarrow H^+ b$ is allowed, it is very likely that H^+ mass is sufficiently large to produce $H^+ \rightarrow W^+ h^0$. Since $H^+ \rightarrow t\bar{b}$ is not allowed then $H^+ \rightarrow W^+ h^0$ will be dominant because of the $H^+ W^- h^0$ coupling

$((g/2) \cos(\beta - \alpha))$, as long as it is not very suppressed. So a possible scenario for H^- discovery could be $t\bar{t}$ production followed by the conventional $t \rightarrow W^+b$ and $\bar{t} \rightarrow H^-\bar{b} \rightarrow W^-h^0\bar{b}$. Since the h^0 is most likely to decay to $b\bar{b}$, we would have to distinguish between a $W^+b\bar{b}b$ final state from a W^+b final state.

Furthermore, the loop induced $H^+ \rightarrow W^+Z$ decay, though highly suppressed in most of the parameter space, can be significantly enhanced owing to non-decoupling effects of Heavy Higgs bosons on the $H^\pm W^\mp Z$ vertices. As we explained in Sec. (2.2.2), these vertices are forbidden at tree level in multi-Higgs doublet models and in particular in the 2HDM because of the isospin symmetry, but might arise at loop levels due to the breaking of the isospin symmetry through the loop particles. The quark loop contributions for the $H^\pm W^\mp Z$ couplings have been studied in [18]. The full one loop calculation in the 2HDM was carried out in [19], finding that the inclusion of non-decoupling heavy Higgs modes with large mass splitting between H^+ and A^0 could yield a substantial enhancement for the decay width $H^+ \rightarrow W^+Z$ due to the strong breakdown of the custodial $SU(2)_V$ invariance [34] in the Higgs sector. Ref. [19], found that the branching ratio for this decay could reach values up to $10^{-2} \sim 10^{-1}$ for $m_{H^+} = 300$ GeV, giving a detectable mode at LHC or future e^+e^- colliders. On the other hand, Diaz-Cruz *et. al.* [20] studied the same decay with an effective Lagrangian approach, finding a branching ratio enhancement up to about 10^{-1} . Additionally, Ref. [20] also studies the rare decays $H^+ \rightarrow W^+\gamma$, and $H^+ \rightarrow W^+h^0$ with an effective Lagrangian approach, finding that they can have ratios of order 10^{-5} and $O(1)$ respectively. Moreover, the relative behavior among the three decays $H^+ \rightarrow W^+(\gamma, Z, h^0)$ could give clues about the underlying Higgs structure [20].

Since detection of a charged Higgs would be an unambiguous signal of physics beyond the SM, many estimations of the potential of either hadron or electron positron colliders to discover such Higgs boson and its properties have been carried out. The production of charged Higgs at the Tevatron and the LHC proceeds via the partonic processes: $gb \rightarrow tH^+$ and $gg \rightarrow tbH^+$ [53]. Other partonic processes could generate pair production of charged Higgs bosons: $gg(q\bar{q}) \rightarrow H^+H^-$ [54] and $gg(b\bar{b}) \rightarrow H^\pm W^\mp$ [55], notwithstanding $H^\pm W^\mp$ production lead to a much smaller rate at Hadron colliders. At e^+e^- colliders, the main source is $e^+e^- \rightarrow \gamma^*, Z^* \rightarrow H^+H^-$. If the collider energy is not enough for pair production the associated $H^\pm W^\mp$ production becomes dominant if kinematically accessible. This latter possibility has been

studied in Ref. [56], where $H^\pm W^\mp$ production is analyzed in both hadron and e^+e^- colliders in the framework of the MSSM and the general 2HDM. At hadron colliders $H^\pm W^\mp$ final states arise via gg fusion and $b\bar{b}$ annihilation, Ref. [56] found that hadronic cross section in the general 2HDM type II, can be much larger than in the MSSM (about a factor 500-1000!), thus, its discovery at hadron colliders could in addition provide a distinctive signature of the Higgs sector it belongs to. In contrast, for e^+e^- colliders the MSSM signals are considerably higher than for the 2HDM type II (up to two orders of magnitude).

On the other hand, Kanemura *et. al.* [57], showed that there are only two channels that offers an opportunity for single H^\pm detection at e^+e^- colliders for $m_{H^\pm} \gtrsim \sqrt{s}/2$, when $\sqrt{s} = 500$ GeV, (1) the one loop $H^\pm W^\mp$ production discussed above, and (2) the tree level scattering $e^+e^- \rightarrow \tau^-\bar{\nu}_\tau H^+, \tau^+\nu_\tau H^-$. The latter is relevant in the large $\tan\beta$ region while the former is relevant in the small $\tan\beta$ regime. Since the rate of process (1) is rather poor [57], Ref. [58] resort to the dominant decay channel $H^+ \rightarrow t\bar{b}$. Such process has as the main background source, the SM process $e^+e^- \rightarrow t\bar{t} \rightarrow \tau^-\bar{\nu}_\tau t\bar{b}$. It was found that for 1 and 5 ab^{-1} of accumulated luminosity, neither evidence ($\gtrsim 3\sigma$) nor discovery ($\gtrsim 5\sigma$) of charged Higgs bosons is possible if $m_{H^\pm} \gtrsim \sqrt{s}/2$, whereas if $m_{H^\pm} \lesssim \sqrt{s}/2$ the signal should be easily observed.

Further, many of the technics to look for the SM Higgs boson, can be extrapolated to the exploration for neutral Higgs bosons of extended Higgs sectors, if a neutral CP even scalar were discovered a precision test of its couplings to fermions and vector bosons, as well as its self couplings, could give us information on the underlying Higgs structure. Linear colliders (LC) will explore the Higgs structure in case of discovery by precise measurements of the Higgs couplings to fermions and vector bosons. However, the structure of the Higgs potential can only be revealed by measuring the Higgs self couplings. The trilinear Higgs coupling $\lambda_{h^0h^0h^0}$ can be directly measured from $e^+e^- \rightarrow Z^* \rightarrow Z h^0 h^0$ and $e^+e^- \rightarrow W^{+*}W^{-*}\nu\bar{\nu} \rightarrow h^0 h^0 \nu\bar{\nu}$, when the Higgs boson is light [59]. Ref. [60] shows that at e^+e^- colliders with the energy of 500 GeV (3TeV) and the integrated luminosity of 1 ab^{-1} (5 ab^{-1}), $\lambda_{h^0h^0h^0}$ can be measured by about 20% (7%) accuracy for $m_h \sim 120$ GeV. It worths to remark that even in the decoupling limit in which the couplings of h^0 to fermions and vector bosons are SM-like, the one loop corrections to the trilinear self coupling $\lambda_{h^0h^0h^0}$ can undergo a significant deviation from the SM behavior in both the MSSM and the general 2HDM [61]. In particular, they find that quantum corrections can be of the order of 100% in the general

2HDM due to the quartic mass terms of heavier Higgses. In the case of the MSSM they find that the deviation can exceed 5% in light stop scenarios.

The $\tau\bar{\tau}$ decay mode [62] is a promising discovery channel for A^0 and H^0 at the CERN LHC for large $\tan\beta$. On the other hand, the potential of the muon pair channel for MSSM Higgs bosons was studied in [62, 63]. Ref. [64] focus on the potentiality to look for neutral Higgs bosons of the MSSM via $pp \rightarrow b\bar{b}H \rightarrow b\bar{b}\mu\bar{\mu} + X$ at the LHC. He estimated that such process could serve to discover A^0 and H^0 at the LHC with an integrated luminosity of 30 fb^{-1} if $m_{A^0} \lesssim 300 \text{ GeV}$. At a higher luminosity of 300 fb^{-1} , the discovery reach is not expanded much. In addition, the inclusive final state $H \rightarrow \mu\bar{\mu}$ could allow the discovery of A^0 and H^0 at the LHC with an integrated luminosity of 30 fb^{-1} if $m_A \lesssim 450 \text{ GeV}$. At a higher luminosity of 300 fb^{-1} , the discovery region in m_{A^0} increases significantly to $m_A \lesssim 650 \text{ GeV}$ for $\tan\beta = 50$.

In this section we have examined the most hopeful channels for possible direct and indirect detection of the 2HDM Higgs sector. However, the importance of this channels depend strongly on the specific scenario, in what follows we describe some interesting scenarios of the general 2HDM.

3.2.1 The fermiophobic limit

If we take into account the relative Yukawa couplings given in Eqs. (2.34) we can see that in model I the heaviest (lightest) CP even Higgs becomes totally fermiophobic (i.e. all $h f\bar{f}$ couplings vanish) if $\alpha = 0 (\pi/2)$. In contrast, model type II does not exhibit a totally fermiophobic limit for any Higgs boson, see Eqs. (2.37); for instance, if $\alpha = \pi/2$ then $h^0 (H^0)$ become fermiophobic to fermions of up(down)-type, while couplings to the down(up)-type fermions are maximal, the opposite occurs when $\alpha = 0$. On the other hand, in model III, there is still a possible fermiophobic scenario, nevertheless in order for a certain Higgs boson to be totally fermiophobic, a non natural fine tuning must be accomplished²; see details in section (2.2.3).

Consequently, only the model type I provides a natural totally fermiophobic framework. The fermiophobic limit for h^0 ($\alpha = \pi/2$) in the model I can be obtained in the potential V'_A in two ways: $\lambda_+ = 0$, or $v_1 = 0$; the latter assumption leads to a massless h^0 . In potential V_B there is only one

²There are other scenarios with fermiophobic Higgs bosons such as the Higgs triplet model of Refs. [23], and some models with extra dimensions [24]. Ref. [24] shows that the latter can exhibit a more natural fermiophobic limit with less fine tuning.

way: $2v_1v_2\lambda_+ = \frac{1}{2}\mu_3^2$. We have assumed $v_1 < v_2$ but of course we can interchange the role of each VEV. Despite h^0 becomes totally fermiophobic by setting $\alpha = \pi/2$; h^0 can still decay into fermions by the channels $h^0 \rightarrow W^*W (Z^*Z) \rightarrow 2\bar{f}f$ or by means of decays of the type $h^0 \rightarrow \bar{f}f$ through scalar and vector boson loops; the dominant fermionic decay in the fermiophobic limit is $h^0 \rightarrow b\bar{b}$.

If we additionally assume $\alpha - \beta \equiv \delta = 0$ then h^0 becomes bosophobic and ghostophobic as well. Besides, in this scenario A^0, H^\pm are also fermiophobic. In that case, h^0 needs another scalar particle to be able to decay. Moreover, in the 2HDM type I with these assumptions, H^0 acquires the couplings of the SM Higgs. In contrast, the signature of h^0 is model dependent.

Brüicher and Santos [25] shows that in the fermiophobic limit the most important three level decays for h^0 are

$$h^0 \rightarrow WW, ZZ, ZA, WH, AA, H^+H^-$$

and the most important one loop decays are

$$h^0 \rightarrow \gamma\gamma, Z\gamma, b\bar{b}$$

and decays into fermions via virtual vector bosons. The dominance of any of them depend on the parameters of the model, especially on $\delta \equiv \alpha - \beta = \pi/2 - \beta$ see details in Ref. [25]. The fact to emphasize is that the branching fractions depend strongly on the potential chosen and that $h^0 \rightarrow b\bar{b}$ is the fermionic dominant decay. In addition, the decay $h^0 \rightarrow \gamma\gamma$ is always important for light h^0 (and sometimes for intermediate h^0), but for h^0 sufficiently heavy it is suppressed.

As for the pseudoscalar, below the Zh^0 and the $W^\pm H^\mp$ thresholds A^0 decays mainly into fermions, but if $\delta \rightarrow 0$, A^0 becomes stable or decay outside the detector; thus the only signature would be missing energy or momentum. Over the threshold of Zh^0 or $W^\pm H^\mp$ the pseudoscalar Higgs boson decays inside the detector. Finally, the signature of A^0 is the same for both V'_A and V_B .

Now for the charged Higgs boson, if m_{H^\pm} is below m_{W^\pm} the decays are fermionic and independent of δ , but if δ decreases the branching is unchanged while the total decay width decreases (so H^\pm becomes stable), if $m_{H^\pm} \geq m_{W^\pm}$ then $H^\pm \rightarrow W^\pm\gamma$ becomes dominant for tiny δ but for large values the signature is again fermionic, but as soon as $H^\pm \rightarrow W^\pm A^0 (h^0)$ is possible the sum of both becomes dominant, except in the case in which $m_{H^\pm} \geq m_t + m_b$ in

whose case $H^+ \rightarrow t\bar{b}$ will be dominant. In the case of potential V_B below the $W^\pm\gamma$ and above the $W^\pm h^0$ or $W^\pm A^0$ thresholds, the situation is the same as in the potential V_A . But in the regime of $H^\pm \rightarrow W^\pm\gamma$ dominance, the situation depends strongly on the choice of parameters; for instance, when $\delta \rightarrow 0$ the unitarity constraint for V_B given by Eq. (3.4) predicts a degeneracy between m_{A^0} and m_{h^0} ; such degeneracy can suppress $H^\pm \rightarrow W^\pm\gamma$ to a few percent respect to the fermionic decays even above the $m_{H^\pm} \geq m_{W^\pm}$ threshold unlike the case of V'_A .

Finally, H^0 is not fermiophobic in this scenario so the one loop decays are not important, the dominant decay is obviously $H^0 \rightarrow b\bar{b}$ and $H^0 \rightarrow WW$ above the WW threshold like in SM, this situation is the same in both potentials. A difference in signature can only be detected by purely scalar decay modes.

From the experimental point of view, LEP and Tevatron have looked for fermiophobic Higgs bosons. The main channel at LEP has been $e^+e^- \rightarrow h^0Z$, $h^0 \rightarrow \gamma\gamma$ obtaining a lower bound of about 100 GeV [26], the channels $e^+e^- \rightarrow h^0A^0$, $h^0 \rightarrow \gamma\gamma$ and $h^0 \rightarrow WW^*$ have also been considered [26]. As for Tevatron run I, the mechanism used is $qq' \rightarrow V^* \rightarrow h^0V$, $h^0 \rightarrow \gamma\gamma$ and a lower limit of about 80 GeV was obtained [27]. Nevertheless, such limits were obtained assuming that the couplings of the type g_{h^0VV} are of the same order as the ones in SM. Notwithstanding, in the limit of fermiophobia we can see that the relative couplings $\chi_V^{h^0}$ behave like

$$\chi_V^{h^0} \sim \cos^2 \beta = \frac{1}{1 + \tan^2 \beta}$$

therefore, in scenarios with large values of $\tan \beta$ the couplings g_{h^0VV} might be highly suppressed and the bounds described above would not be valid. If it is the case, a light Higgs boson ($h^0 \ll 100$ GeV) could have eluded the LEP and Tevatron constraints and may also escape detection at Tevatron run II [28]. Owing to it, Akeroyd and M. A. Diaz [28], have proposed new production mechanisms at Tevatron run II, they are: (1) $q\bar{q} \rightarrow \gamma^*, Z^* \rightarrow H^+H^-$; (2) $qq' \rightarrow W^* \rightarrow H^\pm h^0$; (3) $qq' \rightarrow W^* \rightarrow H^\pm A^0$; (4) $q\bar{q} \rightarrow Z^* \rightarrow A^0 h^0$.

The subsequent decays $H^\pm \rightarrow h^0W^*$, $A^0 \rightarrow Z^*h^0$, $h^0 \rightarrow \gamma\gamma$ would give rise to $\gamma\gamma\gamma\gamma$ final states very easy to measure accurately. In the fermiophobic scenarios, these new channels are effective even when h^0VV are very suppressed [28]. These mechanisms are complementary to the traditional one $qq' \rightarrow Vh^0$ which could suffer a strong suppression in realistic models. Note

that gluon gluon fussion is not relevant in this framework and that the four additional channels proposed are based on the couplings g_{HHV} .

3.2.2 The decoupling limit

The discussion of the decoupling limit will be given based on the following parametrization of the most general CP invariant potential[46]

$$\begin{aligned} V = & m_{11}^2 \Phi_1^\dagger \Phi_1 + m_{22}^2 \Phi_2^\dagger \Phi_2 - \left[m_{12}^2 \Phi_1^\dagger \Phi_2 + h.c. \right] + \frac{1}{2} \lambda_1 \left(\Phi_1^\dagger \Phi_1 \right)^2 \\ & + \frac{1}{2} \lambda_2 \left(\Phi_2^\dagger \Phi_2 \right)^2 + \lambda_3 \left(\Phi_1^\dagger \Phi_1 \right) \left(\Phi_2^\dagger \Phi_2 \right) + \lambda_4 \left(\Phi_1^\dagger \Phi_2 \right) \left(\Phi_2^\dagger \Phi_1 \right) \\ & + \left\{ \frac{1}{2} \lambda_5 \left(\Phi_1^\dagger \Phi_2 \right)^2 + \left[\lambda_6 \left(\Phi_1^\dagger \Phi_1 \right) + \lambda_7 \left(\Phi_2^\dagger \Phi_2 \right) \right] \Phi_1^\dagger \Phi_2 + h.c \right\} . \end{aligned}$$

In principle m_{12}^2 , λ_5 , λ_6 and λ_7 can be complex, but for simplicity all of them are chosen real. The exploration of the decoupling limit is inspired in the idea that the standard model could be an effective theory embedded in a more fundamental structure characterized by a scale Λ which is supposed to be much larger than the ElectroWeak Symmetry Breaking (EWSB) scale, $v = 246\text{GeV}$. In particular, many models end up in a low energy model with a non-minimal Higgs sector, as is the case of the MSSM whose low energy Higgs sector correspond to that of a 2HDM.

Based on this idea, there are two important scenarios to differenciate in the 2HDM, in the first one there is not a low energy theory containing only one light Higgs boson i.e. no decoupling limit exists. In the second case, the lightest CP even Higgs boson is much lighter than the other Higgs bosons whose masses are of the order of a new scale Λ_{2HDM} . In particular, if $\Lambda_{2HDM} \gg v$ and all dimensionless Higgs self-coupling parameters accomplish the condition $\lambda_i \lesssim O(1)$, then all couplings of the light Higgs are SM-like, the deviations lie on the order of $O(v^2/\Lambda_{2HDM}^2)$, this is called the decoupling limit. What we do in an effective theory is to integrate out the heavy modes; if we believe that the SM is an effective theory of a 2HDM then one of the doublets should be integrated out. Since only one Higgs boson must exist in the low energy theory then the mass of the light Higgs should be of the order of EWSB scale while the heavy scalars masses should be of the order of Λ_{2HDM} . And as the low energy theory only contain one doublet, then h^0 should be indistinguishable from the SM Higgs. For some choices of the scalar potential, no decoupling limit exists. Haber and Gunion [46]

has established that *no decoupling limit exists if and only if* $\lambda_6 = \lambda_7 = 0$ *in the basis where* $m_{12}^2 = 0$. Thus, the absence of a decoupling limit implies a discrete symmetry for the scalar potential (this symmetry could be hidden in other bases). The low energy effective theory reduces the potential to the potential of the SM with all the SM constraints.

When we assume that $m_{h^0} \ll m_{H^0}, m_{A^0}, m_{H^\pm}$ one can simply impose tree level unitarity constraints to the low energy effective scalar theory i.e. to the SM in this case. However, at one loop, the heavier scalars can contribute by virtual exchanges so the restrictions on the self couplings involves all Higgs bosons, to maintain unitarity and perturbativity the splitting of the squared masses among the heavier states should be of order $O(v^2)$ so they should be rather degenerate [46].

In MSSM the decoupling limit is achieved by setting $m_{A^0} \gg m_Z$. However, one loop effects mediated by loops of SUSY particles can generate a deviation from the SM expectations (e.g. light squarks contributions to $h^0 \rightarrow \gamma\gamma, gg$), so to avoid significant SUSY contributions we should assume heavy SUSY particles (say of order 1TeV). If the latter condition is fulfilled, h^0 is SM-like even at one loop level. The leading one loop radiative correction to $g_{h^0 b\bar{b}}$ is of order $O(m_Z^2 \tan \beta / (m_{A^0}^2))$ and formally decouples in the regime in which $m_{A^0}^2 \gg m_Z^2 \tan \beta$ which is more demanding in the case of large $\tan \beta$ regime. This behavior is called delay decoupling in Ref. [47], this phenomenon can also occur in the general 2HDM, with tree level couplings.

In general, the amplitudes of all loop induced processes which involve h^0 and SM particles as external states approaches the SM values whenever $\lambda_i \lesssim O(1)$ and $m_{A^0} \rightarrow \infty$, this is guaranteed by the applequist-Carazzone decoupling theorem.

After describing the framework of the decoupling limit, phenomenological consequences must be discussed. For instance, in the most general Yukawa Lagrangian (model type III) FCNC are generated through the mixing matrices $\xi_{ij}^{U,D}$ and $\eta_{ij}^{U,D}$. These matrices are in general complex and non-diagonal; thus, they could be also a source for CP violating couplings between the neutral Higgs bosons and fermions. Notwithstanding, in the decoupling limit (which correspond to the condition $\cos(\beta - \alpha) = 0$ in the Yukawa Lagrangian), both non-diagonal and CP violating couplings of h^0 vanish (but not for H^0, A^0) and the h^0 couplings to fermions reduces to the SM ones. However, FCNC and CP violating processes mediated by H^0 or A^0 are suppressed by their square masses (relative to v), due to the propagator suppression, and since $\cos(\beta - \alpha) \simeq O(v^2/m_A^2)$ the suppression factor is roughly

the same for h^0, H^0, A^0 . Therefore, the decoupling limit is a natural mechanism to suppress Higgs mediated FCNC and to suppress Higgs mediated CP violating couplings in the most general 2HDM. Additionally, all vertices containing at least one vector boson and exactly one of the heavy Higgs states are proportional to $\cos(\beta - \alpha)$ and hence vanish in the decoupling limit.

Nevertheless, Ref. [46] shows that there are some alternative scenarios in which $\cos(\beta - \alpha) = 0$, but all Higgs bosons masses are of $O(v)$, although h^0 is SM-like, there is not an effective theory with only one light Higgs. Radiative corrections introduce in this case significant deviation respect to the tree-level h^0 behavior.

The scenario in which $\sin(\beta - \alpha) = 0$, is usually called the non-decoupling regime, since h^0 couplings deviate maximally from SM, while H^0 ones are SM-like.

Now the following question arise, if only one CP even Higgs boson were discovered, how could we distinguish whether this scalar belongs to the minimal Higgs sector of the SM or to a non minimal Higgs sector?. Far from the decoupling limit, the deviation from the coupling of the Higgs boson to fermions and gauge bosons (respect to the ones in SM) could provide the answer. However, in the decoupling regime couplings of this Higgs boson are similar to the SM ones and the discrimination becomes problematic; in that case there are two alternatives: (1) Direct production of heavy states and (2) High precision measurements of the couplings of the light Higgs to look even for tiny deviations.

As for the first alternative, at the LHC $gg \rightarrow A^0, H^0$ and $gb \rightarrow H^-t$ signatures could be suppressed in the decoupling scenario. In addition, the branching $H^0 \rightarrow ZZ$ which is the gold plated in SM is almost absent in this regime. An interesting method could be from $gg \rightarrow Q\bar{Q}'(H^0, A^0, H^\pm)$ where Q is a heavy quark (b or t) and the Higgs decays into a Heavy quark pair because these couplings are not suppressed in the decoupling limit. In e^+e^- colliders with sufficiently high energy the heavy states can be produced via $e^+e^- \rightarrow H^+H^-$ or $e^+e^- \rightarrow H^0A^0$ without a rate suppression, the mechanism $e^+e^- \rightarrow Z \rightarrow h^0A^0$ discussed in section (3.2) is suppressed by $\cos(\beta - \alpha)$. These production mechanisms requires very high \sqrt{s} since they involve a pair of heavy states. Another possibility is to consider the production of one heavy state in association with light states (the light Higgs and the top quark are considered light states), however this option seems to be hopeless[46].

On the other hand, for the second alternative, one of the most promising channels seems to be $Br(h^0 \rightarrow \bar{b}b)$. Additionally, $\gamma\gamma$ colliders could play an

important role by either measuring the $h^0 \rightarrow \gamma\gamma$ coupling with sufficient precision or directly producing A^0 and/or H^0 in $\gamma\gamma$ fusion, only the latter is viable in the decoupling regime. Finally, as it was pointed out by Kanemura *et. al.* [61], another promising coupling to distinguish the underlying Higgs structure could be the trilinear self coupling $\lambda_{h^0 h^0 h^0}$ which has been estimated to be very sensitive to the introduction of new physics in both the 2HDM type II and the MSSM, see discussion in Sec. (3.2).

3.2.3 Scenarios with a light Higgs boson

As we saw above, SM estimation of the muon anomalous magnetic moment differs from the experimental measurement by about 3σ deviations. In the SM the Higgs contribution to a_μ is negligible since it is proportional to the factor m_μ^2/m_h^2 , and the present SM Higgs mass limit provided by LEP is $m_h \gtrsim 114.4$ GeV. If we believe that an extended Higgs sector provides the necessary enhancement to get a value of the $(g-2)_\mu$ compatible with experimental measurement, we should examine possible factors to generate such enhancement. In a general 2HDM with no FCNC, it might occur due to two factors. First, an increment on the $h^0 \mu^+ \mu^-$ coupling proportional to $\tan\beta$, and second owing to the possibility of a light Higgs boson arising from the suppression of the vertex $h^0 ZZ$ from which the LEP bound could be avoided. The total enhancement at one loop level would be of the order of [71]

$$\frac{m_\mu^2}{m_{h^0}^2} \tan^2 \beta \ln \left(\frac{m_\mu^2}{m_{h^0}^2} \right) \quad (3.8)$$

The couplings of $h^0 ZZ$ and $h^0 A^0 Z$ for the 2HDM read

$$g_{h^0 ZZ} = \frac{gm_Z \sin(\beta - \alpha)}{\cos \theta_W} ; \quad g_{h^0 AZ} = \frac{g \cos(\beta - \alpha)}{2 \cos \theta_W}$$

so we can evade the LEP constraint by assuming $\sin(\beta - \alpha) \simeq 0$, i.e. a non decoupling scenario, in that case, a light CP even scalar can be considered. Exploration of light scalar and pseudoscalar modes has been studied by a variety of authors [24, 52, 71, 72]. In general, one light Higgs boson is necessary in the 2HDM type I and II, in order to get a sufficient value of Δa_μ to be compatible with present experimental measurement. M. Krawczyk [72]

explores the possibility of having a light scalar or pseudoscalar Higgs boson in the framework of the 2HDM (II), considering only the case in which the soft breaking term μ_3^2 vanishes. The LEP data allows the existence of a light neutral Higgs in the 2HDM, but not two of them could be light simultaneously [73, 74, 75, 76], the constraints are given in a (m_{h^0}, m_{A^0}) plane and they indicate roughly that $m_{h^0} + m_{A^0} \gtrsim 90$ GeV. On the other hand, the Bjorken process gives an upper limit on the relative coupling $\chi_V^{h^0}$ [72], for instance, it is found that at 95% CL, $\chi_V^{h^0} \ll 1$ for $m_{h^0} \lesssim 50$ GeV. Moreover, the Yukawa couplings $\chi_d^{h^0, A^0}$ are constrained by low energy data coming from $\Upsilon \rightarrow h^0 (A^0) \gamma$ [77, 78] while LEP do it for masses $\gtrsim 4$ GeV. Additionally, the analysis of the decay $Z \rightarrow h^0 (A^0) \gamma$ at LEP [73] gives both the upper and lower limits for $|\chi_d|$.

Assuming that the light Higgs (h^0 or A^0), is the only one contributing at one loop to the muon anomalous magnetic moment, the one loop diagram gives a positive (negative) contribution for $h^0 (A^0)$. However, calculation of the two loops diagram with a charged Higgs in one of the loops produce a contribution that is positive (negative) for $A^0 (h^0)$. Taking into account both contributions Ref. [72] found that the scalar Higgs gives a positive (negative) contribution for m_{h^0} below (above) 5 GeV, while the pseudoscalar gives a positive (negative) contribution for m_{h^0} above (below) 3 GeV.

Constraints from $(g - 2)_\mu$ [70], current upper limits of LEP from the Yukawa processes [76], lower limits from $Z \rightarrow h^0 (A^0) \gamma$ [73], upper 90% CL limits from $\Upsilon \rightarrow h^0 (A^0) \gamma$ and upper limits from the Tevatron [79] are combined to obtain exclusion regions in $m_{h^0} - \tan \beta$ and $m_{A^0} - \tan \beta$ planes. The two loop analysis of [72] shows that light scalars are excluded at 95% CL, but pseudoscalar masses between ~ 25 GeV and 70 GeV with $25 \lesssim \tan \beta \lesssim 115$ are still allowed.

An alternative study of very light pseudoscalar scenarios (of the order of 0.2 GeV) has been carried out in Ref. [52], they show that in the 2HDM type I and II this very light CP-odd scalar can be compatible with the ρ parameter, $\text{Br}(b \rightarrow s\gamma)$, R_b , A_b , $(g - 2)_\mu$ $\text{Br}(\Upsilon \rightarrow A^0 \gamma)$, and direct searches via the Yukawa process at LEP. For a mass of around $m_{A^0} \sim 0.2$ GeV, they got that $\tan \beta \sim 1$ and that A^0 behaves as a CP odd fermiophobic scalar, decaying predominantly into a $\gamma\gamma$ pair. The second of Refs. [52] found that a very light CP odd Scalar can be either allowed or excluded depending on the statistic used for the Hadronic contributions for a_μ . Therefore, a better stabilization of the Hadronic contributions for a_μ^{SM} is necessary to elucidate this point.

Recently, Ref. [24] showed that additional constraints on light pseudoscalars belonging to a 2HDM are obtained from K and B decays. They showed that masses between 100 MeV and 200 MeV might evade such stringent constraints owing to a possible cancellation in the decay amplitude. In that case, the coupling of A^0 to quarks is strong and may produce sufficient pseudoscalar states via photoproduction. This kind of test could be performed by the Jefferson laboratory and Ref. [24] shows the perspective for detection of this modes in this laboratory.

3.2.4 The 2HDM with FCNC

FCNC, general framework

Flavor Changing Neutral Currents (FCNC) are processes highly suppressed by some underlying principle still unknown, despite they seem not to violate any fundamental law of nature. On the other hand, Standard Model (SM) observables are compatible with experimental constraints on FCNC so far, with the remarkable exception of neutrino oscillations [8]. In the case of the lepton sector, the high suppression of FCNC suggested by direct search is “explained” by the implementation of the Lepton Number Conservation (LFC), a new symmetry that protects the phenomenology from these dangerous processes. Notwithstanding, the observation of oscillation of neutrinos [81] coming from the sun and the atmosphere, seem to indicate the existence of such rare couplings. Neutrino oscillations can be explained by introducing mass terms for these particles, in whose case the mass eigenstates are different from the interaction eigenstates. It should be emphasized that the oscillation phenomenon implies that the lepton family number is violated, and such fact leads us in turn to consider the existence of physics beyond the standard model (SM), because in SM neutrinos are predicted to be massless and lepton flavor violating mechanisms are basically absent. These considerations motivate the study of scenarios with Lepton Flavor Violation (LFV).

The original motivation for the introduction of neutrino oscillations comes from the first experiment designed to measure the flux of solar neutrinos [82], such measurement was several times smaller than the value expected from the standard solar model, so Ref. [83] suggested the neutrino oscillation mechanism as a possible explanation of the neutrino deficit problem. In addition, models of neutrino oscillations in matter [84] arose to solve the neutrino deficit confirmed by SuperKamiokande [85]. Since then, further

evidence of solar neutrino oscillations has been found by SuperKamiokande and SNO [86]. Besides, this phenomenon can be inferred from experiments with atmospheric neutrinos as well [8].

On the other hand, since neutrino oscillations imply LFV in the neutral lepton sector, it is generally expected to find out LFV processes involving the charged lepton sector as well. Experiments to look directly for LFV have been performed for many years, all with null results so far, those searches for these processes have only provided some upper limits, some examples are $\mu - e$ conversion in nuclei [87], $\mu \rightarrow eee$ [88], $\mu \rightarrow e\gamma$ [89], and $\mu^- \rightarrow \nu_e e^- \bar{\nu}_\mu$ [90]. In addition, the search for LFV can also be made by analyzing semileptonic decays, upper bounds from LFV meson decays have been estimated, some examples are $K_L^0 \rightarrow \mu^+ e^-$ [91], and $K_L^0 (K^+) \rightarrow \pi^0 (\pi^+) \mu^+ e^-$ [92].

As for experimental perspectives, a muon muon collider could provide very interesting new constraints on FCNC, for example $\mu\mu \rightarrow \mu\tau(e\tau)$ mediated by Higgs exchange [21] which test the mixing between the second and third generations. Additionally, the muon collider could be a Higgs factory and it is well known that the Higgs sector is crucial for FCNC. Several authors have studied the potentiality of $\mu\mu$ colliders as a Higgs factory and as a source of Higgs mediated FCNC [21].

Other interesting perspectives consist of improving the sensitivity of experiments that look for LFV processes. For example, in the case of $\mu \rightarrow e\gamma$, the present upper bound of its branching ratio comes from MEGA collaboration (1.2×10^{-11}) [98]. A new experiment is under construction at PSI whose aim is to improve present bound by about three orders of magnitude [99]. On the other hand, the SINDRUM II experiment at PSI provides the current upper bound of $\mu - e$ conversion branching ratio (6.1×10^{-13}) [100]. The MECO experiment at BNL [101] is planned to analyse such conversion in aluminum nuclei with a sensitivity below 10^{-16} . In addition, the PRISM project [102] aims to improve upper limits for $\mu \rightarrow e\gamma$, and $\mu - e$ conversion in nuclei, by one or two orders of magnitude.

Another possible source to study LFV is by means of lepton flavor violating decays of a Higgs, in Higgs factories. In particular, the Fermilab Tevatron and the CERN Large Hadron Collider have the potentiality to study LFV Higgs boson decays such as $h \rightarrow \tau\mu$ [64, 65].

From the theoretical point of view, the phenomenon of LFV has been widely studied in different scenarios such as Two Higgs Doublet Models, Supersymmetry, Grand Unification, effective theories, leptoquark models, technicolor, Superstrings and SM extensions with heavy neutrinos [93]. For

instance, LFV processes in SU(5) SUSY models with right-handed neutrinos have been examined based on recent results of neutrino oscillation experiments [94]. On the other hand, Ref. [95] discuss how the supersymmetric SM with a see-saw mechanism could face the flavor problem; in particular, current constraints on the leptonic soft supersymmetry breaking terms and possible improvement on those constraints are studied in this reference. Moreover, Grimus *et. al.* [96] explores the generation of LFV by using a multi-Higgs doublet model with additional right-handed neutrinos for each lepton generation, finding a non-decoupling behavior of some LFV amplitudes respect to the right-handed neutrino masses.

Further, Babu and Pakvasa [97], studied the $\Delta L = 2$ process $\mu^+ \rightarrow e^+ \bar{\nu}_e \bar{\nu}_i$ ($i = e, \mu, \tau$), in an effective Lagrangian approach showing that it can explain the neutrino anomaly reported by the LSND experiment. Ref. [97], found two effective operators in SM that lead to such decays and no other processes. These operators arise from integrating out scalar fields with LFV interactions.

In addition, Cvetic *et. al.* [42], studied lepton flavor violation in tau decays induced by heavy Majorana neutrinos within two models (1) the SM with additional right-handed heavy Majorana neutrinos which is a typical see-saw model; and (2) the SM with left-handed and right-handed neutral singlets. The first of these models predicts very small branching ratios of the LFV tau decays considered, in most of the parameter space. Unlike the second of these models, which might show large enough branching ratios for such decays to be tested in near future experiments.

Now, since there are interesting perspectives to improve the experimental sensitivity for the LFV processes $\mu \rightarrow e\gamma$, and $\mu \rightarrow e$ conversion in nuclei. It might also be interesting to check for theoretical predictions for them coming from different scenarios. Both processes might occur in many models with LFV. Nevertheless, the simple see-saw neutrino model does not induce experimentally observable rates for the $\mu \rightarrow e\gamma$ decay [103]. But in the case of SUSY models the rate for this decay can be significant owing to the production of LFV processes by means of one loop diagrams of sleptons. Particularly interesting are SUSY models with R -parity broken because LFV interactions could arise even at tree level [104]. The branching ratios of LFV processes has been calculated for a variety of models such as SUSY-GUTs and SUSY models with right-handed neutrinos [105]. These references show that the branching ratios for $\mu \rightarrow e\gamma$, and $\mu - e$ conversion could get values near to the observable threshold in forthcoming experiments.

The $\mu - e$ conversion rate in nuclei, has been calculated by a variety of authors with a variety of approaches [106]. In particular, Kitano *et. al.* [103] have evaluated the $\mu - e$ conversion by using the method of Czarnecki *et. al.* [106]. These calculations were carried out for nuclei in a wide range of atomic numbers with an effective theory approach. In general they found that the conversion branching ratios grow along with the atomic number (Z) up to $Z \sim 30$, those branching ratios become the largest for $Z \sim 30 - 60$, and decrease for heavy nuclei $Z \gtrsim 60$. Though this tendency is general, the Z dependence on conversion rates is significantly different for several LFV couplings. Therefore, the atomic number dependence of the conversion branching ratio could be useful to discriminate among the theoretical models with LFV. Additionally, the conversion rate also depends on proton and neutron densities for each nucleus, Ref. [103] uses several models for proton and neutron density distributions (see appendix A on that reference), finding a reasonable agreement among them.

In general, many extensions of the SM permit FCNC at tree level. The introduction of new representations of fermions different from doublets produce them by means of the Z-coupling [107]. In addition, they are generated at tree level in the Yukawa sector by adding a second doublet to the SM [9]. Such couplings also appear in SUSY theories with R-parity broken [108], because FCNC coming from R-parity violation generates massive neutrinos and neutrino oscillations [109]. In this work we shall concentrate on the FCNC arising from the general 2HDM. For other scenarios with FCNC, I refer the reader to the literature [80, 107, 108].

On the other hand, scenarios with FCNC in the lepton sector automatically generates FCNC in the quark sector as well, experimental bounds on FCNC in the quark sector come from $\Delta F = 2$ processes, rare B-decays, $Z \rightarrow \bar{b}b$ and the ρ -parameter [31]. Reference [31] also explored the implications of FCNC at tree level for $e^+e^- (\mu^+\mu^-) \rightarrow t\bar{c} + \bar{t}c$, $t \rightarrow c\gamma (Z, g)$, $D^0 - \bar{D}^0$ and $B_s^0 - \bar{B}_s^0$. Moreover, there are other important processes involving FCNC. For instance, the decay $B^-(D^-) \rightarrow K^-\mu^+\tau^-$ which depends on $\mu - \tau$ mixing and vanishes in the SM. Another one is $B^-(D^-) \rightarrow K^-\mu^+e^-$ whose form factors have been calculated in [4], [110].

As explained above, FCNC in the lepton sector are basically absent in the SM. On the other hand, in the quark sector FCNC are very tiny because they are prohibited at the tree level and are further suppressed at one loop by the GIM mechanism [6]. Consequently, SM provides a hopeless framework

for this rare processes since predictions from it, are by far out of the scope of next generation colliders [31]. So detection of these kind of events in near future experiments in either the lepton or quark sector, would imply the existence of new Physics.

Since FCNC are strongly constrained by experimental data, several mechanism to avoid potentially larger contribution to these exotic processes have been developed. For instance, Glashow and Weinberg [30] proposed a discrete symmetry in the Two Higgs Doublet Model (2HDM) which forbids the couplings that generate such rare decays, hence they do not appear at tree level. This discrete symmetry led to the so called 2HDM type I and II discussed in section (2.2.3). Another possibility is to consider heavy exchange of scalar or pseudoscalar Higgs fields [4] or by cancellation of large contributions with opposite sign. Another mechanism was proposed by Cheng and Sher arguing that a natural value for the FC couplings from different families should be of the order of the geometric average of their Yukawa couplings [5]. On the other hand, the possibility of having a flavor conserving type III model at the tree level has been considered in Ref. [22] by demanding an S_3 permutation symmetry on the fermion families, see details in Sec. (3.1). Finally, as dicussed in Sec. (3.1), the decoupling limit provides another natural scenario for suppression of both FCNC and CP violating couplings in the 2HDM type III.

FCNC in the 2HDM

Although FCNC in SM are very suppressed because of the GIM mechanism, FC transitions involving down-type quarks get enhanced because of the presence of a top quark in the loop. In contrast, transitions involving up-type quarks are usually very small. Therefore in SM processes like $b \rightarrow (s, d) \gamma$, $K - \overline{K}^0$, $B - \overline{B}^0$; are more interesting than for example $t \rightarrow c(\gamma, Z)$, $D - \overline{D}^0$. However, by introducing FCNC at tree level (as is the case of the 2HDM type III) transitions like $t \rightarrow c(\gamma, Z)$ could be enhanced too, giving a clear signal of new physics [31, 35].

In e^+e^- colliders a very interesting FCNC reaction is $e^+e^- \rightarrow t\bar{c}$. Its signature would be very clear and could compensate the lower statistics respect to hadron colliders. This process can proceeds by a Higgs in the s –channel at the tree level, and at one loop via corrections to the Ztc , γtc vertices.

The former is negligible and only the latter have to be considered. Defining

$$R^{tc} \equiv \frac{\sigma(e^+e^- \rightarrow t\bar{c} + \bar{t}c)}{\sigma(e^+e^- \rightarrow \gamma^* \rightarrow \mu^+\mu^-)}$$

and using the following parametrization for the mixing matrix elements

$$\xi_{ij} = \lambda_{ij} \frac{\sqrt{m_i m_j}}{v}$$

Atwood *et. al.* [31] found that assuming $\lambda_{tt} = \lambda_{ct} \equiv \lambda$, values of R^{tc}/λ^4 up to 10^{-5} are reached at $\sqrt{s} = 400 - 500 \text{ GeV}$ and that not much is gained for larger values of \sqrt{s} .

The decay $t \rightarrow c\gamma$ is highly suppressed in SM since the GIM mechanism suppresses it strongly owing to the smallness of the quarks running into the loop (down type quarks) and also because of the large tree level rate $t \rightarrow bW$. This process as well as the processes $t \rightarrow c(Z, g)$ can be substantially enhanced in model type III respect to SM and also respect to type I and type II [31, 35].

Due to the great agreement between *SM* and experimental determination of the mass difference in the $K - \bar{K}^0$, and $B_d - \bar{B}_d^0$ systems, any tree level contribution from elementary flavor changing couplings needs to be strongly suppressed. This was the original motivation to impose the discrete symmetry given in Ref. [30] on the 2HDM. If we were to work on a model with FCNC a very usual assumption is that $\xi_{ij} = \lambda_{ij} \frac{\sqrt{m_i m_j}}{v}$ [5]. If we assume that all λ_{ij} are equal in the quark sector then $\Delta F = 2$ mixing imposes severe constraints to the common λ . If on the other hand, we assume that the mixings involving the first family are negligible then these processes do not place further constraints on the remaining *FC* couplings, allowing quite strong mixing between the second and third family [31]. Finally, further constraints coming from R_b seems to indicate that $\lambda_{bb} \gg 1$, $\lambda_{tt} \ll 1$ and $\lambda_{sb} \gg 1$, $\lambda_{ct} \ll 1$. i.e. only the down sector of the second and third family is strongly mixed. Disregarding constraints coming from R_b the latter assumptions are not necessary and the assumption of negligible mixing with the first family is compatible with constraints given by processes like $Br(B \rightarrow X_s \gamma)$ and the ρ parameter. In general, the mixing between the second and third generation of down-type quarks stays almost unconstrained, for example the contribution of new Physics for $\Gamma(b \rightarrow sc\bar{c})$ is appreciably smaller than SM one for $\lambda_{sb} < 40$, i.e. in a large range of values.

As for the lepton sector, FCNC (i.e. LFV processes) in extended Higgs sectors have been analyzed by several authors [4, 15, 37, 38, 39, 121]. Nie and Sher examined the contribution on a_μ from Higgs mediated FCNC coming from a very general model with extended Higgs sector. They found that those contributions can be significantly enhanced if the mass of the scalar is light enough [15], and obtained a bound on $\xi_{\mu\tau}$ from a_μ by assuming that the heavier generations have larger flavor changing couplings [5]. Kang and Lee [121], got constraints on some LFV couplings ($\xi_{\tau\tau}$, $\xi_{e\tau}$, $\xi_{\mu\tau}$, $\xi_{\mu\mu}$, $\xi_{e\mu}$, ξ_{ee}), in the framework of a general extended Higgs sector by means of the $g-2$ muon factor and several LFV decays. These limits are gotten by setting the lightest scalar mass as $m_{h^0} = 100$ GeV, 1000 GeV, and assuming that the other Higgs bosons are decoupled. On the other hand, Ref. [38] provides bounds on the mixing vertices ($\xi_{\tau\tau}$, $\xi_{e\tau}$, $\xi_{\mu\tau}$, $\xi_{\mu\mu}$) in the framework of the 2HDM type III, by a similar approach but sweeping a wide region of the free parameters of the model. For instance, since the contribution of the scalars and the pseudoscalar have opposite signs, those limits could change significantly if the pseudoscalar Higgs is not decoupled. Specifically, Ref. [38] shows that lower limits on $\xi_{\mu\tau}^2$ are obtained by using light values of the pseudoscalar Higgs boson, while upper limits are found by using scenarios with very heavy pseudoscalar, details in next chapter. Finally, Diaz *et. al.* [39] have found the constraint $|\xi_{\mu e}/m_{H^+}| \leq 3.8 \times 10^{-3} \text{GeV}^{-1}$, based on the flavor changing charged current decay $\mu \rightarrow \nu_e e \bar{\nu}_\mu$. Despite the bound is not so strong, it should be pointed out that it is independent on the other parameters of the model, so improvements on the upper limit of $\mu \rightarrow \nu_e e \bar{\nu}_\mu$ could provide very useful information on $\xi_{\mu e}$.

Chapter 4

Flavor Changing Neutral Currents in the Lepton Sector of the 2HDM (III)

Having motivated the study of Higgs mediated FCNC in the previous chapter, we shall concentrate on the lepton sector of the 2HDM type III henceforth. Now, since neutrino oscillations seem to indicate the existence of Lepton Flavor Violation (LFV) in the neutral lepton sector; we shall consider the possibility of having LFV couplings in the form of either FCNC in the charged sector, or Flavor Changing Charged Currents (FCCC) between the charged and neutral sector.

For easy reference, I write the Yukawa Lagrangian type III Eq. (2.39) in the fundamental parametrization, for the lepton sector only

$$\begin{aligned}
 -\mathcal{L}_Y = & \overline{E} \left[\frac{g}{2M_W} M_E^{diag} \right] E (\cos \alpha H^0 - \sin \alpha h^0) \\
 & + \frac{1}{\sqrt{2}} \overline{E} \xi^E E (\sin \alpha H^0 + \cos \alpha h^0) \\
 & + \overline{\vartheta} \xi^E P_R E H^+ + \frac{i}{\sqrt{2}} \overline{E} \xi^E \gamma_5 E A^0 + h.c.
 \end{aligned} \tag{4.1}$$

In order to get information on LFV couplings in the 2HDM type III, we shall use the following observables: the anomalous magnetic moment of the muon $(g-2)_\mu$ and the LFV decays: $\mu \rightarrow e\gamma$, $\mu \rightarrow eee$, $\tau \rightarrow eee$, $\tau \rightarrow \mu\mu\mu$, $\tau \rightarrow e\gamma$, $\tau \rightarrow \mu\gamma$, $\mu^- \rightarrow \nu_e e^- \overline{\nu}_\mu$.

In general, the muon anomalous magnetic moment a_μ , is one of the most important observables to constrain contributions coming from new Physics. Since, it is perhaps the most important source to obtain our bounds, we shall make a brief survey on the present status of its experimental and theoretical estimations.

4.1 Brief survey on $(g - 2)_\mu$

The first study of g -factors of subatomic particles was realized by Stern in 1921 [111], the famous Stern Gerlach experiment was done in 1924 [112] the conclusion was that the magnetic moment of the electron was one Bohr magneton i.e. that the gyromagnetic ratio g was 2. This gyromagnetic factor is the proportionality constant between the magnetic moment and the spin,

$$\vec{\mu} = g \left(\frac{e}{2m} \right) \vec{s}$$

the discovery that $g_e \neq 2$ [113] and the calculation by Swinger [114] was one of the great success of quantum electrodynamics. Additionally the long lifetime of the muon allows a precision measurement of its anomalous magnetic moment at ppm level. The anomalous muon magnetic moment is given by

$$\mu_\mu = (1 + a_\mu) \frac{e\hbar}{2m_\mu} \quad a_\mu \equiv \frac{g - 2}{2}$$

A series of experiments to evaluate a_μ were carried out at CERN [115]. Nowadays, an ongoing experiment at BNL has been running with much higher statistics and a very stable magnetic field in its storage ring [116]. By combining CERN and BNL statistics the present world average result is [68]

$$a_\mu^{\text{exp}} \equiv \frac{(g - 2)_\mu^{\text{exp}}}{2} = 11\,659\,203 (8) \times 10^{-10}$$

the ultimate goal of the E821 experiment at BNL is to reduce present uncertainty by a factor of two.

In the framework of the SM, theoretical predictions of a_μ comes from QED, electroweak, and hadronic contributions

$$a_\mu = a_\mu^{\text{QED}} + a_\mu^{\text{EW}} + a_\mu^{\text{Had}}$$

a_μ^{QED} constitute the bulk of the SM contributions ($11\,658\,470.57 \times 10^{-10}$) and its uncertainty is small (2.9×10^{-11}) [117], the EW contribution is small (152.0×10^{-11}) and it is known with a similar accuracy (4.0×10^{-11}) [118], noteworthy, the EW contribution has the same order of magnitude as the current experimental uncertainty. Hadronic contributions are the second largest ones ($\sim 7000 \times 10^{-11}$) [69, 70] and their uncertainty constitutes the bulk of the uncertainty contributions ($\sim 70.7 \times 10^{-11}$).

As for the hadronic contributions, the most important ones in terms of both contributions to a_μ and its uncertainties are the leading vacuum polarization terms, they have been estimated recently by a set of authors [70]. The first of Refs. [70] has used the most recent data on hadron production from e^+e^- collisions from BES, CMD-2, and SND [119]. The HMNT group (see fourth of Refs. [70]) has made estimations based on both inclusive and exclusive analysis of $e^+e^- \rightarrow \text{hadrons}$. Combining such exclusive and inclusive sets of data, they obtain a more optimum estimate, and evaluate QCD sum rules in order to solve a discrepancy between the inclusive and exclusive analysis. In addition, the second and third Refs. [70] presents an analysis based on e^+e^- data as well as τ hadronic decays data. All of Refs. [70] found that analysis based on $e^+e^- \rightarrow \text{hadrons}$, predicts a SM value which is roughly 3σ below the present world average measurement, however, the second and third of Refs. [70] have showed that data based on hadronic τ decays only differs with the experimental world average by about 1.6σ . Stabilization of the predictions coming from e^+e^- based data and τ decays data is necessary in order to say something definitive. For our purposes we shall use the estimation given by Jegerlehner [70] whose analysis is based on e^+e^- data by taking the most recent results from CMD-2 [119]. Furthermore, other important contribution is the light by light scattering whose sign has been corrected recently [69].

On the other hand, it is important to emphasize that despite the measurement of the muon anomalous magnetic moment of the muon is about 180 times less accurate than the electron anomalous magnetic moment; the former is more sensitive to new physics by a factor of $\sim (m_\mu^2/m_e^2)$, this factor more than compensates the difference in precision. Therefore, a_μ is more important than a_e in looking for new physics.

In constraining the 2HDM type III we shall use the estimation for Δa_μ at 95% CL reported by [72]

$$9.38 \times 10^{-10} \leq \Delta a_\mu \leq 51.28 \times 10^{-10} \quad (4.2)$$

which in turn are based on preliminary results by Jegerlehner [70].

4.2 The $(g - 2)_\mu$ factor in the 2HDM type III

The first one loop electroweak corrections for a_μ coming from new Physics (Δa_μ) were calculated in Refs. [120]. For Δa_μ the integral expression [17] is given by

$$\begin{aligned}\Delta a_\mu &= \sum_S I_S + \sum_P I_P, \\ I_{S(P)} &= C_{S(P)}^2 \frac{m_\mu^2}{8\pi^2} \int_0^1 \frac{x^2 (1 - x \pm m_\tau/m_\mu)}{m_\mu^2 x^2 + (m_\tau^2 - m_\mu^2) x + M_{S(P)}^2 (1 - x)} dx\end{aligned}\quad (4.3)$$

where $I_{S(P)}$ is an integral involving an Scalar (Pseudoscalar) Higgs boson with mass $M_{S(P)}$, and $C_{S(P)}$ is the corresponding coefficient in the Yukawa Lagrangian Eq. (4.1). If we assume that $m_\mu^2 \ll m_\tau^2$ and $m_\mu^2 \ll m_{h^0, H^0, A^0}^2$ in the calculation of (4.3), the one loop contribution from all neutral Higgs bosons reads [37]

$$\begin{aligned}\Delta a_\mu &= \frac{m_\mu m_\tau}{16\pi^2} \left\{ \left[\sum_S C_S^2 \left(F(M_S) - \frac{m_\mu}{3m_\tau} G(M_S) \right) \right] + \right. \\ &\quad \left. \left[\sum_P C_P^2 \left(F(M_P) + \frac{m_\mu}{3m_\tau} G(M_P) \right) \right] \right\}\end{aligned}\quad (4.4)$$

where

$$\begin{aligned}G(M) &\equiv \frac{2 + 3\widehat{M}^2 + 6\widehat{M}^2 \ln(\widehat{M}^2) - 6\widehat{M}^4 + \widehat{M}^6}{M^2 (1 - \widehat{M}^2)^4} \\ F(M) &\equiv \frac{\left[3 + \widehat{M}^2 (\widehat{M}^2 - 4) + 2 \ln(\widehat{M}^2) \right] \widehat{M}}{M^2 (1 - \widehat{M}^2)^3} \\ \widehat{M} &\equiv \frac{m_\tau}{m_H}\end{aligned}\quad (4.5)$$

We have neglected the contribution of the charged Higgs boson because of two reasons [37]: on one hand this contribution involves the neutrino mass and on the other hand, the CERN e^+e^- collider LEP bound on its mass is $m_{H^+} \geq 80.5$ GeV.

4.3 Lepton Flavor Violating decays

As we explained below, some lepton flavor violating decays are useful to constrain the 2HDM type III. The relevant expressions of the lepton decays involved at leading order are given by [38]:

$$\begin{aligned}\Gamma(\tau \rightarrow l\gamma) &= \xi_{l\tau}^2 \frac{G_F \alpha_{em} m_\tau^5}{4\pi^4 \sqrt{2}} R(m_{H^0}, m_{h^0}, m_{A^0}, \alpha, \xi_{\tau\tau}) , \\ \Gamma(\mu \rightarrow e\gamma) &= \xi_{\mu\tau}^2 \xi_{e\tau}^2 \frac{\alpha_{em} m_\tau^4 m_\mu}{16\pi^4} S(m_{H^0}, m_{h^0}, m_{A^0}, \alpha, \xi_{\tau\tau}) .\end{aligned}\quad (4.6)$$

where $l \equiv e, \mu$ denotes a light charged lepton. In addition, we have defined

$$\begin{aligned}R(m_{H^0}, m_{h^0}, m_{A^0}, \alpha, \xi_{\tau\tau}) &= \left| \left(m_\tau \sin 2\alpha + \frac{\sqrt[4]{2} \xi_{\tau\tau} \sin^2 \alpha}{\sqrt{G_F}} \right) \frac{\ln [m_{H^0}/m_\tau]}{m_{H^0}^2} \right. \\ &\quad \left. - \left(m_\tau \sin 2\alpha - \frac{\sqrt[4]{2} \xi_{\tau\tau} \cos^2 \alpha}{\sqrt{G_F}} \right) \frac{\ln [m_{h^0}/m_\tau]}{m_{h^0}^2} \right. \\ &\quad \left. - \frac{2\sqrt[4]{2} \xi_{\tau\tau} \ln [m_{A^0}/m_\tau]}{\sqrt{G_F} m_{A^0}^2} \right|^2 , \\ S(m_{H^0}, m_{h^0}, m_{A^0}, \alpha, \xi_{\tau\tau}) &= \left| \sin^2 \alpha \frac{\ln [m_{H^0}/m_\tau]}{m_{H^0}^2} + \cos^2 \alpha \frac{\ln [m_{h^0}/m_\tau]}{m_{h^0}^2} \right. \\ &\quad \left. + \frac{\ln [m_{A^0}/m_\tau]}{m_{A^0}^2} \right|^2 .\end{aligned}\quad (4.7)$$

On the other hand, the expression for a lepton L going to three leptons of the same flavor l is given by

$$\begin{aligned}\Gamma(L \rightarrow \bar{l}ll) &= \frac{m_L^5}{2048\pi^3} \left[\sin 2\alpha \sqrt{\frac{G_F}{\sqrt{2}}} \left(\frac{1}{m_{H^0}^2} - \frac{1}{m_{h^0}^2} \right) m_l \right. \\ &\quad \left. + \xi_{ll} \left(\frac{\sin^2 \alpha}{m_{H^0}^2} + \frac{\cos^2 \alpha}{m_{h^0}^2} - \frac{1}{m_{A^0}^2} \right) \right]^2 .\end{aligned}\quad (4.8)$$

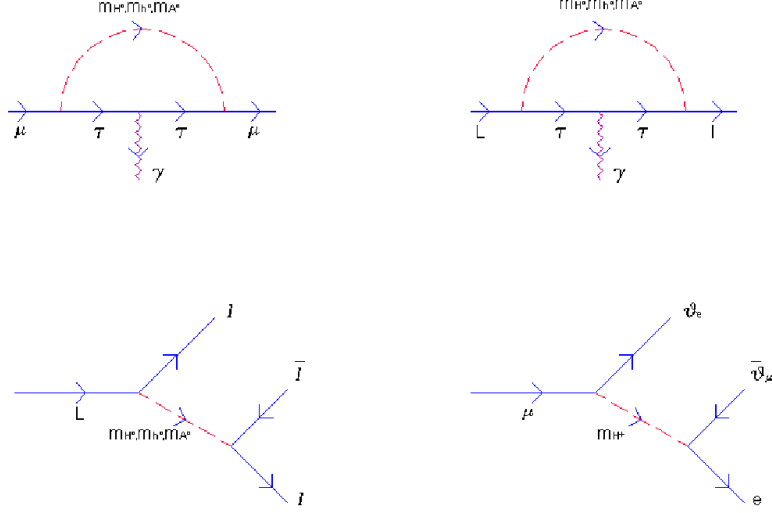


Figure 4.1: Leading order diagrams for the processes: $(g - 2)_\mu$ (top left), $L \rightarrow l\gamma$ (top right), $L \rightarrow \bar{l}l$ (bottom left), and $\mu^- \rightarrow \vartheta_e \bar{\vartheta}_\mu e^-$ (bottom right). In the two former, we have neglected the contribution of the charged Higgs and a neutrino into the loop.

Finally, the decay width for $\mu^- \rightarrow \nu_e e^- \bar{\nu}_\mu$, reads

$$\Gamma(\mu^- \rightarrow \nu_e e^- \bar{\nu}_\mu) = \frac{m_\mu^5}{24576\pi^3} \left(\frac{\xi_{\mu e}}{m_{H^+}} \right)^4 \quad (4.9)$$

the latter is a process with Flavor Changing Charged Currents (FCCC) mediated by a charged Higgs boson as we see in figure (4.1).

In calculating Δa_μ and the leptonic decays of the type $L \rightarrow l\gamma$, we neglect the contribution of light leptons into the loop, so only the contribution with a tau into the loop is considered, see figure (4.1).

4.4 Obtaining the bounds for the flavor changing vertices

From the previous section, we see that the free parameters that we are involved with, are: the three neutral Higgs boson masses ($m_{h^0}, m_{H^0}, m_{A^0}$), the mixing angle α , and some flavor changing vertices ξ_{ij} . Based on the present

	Bounds on $\xi_{\mu\tau}^2$	Bounds on $\xi_{e\tau}^2 \xi_{\mu\tau}^2$	Bounds on $\xi_{e\tau}^2$
case 1	$7.62 \times 10^{-4} \lesssim \xi_{\mu\tau}^2 \lesssim 8.31 \times 10^{-3}$	$\xi_{e\tau}^2 \xi_{\mu\tau}^2 \lesssim 7.33 \times 10^{-18}$	$\xi_{e\tau}^2 \lesssim 4.82 \times 10^{-15}$
case 2	$1.29 \times 10^{-3} \lesssim \xi_{\mu\tau}^2 \lesssim 4.42 \times 10^{-2}$	$\xi_{e\tau}^2 \xi_{\mu\tau}^2 \lesssim 2.24 \times 10^{-16}$	$\xi_{e\tau}^2 \lesssim 2.77 \times 10^{-14}$
case 3	$1.53 \times 10^{-3} \lesssim \xi_{\mu\tau}^2$	$\xi_{e\tau}^2 \xi_{\mu\tau}^2 \lesssim 2.24 \times 10^{-16}$	$\xi_{e\tau}^2 \lesssim 2.76 \times 10^{-14}$
case 4	$9.57 \times 10^{-4} \lesssim \xi_{\mu\tau}^2 \lesssim 1.40 \times 10^{-2}$	$\xi_{e\tau}^2 \xi_{\mu\tau}^2 \lesssim 2.10 \times 10^{-17}$	$\xi_{e\tau}^2 \lesssim 8.22 \times 10^{-15}$
case 5	$1.02 \times 10^{-3} \lesssim \xi_{\mu\tau}^2 \lesssim 1.66 \times 10^{-2}$	$\xi_{e\tau}^2 \xi_{\mu\tau}^2 \lesssim 2.93 \times 10^{-17}$	$\xi_{e\tau}^2 \lesssim 9.65 \times 10^{-15}$

Table 4.1: Constraints on the mixing parameters $\xi_{\mu\tau}^2$, $\xi_{e\tau}^2 \xi_{\mu\tau}^2$ and $\xi_{e\tau}^2$ for the five cases mentioned in the text. The two former are generated from Δa_μ and $\Gamma(\mu \rightarrow e\gamma)$ respectively, while the latter comes from the combination of the lower limit on $\xi_{\mu\tau}^2$ and the upper bound on $\xi_{e\tau}^2 \xi_{\mu\tau}^2$.

bounds from LEP2 we shall assume that $m_{h^0} \approx 115$ GeV. In addition, we shall assume that $m_{A^0} \gtrsim m_{h^0}$, both assumptions will be held throughout this section. Now, since we are going to consider plots in the $\xi_{ij} - m_{A^0}$ plane, we should manage to use appropriate values of (m_{H^0}, α) in order to sweep a wide region of parameters. To sweep a reasonable set of this pair of parameters we utilize for m_{H^0} values of the order of 115 GeV (light), 300 GeV (intermediate), and very large masses (heavy). As for the angle α , we consider values of $\alpha = 0$ (minimal mixing), $\alpha = \pi/4$ (intermediate mixing), and $\alpha = \pi/2$ (maximal mixing). It can be seen that all possible combinations of (m_{H^0}, α) could be done by considering five cases 1) when $m_{H^0} \simeq 115$ GeV; 2) when $m_{H^0} \simeq 300$ GeV and $\alpha = \pi/2$; 3) when m_{H^0} is very large and $\alpha = \pi/2$; 4) when $m_{H^0} \simeq 300$ GeV and $\alpha = \pi/4$; 5) when m_{H^0} is very large, and $\alpha = \pi/4$. In all these cases the mass of the pseudoscalar will be considered in the range 115 GeV $\lesssim m_{A^0}$.

It is worthwhile to remark that these five cases cover all possible combinations of (m_{H^0}, α) , with the three different values for m_{H^0} (115 GeV, 300 GeV, and very heavy) and the three different values for α ($0, \pi/4, \pi/2$), though at the first glance some cases seem to miss. For example, in the first case we have $m_{H^0} \simeq m_{h^0}$. In this scenario, all the processes that we calculate become independent on α and therefore no distinction is necessary among the three different values of it. The cases a) $m_{H^0} = 300$ GeV, with $\alpha = 0$; and b) m_{H^0} very large, with $\alpha = 0$; are also included in case 1, because when $\alpha = 0$ the processes in the previous section does not depend on m_{H^0} .

The first bounds come from Δa_μ . We use the estimated value of it, given by [72] at 95% C.L. Eq. (4.2). Since Δa_μ in Eq. (4.2) is positive, lower and upper bounds for the FC vertex $\xi_{\mu\tau}$ can be gotten at 95% C.L. The results are indicated in table (4.1) column 1. The lower bounds in each case are obtained when $m_{A^0} \approx 115$ GeV, and using the minimum value of Δa_μ in Eq. (4.2), while the upper bounds are obtained when A^0 is very heavy, and using the maximum value of Δa_μ in Eq. (4.2). From these results a quite general and conservative allowed interval can be extracted [38]

$$7.62 \times 10^{-4} \lesssim \xi_{\mu\tau}^2 \lesssim 4.44 \times 10^{-2}. \quad (4.10)$$

Furthermore, upper bounds for the product $\xi_{\mu\tau}^2 \xi_{e\tau}^2$ are obtained from the expression of the decay width $\Gamma(\mu \rightarrow e\gamma)$ in Eq. (4.6) and from the experimental upper limit $\Gamma(\mu \rightarrow e\gamma) \leq 3.6 \times 10^{-30}$ GeV [122]. The most general upper bounds are obtained for A^0 very heavy. The results are shown in table (4.1) column 2. From this table we infer that quite generally the bound is [38]

$$\xi_{e\tau}^2 \xi_{\mu\tau}^2 \lesssim 2.24 \times 10^{-16} \quad (4.11)$$

Moreover, combining these upper limits with the lower bounds on $\xi_{\mu\tau}^2$ given in the first column of table (4.1), we find upper limits on $\xi_{e\tau}^2$. The results appear on table (4.1) third column, and the general bound can be written as

$$\xi_{e\tau}^2 \lesssim 2.77 \times 10^{-14}. \quad (4.12)$$

Noteworthy, these constraints predict a strong hierarchy between the mixing elements $\xi_{\mu\tau}$ and $\xi_{e\tau}$ i.e. $|\xi_{e\tau}| \ll |\xi_{\mu\tau}|$ and they differ by at least five orders of magnitude.

On the other hand, from Eq. (4.6) we see that the decay widths $\Gamma(\tau \rightarrow \mu\gamma)$ and $\Gamma(\tau \rightarrow \mu\mu\mu)$ depend on two mixing vertices $\xi_{\mu\tau}^2, \xi_{\tau\tau}$ and $\xi_{\mu\tau}^2, \xi_{\mu\mu}$ respectively. Then, we can get conservative constraints on the diagonal mixing vertices $\xi_{\tau\tau}, \xi_{\mu\mu}$ by using once again the lower bounds on $\xi_{\mu\tau}^2$ obtained from Δa_μ . Since $\Gamma(\tau \rightarrow \mu\gamma)$, and $\Gamma(\tau \rightarrow \mu\mu\mu)$ are rather complicate functions of $\xi_{\tau\tau}$, and $\xi_{\mu\mu}$ respectively, we present these constraints in the form of contour-plots in the $m_{A^0} - \xi_{\tau\tau}$ plane and the $m_{A^0} - \xi_{\mu\mu}$ plane, figures 4.2 and 4.3, each one for the five cases.

We can check that for each contourplot there is a value of m_{A^0} for which $\xi_{\tau\tau}$ or $\xi_{\mu\mu}$ stays unconstrained, and they are shown in tables 4.2, and 4.3

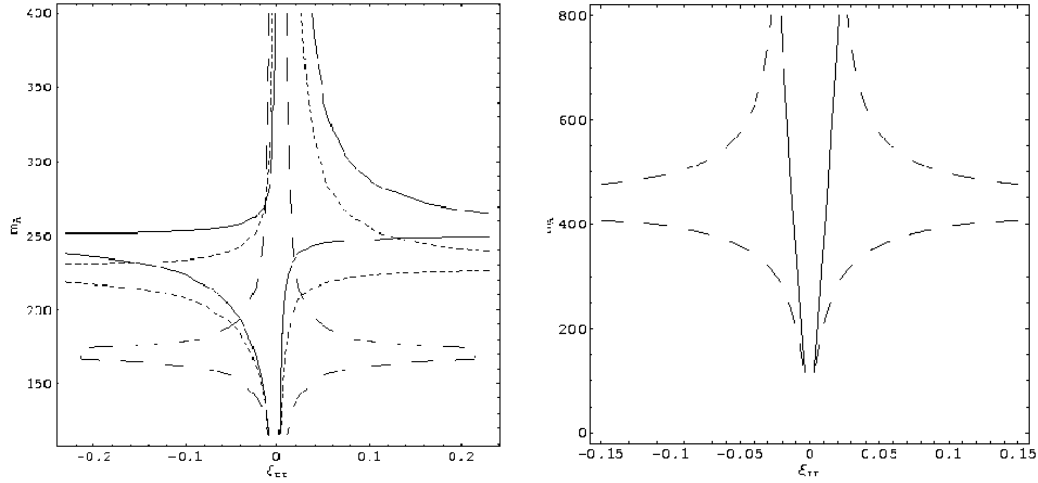


Figure 4.2: Contourplots in the $\xi_{\tau\tau} - m_{A^0}$ plane for each of the five cases cited in the text. On left: case 1 corresponds to the long-dashed line, case 4 to the short-dashed line, and case 5 to the solid line. On right: case 2 corresponds to dashed line, and case 3 is solid line.

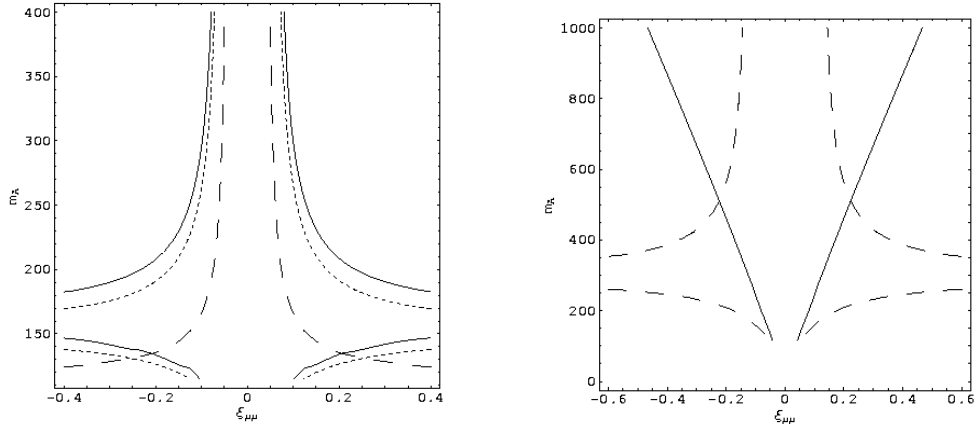


Figure 4.3: Contourplots in the $\xi_{\mu\mu} - m_{A^0}$ plane for each of the five cases cited in the text. On left: case 1 corresponds to the long-dashed line, case 4 to the short-dashed line, and case 5 to the solid line. On right: case 2 corresponds to dashed line, and case 3 is solid line.

respectively. Additionally, the bounds for $\xi_{\tau\tau}$, $\xi_{\mu\mu}$ when m_{A^0} is very large and when $m_{A^0} \approx 115$ GeV are also included in tables 4.2, 4.3 respectively. We see that the general constraints for $\xi_{\tau\tau}$ read

$$\begin{aligned} -1.8 \times 10^{-2} &\lesssim \xi_{\tau\tau} \lesssim 2.2 \times 10^{-2}, \text{ for } m_{A^0} \text{ very large} \\ -1.0 \times 10^{-2} &\lesssim \xi_{\tau\tau} \lesssim 1.0 \times 10^{-2}, \text{ for } m_{A^0} \approx 115 \text{ GeV} \end{aligned} \quad (4.13)$$

These constraints are valid for all cases, except for the third case with m_{A^0} very large, since in that scenario $\xi_{\tau\tau}$ remains unconstrained. Now, for $\xi_{\mu\mu}$ the general bounds read

$$\begin{aligned} |\xi_{\mu\mu}| &\lesssim 0.12, \text{ for } m_{A^0} \text{ very large} \\ |\xi_{\mu\mu}| &\lesssim 0.13, \text{ for } m_{A^0} \approx 115 \text{ GeV} \end{aligned} \quad (4.14)$$

Once again these constraints are not valid for the third case when m_{A^0} is very large, but are valid in all the other cases.

We should remember that the diagonal mixing vertices generate differences among the relative couplings in model type III, and that this lack of universality could be a distinctive signature for it. This fact might lead us to scenarios in which a certain Higgs boson (say h^0) may be tau-phobic¹ but not muon-phobic or electron-phobic (see section 2.2.3).

We also ought to remember that in model type III, the pseudoscalar Higgs boson couples to fermions only by means of the matrix element ξ_{ff} , while in models I and II it couples through the mass of the corresponding fermion. Therefore in model III, if $\xi_{ff} = 0$ for a certain specific fermion, then A^0 becomes fermiophobic to it (and only to it).

At this step, it is important to remark that our bounds are compatible with all tau-phobic limits for each Higgs boson. It is easy to check that h^0 becomes tau-phobic if $\xi_{\tau\tau} = 0$ for $\alpha = 0$, and if $\xi_{\tau\tau} \simeq 0.01$ for $\alpha = \pi/4$; for $\alpha = \pi/2$ there is not tau-phobic limit. On the other hand, H^0 becomes tau-phobic if $\xi_{\tau\tau} = 0$ for $\alpha = \pi/2$, and if $\xi_{\tau\tau} \simeq -0.01$ for $\alpha = \pi/4$; and there is no tau-phobic limit for $\alpha = 0$. The tau-phobic limit for the pseudoscalar is the simplest one, $\xi_{\tau\tau} = 0$. Finally, if $\xi_{\tau\tau} = 0$ and $\alpha = 0$ ($\pi/2$) then A^0 and h^0 (H^0) become tau-phobic simultaneously.

On the other hand, bounds given above could in contrast produce a significant enhancement to the Yukawa couplings. As a matter of example, in

¹With the tau-phobic limit for certain Higgs, we mean that the coupling of that Higgs to a pair of tau leptons vanishes. Nevertheless, the couplings of such Higgs to a tau and any other lepton could exist.

	Values of m_{A^0} for $\xi_{\tau\tau}$ unconstrained	$\xi_{\tau\tau}$ intervals for m_{A^0} very large	$\xi_{\tau\tau}$ intervals for $m_{A^0} \approx 115$ GeV
case 1	$m_{A^0} \approx 170$ GeV	$-0.0072 \lesssim \xi_{\tau\tau} \lesssim 0.0072$	$-0.010 \lesssim \xi_{\tau\tau} \lesssim 0.010$
case 2	$m_{A^0} \approx 440$ GeV	$-0.018 \lesssim \xi_{\tau\tau} \lesssim 0.018$	$-0.0043 \lesssim \xi_{\tau\tau} \lesssim 0.0043$
case 3	—	unconstrained	$-0.0036 \lesssim \xi_{\tau\tau} \lesssim 0.0036$
case 4	$m_{A^0} \approx 228$ GeV	$-0.0075 \lesssim \xi_{\tau\tau} \lesssim 0.022$	$-0.0094 \lesssim \xi_{\tau\tau} \lesssim 0.0036$
case 5	$m_{A^0} \approx 250$ GeV	$0.00024 \lesssim \xi_{\tau\tau} \lesssim 0.021$	$-0.0093 \lesssim \xi_{\tau\tau} \lesssim 0.0026$

Table 4.2: Bounds extracted from the contourplots shown in Fig. 4.2. The first column indicates the values of m_{A^0} for which $\xi_{\tau\tau}$ stays unconstrained for each of the five cases. The second and third columns show the allowed intervals on $\xi_{\tau\tau}$ when m_{A^0} is very large and when $m_{A^0} \approx 115$ GeV respectively.

	Values of m_{A^0} for $\xi_{\mu\mu}$ unconstrained	$\xi_{\mu\mu}$ intervals for $m_A \gg m_{h^0}$	$\xi_{\mu\mu}$ intervals for $m_{A^0} \approx 115$ GeV
case 1	$m_{A^0} \approx 115$ GeV	$ \xi_{\mu\mu} \lesssim 0.043$	unconstrained
case 2	$m_{A^0} \approx 300$ GeV	$ \xi_{\mu\mu} \lesssim 0.12$	$ \xi_{\mu\mu} \lesssim 0.055$
case 3	—	unconstrained	$ \xi_{\mu\mu} \lesssim 0.043$
case 4	$m_{A^0} \approx 152$ GeV	$ \xi_{\mu\mu} \lesssim 0.058$	$ \xi_{\mu\mu} \lesssim 0.13$
case 5	$m_{A^0} \approx 163$ GeV	$ \xi_{\mu\mu} \lesssim 0.061$	$ \xi_{\mu\mu} \lesssim 0.11$

Table 4.3: Bounds extracted from the contourplots shown in Fig. 4.3. The first column indicates the values of m_{A^0} for which $\xi_{\mu\mu}$ stays unconstrained for each one of the five cases. The second and third columns show the allowed intervals on $\xi_{\mu\mu}$ when m_{A^0} is very large and when $m_{A^0} \approx 115$ GeV respectively.

the case 5 with $\alpha = \pi/4$ using $\xi_{\tau\tau} \approx 0.1$ ² we see that the contribution coming from the term proportional to $\xi_{\tau\tau}$, is about 10 times larger in magnitude than the contribution coming from the term proportional to the tau mass, for both the H^0 and h^0 couplings. So it is even possible for the couplings of the CP -even Higgs bosons to be overwhelmed by the $\xi_{\tau\tau}$ contribution. Of course, since the bounds for $\xi_{\mu\mu}$ are weaker than the constraints on $\xi_{\tau\tau}$ as we can see from Fig. 4.3 and table 4.3, we can also have highly suppressed or highly enhanced Yukawa couplings to a pair of muon fermions.

Based on the bounds obtained above, we are able to estimate upper limits for some leptonic decays by using the expressions (4.6,4.7,4.8). We shall assume that $|\xi_{\tau\tau}| \lesssim 0.1$, and that $|\xi_{ee}| \lesssim 0.1$; from these assumptions we can infer the following upper bounds [38]

$$\begin{aligned}\Gamma(\tau \rightarrow e\gamma) &\lesssim 1.5 \times 10^{-27}, \\ \Gamma(\tau \rightarrow eee) &\lesssim 5 \times 10^{-29}.\end{aligned}\quad (4.15)$$

If we compare with the current experimental upper bounds, [122]

$$\begin{aligned}\Gamma(\tau \rightarrow e\gamma) &\leq 6.12 \times 10^{-18} \\ \Gamma(\tau \rightarrow eee) &\leq 6.57 \times 10^{-18}\end{aligned}$$

We see that these decays are predicted to be very far from the reach of next generation experiments in the context of the 2HDM type III, unless that $\xi_{\tau\tau}$, and/or ξ_{ee} acquire unexpectedly large values, this remarkably strong suppression owes to the dependence of these decays on the mixing vertex $\xi_{e\tau}$. For the sake of comparison, Ref. [42] has obtained upper limits for these decays in the context of two models with heavy Majorana neutrinos: (I) the SM with additional right-handed heavy Majorana neutrinos i.e. a typical see-saw type model and (II) the standard model with right-handed and left-handed neutral singlets. The first of these models predicts very small decay widths for LFV processes in most of the parameter space, but the second one might show large enough decay widths. Namely, the upper limits in the context of the second of these models read [42]

$$\begin{aligned}\Gamma(\tau \rightarrow e\gamma) &\lesssim 2.27 \times 10^{-20} \text{ GeV}, \\ \Gamma(\tau \rightarrow eee) &\lesssim 2.27 \times 10^{-21} \text{ GeV}.\end{aligned}\quad (4.16)$$

²In the case 5 both values $\xi_{\tau\tau} = 0.01$ and $\xi_{\tau\tau} = 0.1$ are allowed at least for m_{A^0} around 250 GeV, as it is shown in Fig. (4.2). However, for a very light ($m_{A^0} \approx 115$ GeV), or a very heavy pseudoscalar Higgs boson ($m_{A^0} >> m_{h^0}$), constraints on $\xi_{\tau\tau}$ are considerably stronger in all cases, see table 4.2.

which are not so far from the present experimental threshold and could be tested by near future experiments, unlike the case of the 2HDM (III). Such fact could be useful to discriminate between these models.

On the other hand, the decay $\mu^- \rightarrow \nu_e e^- \bar{\nu}_\mu$ provides information about the mixing between the first and second lepton family. The leptonic processes analyzed so far, involves FCNC mediated by neutral Higgs bosons. Instead, the process $\mu^- \rightarrow \nu_e e^- \bar{\nu}_\mu$, involves Flavor Changing Charged Currents mediated by a charged Higgs boson. Nevertheless, from Lagrangian (4.1) we see that the matrix elements ξ_{ij}^E that generates FCNC automatically generates FCCC which are strongly suppressed in the leptonic sector. Consequently, by constraining flavor changing charged currents we are indirectly constraining flavor changing neutral currents as well. In the case of the 2HDM (III), interactions involving FCCC at tree level only contains the contribution from the charged Higgs boson, reducing the free parameters to manage. Thus, from the decay width $\Gamma(\mu^- \rightarrow \nu_e e^- \bar{\nu}_\mu)$ we are able to extract a bound for the quotient $\xi_{e\mu}/m_{H^+}$ independent on the other free parameters of the model. Taking the analytical expression for the decay width Eq. (4.9) and the current experimental upper bound for it [122]

$$\Gamma(\mu^- \rightarrow \nu_e e^- \bar{\nu}_\mu) \leq 3.6 \times 10^{-21} \text{ GeV}, \quad (4.17)$$

the following constraint is gotten

$$\left| \frac{\xi_{e\mu}}{m_{H^+}} \right| \leq 3.8 \times 10^{-3} \text{ GeV}^{-1}. \quad (4.18)$$

Despite this constraint is not so strong, it is interesting since it does not depend on the other free parameters of the model, because the calculation does not involve neutral Higgs bosons nor mixing angles. This is a good motivation to improve the experimental upper limit for processes involving FCCC in the leptonic sector.

4.5 Bounds on the Higgs boson masses

In the previous section, we obtained constraints for the mixing vertices based on some sets of values for the Higgs masses. Conversely, we can assume a set of values for the flavor changing vertices and try to get constraints on the Higgs boson masses. We shall do it in the framework of the new parametrization developed in Ref. [36] and in section (2.2.3) of this work. We should

be very careful in interpreting such results because a different basis has been used for the Yukawa Lagrangian. For instance, we shall show allowed regions in the $m_{A^0} - \tan \beta$ plane by using fixed values for $\tilde{\xi}_{\mu\tau}$, m_{H^0} , m_{h^0} . However, we ought to bear in mind that $\tilde{\xi}_{\mu\tau}$ depends explicitly on $\tan \beta$ as we see in Eqs. (2.50), checking Eqs. (2.50) we see that the only way to keep $\tilde{\xi}_{\mu\tau}$ fixed with changing $\tan \beta$, is by varying the $\xi_{\mu\tau}$ parameter of the fundamental parametrization; applying the last of Eqs. (2.50) to the vertex $\xi_{\mu\tau}$ we get

$$\xi_{\mu\tau} = \left(\sqrt{1 + \tan^2 \beta} \right) \tilde{\xi}_{\mu\tau} \quad (4.19)$$

so by using a fixed value of $\tilde{\xi}_{\mu\tau}$ and varying $\tan \beta$ (say from 0 to N), what we are really doing from the point of view of the fundamental parametrization, is sweeping $\xi_{\mu\tau}$ from $\tilde{\xi}_{\mu\tau}$ to $\sqrt{1 + N^2} \tilde{\xi}_{\mu\tau}$. In addition, we should take into account that $\alpha' = \alpha + \beta$; Therefore, if we want to keep α' constant as well, α should be varied accordingly. Consequently, to vary $\tan \beta$ while keeping fixed $\tilde{\xi}_{\mu\tau}$ and α' , it is necessary to vary the parameters $\xi_{\mu\tau}$ and α in the fundamental parametrization³. It should be pointed out then, that changing $\tan \beta$ would imply a correlation among the variation of α and $\xi_{\mu\tau}$ which is not a necessary condition. A more appropriate picture would be fixing $\tan \beta$ (the basis) and use the other parameters as variables. Notwithstanding, we shall show some plots in the $m_{A^0} - \tan \beta$ plane, assuming that correlation.

The possibility of plotting in a $m_{A^0} - \tan \beta$ plane for the model type III, facilitates the comparison of the model type III with the models type I or II.

With this clarification we proceed to constrain the FC vertex involving the second and third charged leptonic sector by using the estimated value for Δa_{μ}^{NP} . Additionally, we get lower bounds on the Pseudoscalar Higgs mass by taking into account the lower experimental value of Δa_{μ}^{NP} at 95% CL reported in [72] and making reasonable assumptions on the FC vertex.

For easy reference, I include the Yukawa Lagrangian type III for the leptonic sector by using parametrizations of type I and II explained in section

³We can assume another point of view in which $\tan \beta$ and α' are changed in such a way that only $\xi_{\mu\tau}$ varies in the fundamental parametrization. But it implies to work with an additional variable in the non-trivial parametrization.

(2.2.3).

$$\begin{aligned}
-\mathcal{L}_{Y(E)}^{(I)} = & \frac{g}{2M_W \sin \beta} \overline{E} M_E^{diag} E (\sin \alpha' H^0 + \cos \alpha' h^0) \\
& + \frac{ig}{2M_W} \overline{E} M_E^{diag} \gamma_5 E G^0 + \frac{ig \cot \beta}{2M_W} \overline{E} M_E^{diag} \gamma_5 E A^0 \\
& - \frac{1}{\sqrt{2} \sin \beta} \overline{E} \tilde{\eta}^E E [\sin (\alpha' - \beta) H^0 + \cos (\alpha' - \beta) h^0] \\
& - \frac{i}{\sqrt{2} \sin \beta} \overline{E} \tilde{\eta}^E \gamma_5 E A^0 + h.c.
\end{aligned} \tag{4.20}$$

where the superindex (I) refers to the parametrization type I. It is easy to check that Lagrangian (4.20) is just the one in the 2HDM type I, plus some FC interactions. Therefore, we obtain the Lagrangian of the 2HDM type I from Eq. (4.20) by setting $\tilde{\eta}^E = 0$. In this case, it is clear that when $\tan \beta \rightarrow 0$ then $\tilde{\eta}^E$ should go to zero, in order to have a finite contribution for FCNC at the tree level.

In the parametrization of type II, the Yukawa Lagrangian reads

$$\begin{aligned}
-\mathcal{L}_{Y(E)}^{(II)} = & \frac{g}{2M_W \cos \beta} \overline{E} M_E^{diag} E (\cos \alpha' H^0 - \sin \alpha' h^0) \\
& + \frac{ig}{2M_W} \overline{E} M_E^{diag} \gamma_5 E G^0 - \frac{ig \tan \beta}{2M_W} \overline{E} M_E^{diag} \gamma_5 E A^0 \\
& + \frac{1}{\sqrt{2} \cos \beta} \overline{E} \tilde{\xi}^E E [\sin (\alpha' - \beta) H^0 + \cos (\alpha' - \beta) h^0] \\
& + \frac{i}{\sqrt{2} \cos \beta} \overline{E} \tilde{\xi}^E \gamma_5 E A^0 + h.c.
\end{aligned} \tag{4.21}$$

The Lagrangian (4.21) coincides with the one of the 2HDM type II [17], plus some FC interactions. So, the Lagrangian of the 2HDM type II is obtained setting $\tilde{\xi}^E = 0$. In this case it is clear that when $\tan \beta \rightarrow \infty$, then $\tilde{\xi}^E$ should go to zero, in order to have a finite contribution for FCNC at the tree level.

We now use the expression for Δa_μ from either Eq. (4.3) or Eq. (4.4) to get bounds on the Higgs boson masses. Additionally, we can notice that in Eq. (4.5) for Higgs bosons heavier than 100 GeV we find

$$\frac{m_\mu}{3m_\tau} G(m_{H_i}) \ll F(m_{H_i})$$

and the contribution of the factor involving $G(m_{H_i})$ is negligible [37]. However, we put it for completeness.

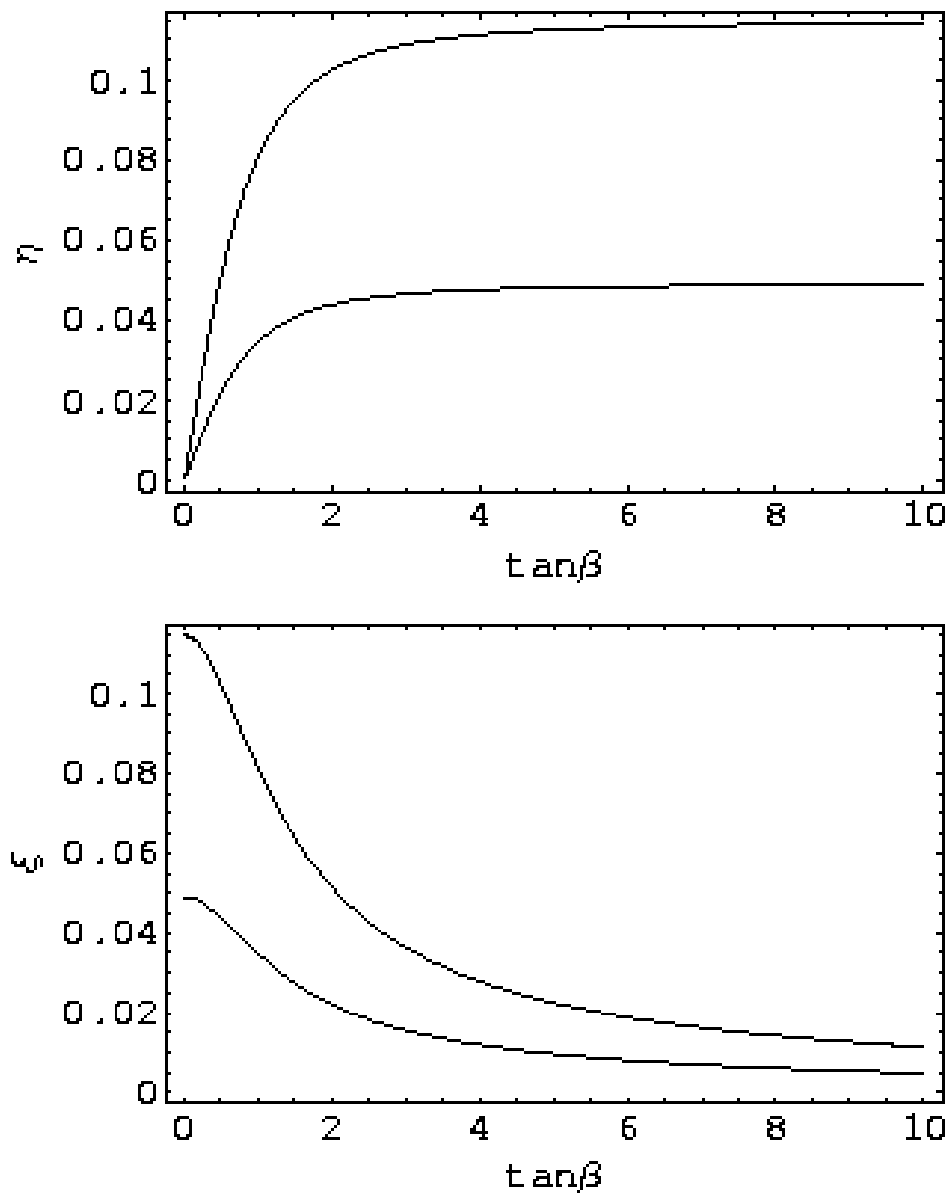


Figure 4.4: Lower and upper bounds for $\tilde{\eta}_{\mu\tau}(\tilde{\xi}_{\mu\tau})$ vs $\tan\beta$, for parametrizations I and II using $m_{h^0} = m_{H^0} = 150$ GeV and $m_{A^0} \rightarrow \infty$.

In Ref. [37] the estimated value for Δa_μ has been taken from [116]. In this section we are going to use the basic procedure developed in Ref. [37], but using a more updated value for Δa_μ i.e. the one reported in Ref. [72], instead of the one reported in [116]. We get some lower and upper bounds on the mixing vertex $\tilde{\eta}(\tilde{\xi})_{\mu\tau}$ for the parametrizations of type I (II). In Fig. (4.4), we display lower and upper bounds for the FC vertices as a function of $\tan\beta$ for both types of parametrizations with $m_{h^0} = m_{H^0} = 150$ GeV and $m_{A^0} \rightarrow \infty$. In the first case, with parametrization type I, the allowed region for $\tilde{\eta}_{\mu\tau}$ is $0.045 \lesssim \tilde{\eta}_{\mu\tau} \lesssim 0.12$ for large values of $\tan\beta$. Meanwhile, for parametrization type II, the allowed region for small $\tan\beta$ is the same. From the first of Figs. (4.4) we can see that when $\tan\beta \rightarrow 0$, $\tilde{\eta}_{\mu\tau}$ goes to zero as expected. Similarly, the second of these figures, shows that when $\tan\beta \rightarrow \infty$, $\tilde{\xi}_{\mu\tau}$ goes to zero as expected too.

In addition, the Figs. (4.4) show us that the FC vertices are basis dependent. We can realize that by varying $\tan\beta$, what we are doing is changing the basis. Figs. (4.4) show that for different values of $\tan\beta$ (i.e. different bases) we get different values for the lower and upper limits on $\tilde{\eta}_{\mu\tau}(\tilde{\xi}_{\mu\tau})$.

In figure (4.5), we show lower and upper bounds for the FC vertex as a function of m_{H^0} for parametrization of type II when $m_{h^0} = m_{H^0}$ and $m_{A^0} \rightarrow \infty$. We see that the larger value for $\tan\beta$ the smaller value of $\tilde{\xi}_{\mu\tau}$. We only consider the case of parametrization type II because there is a complementary behaviour between both parametrizations as could be seen in figure (4.4). In particular, for $\tan\beta = 1$, the behaviour of the bounds for both parametrizations is the same. Since in this case we are fixing $\tan\beta$, we are fixing the basis and the interpretation is clear. It should be emphasized that according to Eq. (4.19) for different values of $\tan\beta$, the same value of $\tilde{\xi}_{\mu\tau}$ correspond to different values of $\xi_{\mu\tau}$ in the fundamental parametrization. Thus, we see again that the values of the FC vertices are basis dependent.

Observe that according to its current estimated value, Δa_μ^{NP} is positive definite, and it is a new feature from most updated results [70]. On the other hand, the Feynman rules from (4.20) and (4.21), show that the Scalar (Pseudoscalar) contribution to Δa_μ^{NP} Eqs. (4.3, 4.4) is positive (negative). Such fact permits us to impose lower bounds on the pseudoscalar Higgs mass, by using the lower limit for Δa_μ^{NP} . However, it is very important to clarify that for very light Pseudoscalars (i.e. $m_{A^0} \ll 100$ GeV), the contributions up to two loops become important [72]. Further, the diagrams at two loops

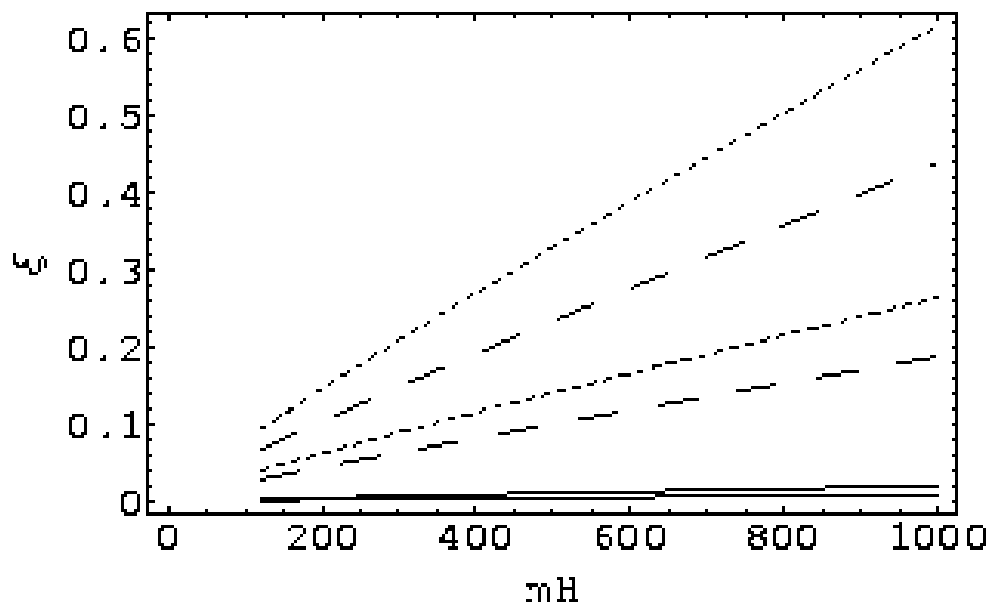


Figure 4.5: Lower and upper bounds for $\tilde{\xi}_{\mu\tau}$ vs m_{H^0} , for parametrization of type II, taking $m_{h^0} = m_{H^0}$ and $m_{A^0} \rightarrow \infty$, the pair of dotted lines correspond to $\tan \beta = 0.1$, the dashed lines are for $\tan \beta = 1$, and the solid lines are for $\tan \beta = 30$.

for the scalars and the pseudoscalar could have opposite signs respect to the contribution at one loop. Consequently, the lower bounds shown here are not valid in the very light pseudoscalar regime, and they are only valid if we assume that $m_{A^0} \gtrsim 100$ GeV.

Now, to take into account the experimental value, we should make a supposition about the value of the FC vertex. A reasonable assumption consists of taking the geometric average of the Yukawa couplings [5] i.e. $\tilde{\eta}(\tilde{\xi})_{\mu\tau} \approx 2.5 \times 10^{-3}$. Additionally, we shall use also the values $\tilde{\eta}(\tilde{\xi})_{\mu\tau} \approx 2.5 \times 10^{-2}$ and $\tilde{\eta}(\tilde{\xi})_{\mu\tau} \approx 2.5 \times 10^{-4}$ which are one order of magnitude larger and smaller than the former. Notwithstanding, we should remember that these values are basis dependent. Therefore, in this work we shall take the values yielded above for the FC vertex among the second and third family by using different bases, i.e. different values of $\tan\beta$. Using these suppositions and the experimental value for Δa_μ^{NP} reported in Ref. [72] we get lower bounds for m_{A^0} and they are plotted in figures (4.6-4.8).

Figure 4.6 displays m_{A^0} vs $\tan\beta$ utilizing the parametrization type II and using $\tilde{\xi}_{\mu\tau} = 2.5 \times 10^{-2}$, and $\tilde{\xi}_{\mu\tau} = 2.5 \times 10^{-3}$. Additionally it is assumed that $m_{h^0} = m_{H^0}$ with $m_{h^0} = 115, 300$ GeV⁴. According to the interpretation explained above, since we are using $0 \leq \tan\beta \leq 100$, it is equivalent to use a range of $\xi_{\mu\tau}$ from $\tilde{\xi}_{\mu\tau}$ to $100\tilde{\xi}_{\mu\tau}$ in the fundamental parametrization. It could be seen that in the limit of large $\tan\beta$, the lower limit reduces to $m_{A^0} \approx m_{h^0}$. The same behavior can be seen in parametrization type I but the bound $m_{A^0} \approx m_{h^0}$ is gotten in the limit of small $\tan\beta$. We also see that the smaller value of $\xi_{\mu\tau}$ the stronger lower limit for m_{A^0} .

As a proof of consistency, we can see that for instance in the case $m_{h^0} = m_{H^0} = 115$ GeV with $\tilde{\xi}_{\mu\tau} = 2.5 \times 10^{-3}$ the allowed region starts at about $\tan\beta \approx 13$. If we calculate the value of $\xi_{\mu\tau}$ in the fundamental parametrization corresponding to $\tan\beta \approx 13$ we obtain from Eq. (4.19) that $\xi_{\mu\tau}^2 \approx 1 \times 10^{-3}$, in rough agreement with the minimum allowed value for $\xi_{\mu\tau}^2$ reported in table (4.1) for the case 1⁵.

⁴By using $\tilde{\xi}_{\mu\tau} = 2.5 \times 10^{-4}$ we still have an allowed region but it appears only for $\tan\beta \gtrsim 155$ and for $\tan\beta \gtrsim 360$ when $m_{h^0} = 115$ GeV and when $m_{h^0} = 300$ GeV respectively. The behavior of those curves is similar to the others and is not shown in Fig. 4.6.

⁵The difference owes to the fact that here we have used the approximate expression for Δa_μ given in Eq. (4.4), instead of the Eq. (4.3) which was the one used to obtain the table (4.1). Additional differences could be traced to the errors involved in the calculation

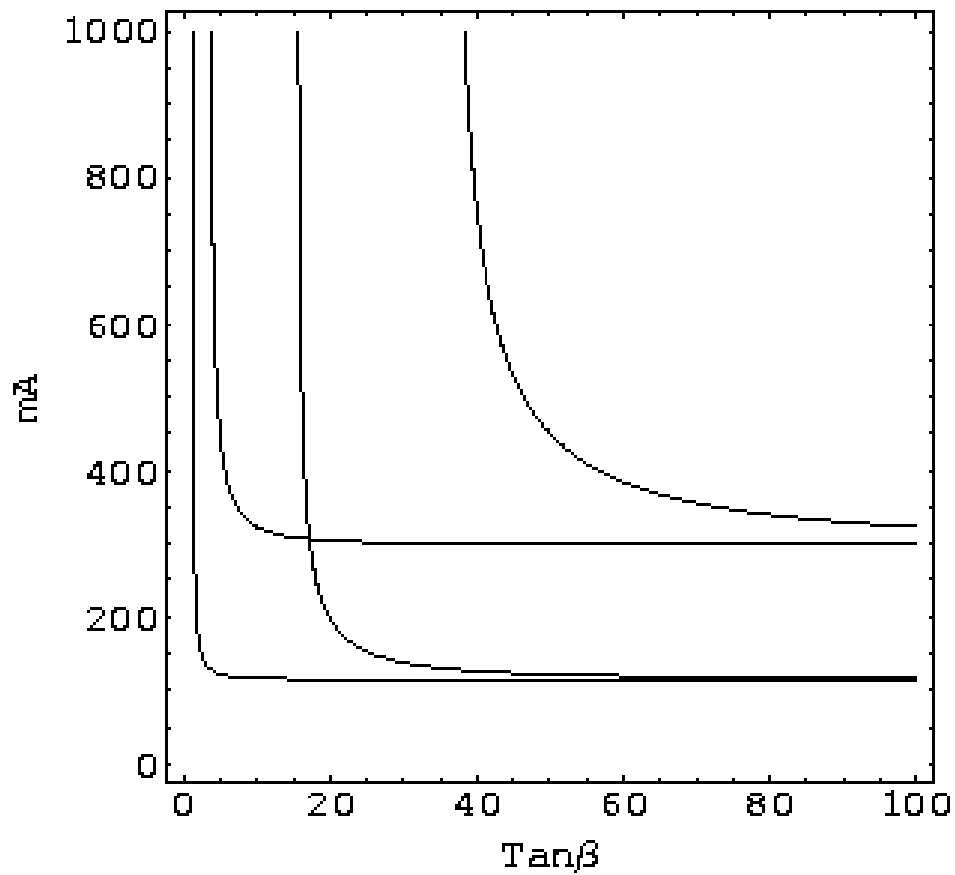


Figure 4.6: Contourplot of m_{A^0} vs $\tan \beta$ using parametrization type II and assuming $m_{h^0} = m_{H^0}$. From left to right: (1) $m_{h^0} = 115$ GeV, $\xi_{\mu\tau} = 2.5 \times 10^{-2}$ (2) $m_{h^0} = 300$ GeV, $\xi_{\mu\tau} = 2.5 \times 10^{-2}$ (3) $m_{h^0} = 115$ GeV, $\xi_{\mu\tau} = 2.5 \times 10^{-3}$ (4) 300 GeV, $\xi_{\mu\tau} = 2.5 \times 10^{-3}$.

Figure 4.7 shows m_{A^0} vs m_{H^0} with $\tilde{\xi}_{\mu\tau} = 2.5 \times 10^{-2}$ and $\tan\beta = 2$, using $m_{h^0} = m_{H^0}$ and $m_{h^0} = 115$ GeV. With these settings, the values $\tilde{\xi}_{\mu\tau} = 2.5 \times 10^{-3}$ and $\tilde{\xi}_{\mu\tau} = 2.5 \times 10^{-4}$ are excluded.

Once again, we can see the consistency with the analysis in Sec. (4.4) noting that for $\tilde{\xi}_{\mu\tau} = 2.5 \times 10^{-3}$ and $\tilde{\xi}_{\mu\tau} = 2.5 \times 10^{-4}$ with $\tan\beta = 2$, we get $\xi_{\mu\tau}^2 = 3.125 \times 10^{-5}$ and $\xi_{\mu\tau}^2 = 3.125 \times 10^{-7}$ respectively. Looking at the case 1 in table (4.1) we see that these values are not allowed, and hence they are excluded in Fig. 4.7. By contrast, the value $\tilde{\xi}_{\mu\tau} = 2.5 \times 10^{-2}$ with $\tan\beta = 2$, leads to $\xi_{\mu\tau}^2 = 3.1 \times 10^{-3}$ which is clearly allowed according to the table (4.1) in the case 1.

In figure 4.8 we suppose that $m_{h^0} = 115$ GeV, $m_{H^0} = 300$ GeV. The figure above shows the sensitivity of lower bounds on m_{A^0} with the mixing angle α' , for parametrization type II, taking $\tan\beta = 20$. The value $\tilde{\xi}_{\mu\tau} = 2.5 \times 10^{-4}$ is excluded again. The constraints are very sensitive to the α' mixing angle for $\tilde{\xi}_{\mu\tau} = 2.5 \times 10^{-3}$ but less sensitive for $\tilde{\xi}_{\mu\tau} = 2.5 \times 10^{-2}$. The figure below shows m_{A^0} vs $\tan\beta$ for $m_{h^0} = 115$ GeV, $m_{H^0} = 300$ GeV, $\alpha' = \pi/6$, for parametrization type II and considering the $\tilde{\xi}_{\mu\tau} = 2.5 \times 10^{-2}$ and $\tilde{\xi}_{\mu\tau} = 2.5 \times 10^{-3}$. The value $\tilde{\xi}_{\mu\tau} = 2.5 \times 10^{-4}$ is excluded. The m_{A^0} lower asymptotic limit for large $\tan\beta$ is approximately m_{h^0} .

of the contourplots. A more careful numerical analysis could improve the agreement, but it is beyond the purpose of the present work.

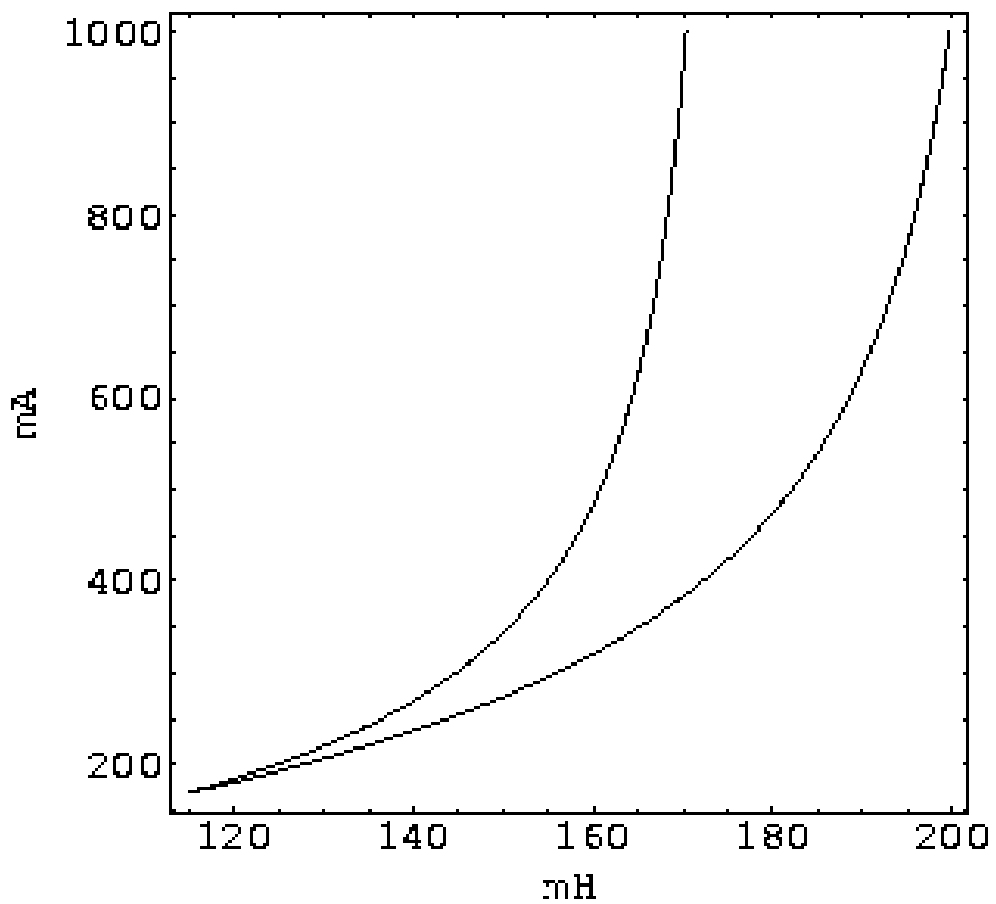


Figure 4.7: Contourplot of m_{A^0} vs m_{H^0} setting $\tan \beta = 2$, the line above correspond to $\tilde{\xi}_{\mu\tau} = 2.5 \times 10^{-2}$ and $m_{h^0} = m_{H^0}$, while the line below correspond to $\tilde{\xi}_{\mu\tau} = 2.5 \times 10^{-2}$ for $m_{h^0} = 115$ GeV.

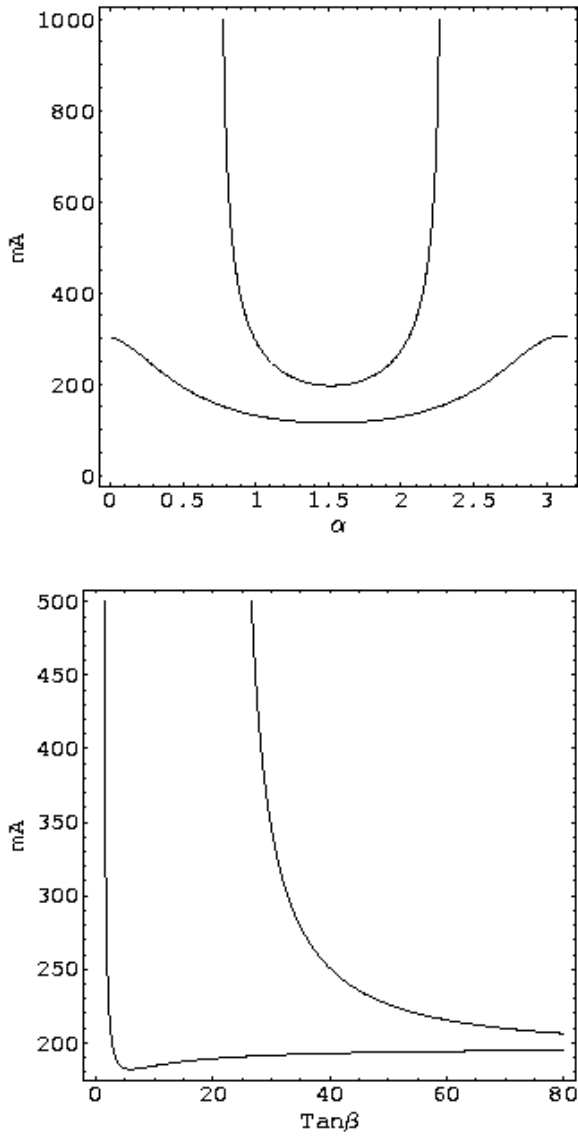


Figure 4.8: (top) Contourplot of m_{A^0} vs α' , for parametrization type II, with $m_{h^0} = 115$ GeV, $m_{H^0} = 300$ GeV and $\tan\beta = 20$. Line above corresponds to $\tilde{\xi}_{\mu\tau} = 2.5 \times 10^{-3}$, and line below corresponds to $\tilde{\xi}_{\mu\tau} = 2.5 \times 10^{-2}$. (bottom) Contourplot of m_{A^0} vs $\tan\beta$ for $m_{h^0} = 115$ GeV, $m_{H^0} = 300$ GeV, $\alpha = \pi/6$, and for parametrization type II. Line above corresponds to $\tilde{\xi}_{\mu\tau} = 2.5 \times 10^{-3}$, and line below corresponds to $\tilde{\xi}_{\mu\tau} = 2.5 \times 10^{-2}$.

Chapter 5

Addendum: Top-squark searches at the Fermilab Tevatron in models of low-energy supersymmetry breaking

5.1 General framework

This chapter describes the work developed at the Fermi National Accelerator Laboratory, along with M. Carena, D. Choudhury, H. E. Logan, and C.E.M. Wagner [41]. It is about the perspectives for detection of the lightest top squark at the Tevatron collider in the case in which such stop comes from a supersymmetric model with low energy supersymmetry breaking pattern. Since it is an addendum, I will provide only a very brief survey on the framework of supersymmetric models and supersymmetry breaking schemes. For more details I refer the reader to the literature [123, 124]

One of the greatest problems of the SM is the so called “naturalness problem”. The radiative corrections of the Higgs mass squared depend quadratically on the cut off scale energy used. If one hopes to have a Higgs mass of the order of the EWSB scale, it is required a very precise fine tuning (of about one part in 10^{16}), in order to get the cancellation necessary at the Planck scale, the apparent necessity of such extremely accurate cancellation

is known as the naturalness problem. On the other hand, it is well known that such radiative corrections with fermions and bosons into the loops have opposite signs. Consequently, if we had a fermion of the same mass for each boson and vice versa, the necessary cancellation would occur. Supersymmetry provides a framework in which each SM particle possesses a superpartner i.e. a particle with the same mass and quantum numbers under the gauge symmetry but with different spin. Therefore, imposition of SUSY provides an elegant solution to the naturalness problem.

Supersymmetry consists of an extension to the Poincaré group by the introduction of new generators. The algebra of the group is determined by a set of commuting and anticommuting relations among the poincaré generators and the new generators. The new supersymmetric generators permits to relate fermion fields with boson fields providing a unified description of them. In order to keep the supersymmetry, the spectrum of the SM should be doubled arising the so called superpartners.

Nevertheless, since the superpartners have not been detected yet, they cannot have the same mass as their corresponding SM partners. Consequently, supersymmetry must be broken in such a way that the superpartners should be heavier than their partners. However, such breaking have to preserve the cancellation of quadratic divergencies that was one of the original motivations, this fact imposes constraints on the splittings among the partner and superpartner masses, in general such splitting cannot be larger than a few TeV. As a consequence, some of the lightest superpartners could have masses within the reach of accelerators like the Tevatron or the LHC. As we shall see later, the lightest stop (i.e. one of the superpartners of the top quark), is a good candidate to be one of the lightest supersymmetric particles. Before discussing that point, let us describe briefly the particle content of the Minimal Supersymmetric Standard Model (MSSM), and some breaking schemes of supersymmetric models.

5.1.1 The MSSM

In the MSSM, the particle spectrum of the SM is doubled. On the other hand, in order to get cancellation of anomalies and preserve SUSY, two Higgs doublets must be introduced. The Higgs spectrum is similar to the one of the general 2HDM i.e. two CP-even scalars (H^0, h^0), one CP-odd scalar (A^0), and two charged Higgs bosons (H^\pm). The Higgs bosons and the SM particles have superpartners with the same quantum numbers under the gauge

symmetry but with different spin. The superpartners of the gauge bosons (gauginos) are spin 1/2 particles denoted as photinos ($\tilde{\gamma}$), Winos (\tilde{W}), Zinos (\tilde{Z}) and gluinos (\tilde{g}). The fermionic superpartners of the Higgs bosons (Higgsinos) are \tilde{H}_1 , \tilde{H}_2 , \tilde{H}^\pm . Owing to the EWSB, the Higgsinos and the gauginos of the electroweak symmetry can be mixed to give the mass eigenstates, arising two charged Dirac fermions called charginos $\tilde{\chi}^\pm$, and four neutral majorana fermions (the neutralinos $\tilde{\chi}^0_{1-4}$). By contrast, the gaugino of the color symmetry (gluino \tilde{g}) does not mix with Higgsinos nor electroweak gauginos, because it belongs to an unbroken symmetry. Finally, the spin-0 partners of the fermion fields (the sfermions) are the squarks \tilde{q} , charged sleptons \tilde{l} and sneutrinos $\tilde{\nu}$. There are two superpartners associated to each quark or charged slepton, one for each chirality, the left-handed sfermions transform as $SU(2)_L$ doublets while right-handed ones are $SU(2)_L$ singlets, there are only left-handed sneutrinos because of the lack of right-handed partners in the SM. The gluino is a $SU(3)_C$ octet while the squarks are $SU(3)_C$ triplets.

As well as the interactions of SUSY particles with SM particles, the Lagrangian of Supersymmetry should contain some soft SUSY breaking terms. The term “soft” means that these terms breaks SUSY and generates splittings among the SUSY particles and their partners but maintaining the gauge symmetry and the cancellation of the quadratic divergencies mentioned above. The soft SUSY breaking parameters are mass terms for gauginos and sfermions as well as trilinear scalar couplings. The number of those kind of terms depend on the specific SUSY breaking scheme.

The chargino and neutralino masses and mixing angles are determined by the gauge boson masses M_W , M_Z , the parameter $\tan\beta$, the SUSY Higgsino mass parameter μ and the two soft breaking parameters associated to the $SU(2)_L$ gaugino mass (M_1) and the $U(1)$ gaugino mass (M_2), evaluated at the EW scale. The neutralino mass matrix in the $\tilde{B} - \tilde{W}^3 - \tilde{H}_1 - \tilde{H}_2$ basis is written as:

$$\begin{aligned} \mathbf{M}_N &= \begin{pmatrix} \mathbf{M}_i & \mathbf{Z} \\ \mathbf{Z}^T & \mathbf{M}_\mu \end{pmatrix}; \quad \mathbf{M}_i = \begin{pmatrix} M_1 & 0 \\ 0 & M_2 \end{pmatrix}; \quad \mathbf{M}_\mu = \begin{pmatrix} 0 & -\mu \\ -\mu & 0 \end{pmatrix} \\ \mathbf{Z} &= \begin{pmatrix} -M_Z \cos\beta \sin\theta_W & M_Z \sin\beta \sin\theta_W \\ M_Z \cos\beta \cos\theta_W & -M_Z \sin\beta \cos\theta_W \end{pmatrix} \end{aligned} \quad (5.1)$$

The values of the parameters M_1 , M_2 , μ , $\tan\beta$ determines the Higgsino and gaugino content of the neutralinos. There are some interesting limits in which the Higgsino and gaugino components become simpler. As a manner of

example, if $|\mu| >> M_Z$ and $M_1, M_2 \approx M_Z$, with $M_1 < M_2$, the lightest neutralinos are gaugino-like and the heaviest are Higgsino like, the eigenvalues of the matrix \mathbf{M}_N in Eq. (5.1) yield the following spectrum

$$M_{\tilde{\chi}_1^0} \approx M_1 ; M_{\tilde{\chi}_2^0} \approx M_2 ; M_{\tilde{\chi}_3^0} \approx M_{\tilde{\chi}_4^0} \approx |\mu|$$

In particular, we shall work under the assumption that the lightest neutralino is a pure bino $\tilde{\chi}_1^0 \approx \tilde{B}$, details later on. The Higgsino and gaugino composition affects strongly the couplings of the neutralinos to gauge bosons and sfermions leading to substantial differences in production and decay rates.

Similarly, the mass matrix for the two charginos can be written in the $\tilde{W}^+ - \tilde{H}^+$ basis, and the production and decay rates depend on their gaugino and Higgsino composition as well.

As for the squarks and sleptons, their mass eigenstates are in general combinations of left-handed and right-handed components. The soft SUSY breaking sfermion mass parameters are strongly constrained by the suppression of FCNC, requiring that (1) the soft SUSY breaking sfermion mass matrix be diagonal and degenerate or (2) the masses of the first and second generation sfermions be very large.

The mixing among left and right-handed sfermions depends on the mass of the corresponding SM fermion. So those mixings are negligible for squarks and sleptons of the first and second generations but could be significant for the fermions of the third generation. In particular, the mass matrix for the stops in the \tilde{t}_L, \tilde{t}_R basis reads

$$M_t^2 = \begin{pmatrix} m_{Q_3}^2 + m_t^2 + D_{\tilde{t}_L} & m_t \left(A_t - \frac{\mu}{\tan \beta} \right) \\ m_t \left(A_t - \frac{\mu}{\tan \beta} \right) & m_{U_3}^2 + m_t^2 + D_{\tilde{t}_R} \end{pmatrix}$$

where $m_{Q_3}^2, A_t$ are SUSY breaking parameters and

$$\begin{aligned} D_{\tilde{f}_L} &= M_Z^2 \cos(2\beta) (T_{3f} - Q_f \sin^2 \theta_W) \\ D_{\tilde{f}_R} &= M_Z^2 \cos(2\beta) Q_f \sin^2 \theta_W \end{aligned}$$

Unless there is a cancellation of the factor $\left(A_t - \frac{\mu}{\tan \beta} \right)$, the mixing will be significant because of the large top mass. This large mixing in turn produces a large splitting between the lightest (\tilde{t}_1) and the heaviest (\tilde{t}_2) top squarks. This fact makes the lightest stop a good candidate to be one of the lightest

superparticles. In this work we shall assume that the stop is the next-to-next-to lightest sparticle, details below.

Another important issue on supersymmetric models is the R –parity, such discrete symmetry is defined as $R = (-1)^{2S+3B+L}$, where S is the particle spin, B the baryon number, and L the lepton number. It can be checked that this quantum number is $R = 1$ for the SM particles and $R = -1$ for the sparticles, if this symmetry were conserved, a SUSY particle could not decay into just SM particles. Specifically, under R –parity conservation each vertex should contain an even number of sparticles. An immediate consequence is that the lightest supersymmetric particle (LSP) must be absolutely stable in the case of R –parity conservation. Thus, from the point of view of collider physics the track of such LSP would be missing energy and momentum. The violation of R –parity conduces to the violation of lepton and/or baryon number. We shall restrict to the case of R –parity conservation.

5.1.2 SUSY breaking schemes

As we have explained above, supersymmetry must be broken and there is a variety of breaking mechanisms. We shall discuss briefly two schemes: supergravity and gauge mediated susy breaking models.

In supergravity (SUGRA) it is assumed the existence of additional superfields (the hidden sector) that couples to the MSSM particles by means of gravitational interactions. After the SUSY breaking, some components of the hidden sector acquire VEV, the soft SUSY breaking terms arise from the interaction among the MSSM superfields with the components of the hidden sector that acquire a VEV, from which it follows that the strength of these SUSY breaking terms is proportional to those VEV divided by the Planck scale. Despite the number of SUSY breaking terms is enormous in those kind of models, in minimal SUGRA they are reduced considerably because the MSSM sparticles couples universally to the hidden sector. This universality is extended to the MSSM mass pattern at a scale of the order of $M_{\text{Planck}} (\sim 10^{19} \text{GeV})$ or at a scale of the order of GUT ($\sim 10^{16} \text{GeV}$); at such a high scale the scalars (Higgs bosons and sfermions) are assumed to have a common mass m_0 , all gauginos (Bino, Wino, and gluino) have a common mass $m_{1/2}$, and all trilinear couplings have a common strength as well (A_0). All these values at GUT or Planck scale can be run by Renormalization Group Equations (RGE) to obtain their values at EW scale. Evolution of the mass pattern by RGE shows that the lightest two neutralinos and the

lightest chargino tend to be gaugino like. In addition, squarks are in general heavier than sleptons. Finally, the lightest neutralino seems to be a good candidate to be the LSP, except in the cases in which m_0 or $m_{1/2}$ are very small, in those cases the best candidates become the sneutrino and the gluino respectively.

As for the scale of supersymmetry breaking, in SUGRA models it is expected to be very high ($\sim 10^{11}$ GeV if we expect the SUSY masses to lie at the TeV scale) as we shall discuss in next section. Thus, SUGRA are in general models with high energy supersymmetry breaking scale.

Another interesting scheme is the gauge mediated SUSY breaking, in which the SUSY breaking terms are generated from gauge interactions. In these models the masses of sfermions with the same quantum numbers under the gauge group i.e. with the same gauge couplings are predicted to be degenerate, in this way FCNC are naturally suppressed. As we shall see in next section, in Gauge Mediated Spontaneously Breaking (GMSB) models the scale of SUSY breaking is much smaller than the Planck or GUT scale avoiding corrections at those scales to the degeneracy. The existence of heavy messenger superfields is assumed. The breaking of SUSY occurs in a hidden sector which also couples to the messenger superfields, thus the fermion components of the messenger superfields acquire a common mass M and the scalar components acquire a common mass $M\sqrt{1 \pm x}$ where x is a dimensionless parameter related to the breaking scale. The gauginos and sfermions masses receive radiative contributions from the messenger fields that generates a splitting among them and their corresponding SM partners. Gaugino and scalar masses lie roughly on the same order of magnitude. Moreover, after evolving by RGE, sfermions with the same quantum numbers continue degenerate if we ignore the effect of Yukawa couplings¹, therefore the mass hierarchy is directly related to the gauge coupling strength; the gauge coupling pattern also determines the gaugino mass hierarchy. In such models the gravitino might be very light, and it is a good candidate to be the LSP, in that case it plays a crucial role in low energy phenomenology. In this work the gravitino will be the LSP.

¹In this work we assume that there are ten degenerate squarks corresponding to the five light quarks. Only the top squarks are considered to have an splitting between them, owing to the large Yukawa coupling of the top quark.

5.2 Introduction

The Standard Model with a light Higgs boson provides a very good description of all experimental data. The consistency of the precision electroweak data with the predictions of the Standard Model suggests that, if new physics is present at the weak scale, it is most probably weakly interacting and consistent with the presence of a light Higgs boson in the spectrum. Extensions of the Standard Model based on softly broken low energy supersymmetry (SUSY) [125] provide the most attractive scenarios of physics beyond the Standard Model fulfilling these properties. If the supersymmetry breaking masses are $\lesssim \mathcal{O}(1 \text{ TeV})$, supersymmetry stabilizes the hierarchy between the Planck scale M_P and the electroweak scale. Furthermore, the minimal supersymmetric extension of the Standard Model (MSSM) significantly improves the precision with which the three gauge couplings unify and leads to the presence of a light Higgs boson with a mass below about 128 GeV [126]².

Perhaps the most intriguing property of supersymmetry is that local supersymmetry naturally leads to the presence of gravity (supergravity). In the case of local supersymmetry, the Goldstino provides the additional degrees of freedom necessary to make the gravitino a massive particle [127]. In the simplest scenarios, the gravitino mass $m_{\tilde{G}}$ is directly proportional to the square of the supersymmetry breaking scale $\sqrt{F_{\text{SUSY}}}$:

$$m_{\tilde{G}} \simeq F_{\text{SUSY}} / \sqrt{3} M_P , \quad (5.2)$$

where M_P denotes the Planck mass.

The relation between the supersymmetry breaking scale $\sqrt{F_{\text{SUSY}}}$ and the masses of the supersymmetric partners depends on the specific supersymmetry breaking mechanism. In general, the superpartner masses M_{SUSY} are directly proportional to F_{SUSY} and inversely proportional to the messenger scale M_m at which the supersymmetry breaking is communicated to the visible sector:

$$M_{\text{SUSY}} \simeq C_M \frac{F_{\text{SUSY}}}{M_m} , \quad (5.3)$$

²This upper limit for the lightest CP even Higgs boson could be moved up in some non-minimal supersymmetric versions. For instance, Ref. [40] shows that in the supersymmetric version of the $SU(3) \times U(1)$ gauge model in which the Higgs triplets are included in the lepton superfields, the upper limit for the lightest CP even Higgs boson can be shifted up to about 140 GeV.

where C_M is the characteristic strength of the coupling between the messenger sector and the visible one. If the breakdown of supersymmetry is related to gravity effects, M_m is naturally of the order of the Planck scale and C_M is of order one; hence, for $\sqrt{F_{\text{SUSY}}} \sim 10^{11}$ GeV, M_{SUSY} is naturally at the TeV scale. In gauge mediated scenarios (GMSB) [128, 129], instead, the couplings C_M are associated with the Standard Model gauge couplings (times a loop suppression factor), so that a $F_{\text{SUSY}}/M_m \lesssim 100$ TeV yields masses of the order of 100 GeV for the lighter Standard Model superpartners.

When relevant at low energies, the gravitino interactions with matter are well described through the interactions of its spin 1/2 Goldstino component [127]. The Goldstino has derivative couplings with the visible sector with a strength proportional to $1/F_{\text{SUSY}}$. In scenarios with a high messenger scale, of order M_P , Eqs. 5.2 and 5.3 imply that the gravitino has a mass of the same order as the other SUSY particles, and its interactions are extremely weak. In such scenarios, the gravitino plays no role in the low-energy phenomenology. However, in low energy supersymmetry breaking scenarios such as GMSB in which the messenger scale is significantly lower than the Planck scale, the supersymmetry breaking scale is much smaller. Typical values in the GMSB case are $M_m \sim 10^5 - 10^8$ GeV, leading to a supersymmetry breaking scale $\sqrt{F_{\text{SUSY}}}$ roughly between 10^5 and a few times 10^6 GeV. The gravitino then becomes significantly lighter than the superpartners of the quarks, leptons and gauge bosons, and its interaction strength is larger. As the lightest supersymmetric particle (LSP), the gravitino must ultimately be produced at the end of all superparticle decay chains if R -parity is conserved (for an analysis of the case of R -parity violation see, Ref. [130]).

Depending on the strength of the gravitino coupling, the decay length of the next-to-lightest supersymmetric particle (NLSP) can be large (so that the NLSP is effectively stable from the point of view of collider phenomenology; this occurs when $\sqrt{F_{\text{SUSY}}} \gtrsim 1000$ TeV), intermediate (so that the NLSP decays within the detector giving rise to spectacular displaced vertex signals; this occurs when 1000 TeV $\gtrsim \sqrt{F_{\text{SUSY}}} \gtrsim 100$ TeV), or microscopic (so that the NLSP decays promptly; this occurs when $\sqrt{F_{\text{SUSY}}} \lesssim 100$ TeV) [131, 132, 133]. The decay branching fractions of the Standard Model superpartners other than the NLSP into the gravitino are typically negligible. However, if the supersymmetry breaking scale is very low, $\sqrt{F_{\text{SUSY}}} \ll 100$ TeV (corresponding to a gravitino mass $\ll 1$ eV), then the gravitino coupling strength can become large enough for superpartners other than the NLSP to decay directly into final states containing a gravitino [133, 134]. In any

case, the SUSY-breaking scale must be larger than the mass of the heaviest superparticle; an approximate lower bound of $\sqrt{F_{\text{SUSY}}} \simeq 1$ TeV corresponds to a gravitino mass of about 10^{-3} eV.

In many models, the lightest amongst the supersymmetric partners of the Standard Model particles is a neutralino, $\tilde{\chi}_1^0$. The partial width for $\tilde{\chi}_1^0$ decaying into the gravitino and an arbitrary SM particle X is given by

$$\Gamma(\tilde{\chi}_1^0 \rightarrow X \tilde{G}) \simeq K_X N_X \frac{m_{\tilde{\chi}_1^0}}{96\pi} \left(\frac{m_{\tilde{\chi}_1^0}}{\sqrt{M_P m_{\tilde{G}}}} \right)^4 \left(1 - \frac{m_X^2}{m_{\tilde{\chi}_1^0}^2} \right)^4, \quad (5.4)$$

where K_X is a projection factor equal to the square of the component in the NLSP of the superpartner \tilde{X} , and N_X is the number of degrees of freedom of X . If X is a photon, for instance, $N_X = 2$ and

$$K_X = |N_{11} \cos \theta_W + N_{12} \sin \theta_W|^2, \quad (5.5)$$

where N_{ij} is the mixing matrix connecting the neutralino mass eigenstates to the weak eigenstates in the basis $\tilde{B}, \tilde{W}, \tilde{H}_1, \tilde{H}_2$.

If the neutralino has a significant photino component, it will lead to observable decays into photon and gravitino. Since the heavier supersymmetric particles decay into the NLSP, which subsequently decays into photon and gravitino, supersymmetric particle production will be characterized by events containing photons and missing energy. This is in contrast to supergravity scenarios, where, unless very specific conditions are fulfilled [135, 136], photons do not represent a characteristic signature. The presence of two energetic photons plus missing transverse energy provides a distinctive SUSY signature with very little Standard Model background.

It might be argued that a $\tilde{\chi}_1^0$, decaying with a large branching ratio into photons, would be severely constrained by LEP data. However, such bounds are extremely model-dependent. For example, there exists no tree-level coupling between a photon (or Z) and either two binos or two neutral winos. Since the bino is associated with the smallest of all gauge interactions and, in addition, its mass is more strongly renormalized downward at smaller scales compared to the wino mass, in many models the lightest neutralino has a significant bino component. Therefore, if the NLSP is approximately a pure bino, the bounds on its mass depend strongly on the selectron mass (since, at LEP, pair-production of binos or neutral winos could occur through t -channel exchange of selectrons). For selectron masses below 200 GeV, the

present bound on such a neutralino is approximately 90 GeV [137] (the bound weakens with increasing selectron mass). As emphasized before, once produced, such a neutralino would decay via $\tilde{\chi}_1^0 \rightarrow \gamma \tilde{G}$. If $\tilde{\chi}_1^0$ is heavy enough, then the decays $\tilde{\chi}_1^0 \rightarrow Z \tilde{G}$ and $\tilde{\chi}_1^0 \rightarrow h^0 \tilde{G}$ are also allowed; however, the decay widths into these final states are kinematically suppressed compared to the $\gamma \tilde{G}$ final state and will be important only if either the photino component of $\tilde{\chi}_1^0$ is small or if $\tilde{\chi}_1^0$ itself is significantly heavier than Z and h^0 [133].

In most SUSY models, it is natural for the lighter top squark, \tilde{t}_1 , to be light compared to the other squarks. In general, due to the large top Yukawa coupling, there is a large mixing between the weak eigenstates \tilde{t}_L and \tilde{t}_R , which leads to a large splitting between the two stop mass eigenstates. In addition, even if all squarks have a common mass at the messenger scale, the large top Yukawa coupling typically results in the stop masses being driven (under renormalization group evolution) to smaller values at the weak scale. An extra motivation to consider light third generation squarks comes from the fact that light stops, with masses of about or smaller than the top quark mass, are demanded for the realization of the mechanism of electroweak baryogenesis within the context of the MSSM [138].

In this chapter, we examine, in detail, the production and decay of top squarks at Run II of the Tevatron collider in low-energy SUSY breaking scenarios wherein the lightest neutralino is the NLSP and decays promptly into $\gamma \tilde{G}$. We also investigate the production and decay of the other squarks, and provide an estimate of the reach of Run II of the Tevatron in the heavy gluino limit. We work in the context of a general SUSY model in which the SUSY particle masses are *not* constrained by the relations predicted in the minimal GMSB models. We assume throughout that the gravitino coupling is strong enough (or, equivalently, that the scale of SUSY breaking is low enough) that the NLSP decays promptly. This implies an upper bound on the supersymmetry breaking scale of a few tens to a few hundred TeV [132, 133, 131], depending on the mass of the NLSP. Our analysis can be extended to higher supersymmetry breaking scales for which the NLSP has a finite decay length, although in this case some signal will be lost on account of the NLSP decaying outside the detector. At least 50% of the diphoton signal cross section remains though for NLSP decay lengths $c\tau \lesssim 40$ cm [131]; this corresponds to a supersymmetry breaking scale below a few hundred to about a thousand TeV, depending on the mass of the NLSP. Moreover, the displaced vertex associated with a finite decay length could be a very good additional discriminator for the signal. Thus, in totality, our choice is

certainly not an overly optimistic one.

This chapter is organized as follows. In Sec. 5.3, we outline models of low-energy supersymmetry breaking wherein the lighter stop is the lightest sfermion and, moreover, is lighter than the charginos as well as the gluino. In the following section, we review the stop pair production cross section at the Tevatron. In Sec. 5.5, we summarize previous studies of stop production and decay at Run II of the Tevatron. This is followed, in Sec. 5.6, by a discussion of the SUSY parameter space and the relative partial widths of the various stop decay modes. In Sec. 5.7, we describe the signal for each of the stop decay modes considered. We describe the backgrounds and the cuts used to separate signal from background in each case, and give signal cross sections after cuts. This gives the reach at Run II. We also note the possibility that stops can be produced in the decays of top quarks. In Sec. 5.8 we consider the production and decay of 10 degenerate squarks that are the supersymmetric partners of the five light quarks. Finally, we summarize our results (along with the results concerning the previous chapters of this Ph. D. thesis) in chapter 6.

5.3 Light Stop in Low Energy Supersymmetry Breaking Models

As discussed above, the mass of the gravitino as well as its interaction strength are governed by the supersymmetry breaking scale $\sqrt{F_{\text{SUSY}}}$. Low energy supersymmetry breaking models are defined as those obtained for low values of $\sqrt{F_{\text{SUSY}}}$ ($\lesssim 10^6$ GeV) and hence resulting in a gravitino lighter than a few keV. Apart from evading cosmological problems [139], a further striking consequence of such models is that sparticle decays into gravitinos may occur at scales that may be of interest for collider phenomenology. As is apparent from Eq. (5.3), in such models the messenger mass scale M_m should be smaller than 10^9 GeV.

In this chapter, we are interested in the presence of light stops in low energy supersymmetry breaking scenarios. The motivation is simple: assuming that the supersymmetry breaking masses are flavor independent, that is the left- and right-handed squark masses of the three generations are the same at the messenger scale, the lighter stop turns out to be the lightest of all the squarks. The reasons are twofold. On the one hand, there are renormal-

ization group effects induced by top-quark Yukawa interactions that tend to reduce the stop mass scale compared to the other squark masses. On the other, there are non-trivial mixing effects that tend to push the lightest stop mass down compared to the overall left- and right-squark masses. For similar reasons, it is also natural to assume that the lightest stop will be lighter than the gluino.

There is a further motivation behind our analysis, namely that of baryogenesis. A crucial requirement for electroweak baryogenesis scenarios within the Minimal Supersymmetric Extension of the Standard Model is the presence of a light stop with mass of the order of, or smaller than, the top quark mass. Since this scenario does not depend on the nature of supersymmetry breaking, it is very important to develop strategies to look for light top squarks in all their possible decay modes, in particular in those related to the possibility of low energy supersymmetry breaking.

In general, light stops can induce large corrections to the precision electroweak parameter $\Delta\rho$ [140, 141, 142], unless they are mainly right-handed or there is some correlation between the masses and mixing angles in the stop and sbottom sector [143]. The most natural way of suppressing potentially large contributions to the rho-parameter is to assume that there is a large hierarchy between the supersymmetry breaking mass parameters for the left- and right-handed stops. The simplest and most efficient way of doing this is to assume that sparticles which are charged under the weak gauge interactions acquire large supersymmetry breaking masses. Observe that, under this assumption, the charged wino will also be naturally heavier than the lightest stop and, for simplicity, we will assume that both charginos are heavier than the particle under study. We will further assume that the superpartner of the $U(1)_Y$ gauge boson, the so-called bino, is the lightest standard model superpartner.

The above mentioned properties are naturally obtained in simple extensions of the minimal gauge mediated model. Indeed, let us assume that there are N copies of messengers, which transform as complete representations (+) of $SU(5)$ and hence do not spoil the unification relations. Under the Standard Model gauge group, some of these fields will then transform as left-handed lepton multiplets (W_i , $i = 1 \dots N$) and their mirror partners (\bar{W}_i), while the others would transform as a right-handed down quark multiplet (C_i) and its mirror partner (\bar{C}_i). We shall assume that $N \leq 4$ in order to keep the gauge couplings weak up to the grand unification scale [144]. Let us further assume

that W_i and C_i couple to two different singlet fields $S_{2,3}$, with

$$\langle S_j \rangle = S_j + \theta^2 F_j , \quad (5.6)$$

and, for simplicity, assume that all couplings are of order one and that $F_j \ll S_j^2$. We will further assume that $S_1 \simeq S_2 \simeq S$, where S characterizes the messenger scale.

In this simple case, the masses of the gauginos at the messenger scale will be given by

$$\begin{aligned} M_3 &= N \frac{\alpha_3}{4\pi} \Lambda_3 , \\ M_2 &= N \frac{\alpha_2}{4\pi} \Lambda_2 , \\ M_1 &= N \frac{\alpha_1}{4\pi} \left(\frac{2 \Lambda_3}{5} + \frac{3 \Lambda_2}{5} \right) , \end{aligned} \quad (5.7)$$

where $\Lambda_3 \approx F_3/S_3$ and $\Lambda_2 \approx F_2/S_2$ [144, 145]. Now, it is easy to see that for $\Lambda_2 > 3\Lambda_3$, the weak gaugino can have a mass similar to that of the gluino (or be even heavier), while the bino is still much lighter than the wino (about three times lighter than the wino at the messenger scale).

The squared scalar masses at the messenger scale are also proportional to the number of messengers N

$$m_Q^2 = 2N \left[\sum_{a=2,3} C_Q^a \left(\frac{\alpha_a}{4\pi} \right)^2 \Lambda_a^2 + C_Q^1 \left(\frac{\alpha_1}{4\pi} \right)^2 \left(\frac{2}{5} \Lambda_3^2 + \frac{3}{5} \Lambda_2^2 \right) \right] , \quad (5.8)$$

where, for a particle transforming in the fundamental representation of $SU(n)$, $C_Q^n = (n^2 - 1)/(2n)$, while $C_Q^1 = 3/5(Q - T_3)^2$. The above quoted masses should be renormalized to the weak scale. The details of this procedure in a general gauge mediated model have been given by one of us in Ref. [145]. We shall not repeat these expressions here. For our purpose, it suffices to stress some important details.

As we mentioned before, after renormalization and mixing effects are added, the right-handed stop is the lightest squark in the spectrum. The large value of the left-handed stop mass increases the negative Yukawa dependent radiative corrections to the right-handed stop mass. Therefore, for Λ_2 larger than a few times Λ_3 and $N > 1$, the lightest stop is lighter than the gluino and the wino. Even for $N = 1$ this tends to be true, for not too small values

of the messenger scale ($S_3 \gtrsim 10^7$ GeV). Notice that, for Λ_2 larger by an order of magnitude than Λ_3 and/or large values of N , the right-stop (or, in extreme cases the right-sbottom) becomes the lightest standard model superpartner. We shall thus concentrate on cases where Λ_2 , though larger than Λ_3 , is still of the same order.

The sleptons do not play a relevant role in stop decays as long as the charginos are heavier than the lightest stop. One has only to ensure that the lightest slepton does not become lighter than the bino. The hierarchy of the right-handed slepton mass and the bino mass is approximately given by

$$m_{\tilde{e}_R}^2 \approx \frac{2M_1^2}{N} r_1 , \quad (5.9)$$

where r_1 is the appropriate renormalization group factor relating the masses at the messenger scale to the masses at the weak scale. This factor is about 1.5–1.7 [144] in the region of interest for this work and therefore we are led to conclude that, as long as $N \leq 3$, the bino is the next-to-lightest supersymmetric particle. Observe that this constraint on N is somewhat weaker than in the minimal model, due to the appearance of the factor 3/5 in front of the dominant Λ_2 contribution.

In all of the above, we have not discussed the process of radiative electroweak symmetry breaking and the determination of the μ parameter. This is due to the fact that in the minimal gauge mediated models of the kind we described above, the generation of a proper value of the parameter $B\mu$ requires the presence of new physics that necessarily modifies the value of the Higgs mass parameters [146]. It is, therefore, justified to treat μ as an independent parameter in such models.

To summarize, we have seen that a mild modification of the simplest gauge mediated models leads to a model where the stop is lighter than all the other squarks and also lighter than the weak and strong gauginos, while the bino remains the next-to-lightest supersymmetric particle. The unification relations are preserved as long as the number of messenger families is less than or equal to 3. The only condition for this to happen is that the effective scale Λ_2 is a few times larger than Λ_3 , but still of the same order of magnitude. The relation between the stop mass and the bino mass will be governed by the hierarchy between Λ_2 and Λ_3 . This modification of the minimal gauge mediated models is well justified in order to get consistency of a light stop with electroweak precision observables. Some of the sleptons might be lighter

than the stop, but, as long as the charginos remain heavy, they have no impact on the stop phenomenology.

Let us stress that the above should be considered only as a simple example in which a light stop, mainly right-handed, can appear in the spectrum in low energy supersymmetry breaking models. As the nature of supersymmetry breaking is unknown, so is the exact spectrum. We only make the simplifying assumptions that the left- and right-handed sfermions receive an approximately common mass at the messenger scale and that the gaugino masses are of the same order of magnitude as the squark masses. The truly defining feature of our assumption is that the wino and the gluino are heavier than the squarks and that the bino is the next-to-lightest supersymmetric particle. Although the left-handed squarks tend to be heavier than the right-handed ones, the exact spectrum obtained in the simple model detailed above does not differ markedly from the simplified spectrum that we choose to work with. In this kind of models, apart from the somewhat lighter stops, there will be ten squarks approximately degenerate in mass, which will predominantly decay into a quark and a bino, which will subsequently decay into photons (or Z bosons) and missing energy.

5.4 Top squark production at Tevatron Run II

Top squarks are produced at hadron colliders overwhelmingly via the strong interaction, so that the tree-level cross sections are model independent and depend only on the stop mass. The production modes of the lightest stop, \tilde{t}_1 , at the Tevatron are $q\bar{q} \rightarrow \tilde{t}_1\tilde{t}_1^*$ and $gg \rightarrow \tilde{t}_1\tilde{t}_1^*$. The cross sections for these processes are well known at leading order (LO) [147, 148], and the next-to-leading order (NLO) QCD and SUSY-QCD corrections have been computed [149] and significantly reduce the renormalization scale dependence. The NLO cross section is implemented numerically in PROSPINO [150, 149].

We generate stop events using the LO cross section evaluated at the scale $\mu = m_{\tilde{t}}$, improved by the NLO K-factor³ obtained from PROSPINO [150, 149] (see Fig. 5.1). The K-factor varies between 1 and 1.5 for $m_{\tilde{t}}$ decreasing from 450 to 100 GeV. We use the CTEQ5 parton distribution functions [151]. We assume that the gluino and the other squarks are heavy

³Although gluon radiation at NLO leads to a small shift in the stop p_T distribution to lower p_T values [150, 149], we do not expect this shift to affect our analysis in any significant way.

enough that they do not affect the NLO cross section. This is already the case for gluino and squark masses above about 200 GeV [149].

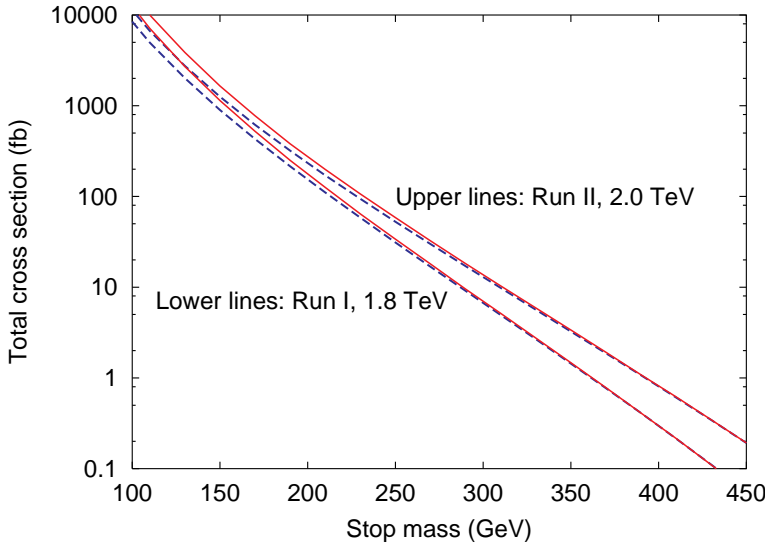


Figure 5.1: LO (dashed) and NLO (solid) cross sections for stop pair production in $p\bar{p}$ collisions at Tevatron Run I (1.8 TeV) and Run II (2.0 TeV), from PROSPINO [150, 149]. Cross sections are evaluated at the scale $\mu = m_{\tilde{t}}$.

Top squarks can also be produced via cascade decays of heavier supersymmetric particles, with a highly model dependent rate. To be conservative, we assume that the masses of the heavier supersymmetric particles are large enough that their production rate at Tevatron energies can be neglected.

5.5 Previous studies of stops at Run II

A number of previous studies have considered the prospects for stop discovery at Run II of the Tevatron, which we summarize here. In general, the most detailed SUSY studies have been done in the context of supergravity; in this case SUSY is broken at the Planck scale so that the gravitino plays no role in the collider phenomenology. Then the lightest neutralino is the LSP and ends all superparticle decay chains. The reach of the Tevatron for a number of stop decay modes has been analyzed in Refs. [152, 153]. The signal depends on the decay chain, which in turn depends on the relative masses

of various SUSY particles. For sufficiently heavy stops, the decay $\tilde{t} \rightarrow t\tilde{\chi}_1^0$ will dominate. This channel is of limited use at Run II because the stop pair production cross section falls rapidly with increasing stop mass, and this channel requires $m_{\tilde{t}} > m_t + m_{\tilde{\chi}_1^0}$, which is quite heavy for the Tevatron in the case of minimal supergravity.⁴ For lighter stops, if a chargino is lighter than the stop then $\tilde{t} \rightarrow b\tilde{\chi}_1^+$ tends to dominate (followed by the decay of the chargino). The details of the signal depend on the Higgsino content of $\tilde{\chi}_1^+$. If $\tilde{\chi}_1^+$ has a mass larger than $m_{\tilde{t}} - m_b$, the previous decay does not occur and the three-body decay $\tilde{t} \rightarrow bW^+\tilde{\chi}_1^0$ dominates; this decay proceeds through the exchange of a virtual top quark, chargino, or bottom squark. If the stop is too light to decay into an on-shell W boson and $\tilde{\chi}_1^0$, then the flavor-changing decay $\tilde{t} \rightarrow c\tilde{\chi}_1^0$ tends to dominate. Finally, if a sneutrino or slepton is light, then $\tilde{t} \rightarrow b\ell^+\tilde{\nu}_\ell$ or $\tilde{t} \rightarrow b\tilde{\ell}^+\nu_\ell$, respectively, will occur (followed by the decays of the slepton or the sneutrino, if it is not the LSP). At Run II with 2 (20) fb^{-1} of total integrated luminosity, in the context of minimal supergravity one can probe stop masses up to 160 (200) GeV in the case of the flavor changing decay, while stop masses as high as 185 (260) GeV can be probed if the stop decays into a bottom quark and a chargino [153]. A similar reach holds in the case of a light sneutrino [153] and in the case of large $\tan\beta$ when the stop can decay into $b\tau\nu\tilde{\chi}_1^0$ [154].

One can also search for stops in the decay products of other SUSY particles [153]. In top decays, the process $t \rightarrow \tilde{t}\tilde{g}$ is already excluded because of the existing lower bound on the gluino mass⁵. Other possibilities are $\tilde{\chi}^- \rightarrow b\tilde{t}^*$ and $\tilde{g} \rightarrow t\tilde{t}^*$. Finally, the decays $\tilde{b} \rightarrow \tilde{t}W^-$ and $\tilde{t}H^-$ have to compete with the preferred decay, $\tilde{b} \rightarrow b\tilde{\chi}_1^0$, and so may have small branching ratios (depending on the masses of \tilde{t} , \tilde{b} , $\tilde{\chi}_1^0$ and H^-). The signals for these processes at the Tevatron Run II have been considered in minimal supergravity in Ref. [153].

If R-parity violation is allowed, then single stop production can occur via the fusion of two quarks. Single stop production is kinematically favored compared to stop pair production and offers the opportunity to measure R-parity violating couplings. This has been considered for the Tevatron in Ref. [157], which showed that the stop could be discovered at Run II for masses below about 400 GeV provided that the R-parity violating coupling

⁴In low-energy SUSY breaking scenarios, however, the mass range $m_{\tilde{t}} > m_t + m_{\tilde{\chi}_1^0}$ is interesting at Tevatron energies because the distinctive signal allows backgrounds to be reduced to a very low level, as we will show.

⁵The bound on the gluino mass is, however, model dependent. Under certain conditions, an allowed window exists for gluino masses below the gauge boson masses [155, 156].

$\lambda'' > 0.02 - 0.1$ and that the stop decays via $\tilde{t}_1 \rightarrow b\tilde{\chi}_1^+$ (followed by $\tilde{\chi}_1^+ \rightarrow l^+\nu_l\tilde{\chi}_1^0$).

Relatively few studies have been done in the context of low-energy SUSY breaking with a gravitino LSP. A study of GMSB signals performed as part of the Tevatron Run II workshop [131] considered the decays of various SUSY particles as the NLSP. As discussed before, the NLSP in such models will decay directly to the gravitino and Standard Model particles. If the stop is the NLSP in such a model, then it will decay via $\tilde{t} \rightarrow t^{(*)}\tilde{G} \rightarrow bW^+\tilde{G}$ (for $m_{\tilde{t}} > m_b + m_W$). Note that because \tilde{G} is typically very light in such models, $m_{\tilde{t}} > m_W + m_b$ is sufficient for this decay to proceed with an on-shell W boson. Ref. [153] found sensitivity at Run II to this decay mode for stop masses up to 180 GeV with 4 fb^{-1} . This stop decay looks very much like a top quark decay; nevertheless, even for stop masses near m_t , such stop decays can be separated from top quark decays at the Tevatron using kinematic correlations among the decay products [158].

Finally, Ref. [133] considered general GMSB signals at the Tevatron of the form $\gamma\gamma \not{E}_T + X$. The authors of Ref. [133] provide an analysis of the possible bounds on the stop mass coming from the Run I Tevatron data. They analyze the stop decay mode into a charm quark and a neutralino, and also possible three body decays, by scanning over a sample of models. They conclude that stop masses smaller than 140 GeV can be excluded already by the Run I Tevatron data within low energy supersymmetry breaking models independent of the stop decay mode, assuming that $m_{\tilde{\chi}_1^0} > 70 \text{ GeV}$.

5.6 Top squark decay branching ratios

The decay properties of the lighter stop depend on the supersymmetric particle spectrum. Of particular relevance are the mass splittings between the stop and the lightest chargino, neutralino and bottom squark. In our analysis, we assume that the charginos and bottom squarks are heavier than the lighter stop, so that the on-shell decays $\tilde{t} \rightarrow bW$ and $\tilde{t} \rightarrow \tilde{\chi}^+ b$ are kinematically forbidden. Then the details of the stop decay depend on the mass splitting between the stop and the lightest neutralino. If $m_{\tilde{t}} < m_W + m_b + m_{\tilde{\chi}_1^0}$, two decay modes are kinematically accessible:

1. the flavor-changing (FC) two-body decay $\tilde{t} \rightarrow c\tilde{\chi}_1^0$. This two-body decay proceeds through a flavor-changing loop involving W^+ , H^+ or

$\tilde{\chi}^+$ exchange or through a tree-level diagram with a $\tilde{t} - \tilde{c}$ mixing mass insertion;

2. the four-body decay via a virtual W boson, $\tilde{t} \rightarrow W^{+*} b \tilde{\chi}_1^0 \rightarrow jjb \tilde{\chi}_1^0$ or $\ell\nu b \tilde{\chi}_1^0$ [159].

The branching ratio of the stop decay into charm and neutralino strongly depends on the details of the supersymmetry breaking mechanism. In models with no flavor violation at the messenger scale, the whole effect is induced by loop effects and receives a logarithmic enhancement which becomes more relevant for larger values of the messenger mass. In the minimal supergravity case, the two-body FC decay branching ratio tends to be the dominant one. In the case of low energy supersymmetry breaking, this is not necessarily the case. Since the analysis of the four-body decay process is very similar to the three-body decay described below for larger mass splittings between the stop and the lighter neutralino, here we shall analyze only the case in which the two-body FC decay $\tilde{t} \rightarrow c \tilde{\chi}_1^0$ is the dominant one whenever $m_{\tilde{t}} < m_W + m_b + m_{\tilde{\chi}_1^0}$.

For larger mass splittings, so that $m_W + m_b + m_{\tilde{\chi}_1^0} < m_{\tilde{t}} < m_t + m_{\tilde{\chi}_1^0}$, the three-body decay $\tilde{t} \rightarrow W^+ b \tilde{\chi}_1^0$ becomes accessible, with $\tilde{\chi}_1^0 \rightarrow \gamma \tilde{G}$. This stop decay proceeds through a virtual top quark, virtual charginos, or virtual sbottoms. Quite generally, this 3-body decay will dominate over the 2-body FC decay in this region of phase space.

For still heavier stops, $m_{\tilde{t}} > m_t + m_{\tilde{\chi}_1^0}$, the two-body tree-level decay mode $\tilde{t} \rightarrow t \tilde{\chi}_1^0$ becomes kinematically accessible and will dominate. Although the 3-body and 2-body FC decays are still present, their branching ratios are strongly suppressed.

Let us emphasize that, since the bino is an admixture of the zino and the photino, a pure bino neutralino can decay into either $\gamma \tilde{G}$ or $Z \tilde{G}$ (see Eq. 5.4). If the lightest neutralino is a mixture of bino and wino components, then the relative zino and photino components can be varied arbitrarily, leading to a change in the relative branching ratios to $\gamma \tilde{G}$ and $Z \tilde{G}$. If the lightest neutralino contains a Higgsino component, then the decay to $h^0 \tilde{G}$ is also allowed. We show in Fig. 5.2 the branching ratio of the lightest neutralino into $\gamma \tilde{G}$ as a function of its mass and Higgsino content.

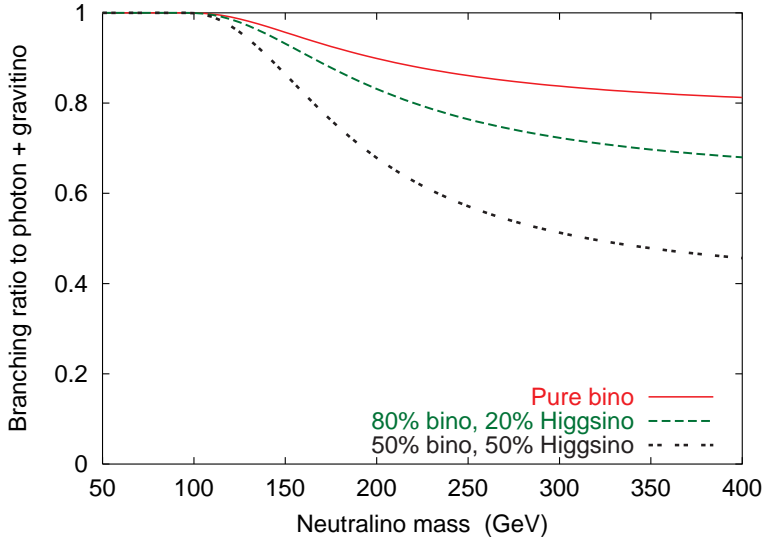


Figure 5.2: Branching ratio for the decay of the lightest neutralino into a photon and a gravitino as a function of the neutralino mass. Shown are the branching ratio if the neutralino is a pure bino (solid line) and for 20% and 50% Higgsino admixtures (long and short dashed lines, respectively) assuming that $m_{h^0} = 120$ GeV and that the other MSSM Higgs bosons are very heavy. For the Higgsino admixture in the lightest neutralino, we choose the \tilde{H}_1 – \tilde{H}_2 mixing so that the field content is aligned with that of h^0 and the longitudinal component of the Z boson in order to minimize the branching ratio to photons.

5.7 Top squark signals in low-energy SUSY breaking

As discussed in the previous section, the decay properties of the lighter stop depend primarily on the mass splitting between the stop and the lightest neutralino. In this section, we proceed with the phenomenological analysis of the signatures of top squark production associated with the different decay modes. In Sec. 5.7.1 we shall analyze the signatures associated with the two-body FC decay, which after the neutralino decay leads to $\tilde{t} \rightarrow c\gamma\tilde{G}$. In Sec. 5.7.2 we shall analyze the signatures associated with the three-body decay, which after neutralino decay leads to $\tilde{t} \rightarrow bW^+\gamma\tilde{G}$. The two-body decay $\tilde{t} \rightarrow t\tilde{\chi}_1^0$, which typically dominates for $m_{\tilde{t}} > m_t + m_{\tilde{\chi}_1^0}$, leads to the

same final state as the three-body decay and therefore the discussion of this case will be included in Sec. 5.7.2. Finally, in Sec. 5.7.3 we consider the possibility that stops are produced in the decays of top quarks.

5.7.1 Two-body FC decay: $\tilde{t} \rightarrow c\gamma\tilde{G}$

With the stop undergoing the aforementioned decay, the final state consists of a pair each of charm jets, photons and (invisible) gravitinos. As we will show below, the backgrounds to this process are small enough that we need not require charm tagging. Thus the signal consists of

$$2(\text{jets}) + 2\gamma + \cancel{E}_T.$$

The selection criteria we adopt are:

1. each event must contain two jets and two photons, each of which should have a minimum transverse momentum ($p_T > 20$ GeV) and be contained in the pseudorapidity range $-2.5 < \eta < 2.5$;
2. the jets and the photons should be well separated from each other; namely,

$$\delta R_{jj} > 0.7, \quad \delta R_{\gamma\gamma} > 0.3, \quad \delta R_{j\gamma} > 0.5$$

where $\delta R^2 = \delta\eta^2 + \delta\phi^2$, with $\delta\eta$ ($\delta\phi$) denoting the difference in pseudorapidity (azimuthal angle) of the two entities under consideration;

3. the invariant mass of the two jets should be sufficiently far away from the W - and Z -masses:
 $m_{jj} \notin (75 \text{ GeV}, 95 \text{ GeV});$
4. each event should be associated with a minimum missing transverse momentum ($\cancel{p}_T > 30$ GeV).

The photons and jets in signal events tend to be very central; in particular, reducing the pseudorapidity cut for the two photons to $-2.0 < \eta < 2.0$ would reduce the signal by less than about 3%. (This change would reduce the background by a somewhat larger fraction.) Apart from ensuring observability, these selection criteria also serve to eliminate most of the backgrounds, which are listed in Table 5.1.

Background	Cross section after cuts	after γ ID
$jj\gamma\gamma Z, Z \rightarrow \nu\bar{\nu}$	~ 0.2 fb	~ 0.13 fb
$jj\gamma\nu\bar{\nu} + \gamma$ radiation	~ 0.002 fb	~ 0.001 fb
$bb\gamma\gamma, c\bar{c}\gamma\gamma$	$\lesssim 0.1$ fb	~ 0.06 fb
$jj\gamma\gamma$	~ 0.2 fb	~ 0.13 fb
Backgrounds with fake photons:		
$jj(ee \rightarrow \gamma\gamma)$	$\sim 5 \times 10^{-4}$ fb	$\sim 5 \times 10^{-4}$ fb
$jj\gamma(j \rightarrow \gamma)$	~ 0.8 fb	~ 0.8 fb
$jj(jj \rightarrow \gamma\gamma)$	~ 0.8 fb	~ 0.8 fb
Total	~ 2 fb	~ 2 fb

Table 5.1: Backgrounds to $\tilde{t}\tilde{t}^* \rightarrow jj\gamma\gamma \cancel{E}_T$. The photon identification efficiency is taken to be $\epsilon_\gamma = 0.8$ for each real photon. See text for details.

A primary source of background is the SM production of $jj\gamma\gamma\nu_i\bar{\nu}_i$ where the jets could have arisen from either quarks or gluons in the final state of partonic subprocesses. A full diagrammatic calculation would be very computer-intensive and is beyond the scope of this work. Instead, we consider the subprocesses that are expected to contribute the bulk of this particular background, namely $p\bar{p} \rightarrow 2j + 2\gamma + Z + X$ with the Z subsequently decaying into neutrinos. These processes are quite tractable and were calculated with the aid of the helicity amplitude program MADGRAPH [160]. On imposition of the abovementioned set of cuts, this background at the Run II falls to below ~ 0.2 fb.

An independent estimate of the $jj\gamma\gamma\nu_i\bar{\nu}_i$ background may be obtained through the consideration of the single-photon variant, namely $jj\gamma\nu_i\bar{\nu}_i$ production, a process that MADGRAPH can handle. After imposing the same kinematic cuts (other than requiring only one photon) as above, this process leads to a cross section of roughly 0.2 fb. Since the emission of a second hard photon should cost us a further power of α_{em} , the electromagnetic coupling constant, this background falls to innocuous levels. We include both this estimate and the one based on Z production from the previous paragraph in Table 5.1. Though a naive addition of both runs the danger of overcounting, this is hardly of any importance given the overwhelming dominance of one.

A second source of background is $b\bar{b}\gamma\gamma$ ($c\bar{c}\gamma\gamma$), with missing transverse energy coming from the semileptonic decay of one or both of the b (c) mesons.

In this case, though, the neutrinos tend to be soft due to the smallness of the b and c masses. Consequently, the cut on p_T serves to eliminate most of this background, leaving behind less than 0.1 fb. This could be further reduced (to $\lesssim 0.001$ fb) by vetoing events with leptons in association with jets. However, such a lepton veto would significantly impact the selection efficiency of our signal, which contains $c\bar{c}$, thereby reducing our overall sensitivity in this channel.

A third source of background is $jj\gamma\gamma$ production, in which the jet (light quark or gluon) and/or photon energies are mismeasured leading to a fake p_T . To simulate the effect of experimental resolution, we use a (very pessimistic) Gaussian smearing: $\delta E_j/E_j = 0.1 + 0.6/\sqrt{E_j(\text{GeV})}$ for the jets and $\delta E_\gamma/E_\gamma = 0.05 + 0.3/\sqrt{E_\gamma(\text{GeV})}$ for the photons.⁶ While the production cross section is much higher than that of any of the other backgrounds considered, the ensuing missing momentum tends to be small; in particular, our cut on \cancel{E}_T reduces this background by almost 99%.⁷ On imposition of our cuts, this fake background is reduced to ~ 0.2 fb.⁸

Finally, we consider the instrumental backgrounds from electrons or jets misidentified as photons. Based on Run I analyses [162] of electron pair production and taking the probability for an electron to fake a photon to be about 0.4%, we estimate the background due to electrons faking photons to be of order 5×10^{-4} fb. More important is the background in which a jet fakes a photon. Based on a Run I analysis [161] and taking the probability for a jet to fake a photon to be about 0.1%, we estimate the background due to $jjj\gamma$ in which one of the jets fakes a second photon to be about 0.8 fb. Similarly, we estimate that the background due to $jjjj$ in which two of the jets fake photons is somewhat smaller; to be conservative we take it to be of the same order, *i.e.*, 0.8 fb.

Having established that the backgrounds are small, let us now turn to the signal cross section that survives the cuts. In Fig. 5.3, we present these

⁶We have also performed similar smearing for the other background channels as well as for the signal. However, there it hardly is of any importance as far as the estimation of the total cross section is concerned.

⁷This reduction factor is in rough agreement with that found for $\gamma + j$ events in CDF Run I data in Ref. [161].

⁸We note that in the squark searches in supergravity scenarios the signal is $jj \cancel{E}_T$; in this case a similar background due to dijet production with fake p_T is present. This background is larger by two powers of α than the $jj\gamma\gamma$ background, yet it can still be reduced to an acceptable level by a relatively hard cut on p_T (see, *e.g.*, Ref. [153]).

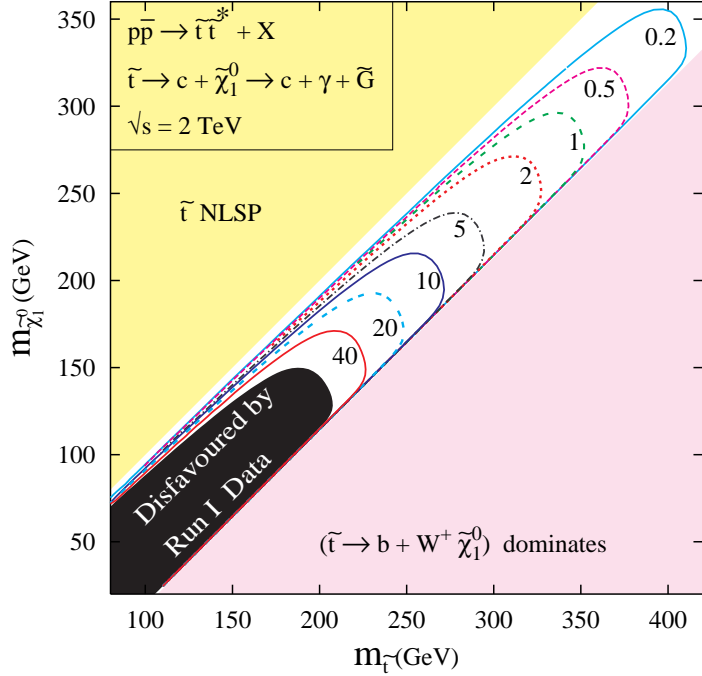


Figure 5.3: Cross sections in fb for stop pair production in Run II with $\tilde{t} \rightarrow c\gamma\tilde{G}$, after cuts. No efficiencies have yet been applied. The black area is excluded by non-observation of $jj\gamma\gamma \not{E}_T$ events in Run I.

as contours in the $m_{\tilde{t}}-m_{\tilde{\chi}_1^0}$ plane. We assume that the branching ratio of $\tilde{t} \rightarrow c\tilde{\chi}_1^0$ dominates in the region of parameter space that we consider here. The branching ratio of $\tilde{\chi}_1^0 \rightarrow \gamma\tilde{G}$ is taken from Fig. 5.2 assuming that $\tilde{\chi}_1^0$ is a pure bino.⁹ All our plots are made before detector efficiencies are applied. With a real detector, each photon is identified with about $\epsilon_\gamma = 80\%$ efficiency; thus the cross sections shown in Fig. 5.3 must be multiplied by $\epsilon_\gamma^2 = 0.64$ in order to obtain numbers of events.¹⁰ While the production cross sections are independent of the neutralino mass, the decay kinematics have a strong

⁹If $\tilde{\chi}_1^0$ is not a pure bino, its branching ratio to $\gamma\tilde{G}$ will typically be reduced somewhat when its mass is large (see Fig. 5.2). This will lead to a reduction of the signal cross section at large $m_{\tilde{\chi}_1^0}$ by typically a few tens of percent.

¹⁰The diphoton trigger efficiency is close to 100%, so we neglect it here.

dependence on $m_{\tilde{\chi}_1^0}$. For a given $m_{\tilde{t}}$, a small mass splitting between $m_{\tilde{t}}$ and $m_{\tilde{\chi}_1^0}$ would imply a soft charm jet, which would often fail to satisfy our selection criteria. This causes the gap between the cross section contours and the upper edge of the parameter space band that we are exploring in Fig. 5.3. This is further compounded at large $m_{\tilde{\chi}_1^0}$ by the fact that a large neutralino mass typically implies a smaller $\tilde{\chi}_1^0 \rightarrow \gamma \tilde{G}$ branching fraction (see Fig. 5.2). On the other hand, a small $m_{\tilde{\chi}_1^0}$ results in reduced momenta for the gravitino and the photon, once again resulting in a loss of signal; however, this is important only for $m_{\tilde{\chi}_1^0} \lesssim 70$ GeV, which is not relevant in this search channel.

The signal cross sections are fairly substantial. In particular, the dark area in Fig. 5.3 corresponds to a signal cross section of 50 fb or larger at Run I of the Tevatron. Taking into account the identification efficiency of 64% for the two photons, such a cross section would have yielded 3 signal events in the 100 pb^{-1} collected in Run I over a background of much less than 1 event. Run I can thus exclude this region at 95% confidence level. In particular, we conclude that Run I data excludes stop masses up to about 200 GeV, for large enough mass splitting between the stop and the neutralino. When the stop-neutralino mass splitting is small (*i.e.*, less than about 10 – 20 GeV), the charm quark jets become too soft and the signal efficiency decreases dramatically. For comparison, a DØ search [163] for inclusive $p\bar{p} \rightarrow \tilde{\chi}_2^0 + X$ with $\tilde{\chi}_2^0 \rightarrow \gamma \tilde{\chi}_1^0$ in the context of minimal supergravity yields a limit on the production cross section of about 1 pb for parent squark masses of order 150–200 GeV. Interpreting this in terms of stop pair production with $\tilde{\chi}_2^0 \rightarrow \gamma \tilde{\chi}_1^0$ reidentified as $\tilde{\chi}_1^0 \rightarrow \gamma \tilde{G}$ increases the signal efficiency by a factor of ~ 2.7 because every SUSY event now contains two photons [163]; the DØ analysis then yields a stop mass bound of about 180 GeV, in rough agreement with our result.¹¹ In addition, Ref. [133] projected a Run I exclusion of stops in this decay channel for masses below about 160–170 GeV, again in rough agreement with our result.

To claim a discovery at the 5σ level, one must observe a large enough number of events that the probability for the background to fluctuate up to that level is less than 5.7×10^{-7} . Because the number of expected background events in this analysis is small, we use Poisson statistics to find the number

¹¹Note, however, that the non-negligible mass of the LSP of about 35 GeV assumed in Ref. [163] leads to kinematics that differ significantly from those in our analysis, in which the gravitino is essentially massless.

of signal events required for a 5σ discovery. Taking the total background cross section to be 2 fb from Table 5.1, we show in Table 5.2 the expected maximum stop discovery mass reach at Tevatron Run II for various amounts of integrated luminosity.¹² In particular, with 4 fb^{-1} a stop discovery can be expected in this channel if $m_{\tilde{t}} < 285$ GeV, with S/B of more than 2/1.¹³ Including the effects of mixing in the composition of the lightest neutralino, a 50% reduction in the $\tilde{\chi}_1^0 \rightarrow \gamma \tilde{G}$ branching ratio compared to the pure bino case would reduce the stop mass reach by only about 20 GeV. For such a reduction to occur in the relevant neutralino mass range of about 200 – 250 GeV, the lightest neutralino would have to be less than half bino.

$\int \mathcal{L}$	B	S for a 5σ discovery	$\sigma_S \times \epsilon_\gamma^2$	Maximum stop mass reach
2 fb^{-1}	4	14	7.0 fb	265 GeV
4 fb^{-1}	8	18	4.5 fb	285 GeV
15 fb^{-1}	30	31	2.1 fb	310 GeV
30 fb^{-1}	60	42	1.4 fb	325 GeV

Table 5.2: Number of signal events (S) required for a 5σ stop discovery at Tevatron Run II in the $jj\gamma\gamma \not{E}_T$ channel and the corresponding signal cross section after cuts and efficiencies and maximum stop mass reach. We assume a photon identification efficiency of $\epsilon_\gamma = 0.80$. The number of background events (B) is based on a background cross section of 2 fb from Table 5.1.

5.7.2 Three-body decay: $\tilde{t} \rightarrow bW^+\gamma\tilde{G}$

For a large enough splitting between the stop and neutralino masses, the signature of stop pair production would be¹⁴ $jjWW\gamma\gamma \not{E}_T$. In this analysis,

¹²The cross sections and numbers of events required for discovery are quoted in terms of integrated luminosities at a single detector. If data from the CDF and DØ detectors are combined, the integrated luminosity of the machine is effectively doubled.

¹³For comparison, in the case of minimal supergravity a reach of $m_{\tilde{t}} < 180$ GeV can be expected in the $\tilde{t} \rightarrow c\tilde{\chi}_1^0$ channel with 4 fb^{-1} at Tevatron Run II; the same reach is obtained in low-energy SUSY breaking scenarios in which the stop is the NLSP rather than the neutralino [153]. In both of these cases, the signal consists of $jj \not{E}_T$, with no photons in the final state.

¹⁴The backgrounds are again small enough after cuts in this channel that we do not need to tag the b quarks. In the case of a discovery, one could imagine tagging the b quarks

we consider only the dominant hadronic decay mode of both W bosons.

This decay mode of the stop proceeds via three Feynman diagrams, involving an intermediate off-shell top quark, chargino or sbottom. We use the full decay matrix elements as given in Ref. [164]. Although this introduces several additional parameters into the analysis, a few simplifying assumptions may be made without becoming too model dependent. For example, assuming that the lightest stop is predominantly the superpartner of the right-handed top-quark (\tilde{t}_R), eliminates the sbottom exchange diagram altogether. Even if the stop contains a mixture of \tilde{t}_R and \tilde{t}_L , under our assumption that the lighter stop is the next-to-lightest Standard Model superpartner, the sbottom exchange diagram will be suppressed by the necessarily larger sbottom mass. As for the chargino exchange, the wino component does not contribute for a \tilde{t}_R decay. Thus the chargino contribution is dominated by its Higgsino component. Furthermore, if we concentrate on scenarios with large values of the supersymmetric mass parameter μ and of the wino mass parameter (in which case the charginos are heavy and the neutralino is almost a pure bino), the chargino exchange contribution is also suppressed and the dominant decay mode is via the diagram involving an off-shell top quark. To simplify our numerical calculations, we have then assumed that only this diagram contributes to the stop decay matrix element. We have checked for a few representative points though, that the inclusion of the sbottom and chargino diagrams does not significantly change the signal efficiency after cuts as long as we require that $m_{\tilde{b}}, m_{\tilde{\chi}^+} > m_{\tilde{t}}$.

As the W bosons themselves decay, it might be argued that their polarization information needs to be retained. However, since we do not consider angular correlations between the decay products, this is not a crucial issue; the loss of such information at intermediate steps in the decay does not lead to a significant change in the signal efficiency after cuts. This is particularly true for the hadronic decay modes of the W , for which the profusion of jets frequently leads to jet overlap, thereby obscuring detailed angular correlations. It is thus safe to make the approximation of neglecting the polarization of the W bosons in their decay distributions, and we do so in our analysis.

Before we discuss the signal profile and the backgrounds, let us elaborate on the aforementioned jet overlapping. With six quarks in the final state, some of the resultant jets will very often be too close to each other to be recognizable as coming from different partons. We simulate this as follows.

and reconstructing the W bosons in order to help identify the discovered particle.

We count a final-state parton (quark or gluon) as a jet only if it has a minimum energy of 5 GeV and lies within the pseudorapidity range $-3 < \eta < 3$. We then merge any two jets that fall within a δR separation of 0.5; the momentum of the resultant jet is the sum of the two momenta. We repeat this process iteratively, starting with the hardest jet. Our selection cuts are then applied to the (merged) jets that survive this algorithm.

The signal thus consists of:

$$n \text{ jets} + 2\gamma + \cancel{E}_T \quad (n \leq 6)$$

Hence, all of the SM processes discussed in the previous section yield backgrounds to this signal when up to four additional jets are radiated. Now, the radiation of each hard and well separated jet suppresses the cross section by a factor of order $\alpha_s \simeq 0.118$. Then, since the $jj\gamma\gamma \cancel{E}_T$ backgrounds are already quite small after the cuts applied in the previous section (see Table 5.1), the backgrounds with additional jets are expected to be still smaller.¹⁵

There exists a potential exception to the last assertion, namely the background due to $t\bar{t}\gamma\gamma$ production. To get an order of magnitude estimate, the cross section for $t\bar{t}$ production at Tevatron Run II is 8 pb [165]. If both of the photons are required to be energetic and isolated, we would expect a suppression by a factor of order α_{em}^2 , leading to a cross section of the order of 0.5 fb. This cross section is large enough that we need to consider it carefully.

If both W bosons were to decay hadronically, then a sufficiently large missing transverse energy can only come from a mismeasurement of the jet or photon energies. As we have seen in the previous section, this missing energy is normally too small to pass our cuts, thereby suppressing the background. If one of the W bosons decays leptonically, however, it will yield a sizable amount of \cancel{E}_T . This background can be largely eliminated by requiring that no lepton (e or μ) is seen in the detector. This effectively eliminates the W decays into e or μ or decays to τ followed by leptonic τ decays; the remaining background with hadronic τ decays is naturally quite small without requiring additional cuts. Considerations such as these lead us to an appropriate choice of criteria for an event to be selected:

1. At least four jets, each with a minimum transverse momentum $p_{Tj} > 20$ GeV and contained in the pseudorapidity interval of $-3 < \eta_j < 3$. Any

¹⁵For the backgrounds in which one or both of the photons are faked by misidentified jets, we have taken into account the larger combinatoric factor that arises when more jets are present to be misidentified.

two jets must be separated by $\delta R_{jj} > 0.7$. As most of the signal events do end up with 4 or more energetic jets (the hardest jets coming typically from the W boson decays), this does not cost us in terms of the signal, while reducing the QCD background significantly. In addition, the $t\bar{t}\gamma\gamma$ events with both W 's decaying leptonically are reduced to a level of order 10^{-4} fb by this requirement alone.

2. Two photons, each one with $p_{T\gamma} > 20$ GeV and pseudorapidity $-2.5 < \eta_\gamma < 2.5$. The two photons must be separated by at least $\delta R_{\gamma\gamma} > 0.3$.
3. Any photon-jet pair must have a minimum separation of $\delta R_{j\gamma} > 0.5$.
4. A minimum missing transverse energy $\cancel{E}_T > 30$ GeV.
5. The event should not contain any isolated lepton with $p_T > 10$ GeV and lying within the pseudorapidity range $-3 < \eta < 3$.

As in the previous section, the cut on \cancel{E}_T serves to eliminate most of the background events with only a fake missing transverse momentum (arising out of mismeasurement of jet energies). In association with the lepton veto, it also eliminates the bulk of events in which one of the W bosons decays leptonically (including the τ channel). A perusal of Table 5.3, which summarizes the major backgrounds after cuts, convinces us that the backgrounds to this channel are very small, in fact much smaller than those for the previous channel.

The signal cross section after cuts (but before photon identification efficiencies) is shown in Fig. 5.4 as a function of the stop and $\tilde{\chi}_1^0$ masses. We assume that the branching ratio of $\tilde{t} \rightarrow bW\tilde{\chi}_1^0$ dominates in the region of parameter space under consideration. The branching ratio of $\tilde{\chi}_1^0 \rightarrow \gamma\tilde{G}$ is again taken from Fig. 5.2 assuming that $\tilde{\chi}_1^0$ is a pure bino. The signal efficiency after cuts is about 45%. For small neutralino masses ($m_{\tilde{\chi}_1^0} \lesssim 50$ GeV), though, both the photons and the gravitinos (\cancel{E}_T) tend to be soft, leading to a decrease in the signal efficiency. For small stop masses (as well as for large stop masses when the stop-neutralino mass difference is small), on the other hand, the jets are soft leading to a suppression of the signal cross section after cuts. As one would expect, both of these effects are particularly pronounced in the contours corresponding to large values of the cross section. The additional distortion of the contours for large neutralino masses can, once again, be traced to the suppression of the $\tilde{\chi}_1^0 \rightarrow \gamma\tilde{G}$ branching fraction (see Fig. 5.2).

Background	Cross section after cuts	after γ ID
$(jj\gamma\gamma Z, Z \rightarrow \nu\bar{\nu}) + 2j$	$\sim 0.003 \text{ fb}$	$\sim 0.002 \text{ fb}$
$jj\nu\bar{\nu}\gamma\gamma + 2j$	$\sim 3 \times 10^{-5} \text{ fb}$	$\sim 2 \times 10^{-5} \text{ fb}$
$(bb\gamma\gamma, c\bar{c}\gamma\gamma) + 2j$	$\sim 0.001 \text{ fb}$	$\sim 0.0006 \text{ fb}$
$jj\gamma\gamma + 2j$	$\lesssim 0.003 \text{ fb}$	$\lesssim 0.002 \text{ fb}$
$t\bar{t}\gamma\gamma, WW \rightarrow jjjj$	$\lesssim 10^{-4} \text{ fb}$	$\lesssim 10^{-4} \text{ fb}$
$t\bar{t}\gamma\gamma, WW \rightarrow jj\ell\nu, \ell = e, \mu, \text{ or } \tau \rightarrow \ell$	$\sim 0.001 \text{ fb}$	$\sim 0.0006 \text{ fb}$
$t\bar{t}\gamma\gamma, WW \rightarrow jj\tau\nu, \tau \rightarrow j$	$\lesssim 0.01 \text{ fb}$	$\lesssim 0.006 \text{ fb}$
Backgrounds with fake photons:		
$jj(ee \rightarrow \gamma\gamma) + 2j$	$\sim 7 \times 10^{-6} \text{ fb}$	$\sim 7 \times 10^{-6} \text{ fb}$
$jj\gamma(j \rightarrow \gamma) + 2j$	$\sim 0.02 \text{ fb}$	$\sim 0.02 \text{ fb}$
$jj(jj \rightarrow \gamma\gamma) + 2j$	$\sim 0.03 \text{ fb}$	$\sim 0.03 \text{ fb}$
Total	$\lesssim 0.07 \text{ fb}$	$\sim 0.06 \text{ fb}$

Table 5.3: Backgrounds to $\tilde{t}\tilde{t}^* \rightarrow jjWW\gamma\gamma \not{E}_T$ with both W bosons decaying hadronically. The photon identification efficiency is taken to be $\epsilon_\gamma = 0.8$ for each real photon. See text for details.

The non-observation of $jjWW\gamma\gamma \not{E}_T$ events at Run I of the Tevatron already excludes the region of parameter space shown in black in Fig. 5.4. As in the previous section, in this excluded region at least 3 signal events would have been produced after cuts and detector efficiencies in the 100 pb^{-1} of Run I data, with negligible background. In particular, Run I data excludes stop masses below about 200 GeV, for neutralino masses larger than about 50 GeV.

We show in Table 5.4 the expected maximum stop discovery mass reach at Tevatron Run II for various amounts of integrated luminosity.¹⁶ In particular, with 4 fb^{-1} , a stop discovery can be expected in this channel if $m_{\tilde{t}} < 320 \text{ GeV}$.¹⁷ If the lightest neutralino is not a pure bino, the reach at large neutralino masses will be reduced. However, the maximum stop mass reach quoted here will not be affected, because it occurs for $m_{\tilde{\chi}_1^0} \sim 50 - 100 \text{ GeV}$;

¹⁶Again, if data from the CDF and DØ detectors are combined, the integrated luminosity of the machine is effectively doubled.

¹⁷For comparison, in the case of minimal supergravity a reach of $m_{\tilde{t}} < 190 \text{ GeV}$ can be expected in the $\tilde{t} \rightarrow bW\tilde{\chi}_1^0$ channel with 4 fb^{-1} at Tevatron Run II [153].

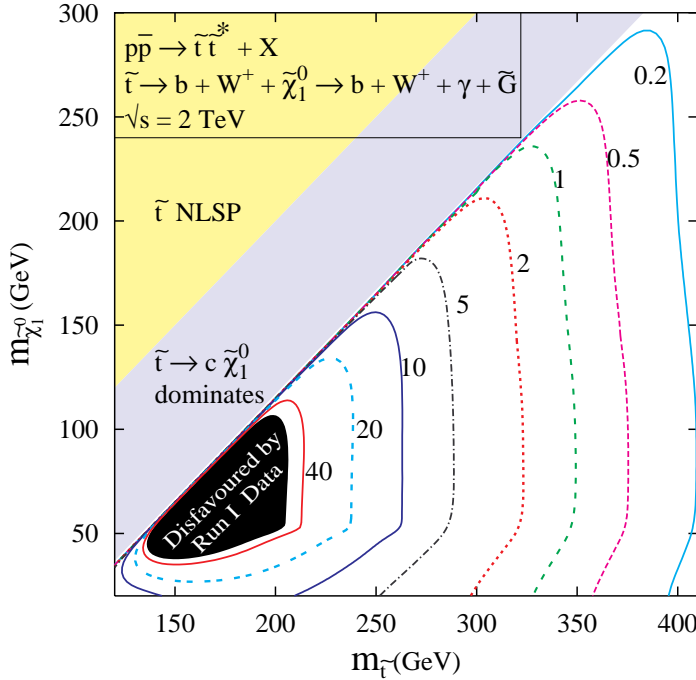


Figure 5.4: Cross section in fb for stop pair production with $\tilde{t} \rightarrow bW\gamma\tilde{G}$, after cuts. Both W bosons are assumed to decay hadronically. The black area is excluded by non-observation of $jjWW\gamma\gamma \not{E}_T$ events in Run I.

in this mass range the lightest neutralino decays virtually 100% of the time to $\gamma\tilde{G}$ due to the kinematic suppression of all other possible decay modes, unless its photino component is fine-tuned to be tiny.

Including a separate analysis of stop production and decay with one or more of the W bosons decaying leptonically would yield an increase in the overall signal statistics; however, we do not expect this increase to dramatically alter the stop discovery reach.

5.7.3 Stop production in top quark decays

If $m_{\tilde{t}} + m_{\tilde{\chi}_1^0} < m_t$, then stops can be produced in the decays of top quarks. As we will explain here, most of the parameter space in this region is excluded by the non-observation of stop events via direct production or in top quark decays at Run I of the Tevatron. However, some interesting parameter space

$\int \mathcal{L}$	B	S for a 5σ discovery	$\sigma_S \times \epsilon_\gamma^2$	Maximum stop mass reach
2 fb^{-1}	0.1	5	2.5 fb	300 GeV
4 fb^{-1}	0.2	6	1.5 fb	320 GeV
15 fb^{-1}	0.9	8	0.53 fb	355 GeV
30 fb^{-1}	1.8	10	0.33 fb	375 GeV

Table 5.4: Number of signal events (S) required for a 5σ stop discovery at Tevatron Run II in the $jjWW\gamma\gamma$ \cancel{E}_T channel and the corresponding signal cross section after cuts and efficiencies and maximum stop mass reach. We take $\epsilon_\gamma = 0.80$. The number of background events (B) is based on a background cross section of 0.06 fb from Table 5.3.

for this decay remains allowed after Run I, especially if the lighter stop is predominantly \tilde{t}_L .

For $m_{\tilde{t}} < m_b + m_W + m_{\tilde{\chi}_1^0}$, so that the stop decays via $\tilde{t} \rightarrow c\tilde{\chi}_1^0$, the region in which $t \rightarrow \tilde{t}\tilde{\chi}_1^0$ is possible is almost entirely excluded by the limit on stop pair production at Run I, as shown in Fig. 5.3. A sliver of parameter space in which the stop-neutralino mass splitting is smaller than about 10 GeV remains unexcluded. For $m_{\tilde{t}} > m_b + m_W + m_{\tilde{\chi}_1^0}$, so that the stop decays via $\tilde{t} \rightarrow bW\tilde{\chi}_1^0$, the signal efficiency in the search for direct stop production is degraded for light neutralinos with masses below about 50 GeV and for stops lighter than about 150 GeV . This prevents Run I from being sensitive to stop pair production in the region of parameter space in which top quark decays to stops are possible with the stops decaying to $bW\tilde{\chi}_1^0$, as shown in Fig. 5.4. In what follows, we focus on this latter region of parameter space.

As discussed before, if the lightest neutralino is mostly bino, the constraints on its mass are model-dependent. The constraints from Tevatron Run I are based on inclusive chargino and neutralino production [133, 166] under the assumption of gaugino mass unification; the cross section is dominated by production of $\tilde{\chi}_1^\pm \tilde{\chi}_1^\mp$ and $\tilde{\chi}_1^\pm \tilde{\chi}_2^0$. If the assumption of gaugino mass unification is relaxed, then Run I puts no constraint on the mass of $\tilde{\chi}_1^0$. At LEP, while the pair production of a pure bino leads to an easily detectable diphoton signal, it proceeds only via t -channel selectron exchange. The mass bound on a bino $\tilde{\chi}_1^0$ from LEP thus depends on the selectron mass [137]. In particular, for selectrons heavier than about 600 GeV , bino masses down to 20 GeV are still allowed by the LEP data. If $\tilde{\chi}_1^0$ contains a Higgsino admix-

ture, it couples to the Z and can be pair-produced at LEP via Z exchange. For an NLSP with mass between 20 and 45 GeV, as will be relevant in our top quark decay analysis, the LEP search results limit the \tilde{H}_2 component to be less than 1%. Such a small \tilde{H}_2 admixture has no appreciable effect on the top quark partial width to $\tilde{t}\tilde{\chi}_1^0$. We thus compute the partial width for $t \rightarrow \tilde{t}\tilde{\chi}_1^0$ assuming that the neutralino is a pure bino. Taking the lighter stop to be $\tilde{t}_1 = \tilde{t}_L \cos \theta_{\tilde{t}} + \tilde{t}_R \sin \theta_{\tilde{t}}$, we find,

$$\Gamma(t \rightarrow \tilde{t}_1 \tilde{B}) = \left[\frac{4}{9} \sin^2 \theta_{\tilde{t}} + \frac{1}{36} \cos^2 \theta_{\tilde{t}} \right] \frac{\alpha}{\cos^2 \theta_W} \frac{E_{\tilde{B}}}{m_t} \sqrt{E_{\tilde{B}}^2 - m_{\tilde{B}}^2}, \quad (5.10)$$

where $E_{\tilde{B}} = (m_t^2 + m_{\tilde{B}}^2 - m_{\tilde{t}}^2)/2m_t$. The numerical factors in the square brackets in Eq. 5.10 come from the hypercharge quantum numbers of the two stop electroweak eigenstates. Clearly, the partial width is maximized if the lighter stop is a pure \tilde{t}_R state; it drops by a factor of 16 if the lighter stop is a pure \tilde{t}_L state. In any case, the branching ratio for $t \rightarrow \tilde{t}\tilde{B}$ does not exceed 6% for $m_{\tilde{t}} > 100$ GeV and $m_{\tilde{\chi}_1^0} > 20$ GeV.¹⁸

The signal from top quark pair production followed by one top quark decaying as in the Standard Model and the other decaying to $\tilde{t}\tilde{\chi}_1^0$, followed by the stop 3-body decay and the neutralino decays to $\gamma\tilde{G}$, is $bbWW\gamma\gamma \not{E}_T$. This signal is the same (up to kinematics) as that from stop pair production in the 3-body decay region. As in the case of stop pair production followed by the 3-body decay, we expect that the background to this process can be reduced to a negligible level. Run I can then place 95% confidence level exclusion limits on the regions of parameter space in which 3 or more signal events are expected after cuts and efficiencies are taken into account. Using the Run I top quark pair production cross section of 6 pb [165] and a total luminosity of 100 pb^{-1} , we compute the number of signal events as a function of the stop and neutralino masses and the stop composition, assuming various values of the signal efficiency after cuts and detector efficiencies. If $\tilde{t}_1 = \tilde{t}_R$, then Run I excludes most of the parameter space below the kinematic limit for this decay even for fairly low signal efficiency $\sim 20\%$, as shown in Fig. 5.5. If $\tilde{t}_1 = \tilde{t}_L$, on the other hand, the signal cross section is much smaller and Run I gives no exclusion unless the signal efficiency is larger than 75%, which would already be unfeasible including only the identification efficiencies for the two photons; even 100% signal efficiency would only yield an exclusion up to $m_{\tilde{t}} \simeq 118$ GeV.

¹⁸For neutralino masses below m_Z , as are relevant here, the branching ratio into $\gamma\tilde{G}$ is virtually 100% (see Fig. 5.2), almost independent on the neutralino composition.

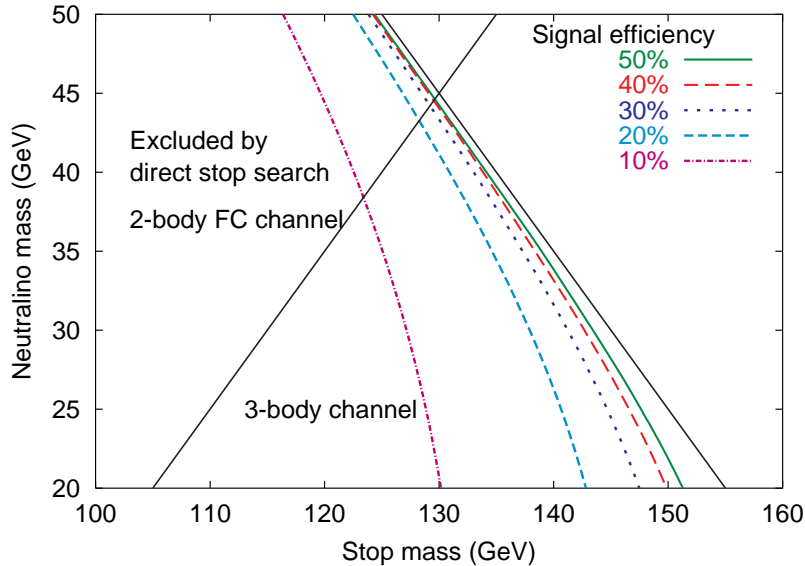


Figure 5.5: 95% confidence level exclusion limits for top quark decays to stops from Run I for various signal efficiencies, in the case that $\tilde{t}_1 = \tilde{t}_R$, which gives the largest event rates. The area to the left of the curves is excluded. The case $\tilde{t}_1 = \tilde{t}_L$ gives no exclusion for the signal efficiencies considered and is not shown here. The solid line from upper left to lower right is the kinematic limit for $m_t = 175$ GeV. The solid line from upper right to lower left separates the regions in which the 2-body FC decay and the 3-body decay of the stop dominate.

At Run II, the top quark pair production cross section is 8 pb [165] and the expected total luminosity is considerably higher. This allows top quark decays to $\tilde{t}\tilde{\chi}_1^0$ to be detected for stop and neutralino masses above the Run I bound. For $\tilde{t}_1 = \tilde{t}_R$, top quark decays to stops will be probed virtually up to the kinematic limit, even with low signal efficiency $\sim 10\%$ and only 2 fb^{-1} of integrated luminosity. If $\tilde{t}_1 = \tilde{t}_L$, so that the signal event rate is minimized, top quark decays to stops would be discovered up to within 10 GeV of the kinematic limit for signal efficiencies $\gtrsim 20\%$ and 4 fb^{-1} of integrated luminosity (see Fig. 5.6). In this region of parameter space, stops would also be discovered in Run II with less than 2 fb^{-1} via direct stop pair production (see Fig. 5.4).

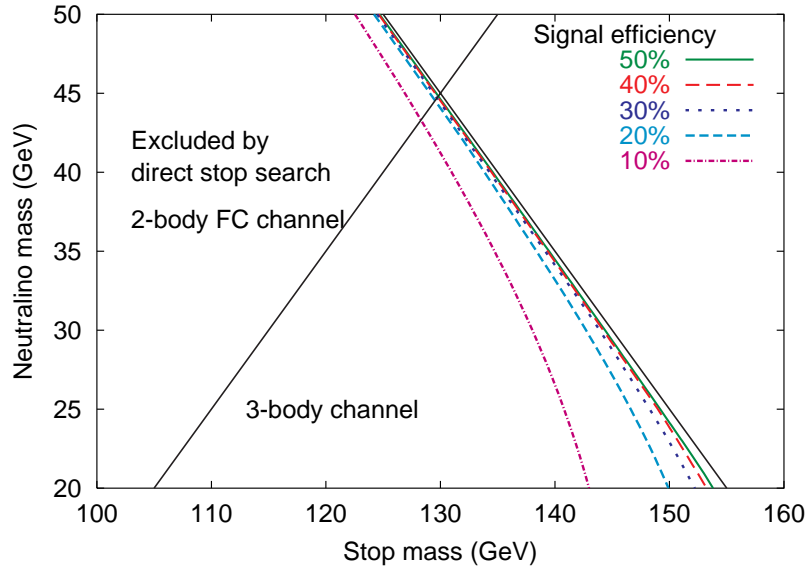


Figure 5.6: 5σ discovery contours for top quark decays to stops at Run II with 4 fb^{-1} for various signal efficiencies, in the case that $\tilde{t}_1 = \tilde{t}_L$, which gives the smallest event rates. The case $\tilde{t}_1 = \tilde{t}_R$ would be discovered virtually up to the kinematic limit even with 10% signal efficiency, and is not shown here. The solid lines are as in Fig. 5.5.

5.8 Ten degenerate squarks

Having concentrated until now on the production and decay of the top squark, let us now consider the other squarks. In the most general MSSM, the spectrum is of course quite arbitrary. However, low energy constraints [167] from flavor changing neutral current processes demand that such squarks be nearly mass degenerate, at least those of the same chirality. Interestingly, in many theoretical scenarios, such as the minimal gauge mediated models, this mass degeneracy between squarks of the same chirality happens naturally; in addition the mass splitting between the left-handed and right-handed squarks associated with the five light quarks turns out to be small. For simplicity, then, we will work under the approximation that all of these 10 squarks (namely, $\tilde{u}_{L,R}$, $\tilde{d}_{L,R}$, $\tilde{c}_{L,R}$, $\tilde{s}_{L,R}$ and $\tilde{b}_{L,R}$) are exactly degenerate.

5.8.1 Production at Tevatron Run II

While the cross sections for the individual pair-production of the $\tilde{c}_{L,R}$, $\tilde{s}_{L,R}$ and $\tilde{b}_{L,R}$ are essentially the same as that for a top-squark of the same mass, the situation is more complicated for squarks of the first generation. The latter depend sensitively on the gluino mass because of the presence of t -channel diagrams. Moreover, processes such as $\bar{u}u \rightarrow \tilde{u}_L \tilde{u}_R^*$ or $dd \rightarrow \tilde{d}_{L,R} \tilde{d}_{L,R}$ become possible and relevant. Of course, in the limit of very large gluino mass, the squark production processes are driven essentially by QCD and dominated by the production of pairs of mass eigenstates, analogous to the top squark production considered already. In particular, at the leading order, the total production cross section for the ten degenerate squarks of a given mass is simply ten times the corresponding top squark production cross section.

Since a relatively light gluino only serves to increase the total cross section (see Fig. 5.7), it can be argued that the heavy gluino limit is a *conservative one*. To avoid considering an additional free parameter, we shall perform our analysis in this limit. To a first approximation, the signal cross sections presented below will scale¹⁹ with the gluino mass approximately as shown in Fig. 5.7.

Like top squarks, the 10 degenerate squarks can also be produced via cascade decays of heavier supersymmetric particles. To be conservative, we again neglect this source of squark production by assuming that the masses of the heavier supersymmetric particles are large enough that their production rate at Tevatron energies can be neglected.

The NLO cross sections for production of ten degenerate squarks including QCD and SUSY-QCD corrections have been implemented numerically in PROSPINO [150]. We generate squark production events using the LO cross section evaluated at the scale $\mu = m_{\tilde{q}}$, improved by the NLO K-factor obtained from PROSPINO [150] (see Fig. 5.8), in the limit that the gluino is very heavy. The K-factor varies between 1 and 1.25 for $m_{\tilde{q}}$ decreasing from 550 to 200 GeV. As in the case of the top squark analysis, we use the CTEQ5 parton distribution functions [151] and neglect the shift in the p_T distribution of the squarks due to gluon radiation at NLO.

¹⁹That the gluino exchange diagram has a different topology as compared to the (dominant) quark-initiated QCD diagram indicates that corresponding angular distributions would be somewhat different. Thus, the efficiency after cuts is not expected to be strictly independent of the gluino mass. For the most part, though, this is only a subleading effect.

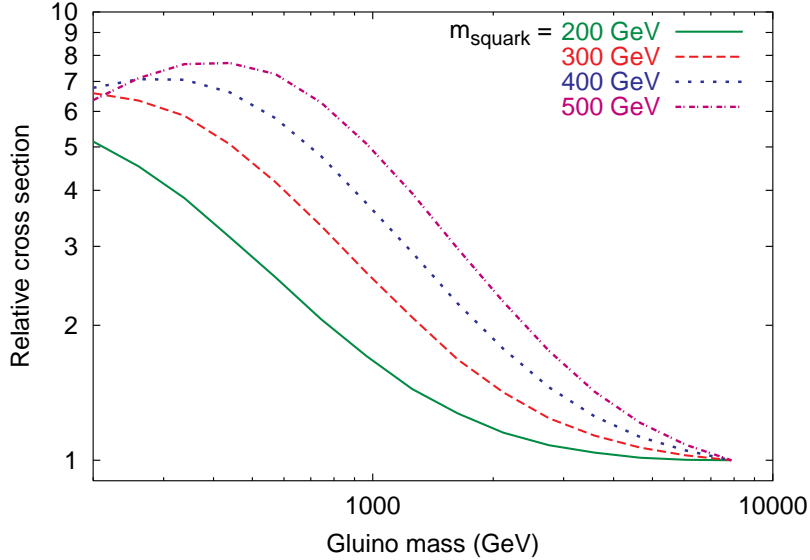


Figure 5.7: Gluino mass dependence of the NLO cross section for production of ten degenerate squarks in 2 TeV $p\bar{p}$ collisions, from PROSPINO [150]. Shown are the cross sections for $\tilde{q}\tilde{q}^*$ production normalized to the value at large $m_{\tilde{q}}$, for common squark masses of 200, 300, 400 and 500 GeV. Production of $\tilde{q}\tilde{q}$ is small at a $p\bar{p}$ collider and is neglected here; it yields an additional 3-15% increase in the total cross section at low $m_{\tilde{q}}$ for this range of squark masses. Cross sections are evaluated at the scale $\mu = m_{\tilde{q}}$.

5.8.2 Signals in low-energy SUSY breaking

The decays of the ten degenerate squarks are very simple. As long as they are heavier than the lightest neutralino,²⁰ they decay via $\tilde{q} \rightarrow q\tilde{\chi}_1^0 \rightarrow q\gamma\tilde{G}$. The signal and backgrounds are then identical to those of the two-body FC stop decay discussed in Sec. 5.7.1, and consequently we use the same selection cuts. In fact, in view of the tenfold increase in the signal strength, we could afford more stringent cuts so as to eliminate virtually all backgrounds, but this is not quite necessary.

The signal cross section after cuts (but before efficiencies) for production of ten degenerate squarks in the heavy gluino limit is shown in Fig. 5.9

²⁰As before, we do not allow the possibility of cascade decays through other neutralinos/charginos. Were we to allow these, the channel we are considering would be somewhat suppressed, but additional, more spectacular, channels would open up.

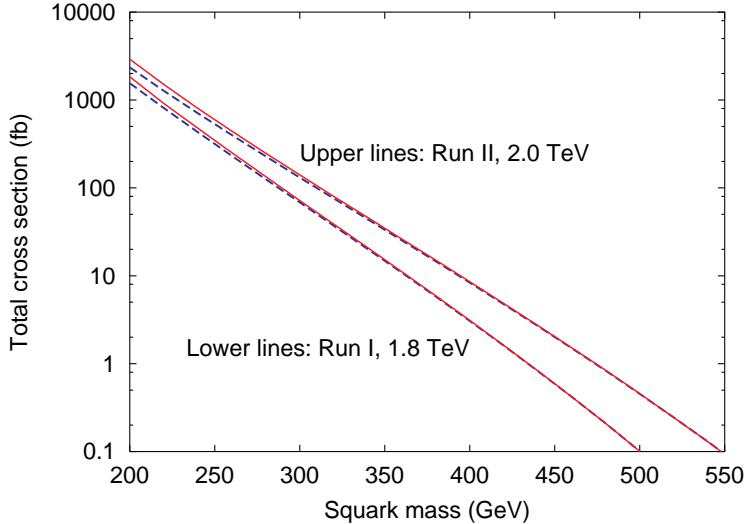


Figure 5.8: LO (dashed) and NLO (solid) cross sections for the production of ten degenerate squarks in the heavy gluino limit in $p\bar{p}$ collisions at Tevatron Run I (1.8 TeV) and Run II (2.0 TeV), from PROSPINO [150]. Cross sections are evaluated at the scale $\mu = m_{\tilde{q}}$.

as contours in the $m_{\tilde{q}}-m_{\tilde{\chi}_1^0}$ plane. We assume that the squark \tilde{q} decays predominantly into $q\tilde{\chi}_1^0$. The branching ratio of $\tilde{\chi}_1^0 \rightarrow \gamma\tilde{G}$ is taken from Fig. 5.2 assuming that $\tilde{\chi}_1^0$ is a pure bino. Clearly, the effect of the kinematic cuts on the signal is very similar to that in the case of the 2-body FC decay of the stop. The mass reach, of course, is much larger due to the tenfold increase in the total cross section; also, unlike in the case of the stop, the 2-body decay is dominant throughout the entire parameter space.

The non-observation of $jj\gamma\gamma E_T$ events at Run I of the Tevatron excludes the region of parameter space shown in black in Fig. 5.9. As in our stop analysis, in this excluded region, at least 3 signal events would have been detected in the 100 pb^{-1} of Run I data, with negligible background. In particular, we estimate that Run I data excludes the ten degenerate squarks up to a common mass of about 280 GeV. As in the case of 2-body FC stop decays, when the mass splitting between the squarks and the neutralino is too small (*i.e.*, less than about 40 GeV), the jets become soft and the signal efficiency decreases dramatically, leaving an unexcluded region of parameter space. The DØ search for inclusive $p\bar{p} \rightarrow \tilde{\chi}_2^0 + X$ with $\tilde{\chi}_2^0 \rightarrow \gamma\tilde{\chi}_1^0$ [163] yields

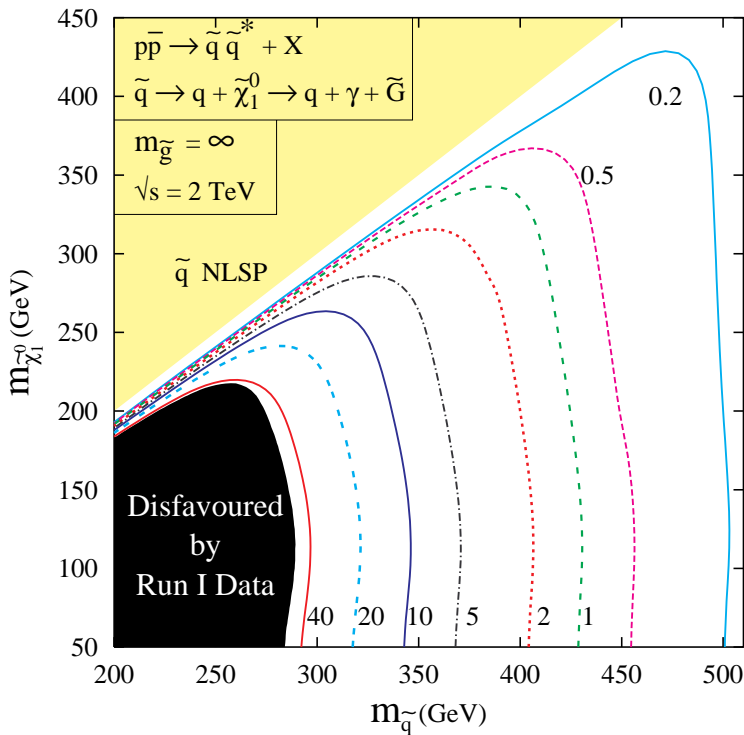


Figure 5.9: Cross section in fb for production of 10 degenerate squarks in Run II in the heavy gluino limit with $\tilde{q} \rightarrow q\gamma\tilde{G}$, after cuts. The black area is excluded by non-observation of $jj\gamma\gamma \not{E}_T$ events in Run I.

a limit on the production cross section of about 0.5 pb for parent squark masses above about 250 GeV. Interpreted in terms of pair production of 10 degenerate squarks in the large $m_{\tilde{q}}$ limit with $\tilde{\chi}_2^0 \rightarrow \gamma \tilde{\chi}_1^0$ reidentified as $\tilde{\chi}_1^0 \rightarrow \gamma \tilde{G}$ again increases the signal efficiency by a factor of ~ 2.7 because every event contains two photons [163]; the D \emptyset analysis then yields a bound on the common squark mass of about 275 GeV, again in rough agreement with our result.²¹

Taking the total background cross section to be 2 fb (see Table 5.1), we show in Table 5.5 the expected maximum discovery mass reach for ten degenerate squarks at Tevatron Run II for various amounts of integrated luminosity.²² In particular, with 4 fb⁻¹ a squark discovery can be expected in this channel if $m_{\tilde{q}} < 360$ GeV. Again, if the lightest neutralino is not a pure bino, the reach at large neutralino masses will be reduced. However, this will have very little effect on the maximum squark mass reach quoted here, because this maximum reach occurs for $m_{\tilde{\chi}_1^0} \sim 100 - 150$ GeV, where all neutralino decay modes other than $\gamma \tilde{G}$ suffer a large kinematic suppression. From Fig. 5.2, it is evident that the neutralino branching fraction into $\gamma \tilde{G}$ will be reduced by no more than 10% in this mass range as long as the neutralino is at least 50% bino; such a reduction in the neutralino branching fraction will lead to a reduction of only a few GeV in the maximum squark mass reach.

²¹Ref. [163] quotes a squark mass bound of 320 GeV for the case $m_{\tilde{q}} \ll m_{\tilde{g}}$ in the context of low-energy SUSY breaking; we expect that this is due to the contribution of chargino and neutralino production to the total SUSY cross section in their analysis.

²²Again, if data from the CDF and D \emptyset detectors are combined, the integrated luminosity of the machine is effectively doubled.

$\int \mathcal{L}$	B	S for a 5σ discovery	$\sigma_S \times \epsilon_\gamma^2$	Maximum squark mass reach
2 fb^{-1}	4	14	7.0 fb	345 GeV
4 fb^{-1}	8	18	4.5 fb	360 GeV
15 fb^{-1}	30	31	2.1 fb	390 GeV
30 fb^{-1}	60	42	1.4 fb	405 GeV

Table 5.5: Number of signal events (S) required for a 5σ squark discovery at Tevatron Run II, assuming production of 10 degenerate squarks in the limit that the gluino is very heavy, and the corresponding signal cross section after cuts and efficiencies and maximum squark mass reach. We take $\epsilon_\gamma = 0.80$. The number of background events (B) is based on a background cross section of 2 fb from Table 5.1.

Chapter 6

Concluding remarks

We have examined the possibility of the existence of a non-minimal Higgs sector. In particular, we consider the next to minimal Higgs sector consisting of two Higgs doublets. There are several motivations to explore those scenarios, among them we have: 1) The fact that the Higgs sector is totally unknown so far, 2) the unnatural hierarchy predicted by SM between the Yukawa couplings of the third family of quarks, 3) the possibility of generating either spontaneous or explicit CP violation, 4) the generation of flavor changing neutral currents (inspired in the increasing evidence on neutrino oscillations) still compatible with the strong experimental limits on them, and 5) the possibility that some models with larger symmetries end up at low energies in a non minimal Higgs sector as in the case of SUSY models. In particular if the SUSY particles are heavy enough, the MSSM Higgs sector acquires the form of a constrained 2HDM type II.

The two Higgs doublet model predicts the existence of five Higgs particles: One CP odd Higgs boson (A^0), two CP even ones (h^0, H^0), and two charged Higgs particles (H^\pm). If a charged Higgs were discovered first, it would be a clear signature of the presence of a non-minimal Higgs sector. The detection of a CP-odd Higgs boson would also yield evidence on physics beyond the SM because of the significant deviations of its couplings to SM particles respect to the ones of a CP even Higgs. In particular, it worths to mention that couplings of $A^0 VV$ should be absent, or at least highly suppressed. Of course, another possible signal would be the discovery of more than one Higgs. Finally, if only one CP even Higgs is discovered and the same experiment is unable to detect other Higgs modes, deviations on its couplings from the ones predicted by the SM can contain the information on certain underlying Higgs

spectrum, in the case of the 2HDM even in the framework of the decoupling limit in which the couplings at tree level of the lighter Higgs boson are SM-like, precision measurements of the couplings could detect such deviations via radiative corrections. If a SM-like Higgs is detected, one of the most promising couplings to look for possible deviations from the SM behavior is the trilinear self coupling $h^0 h^0 h^0$.

The most important sources for production of Higgs bosons in Hadron Colliders are the gluon-gluon fusion and qq' production, while in e^+e^- colliders the most important sources consists of WW, ZZ fusion and Higgstragh lung. Additionally, detection depends on the subsequent decay of the Higgs bosons, the dominant decay channels are highly model dependent and the estimated rate production should be calculated for specific regions of the free parameters. Finally, other interesting perspectives for Higgs production might be provided by $\gamma\gamma$ fusion in $\gamma\gamma$ colliders dominated by ρW^- or $t\bar{t}$ loop, and also by $\mu\mu$ colliders if they run at the Higgs resonance $\sqrt{s} = m_H$.

On the other hand, the presence of FCNC could be an indirect signature of the existence of an extended Higgs sector, perhaps the strongest motivation to look for these rare processes lies on the evidence of neutrino oscillations. Despite processes with FCNC are strongly suppressed by some underlying principle still unknown, there is an important region of parameters in which those processes are still compatible with experimental constraints. As for the quark sector, the FCNC involving the first family are strongly constrained, while the bounds on the other mixings are considerably softened. In this work we concentrate on FCNC in the lepton sector. If LFV is expected in the neutral sector of leptons because of the neutrino oscillations, it is reasonable to consider that those processes are also present in the charged lepton sector as well. Useful constraints involving the vertices $\xi_{\mu\tau}, \xi_{e\tau}, \xi_{\tau\tau}, \xi_{\mu\mu}$ can be derived from the $(g-2)_\mu$ factor, and the decays $\mu \rightarrow e\gamma$, $\tau \rightarrow \mu\gamma$, and $\tau \rightarrow \mu\mu\mu$. In turn, based on the information gotten for these vertices some upper limits on the decay widths $\Gamma(\tau \rightarrow e\gamma)$, and $\Gamma(\tau \rightarrow eee)$ are obtained. Those estimations were calculated by assuming $m_{h^0} \approx 115\text{GeV}$ and $m_{A^0} \gtrsim m_{h^0}$. Since the most recent estimations of Δa_μ , still provides an important window for new Physics, we obtain from it very interesting lower and upper bounds on the mixing vertex $\xi_{\mu\tau}$ at 95% C.L. Specifically, an allowed interval of $7.62 \times 10^{-4} \lesssim \xi_{\mu\tau}^2 \lesssim 4.44 \times 10^{-2}$ was found in a quite wide region of parameters. Of course, we should realize that both SM test and experimental measurements of a_μ are still being scrutinized and current results are not definitive at all. However, if not severe changes occur in forthcoming experi-

ments and/or SM estimations, these constraints could continue being valid at least at a lower confidence level. Future improvements on both estimations should elucidate this point.

Based on these constraints, and on the leptonic decays $\mu \rightarrow e\gamma$, $\tau \rightarrow \mu\gamma$, and $\tau \rightarrow \mu\mu\mu$ we got the following conservative and quite general bounds of LFV vertices

$$\begin{aligned}\xi_{e\tau}^2 &\lesssim 2.77 \times 10^{-14}, \\ -1.8 \times 10^{-2} &\lesssim \xi_{\tau\tau} \lesssim 2.2 \times 10^{-2}; |\xi_{\mu\mu}| \lesssim 0.13 \quad \text{for } m_{A^0} \gg m_{h^0} \\ |\xi_{\tau\tau}| &\lesssim 1.0 \times 10^{-2}; |\xi_{\mu\mu}| \lesssim 0.15 \quad \text{for } m_{A^0} \approx m_{h^0}\end{aligned}$$

It is remarkable the very strong hierarchy among the allowed values for $\xi_{e\tau}^2$ and $\xi_{\mu\tau}^2$. Moreover, these bounds on $\xi_{\tau\tau}$ and $\xi_{\mu\mu}$ are considerably relaxed for certain specific values of m_{A^0} . In that case, the room available for them is such that they permit either a strong enhancement or a strong suppression of the couplings $H\tau\bar{\tau}$ and/or $H\mu\bar{\mu}$ for any neutral Higgs boson.

Furthermore, we estimate upper limits on the decay widths $\Gamma(\tau \rightarrow e\gamma)$, and $\Gamma(\tau \rightarrow eee)$, finding that they are basically hopeless to look for, in near future experiments, at least in the framework of the 2HDM type III with heavy Higgs bosons.

In addition, we see that processes with flavor changing charged currents are intimately related to the processes with flavor changing neutral currents. The same mixing elements that produce the FCNC correct the FCCC in the quark sector (respect to the CKM elements) while producing the FCCC in the leptonic sector. It worths to point out that the study of the FCCC at tree level in the 2HDM (III) depend on a less number of free parameters since only one scalar particle is exchanged, and the Higgs boson involved does not couple through a mixing angle. For instance, based on the decay width $\Gamma(\mu^- \rightarrow \nu_e e^- \bar{\nu}_\mu)$ we can get the upper limit $|\xi_{e\mu}/m_{H^+}| \leq 3.8 \times 10^{-3} GeV^{-1}$ without any further assumption on the free parameters of the model.

It worths to say that the phenomenological constraints described so far, were calculated in the fundamental parametrization of the 2HDM(III) with only one VEV. Nevertheless, it is possible to use other parametrizations for the 2HDM type III in which both VEV's are taken different from zero. In that case, the part of the Lagrangian involving the Higgs sector is written in terms of the spurious parameter $\tan\beta$, in such a way that the Yukawa Lagrangian type III is expressed as the one in the model type I plus some

FC interactions, or as the model type II plus some FC interactions. These particular parametrizations are equivalent to the fundamental one in which one of the VEV is zero and $\tan\beta$ vanishes. However, these non trivial bases could be useful when we want to compare the model type III with the models type I or II. Additionally, these parametrizations facilitates the study of the decoupling limit of the 2HDM. By setting a fixed value of $\tan\beta$ we are using a particular basis to write the model, in that sense, the parameter $\tan\beta$ acts as a “gauge fixing” term.

Now, based on non trivial parametrizations of model III in which models type I and II become apparent, we get bounds on the Higgs boson masses, by making reasonable assumptions on the FC vertices. Since the contribution of the pseudoscalar Higgs boson to Δa_μ is negative while the estimated value is positive definite at 95% CL, the estimated value of Δa_μ impose lower bounds on the Pseudoscalar Higgs mass. Specifically, we have taken for $\tilde{\eta}(\tilde{\xi})_{\mu\tau}$ the geometric average of the Yukawa couplings, and we also utilized values one order of magnitude larger and one order of magnitude smaller. Taking these three values for the FC vertex we find that the smaller value for $\tilde{\eta}(\tilde{\xi})_{\mu\tau}$ the more stringent lower bounds for m_{A^0} . Additionally, assuming $m_{H^0} = m_{h^0}$, we show that in the limit of small (large) $\tan\beta$ the lower bound of m_{A^0} becomes merely $m_{A^0} \approx m_{h^0}$ for parametrization of type I (II). In the case of different scalar masses, there is still a lower asymptotic limit for m_{A^0} . Notwithstanding, these lower constraints on m_{A^0} should be considered carefully, since for $\tilde{\eta}(\tilde{\xi})_{\mu\tau}$ we can only make reasonable estimations but they are unknown so far.

On the other hand, as a matter of addendum, the production and decays of top-squarks at the Tevatron collider is examined in the framework of general low energy supersymmetry breaking models. In models of low-energy SUSY breaking, signatures of SUSY particle production generically contain two hard photons plus missing energy due to the decays of the two neutralino NLSPs produced in the decay chains. Standard Model backgrounds to such signals are naturally small at Run II of the Tevatron. We studied the production and decay of top squarks at the Tevatron in such models in the case where the lightest Standard Model superpartner is a light neutralino that predominantly decays into a photon and a light gravitino. We considered 2-body flavor-changing and 3-body decays of the top squarks. The reach of the Tevatron in such models is larger than in the standard supergravity models

and than in models with low-energy SUSY breaking in which the stop is the NLSP, rather than the neutralino. We estimate that top squarks with masses below about 200 GeV can be excluded based on Run I data, assuming that $50 \text{ GeV} \lesssim m_{\tilde{\chi}_1^0} \lesssim m_{\tilde{t}} - 10 \text{ GeV}$. For a modest final Run II luminosity of 4 fb^{-1} , stop masses up to 285 GeV are accessible in the 2-body decay mode, and up to 320 GeV in the 3-body decay mode.

Top squarks can also be produced in top quark decays. We found that, within the context of low-energy SUSY breaking with the stop as the next-to-next-to-lightest SUSY particle, the region of parameter space in which stop production in top quark decays is possible is almost entirely excluded by Run I data if the lighter stop is predominantly right-handed; however, an interesting region is still allowed if the lighter stop is predominantly left-handed, due to the smaller branching ratio of $t \rightarrow \tilde{t}_L \tilde{\chi}_1^0$. Run II will cover the entire parameter space in which top decays to stop are possible.

We also studied the production and decay of the ten squarks associated with the five light quarks, assumed to be degenerate. In models of low-energy SUSY breaking, the decays of the ten degenerate squarks lead to signals identical to those for the 2-body flavor-changing stop decays. The cross section for production of ten degenerate squarks at the Tevatron is significantly larger than that of the top squark. We estimate that the 10 degenerate squarks with masses below about 280 GeV can be excluded based on Run I data, assuming that $m_{\tilde{\chi}_1^0} \lesssim m_{\tilde{q}} - 40 \text{ GeV}$. For a final Run II luminosity of 4 fb^{-1} , squark masses as large as 360 GeV are easily accessible in the limit that the gluino is very heavy. The production cross section, and hence the discovery reach, increases further with decreasing gluino mass.

Appendix A

Determination of the minima of the potential and the mass eigenstates

A.1 Minimum condition for the potential

The potential can be written in terms of the following hermitian gauge invariant operators

$$\begin{aligned}\widehat{A} &\equiv \Phi_1^\dagger \Phi_1, \quad \widehat{B} \equiv \Phi_2^\dagger \Phi_2, \quad \widehat{C} \equiv \frac{1}{2} (\Phi_1^\dagger \Phi_2 + \Phi_2^\dagger \Phi_1) = \text{Re} (\Phi_1^\dagger \Phi_2), \\ \widehat{D} &\equiv -\frac{i}{2} (\Phi_1^\dagger \Phi_2 - \Phi_2^\dagger \Phi_1) = \text{Im} (\Phi_1^\dagger \Phi_2)\end{aligned}$$

The most general renormalizable and $SU(2) \times U(1)$ invariant potential is given by

$$\begin{aligned}V_g = & -\mu_1^2 \widehat{A} - \mu_2^2 \widehat{B} - \mu_3^2 \widehat{C} - \mu_4^2 \widehat{D} + \lambda_1 \widehat{A}^2 + \lambda_2 \widehat{B}^2 + \lambda_3 \widehat{C}^2 + \lambda_4 \widehat{D}^2 \\ & + \lambda_5 \widehat{A} \widehat{B} + \lambda_6 \widehat{A} \widehat{C} + \lambda_8 \widehat{A} \widehat{D} + \lambda_7 \widehat{B} \widehat{C} + \lambda_9 \widehat{B} \widehat{D} + \lambda_{10} \widehat{C} \widehat{D}\end{aligned}\quad (\text{A.1})$$

For the sake of simplicity, we shall use in this appendix the following parametrization for the doublets

$$\Phi_1 = \begin{pmatrix} \phi_1 + i\phi_2 \\ \phi_3 + i\phi_4 \end{pmatrix} \quad ; \quad \Phi_2 = \begin{pmatrix} \phi_5 + i\phi_6 \\ \phi_7 + i\phi_8 \end{pmatrix} \quad (\text{A.2})$$

we will assume from now on, that both VEV can be taken real (i.e. there is not spontaneous CP – violation) such that $\langle\phi_3\rangle = v_1/\sqrt{2}$; $\langle\phi_7\rangle = v_2/\sqrt{2}$. Now, we examine the minimum conditions (tadpoles).

$$T_i = \frac{\partial V}{\partial \phi_i} \Big|_{\phi_3=v_1/\sqrt{2}, \phi_7=v_2/\sqrt{2}} = 0$$

where ϕ_i , with $i = 1, \dots, 8$ denotes each gauge eigenstate of the scalars defined in (A.2). We obtain the following non trivial equations

$$\begin{aligned} 0 &= T_3 = \frac{1}{4}\lambda_7v_2^3 + \lambda_1v_1^3 + \frac{3}{4}\lambda_6v_1^2v_2 - \mu_1^2v_1 + \frac{1}{2}\lambda_3v_2^2v_1 + \frac{1}{2}\lambda_5v_1v_2^2 - \frac{1}{2}\mu_3^2v_2 \\ 0 &= T_4 = (-2\mu_4^2 + \lambda_9v_2^2 + \lambda_8v_1^2 + \lambda_{10}v_2v_1) v_2 \\ 0 &= T_7 = \frac{3}{4}\lambda_7v_2^2v_1 - \mu_2^2v_2 + \lambda_2v_2^3 - \frac{1}{2}\mu_3^2v_1 + \frac{1}{4}\lambda_6v_1^3 + \frac{1}{2}\lambda_3v_1^2v_2 + \frac{1}{2}\lambda_5v_2v_1^2 \\ 0 &= T_8 = (2\mu_4^2 + \lambda_9v_2^2 + \lambda_8v_1^2 + \lambda_{10}v_2v_1) v_1 \end{aligned} \quad (\text{A.3})$$

Now, the mass matrix elements are gotten from the terms quadratic in the scalars

$$M_{ij}^2 = \frac{1}{2} \frac{\partial^2 V}{\partial \phi_i \partial \phi_j} \Big|_{\phi_3=v_1/\sqrt{2}, \phi_7=v_2/\sqrt{2}} \quad (\text{A.4})$$

from (A.4, A.1), and (A.2) the 8×8 mass matrix becomes

$$\begin{pmatrix} M_{11}^2 & 0 & 0 & 0 & M_{15}^2 & M_{16}^2 & 0 & 0 \\ 0 & M_{22}^2 & 0 & 0 & M_{25}^2 & M_{26}^2 & 0 & 0 \\ 0 & 0 & M_{33}^2 & M_{34}^2 & 0 & 0 & M_{37}^2 & M_{38}^2 \\ 0 & 0 & M_{34}^2 & M_{44}^2 & 0 & 0 & M_{47}^2 & M_{48}^2 \\ M_{15}^2 & M_{25}^2 & 0 & 0 & M_{55}^2 & 0 & 0 & 0 \\ M_{16}^2 & M_{26}^2 & 0 & 0 & 0 & M_{66}^2 & 0 & 0 \\ 0 & 0 & M_{37}^2 & M_{47}^2 & 0 & 0 & M_{77}^2 & M_{78}^2 \\ 0 & 0 & M_{38}^2 & M_{48}^2 & 0 & 0 & M_{78}^2 & M_{88}^2 \end{pmatrix} \quad (\text{A.5})$$

where the matrix elements are given by

$$\begin{aligned}
M_{11}^2 &= -\mu_1^2 + \lambda_1 v_1^2 + \frac{1}{2} \lambda_5 v_2^2 + \frac{1}{2} \lambda_6 v_1 v_2 \\
M_{15}^2 &= -\frac{1}{2} \mu_3^2 + \frac{1}{2} \lambda_3 v_1 v_2 + \frac{1}{4} \lambda_6 v_1^2 + \frac{1}{4} \lambda_7 v_2^2 \\
M_{16}^2 &= -\frac{1}{2} \mu_4^2 + \frac{1}{4} \lambda_{10} v_1 v_2 + \frac{1}{4} \lambda_8 v_1^2 + \frac{1}{4} \lambda_9 v_2^2 \\
M_{22}^2 &= -\mu_1^2 + \lambda_1 v_1^2 + \frac{1}{2} \lambda_5 v_2^2 + \frac{1}{2} \lambda_6 v_1 v_2 \\
M_{25}^2 &= -\frac{1}{4} \lambda_9 v_2^2 - \frac{1}{4} \lambda_{10} v_1 v_2 + \frac{1}{2} \mu_4^2 - \frac{1}{4} \lambda_8 v_1^2 \\
M_{26}^2 &= -\frac{1}{2} \mu_3^2 + \frac{1}{4} \lambda_7 v_2^2 + \frac{1}{4} \lambda_6 v_1^2 + \frac{1}{2} \lambda_3 v_1 v_2 \\
M_{33}^2 &= -\mu_1^2 + 3\lambda_1 v_1^2 + \frac{1}{2} \lambda_3 v_2^2 + \frac{1}{2} \lambda_5 v_2^2 + \frac{3}{2} \lambda_6 v_1 v_2 \\
M_{34}^2 &= -\frac{1}{2} \lambda_8 v_1 v_2 - \frac{1}{4} \lambda_{10} v_2^2 \\
M_{37}^2 &= -\frac{1}{2} \mu_3^2 + \frac{3}{4} \lambda_7 v_2^2 + \frac{3}{4} \lambda_6 v_1^2 + \lambda_5 v_1 v_2 + \lambda_3 v_1 v_2 \\
M_{38}^2 &= \frac{1}{4} \lambda_9 v_2^2 + \frac{1}{2} \lambda_{10} v_1 v_2 - \frac{1}{2} \mu_4^2 + \frac{3}{4} \lambda_8 v_1^2 \\
\\
M_{44}^2 &= -\mu_1^2 + \lambda_1 v_1^2 + \frac{1}{2} \lambda_4 v_2^2 + \frac{1}{2} \lambda_5 v_2^2 + \frac{1}{2} \lambda_6 v_1 v_2 \\
M_{47}^2 &= -\frac{3}{4} \lambda_9 v_2^2 - \frac{1}{2} \lambda_{10} v_1 v_2 + \frac{1}{2} \mu_4^2 - \frac{1}{4} \lambda_8 v_1^2 \\
M_{48}^2 &= -\frac{1}{2} \mu_3^2 + \frac{1}{4} \lambda_7 v_2^2 + \frac{1}{4} \lambda_6 v_1^2 + \frac{1}{2} \lambda_3 v_1 v_2 - \frac{1}{2} \lambda_4 v_1 v_2 \\
M_{55}^2 &= -\mu_2^2 + \lambda_2 v_2^2 + \frac{1}{2} \lambda_5 v_1^2 + \frac{1}{2} \lambda_7 v_1 v_2 \\
M_{66}^2 &= -\mu_2^2 + \lambda_2 v_2^2 + \frac{1}{2} \lambda_5 v_1^2 + \frac{1}{2} \lambda_7 v_1 v_2 \\
M_{77}^2 &= -\mu_2^2 + 3\lambda_2 v_2^2 + \frac{1}{2} \lambda_3 v_1^2 + \frac{1}{2} \lambda_5 v_1^2 + \frac{3}{2} \lambda_7 v_1 v_2 \\
M_{78}^2 &= \frac{1}{2} \lambda_9 v_2 v_1 + \frac{1}{4} \lambda_{10} v_1^2 \\
M_{88}^2 &= -\mu_2^2 + \lambda_2 v_2^2 + \frac{1}{2} \lambda_4 v_1^2 + \frac{1}{2} \lambda_5 v_1^2 + \frac{1}{2} \lambda_7 v_1 v_2
\end{aligned} \tag{A.6}$$

Observe that $v_2 = 0$, is a valid solution for Eqs. (A.3). Now, if we solve using $v_2 = 0$, and replace the other minimum conditions into the mass terms (A.6) we get

$$\begin{aligned}
M_{11}^2 &= 0; \quad M_{15}^2 = 0; \quad M_{16}^2 = \frac{1}{2}\lambda_8 v_1^2; \quad M_{22}^2 = 0; \quad M_{25}^2 = -\frac{1}{2}\lambda_8 v_1^2 \\
M_{26}^2 &= 0; \quad M_{33}^2 = 2\lambda_1 v_1^2; \quad M_{34}^2 = 0; \quad M_{37}^2 = \frac{1}{2}\lambda_6 v_1^2; \quad M_{38}^2 = \lambda_8 v_1^2 \\
M_{44}^2 &= 0; \quad M_{47}^2 = -\frac{1}{2}\lambda_8 v_1^2; \quad M_{48}^2 = 0; \quad M_{55}^2 = -\mu_2^2 + \frac{1}{2}\lambda_5 v_1^2 \\
M_{66}^2 &= -\mu_2^2 + \frac{1}{2}\lambda_5 v_1^2; \quad M_{77}^2 = -\mu_2^2 + \frac{1}{2}\lambda_3 v_1^2 + \frac{1}{2}\lambda_5 v_1^2 \\
M_{78}^2 &= \frac{1}{4}\lambda_{10} v_1^2; \quad M_{88}^2 = -\mu_2^2 + \frac{1}{2}\lambda_4 v_1^2 + \frac{1}{2}\lambda_5 v_1^2
\end{aligned}$$

We can see that the potential A.1 violates CP explicitly by means of the terms M_{16} , M_{25} , M_{34} , M_{38} , M_{47} , M_{78} in the mass matrix (A.5), since they mix real parts with imaginary parts of the complex neutral fields ϕ_1^0 , ϕ_2^0 , see Eqs. (A.2, 2.1). As we shall see below, these terms vanish in the potentials (2.4, 2.5, 2.8) avoiding explicit CP violation. Notwithstanding, potentials (2.4, 2.6) can exhibit spontaneous CP violation while potentials (2.5, 2.8) do not allow spontaneous CP violation either.

Before continuing with some special cases of the potential, we shall introduce some useful formulae. If we have a 2×2 real symmetric matrix

$$A = \begin{pmatrix} a & c \\ c & b \end{pmatrix}$$

its eigenvalues and orthonormal eigenvectors are given by

$$\begin{aligned}
k_{1,2} &= \frac{1}{2} \left[a + b \pm \sqrt{(a - b)^2 + 4c^2} \right] \\
\begin{pmatrix} \cos \delta \\ \sin \delta \end{pmatrix} &\equiv \vec{u}_1 \leftrightarrow k_1; \quad \begin{pmatrix} -\sin \delta \\ \cos \delta \end{pmatrix} \equiv \vec{u}_2 \leftrightarrow k_2 \\
\sin 2\delta &= \frac{2c}{\sqrt{(a - b)^2 + 4c^2}}; \quad \cos 2\delta = \frac{(a - b)}{\sqrt{(a - b)^2 + 4c^2}} \quad (\text{A.7})
\end{aligned}$$

from which we get

$$UAU^\dagger = \begin{pmatrix} k_1 & 0 \\ 0 & k_2 \end{pmatrix}$$

$$U \equiv \begin{pmatrix} \vec{u}_1^T \\ \vec{u}_2^T \end{pmatrix} = \begin{pmatrix} \cos \delta & \sin \delta \\ -\sin \delta & \cos \delta \end{pmatrix}$$

further, if we start from a doublet of gauge eigenstates

$$\Omega \equiv \begin{pmatrix} \Omega_1 \\ \Omega_2 \end{pmatrix}$$

and settle the following definitions

$$H \equiv U\Omega \equiv \begin{pmatrix} H_1 \\ H_2 \end{pmatrix}, \quad M \equiv UAU^\dagger = \begin{pmatrix} k_1 & 0 \\ 0 & k_2 \end{pmatrix}$$

we can check that, owing to the unitarity of the rotation matrix U the following identity is held

$$\Omega^\dagger A \Omega = H^\dagger M H$$

and since M is diagonal, we say that the doublet H contains the mass eigenstates H_1, H_2 . They are obtained by rotating the original gauge eigenstates through the unitary matrix U ; and k_1, k_2 correspond to the squared masses of the mass eigenstates H_1, H_2 respectively. These results will be applied widely in foregoing issues.

From now on, we shall examine some special cases of the potential (A.1).

A.1.1 The potential with C -invariance

According to section (2.2.1), if we demand from the potential to be C -invariant, we ought to settle $\mu_4^2 = \lambda_8 = \lambda_9 = \lambda_{10} = 0$. Additionally, we can always make a rotation on the two doublets in such a way that only one of them get a VEV (see appendix C for details). So we can take $\langle \phi_3 \rangle = v_1/\sqrt{2}$; $\langle \phi_7 \rangle = v_2/\sqrt{2} = 0$, without any loss of generality.

With the assumptions above, the minimum conditions are reduced to only two equations

$$\mu_1^2 = \lambda_1 v_1^2; \quad \mu_3^2 = \frac{\lambda_6 v_1^2}{2}$$

replacing them into the mass matrix elements we get

$$\begin{aligned} M_{15}^2 &= -\frac{1}{2}\mu_3^2 + \frac{1}{4}\lambda_6 v_1^2; \quad M_{33}^2 = 2\lambda_1 v_1^2; \quad M_{37}^2 = \frac{1}{2}\lambda_6 v_1^2 \\ M_{55}^2 &= -\mu_2^2 + \frac{1}{2}\lambda_5 v_1^2; \quad M_{66}^2 = -\mu_2^2 + \frac{1}{2}\lambda_5 v_1^2 \\ M_{77}^2 &= -\mu_2^2 + \frac{1}{2}\lambda_3 v_1^2 + \frac{1}{2}\lambda_5 v_1^2; \quad M_{88}^2 = -\mu_2^2 + \frac{1}{2}\lambda_4 v_1^2 + \frac{1}{2}\lambda_5 v_1^2 \end{aligned}$$

the other terms vanish. Now, we can relabel the matrix in the following way $1, 2, 3, 4, 5, 6, 7, 8 \rightarrow 1, 2, 5, 6, 3, 7, 4, 8$ the new positions of the above elements in this new matrix are¹

$$\begin{pmatrix} 0 & 0 & 0 & 0 & 0 & 0 & 0 & 0 \\ 0 & 0 & 0 & 0 & 0 & 0 & 0 & 0 \\ 0 & 0 & M_{55}^2 & 0 & 0 & 0 & 0 & 0 \\ 0 & 0 & 0 & M_{66}^2 & 0 & 0 & 0 & 0 \\ 0 & 0 & 0 & 0 & M_{33}^2 & M_{37}^2 & 0 & 0 \\ 0 & 0 & 0 & 0 & M_{73}^2 & M_{77}^2 & 0 & 0 \\ 0 & 0 & 0 & 0 & 0 & 0 & 0 & 0 \\ 0 & 0 & 0 & 0 & 0 & 0 & 0 & M_{88}^2 \end{pmatrix} \quad (\text{A.8})$$

which can be decomposed in the following way

$$\begin{pmatrix} 0 & 0 & 0 & 0 \\ 0 & 0 & 0 & 0 \\ 0 & 0 & M_{55}^2 & 0 \\ 0 & 0 & 0 & M_{66}^2 \end{pmatrix} \oplus \begin{pmatrix} M_{33}^2 & M_{37}^2 \\ M_{73}^2 & M_{77}^2 \end{pmatrix} \oplus \begin{pmatrix} 0 & 0 \\ 0 & M_{88}^2 \end{pmatrix} \quad (\text{A.9})$$

Additionally, since $M_{55}^2 = M_{66}^2$ we get for the first matrix

$$\begin{pmatrix} 0 & 0 & 0 & 0 \\ 0 & 0 & 0 & 0 \\ 0 & 0 & M_{55}^2 & 0 \\ 0 & 0 & 0 & M_{66}^2 \end{pmatrix} = \begin{pmatrix} 0 & 0 \\ 0 & M_{55}^2 \end{pmatrix} \otimes I_{2 \times 2} \quad (\text{A.10})$$

With this decomposition it is easier to diagonalize the matrix (A.8) since it is equivalent to diagonalize each of the submatrices given above. Let

¹It is equivalent to relabel the scalar fields ϕ_i which clearly does not affect the physical content of the mass matrix.

us start by diagonalizing the matrix (A.10) corresponding to the indices 1, 2, 5, 6. Its orthonormalized eigenvectors and eigenvalues are given by

$$\begin{aligned} \left\{ \left(\begin{array}{cccc} 1 & 0 & 0 & 0 \end{array} \right)^T, \left(\begin{array}{cccc} 0 & 1 & 0 & 0 \end{array} \right)^T \right\} &\rightarrow m_{G^+}^2 = 0 \\ \left\{ \left(\begin{array}{cccc} 0 & 0 & 1 & 0 \end{array} \right)^T, \left(\begin{array}{cccc} 0 & 0 & 0 & 1 \end{array} \right)^T \right\} &\rightarrow m_{H^+}^2 = -\mu_2^2 + \frac{1}{2}\lambda_5 v_1^2 \end{aligned} \quad (\text{A.11})$$

thus each eigenvalue is doubly degenerate. Therefore, they correspond to charged eigenstates. The eigenvalue $m_{G^+}^2 = 0$ correspond to a would be Goldstone boson (massless scalar) while $m_{H^+}^2 = -\mu_2^2 + \frac{1}{2}\lambda_5 v_1^2$ correspond to the mass of a charged Higgs boson. According to the eigenvectors obtained in (A.11) the mass eigenstates are given by

$$\left(\begin{array}{c} G_1 \\ G_2 \\ H_1 \\ H_2 \end{array} \right) = \left(\begin{array}{cccc} 1 & 0 & 0 & 0 \\ 0 & 1 & 0 & 0 \\ 0 & 0 & 1 & 0 \\ 0 & 0 & 0 & 1 \end{array} \right) \left(\begin{array}{c} \phi_1 \\ \phi_2 \\ \phi_5 \\ \phi_6 \end{array} \right)$$

But taking into account that to define a scalar charged Higgs boson we require two degrees of freedom, we realize that the first two scalar fields define the charged would be Goldstone boson G^+ , which is written as a linear combination of the scalars ϕ_1, ϕ_2 . The assignment of both degrees of freedom can be done as $(\phi_1, \phi_2)^T \rightarrow \phi_1 + i\phi_2 \equiv \phi_1^+$; in the same way $(G_1, G_2)^T \rightarrow G_1 + iG_2 \equiv G^+$, something similar happens to $(\phi_5, \phi_6)^T \equiv \phi_2^+$ and $(H_1, H_2)^T \equiv H^+$. Therefore, the relation among the gauge and mass eigenstates of the charged scalar fields can be simplified as²

$$\left(\begin{array}{c} G^+ \\ H^+ \end{array} \right) = \left(\begin{array}{cc} 1 & 0 \\ 0 & 1 \end{array} \right) \left(\begin{array}{c} \phi_1^+ \\ \phi_2^+ \end{array} \right)$$

The second matrix in (A.9) correspond to the indices 3,7.

$$\left(\begin{array}{cc} M_{33}^2 & M_{37}^2 \\ M_{73}^2 & M_{77}^2 \end{array} \right) = \left(\begin{array}{cc} 2\lambda_1 v_1^2 & \frac{1}{2}\lambda_6 v_1^2 \\ \frac{1}{2}\lambda_6 v_1^2 & -\mu_2^2 + \frac{1}{2}\lambda_3 v_1^2 + \frac{1}{2}\lambda_5 v_1^2 \end{array} \right)$$

²Noteworthy, this is the opposite procedure respect to the one developed in Sec. (2.2.2), in which we extend the dimension of the representation, see for example Eq. (2.17). In this case we are “shrinking” the dimension of the representation.

applying Eqs. (A.7) the eigenvalues and orthonormalized eigenvectors are:

$$m_{H^0, h^0}^2 = \left(\lambda_1 + \frac{1}{2} \lambda_+ \right) v_1^2 - \frac{1}{2} \mu_2^2 \pm \sqrt{\left[\left(\lambda_1 - \frac{1}{2} \lambda_+ \right) v_1^2 + \frac{1}{2} \mu_2^2 \right]^2 + \left(\frac{1}{2} \lambda_6 v_1^2 \right)^2}$$

$$\begin{aligned} \begin{pmatrix} \cos \alpha \\ \sin \alpha \end{pmatrix} &\leftrightarrow m_{H^0}^2 ; \quad \begin{pmatrix} -\sin \alpha \\ \cos \alpha \end{pmatrix} \leftrightarrow m_{h^0}^2 \\ \tan 2\alpha &= \frac{\lambda_6 v_1^2}{(2\lambda_1 - \lambda_+) v_1^2 + \mu_2^2} ; \quad \lambda_+ \equiv \frac{1}{2} (\lambda_3 + \lambda_5) \end{aligned}$$

therefore, the diagonalization process is performed by the following rotation of the gauge eigenstates

$$\begin{pmatrix} \cos \alpha & \sin \alpha \\ -\sin \alpha & \cos \alpha \end{pmatrix} \begin{pmatrix} \sqrt{2}\phi_3 - v_1 \\ \sqrt{2}\phi_7 - v_2 \end{pmatrix} = \begin{pmatrix} H^0 \\ h^0 \end{pmatrix}$$

but according to the parametrizations (A.2) and (2.2) of the Higgs doublets

$$(\sqrt{2}\phi_{3,7} - v_{1,2}) \rightarrow h_{1,2}$$

obtaining

$$\begin{pmatrix} \cos \alpha & \sin \alpha \\ -\sin \alpha & \cos \alpha \end{pmatrix} \begin{pmatrix} h_1 \\ h_2 \end{pmatrix} = \begin{pmatrix} H^0 \\ h^0 \end{pmatrix}$$

Finally, we diagonalize the submatrix corresponding to the elements 4,8 in Eq. (A.9)

$$\begin{pmatrix} M_{44}^2 & M_{48}^2 \\ M_{84}^2 & M_{88}^2 \end{pmatrix} = \begin{pmatrix} 0 & 0 \\ 0 & -\mu_2^2 + \frac{1}{2} (\lambda_4 + \lambda_5) v_1^2 \end{pmatrix}$$

whose eigenvectors and eigenvalues are

$$\left\{ \begin{pmatrix} 1 \\ 0 \end{pmatrix} \right\} \leftrightarrow 0, \left\{ \begin{pmatrix} 0 \\ 1 \end{pmatrix} \right\} \leftrightarrow -\mu_2^2 + \frac{1}{2} v_1^2 \lambda_4 + \frac{1}{2} v_1^2 \lambda_5$$

the first eigenvalue correspond to a neutral, massless would Goldstone boson, while the second one is associated to another neutral Higgs boson.

$$m_{G^0} = 0 ; m_{A^0} = -\mu_2^2 + \frac{1}{2} (\lambda_4 + \lambda_5) v_1^2$$

The mass eigenstates are given by

$$\begin{pmatrix} 1 & 0 \\ 0 & 1 \end{pmatrix} \begin{pmatrix} \phi_4 \\ \phi_8 \end{pmatrix} = \begin{pmatrix} G^0 \\ A^0 \end{pmatrix}$$

A.1.2 The potential with a Z_2 invariance

As explained in section (2.2.1) a way to avoid spontaneous CP violation consists of demanding invariance under the Z_2 symmetry $\Phi_1 \rightarrow \Phi_1$, $\Phi_2 \rightarrow -\Phi_2$ (as well as the C -invariance) and correspond to setting $\mu_3^2 = \mu_4^2 = \lambda_6 = \lambda_7 = \lambda_8 = \lambda_9 = \lambda_{10} = 0$ in (A.1). The minimum conditions (A.3) are reduced to two equations:

$$\begin{aligned} v_1 \left[-\mu_1^2 + \lambda_1 v_1^2 + \lambda_+ v_2^2 \right] &= 0 \\ v_2 \left[-\mu_2^2 + \lambda_2 v_2^2 + \lambda_+ v_1^2 \right] &= 0 \end{aligned}$$

where $\lambda_+ = \frac{1}{2} (\lambda_3 + \lambda_5)$. So we have two sets of independent solutions

a)

$$v_1^2 = \frac{\lambda_2 \mu_1^2 - \lambda_+ \mu_2^2}{\lambda_1 \lambda_2 - \lambda_+^2} ; \quad v_2^2 = \frac{\lambda_1 \mu_2^2 - \lambda_+ \mu_1^2}{\lambda_1 \lambda_2 - \lambda_+^2}$$

or b)

$$v_2^2 = 0 ; \quad v_1^2 = \frac{\mu_1^2}{\lambda_1}$$

First set of solutions

The decomposed mass matrix, after using the minimum conditions, relabeling and taking into account that $M_{15}^2 = M_{26}^2$, $M_{11}^2 = M_{22}^2$, and $M_{55}^2 = M_{66}^2$ becomes

$$M_{tot}^2 = \left[\begin{pmatrix} M_{11}^2 & M_{15}^2 \\ M_{15}^2 & M_{55}^2 \end{pmatrix} \otimes I_{2 \times 2} \right] \oplus \begin{pmatrix} M_{33}^2 & M_{37}^2 \\ M_{37}^2 & M_{77}^2 \end{pmatrix} \oplus \begin{pmatrix} M_{44}^2 & M_{48}^2 \\ M_{48}^2 & M_{88}^2 \end{pmatrix}$$

$$\begin{aligned} M_{11}^2 &= -\frac{1}{2}v_2^2\lambda_3 ; \quad M_{15}^2 = \frac{1}{2}\lambda_3v_1v_2 ; \quad M_{22}^2 = -\frac{1}{2}v_2^2\lambda_3 ; \quad M_{26}^2 = \frac{1}{2}\lambda_3v_1v_2 \\ M_{33}^2 &= 2\lambda_1v_1^2 ; \quad M_{37}^2 = 2\lambda_+v_1v_2 ; \quad M_{44}^2 = \lambda_-v_2^2 ; \quad M_{48}^2 = -\lambda_-v_1v_2 \\ M_{55}^2 &= -\frac{1}{2}v_1^2\lambda_3 ; \quad M_{66}^2 = -\frac{1}{2}v_1^2\lambda_3 ; \quad M_{77}^2 = 2\lambda_2v_2^2 ; \quad M_{88}^2 = \lambda_-v_1^2 \end{aligned}$$

where $\lambda_- \equiv \frac{1}{2}(\lambda_4 - \lambda_3)$. We first diagonalize the submatrix corresponding to 1, 5. The eigenvalues and orthonormal eigenvectors are

$$\begin{aligned} \left\{ \frac{1}{\sqrt{1 + \left(\frac{v_2}{v_1}\right)^2}} \begin{pmatrix} 1 \\ \frac{v_2}{v_1} \end{pmatrix} \right\} &\leftrightarrow 0, \\ \left\{ \frac{1}{\sqrt{1 + \left(\frac{v_2}{v_1}\right)^2}} \begin{pmatrix} -\frac{v_2}{v_1} \\ 1 \end{pmatrix} \right\} &\leftrightarrow \frac{1}{2} \frac{(v_1^2 + v_2^2)(\mu_3^2 - \lambda_3v_1v_2)}{v_1v_2} \end{aligned}$$

which can be written as

$$\begin{aligned} \begin{pmatrix} \cos\beta \\ \sin\beta \end{pmatrix} &\leftrightarrow 0 ; \quad \begin{pmatrix} -\sin\beta \\ \cos\beta \end{pmatrix} \leftrightarrow -\frac{1}{2}v_1^2\lambda_3 - \frac{1}{2}v_2^2\lambda_3 \\ \cos\beta &= \frac{v_1}{\sqrt{v_1^2 + v_2^2}} ; \quad \sin\beta = \frac{v_2}{\sqrt{v_1^2 + v_2^2}} \end{aligned}$$

So the mass Higgs bosons, and mass eigenstates are

$$\begin{aligned} \begin{pmatrix} G^+ \\ H^+ \end{pmatrix} &= \begin{pmatrix} \cos\beta & \sin\beta \\ -\sin\beta & \cos\beta \end{pmatrix} \begin{pmatrix} \phi_1^+ \\ \phi_2^+ \end{pmatrix} \\ m_{G^+}^2 &= 0 , \quad m_{H^+}^2 = -\frac{1}{2}\lambda_3(v_1^2 + v_2^2) \end{aligned}$$

As for the indices 3,7; the eigenvectors and eigenvalues are evaluated from (A.7)

$$\begin{aligned}
m_{H^0, h^0} &= \lambda_1 v_1^2 + \lambda_2 v_2^2 \pm \sqrt{(\lambda_1 v_1^2 - \lambda_2 v_2^2)^2 + 4\lambda_+^2 v_1^2 v_2^2} \\
\tan 2\alpha &= \frac{2v_1 v_2 \lambda_+}{(\lambda_1 v_1^2 - \lambda_2 v_2^2)} \\
\begin{pmatrix} H^0 \\ h^0 \end{pmatrix} &= \begin{pmatrix} \cos \alpha & \sin \alpha \\ -\sin \alpha & \cos \alpha \end{pmatrix} \begin{pmatrix} h_1 \\ h_2 \end{pmatrix}
\end{aligned}$$

Finally, for the indices 4,8; it is obtained

$$\begin{pmatrix} \cos \beta & \sin \beta \\ -\sin \beta & \cos \beta \end{pmatrix} \begin{pmatrix} \phi_4 \\ \phi_8 \end{pmatrix} = \begin{pmatrix} G^0 \\ A^0 \end{pmatrix}$$

$$m_{G^0}^2 = 0, \quad m_{A^0}^2 = \frac{1}{2} (\lambda_4 - \lambda_3) (v_1^2 + v_2^2)$$

Second set of solutions

The mass matrix combined with the minimal conditions is given by:

$$\begin{aligned}
M_{ij}^2 &= \left[\begin{pmatrix} M_{11}^2 & M_{15}^2 \\ M_{15}^2 & M_{55}^2 \end{pmatrix} \otimes I_{2 \times 2} \right] \oplus \begin{pmatrix} M_{33}^2 & M_{37}^2 \\ M_{37}^2 & M_{77}^2 \end{pmatrix} \oplus \begin{pmatrix} M_{44}^2 & M_{48}^2 \\ M_{48}^2 & M_{88}^2 \end{pmatrix} \\
&= \left[\begin{pmatrix} 0 & 0 \\ 0 & -\mu_2^2 + \frac{1}{2}\lambda_5 v_1^2 \end{pmatrix} \otimes I_{2 \times 2} \right] \oplus \begin{pmatrix} 2\lambda_1 v_1^2 & 0 \\ 0 & -\mu_2^2 + \frac{1}{2}\lambda_3 v_1^2 + \frac{1}{2}\lambda_5 v_1^2 \end{pmatrix} \\
&\quad \oplus \begin{pmatrix} 0 & 0 \\ 0 & -\mu_2^2 + \frac{1}{2}\lambda_4 v_1^2 + \frac{1}{2}\lambda_5 v_1^2 \end{pmatrix}
\end{aligned}$$

So in this case the matrix is already diagonal and consequently the mass eigenstates coincide with the gauge eigenstates, the elements in the diagonal are the eigenvalues i.e. the squared masses of the Higgs bosons. Since $M_{55}^2 = M_{66}^2$, they correspond to two particles degenerate in mass (i.e. two charged particles), in addition, other two degrees of freedom should be associated to their corresponding Goldstone bosons. So we get

$$\begin{aligned}
\phi_1^+ &= H^+ ; \phi_2^+ = G^+ ; \phi_3 = H^0 ; \phi_7 = h^0 ; \phi_4 = G^0 ; \phi_8 = A^0 ; \\
m_{G^+}^2 &= 0 ; m_{H^+}^2 = -\mu_2^2 + \frac{1}{2}\lambda_5 v_1^2 ; m_{H^0}^2 = 2\lambda_1 v_1^2 \\
m_{h^0}^2 &= -\mu_2^2 + \frac{1}{2}(\lambda_3 + \lambda_5) v_1^2 ; m_{G^0}^2 = 0 ; m_{A^0}^2 = -\mu_2^2 + \frac{1}{2}(\lambda_4 + \lambda_5) v_1^2
\end{aligned}$$

A.1.3 The potential with the global $U(1)$ symmetry

As explained in section (2.2.1) another way to avoid spontaneous CP violation consists of imposing invariance under the global $U(1)$ symmetry $\Phi_2 \rightarrow e^{i\varphi}\Phi_2$ (as well as the C -invariance) and correspond to setting $\lambda_6 = \lambda_7 = \lambda_8 = \lambda_9 = \lambda_{10} = \mu_4^2 = 0$ and $\lambda_3 = \lambda_4$ in (A.1). In this case, we should assume that in general $v_1, v_2 \neq 0$. The minimum conditions (A.3) are reduced to two equations:

$$\begin{aligned}
\lambda_1 v_1^3 - \mu_1^2 v_1 + \frac{1}{2}\lambda_3 v_2^2 v_1 + \frac{1}{2}\lambda_5 v_1 v_2^2 - \frac{1}{2}\mu_3^2 v_2 &= 0 \\
-\mu_2^2 v_2 + \lambda_2 v_2^3 - \frac{1}{2}\mu_3^2 v_1 + \frac{1}{2}\lambda_3 v_1^2 v_2 + \frac{1}{2}\lambda_5 v_2 v_1^2 &= 0
\end{aligned}$$

and after reorganizing the matrix elements as $1, 2, 3, 4, 5, 6, 7, 8 \rightarrow 1, 2, 5, 6, 3, 7, 4, 8$; using the minimum conditions, and taking into account that $M_{15}^2 = M_{26}^2$, $M_{11}^2 = M_{22}^2$, $M_{55}^2 = M_{66}^2$ the decomposed matrix becomes

$$M_{tot}^2 = \left[\left(\begin{array}{cc} M_{11}^2 & M_{15}^2 \\ M_{15}^2 & M_{55}^2 \end{array} \right) \otimes I_{2 \times 2} \right] \oplus \left(\begin{array}{cc} M_{33}^2 & M_{37}^2 \\ M_{37}^2 & M_{77}^2 \end{array} \right) \oplus \left(\begin{array}{cc} M_{44}^2 & M_{48}^2 \\ M_{48}^2 & M_{88}^2 \end{array} \right)$$

with

$$\begin{aligned}
M_{11}^2 &= \frac{1}{2}\mu_3^2 \frac{v_2}{v_1} - \frac{1}{2}\lambda_3 v_2^2 ; \quad M_{15}^2 = -\frac{1}{2}\mu_3^2 + \frac{1}{2}\lambda_3 v_1 v_2 \\
M_{33}^2 &= \frac{1}{2}\mu_3^2 \frac{v_2}{v_1} + 2\lambda_1 v_1^2 ; \quad M_{37}^2 = -\frac{1}{2}\mu_3^2 + \lambda_5 v_1 v_2 + \lambda_3 v_1 v_2 \\
M_{44}^2 &= \frac{1}{2}\mu_3^2 \frac{v_2}{v_1} ; \quad M_{48}^2 = -\frac{1}{2}\mu_3^2 ; \quad M_{55}^2 = \frac{1}{2}\mu_3^2 \frac{v_1}{v_2} - \frac{1}{2}\lambda_3 v_1^2 \\
M_{77}^2 &= \frac{1}{2}\mu_3^2 \frac{v_1}{v_2} + 2\lambda_2 v_2^2 ; \quad M_{88}^2 = \frac{1}{2}\mu_3^2 \frac{v_1}{v_2}
\end{aligned}$$

the eigenvalues and the matrix of rotation corresponding to the submatrix of indices 1,5 are

$$\begin{aligned} \begin{pmatrix} G^+ \\ H^+ \end{pmatrix} &= \begin{pmatrix} \cos \beta & \sin \beta \\ -\sin \beta & \cos \beta \end{pmatrix} \begin{pmatrix} \phi_1^+ \\ \phi_2^+ \end{pmatrix} \\ m_{G^+} &= 0, \quad m_{H^+} = \frac{1}{2} \frac{(v_1^2 + v_2^2)(\mu_3^2 - \lambda_3 v_1 v_2)}{v_1 v_2} \end{aligned}$$

for the indices 3,7, the eigenvalues and the rotation angle read

$$\begin{aligned} m_{H^0, h^0}^2 &= \lambda_1 v_1^2 + \lambda_2 v_2^2 + \frac{1}{4} \mu_3^2 (\tan \beta + \cot \beta) \pm R_\lambda \\ \tan 2\alpha &= \frac{2v_1 v_2 \lambda_+ - \frac{1}{2} \mu_3^2}{\lambda_1 v_1^2 - \lambda_2 v_2^2 + \frac{1}{4} \mu_3^2 (\tan \beta - \cot \beta)} \\ R_\lambda &\equiv \sqrt{\left[\lambda_1 v_1^2 - \lambda_2 v_2^2 + \frac{1}{4} \mu_3^2 (\tan \beta - \cot \beta) \right]^2 + \left(2v_1 v_2 \lambda_+ - \frac{1}{2} \mu_3^2 \right)^2} \end{aligned}$$

finally for the matrix 4,8, the rotation angle is β once again

$$\begin{pmatrix} \cos \beta & \sin \beta \\ -\sin \beta & \cos \beta \end{pmatrix} \begin{pmatrix} \sqrt{2}\phi_4 - v_1 \\ \sqrt{2}\phi_8 - v_2 \end{pmatrix} = \begin{pmatrix} G^0 \\ A^0 \end{pmatrix}$$

and the eigenvalues are

$$m_{G^0} = 0, \quad m_{A^0} = \frac{1}{2} \mu_3^2 \frac{v_1^2 + v_2^2}{v_1 v_2}$$

Finally, it worths to say that the parametrization of the Higgs Hunter's Guide (in the CP conserving case i.e. $\xi = 0$, and $\lambda_5 = \lambda_6$ in Eq. (4.8) of Ref. [17]), can be gotten from the following associations

$$\begin{aligned} \mu_1^2 &\rightarrow [2\lambda_1 v_1^2 + 2\lambda_3 (v_1^2 + v_2^2)] \\ \mu_2^2 &\rightarrow [2\lambda_2 v_2^2 + 2\lambda_3 (v_1^2 + v_2^2)] \\ \mu_3^2 &\rightarrow 2\lambda_5 v_1 v_2 ; \quad \lambda_1 \rightarrow \lambda_1 + \lambda_3 \\ \lambda_2 &\rightarrow \lambda_2 + \lambda_3 ; \quad \lambda_3 \rightarrow \lambda_5 - \lambda_4 \\ \lambda_4 &\rightarrow \lambda_6 - \lambda_4 = \lambda_5 - \lambda_4 \\ \lambda_5 &\rightarrow \lambda_4 + 2\lambda_3 \end{aligned}$$

where the parameters on left are the ones in our parametrization Eqs. (2.8, 2.7), and the parameters on right correspond to the ones in the Higgs Hunter's Guide.

Appendix B

Rotation of the Yukawa Lagrangian in the 2HDM (III)

We start defining two Higgs doublets with VEV

$$\Phi'_{1,2} = \begin{pmatrix} (\phi_{1,2}^+)' \\ (\phi_{1,2}^0)' \end{pmatrix} \quad \text{and} \quad \langle \Phi'_{1,2} \rangle = v_{1,2} \quad (\text{B.1})$$

and writing the Yukawa Lagrangian as

$$\begin{aligned} -\mathcal{L}_Y = & \tilde{\eta}_{ij}^{U,0} \overline{Q}_{iL}^0 \tilde{\Phi}'_1 U_{jR}^0 + \tilde{\eta}_{ij}^{D,0} \overline{Q}_{iL}^0 \Phi'_1 D_{jR}^0 + \tilde{\xi}_{ij}^{U,0} \overline{Q}_{iL}^0 \tilde{\Phi}'_2 U_{jR}^0 + \tilde{\xi}_{ij}^{D,0} \overline{Q}_{iL}^0 \Phi'_2 D_{jR}^0 \\ & + \text{lepton sector} + h.c. \end{aligned} \quad (\text{B.2})$$

we can make a rotation between the doublets

$$\begin{pmatrix} \Phi_1 \\ \Phi_2 \end{pmatrix} \equiv \begin{pmatrix} \cos \theta & \sin \theta \\ -\sin \theta & \cos \theta \end{pmatrix} \begin{pmatrix} \Phi'_1 \\ \Phi'_2 \end{pmatrix} \quad (\text{B.3})$$

We shall deal with the quark sector only henceforth, the results that we are going to obtain are also valid for the lepton sector with the appropriate replacements. In terms of Φ_1 , Φ_2 , the Yukawa Lagrangian could be rewritten as

$$\begin{aligned} -\mathcal{L}_Y = & \tilde{\eta}_{ij}^{U,0} \overline{Q}_{iL}^0 (\cos \theta \tilde{\Phi}_1 - \sin \theta \tilde{\Phi}_2) U_{jR}^0 \\ & + \tilde{\eta}_{ij}^{D,0} \overline{Q}_{iL}^0 (\cos \theta \Phi_1 - \sin \theta \Phi_2) D_{jR}^0 \\ & + \tilde{\xi}_{ij}^{U,0} \overline{Q}_{iL}^0 (\sin \theta \tilde{\Phi}_1 + \cos \theta \tilde{\Phi}_2) U_{jR}^0 \\ & + \tilde{\xi}_{ij}^{D,0} \overline{Q}_{iL}^0 (\sin \theta \Phi_1 + \cos \theta \Phi_2) D_{jR}^0 + h.c. \end{aligned}$$

$$\begin{aligned}
-\mathcal{L}_Y = & \overline{Q}_{iL}^0 \left(\cos \theta \tilde{\eta}_{ij}^{U,0} + \sin \theta \tilde{\xi}_{ij}^{U,0} \right) \tilde{\Phi}_1 U_{jR}^0 \\
& + \overline{Q}_{iL}^0 \left(\cos \theta \tilde{\eta}_{ij}^{D,0} + \sin \theta \tilde{\xi}_{ij}^{D,0} \right) \Phi_1 D_{jR}^0 \\
& + \overline{Q}_{iL}^0 \left(-\sin \theta \tilde{\eta}_{ij}^{U,0} + \cos \theta \tilde{\xi}_{ij}^{U,0} \right) \tilde{\Phi}_2 U_{jR}^0 \\
& + \overline{Q}_{iL}^0 \left(-\sin \theta \tilde{\eta}_{ij}^{D,0} + \cos \theta \tilde{\xi}_{ij}^{D,0} \right) \Phi_2 D_{jR}^0 + h.c.
\end{aligned}$$

defining

$$\begin{pmatrix} \eta_{ij}^{(U,D),0} \\ \xi_{ij}^{(U,D),0} \end{pmatrix} = \begin{pmatrix} \cos \theta & \sin \theta \\ -\sin \theta & \cos \theta \end{pmatrix} \begin{pmatrix} \tilde{\eta}_{ij}^{(U,D),0} \\ \tilde{\xi}_{ij}^{(U,D),0} \end{pmatrix} \quad (B.4)$$

the Lagrangian could be written as

$$\begin{aligned}
-\mathcal{L}_Y = & \overline{Q}_{iL}^0 \eta_{ij}^{U,0} \tilde{\Phi}_1 U_{jR}^0 + \overline{Q}_{iL}^0 \eta_{ij}^{D,0} \Phi_1 D_{jR}^0 \\
& + \overline{Q}_{iL}^0 \xi_{ij}^{U,0} \tilde{\Phi}_2 U_{jR}^0 + \overline{Q}_{iL}^0 \xi_{ij}^{D,0} \Phi_2 D_{jR}^0 + h.c.
\end{aligned} \quad (B.5)$$

with the same form as the original Lagrangian if we forget the prime notation. Consequently, the combined rotations (B.3,B.4) do not have physical consequences since it is basically a change of basis. In particular we can choose $\theta = \beta$ such that

$$\begin{aligned}
\langle \Phi_1 \rangle &= \cos \beta \langle \Phi'_1 \rangle + \sin \beta \langle \Phi'_2 \rangle = \frac{v_1^2 + v_2^2}{\sqrt{v_1^2 + v_2^2}} = \sqrt{v_1^2 + v_2^2} \equiv v \\
\langle \Phi_2 \rangle &= -\sin \beta \langle \Phi'_1 \rangle + \cos \beta \langle \Phi'_2 \rangle = 0
\end{aligned} \quad (B.6)$$

In whose case we managed to get $\langle \Phi_2 \rangle = 0$. Since this lagrangian contains exactly the same physical information as the first one, we conclude that in model type III the parameter $\tan \beta$ is totally spurious and we can assume without any loss of generality that one of the VEV is zero¹. We shall settle $\theta = \beta$ henceforth.

On the other hand, it is possible to reverse the steps above and start from the representation in which $\langle \Phi_2 \rangle = 0$ (the “fundamental representation”) and

¹Indeed the rotation should be made in all the Lagrangians involving Higgs doublets, consequently, we have to ensure that the physical content of the potential is not altered by the rotation, in appendix (C) we see that the rotation can be performed in the potential V defined in Eq. (2.4).

make a rotation of the Higgs doublets from which the $\tan \beta$ parameter arises. If we assume the fundamental representation as our “starting point”, we see that by making a rotation of the doublets, the mixing matrices are rotated such that

$$\begin{pmatrix} \tilde{\eta}_{ij}^{(U,D),0} \\ \tilde{\xi}_{ij}^{(U,D),0} \end{pmatrix} = \begin{pmatrix} \cos \beta & -\sin \beta \\ \sin \beta & \cos \beta \end{pmatrix} \begin{pmatrix} \eta_{ij}^{(U,D),0} \\ \xi_{ij}^{(U,D),0} \end{pmatrix} \quad (\text{B.7})$$

from this rotation we can see that $\tilde{\eta}_{ij}^{(U,D),0}$ and $\tilde{\xi}_{ij}^{(U,D),0}$ depend on the $\tan \beta$ parameter (since $\eta_{ij}^{(U,D),0}$ and $\xi_{ij}^{(U,D),0}$ come from the fundamental representation, they do not depend on $\tan \beta$). In the non trivial parametrization the VEV’s are v_1 and v_2 where $\tan \beta = v_2/v_1$, $\sin \beta = v_2/\sqrt{v_1^2 + v_2^2}$, and the Yukawa Lagrangian in terms of the mass eigenstates can be written in the following ways (see section (2.2.3))

$$\begin{aligned} -\mathcal{L}_Y^I &= -\mathcal{L}_Y(\text{Type I}, \tan \beta) + \tilde{\eta}^U(\eta^U, \xi^U, \tan \beta) \\ &\quad + \tilde{\eta}^D(\eta^D, \xi^D, \tan \beta) \end{aligned} \quad (\text{B.8})$$

$$\begin{aligned} -\mathcal{L}_Y^{II} &= -\mathcal{L}_Y(\text{Type II}, \tan \beta) + \tilde{\eta}^U(\eta^U, \xi^U, \tan \beta) \\ &\quad + \tilde{\xi}^D(\eta^D, \xi^D, \tan \beta) \end{aligned} \quad (\text{B.9})$$

the fundamental parametrization is clearly independent on $\tan \beta$, and since all these parametrizations are physically equivalent, the parametrizations defined by Eqs. (B.8,B.9) cannot depend on $\tan \beta$ either. I shall restrict the discussion to $-\mathcal{L}_Y^{II}$ but the same ideas are applicable to $-\mathcal{L}_Y^I$. In $-\mathcal{L}_Y^{II}$, it is very clear that $-\mathcal{L}_Y(\text{Type II}, \tan \beta)$ depends on $\tan \beta$ explicitly. However, as the whole Lagrangian must be independent of it; the mixing matrices should depend on $\tan \beta$ in such a way that they cancel the dependence on this parameter from $-\mathcal{L}_Y(\text{Type I}, \tan \beta)$. This emphasize the fact that the mixing matrices are basis dependent (changing the basis means changing $\tan \beta$).

Let us see explicitly the relation among the parameters in the fundamental representation $(\xi^{U,D}, \eta^{U,D}, \Phi_1, \Phi_2, \alpha)$ and the ones in the non trivial representation $(\tilde{\xi}^{U,D}, \tilde{\eta}^{U,D}, \Phi'_1, \Phi'_2, \alpha', \beta)$. First of all, Eqs. (B.3) provides us with the relation between (Φ_1, Φ_2) and (Φ'_1, Φ'_2) . On the other hand, Eq. (B.4) provides the relation among $(\xi^{(U,D),0}, \eta^{(U,D),0})$ and $(\tilde{\xi}^{(U,D),0}, \tilde{\eta}^{(U,D),0})$. Notwithstanding, the most useful relations would be the ones among $(\xi^{U,D}, \eta^{U,D})$ and $(\tilde{\xi}^{U,D}, \tilde{\eta}^{U,D})$ i.e. the mixing matrices when the Lagrangian is written in terms of mass

eigenstates. In the non-trivial basis the relation between gauge and mass Higgs eigenstates can be taken from (2.9) with the appropriate change of notation.

$$\begin{aligned} \begin{pmatrix} (\phi_1^+)' \\ (\phi_2^+)' \end{pmatrix} &= \begin{pmatrix} \cos \beta & -\sin \beta \\ \sin \beta & \cos \beta \end{pmatrix} \begin{pmatrix} G^+ \\ H^+ \end{pmatrix} \\ \begin{pmatrix} h'_1 \\ h'_2 \end{pmatrix} &= \begin{pmatrix} \cos \alpha' & -\sin \alpha' \\ \sin \alpha' & \cos \alpha' \end{pmatrix} \begin{pmatrix} H^0 \\ h^0 \end{pmatrix} \\ \begin{pmatrix} g'_1 \\ g'_2 \end{pmatrix} &= \begin{pmatrix} \cos \beta & -\sin \beta \\ \sin \beta & \cos \beta \end{pmatrix} \begin{pmatrix} G^0 \\ A^0 \end{pmatrix} \end{aligned} \quad (\text{B.10})$$

performing the rotation (B.3) and using (B.1) we get

$$\begin{aligned} \Phi_1 &= \cos \beta \Phi'_1 + \sin \beta \Phi'_2 \\ &= \cos \beta \begin{pmatrix} (\phi_1^+)' \\ (h'_1 + v_1 + ig'_1) / \sqrt{2} \end{pmatrix} + \sin \beta \begin{pmatrix} (\phi_2^+)' \\ (h'_2 + v_2 + ig'_2) / \sqrt{2} \end{pmatrix} \\ &\equiv \begin{pmatrix} \phi_1^+ \\ (h_1 + v + ig_1) / \sqrt{2} \end{pmatrix} \\ \Phi_2 &= -\sin \beta \Phi'_1 + \cos \beta \Phi'_2 \\ &= -\sin \beta \begin{pmatrix} (\phi_1^+)' \\ (h'_1 + v_1 + ig'_1) / \sqrt{2} \end{pmatrix} + \cos \beta \begin{pmatrix} (\phi_2^+)' \\ (h'_2 + v_2 + ig'_2) / \sqrt{2} \end{pmatrix} \\ &\equiv \begin{pmatrix} \phi_2^+ \\ (h_2 + ig_2) / \sqrt{2} \end{pmatrix} \end{aligned}$$

so the conversion from the gauge eigenstates in the non trivial basis to the gauge eigenstates in the fundamental representation is given by

$$\begin{aligned} \begin{pmatrix} \phi_1^+ \\ \phi_2^+ \end{pmatrix} &= \begin{pmatrix} \cos \beta & \sin \beta \\ -\sin \beta & \cos \beta \end{pmatrix} \begin{pmatrix} (\phi_1^+)' \\ (\phi_2^+)' \end{pmatrix}, \\ \begin{pmatrix} h_1 \\ h_2 \end{pmatrix} &= \begin{pmatrix} \cos \beta & \sin \beta \\ -\sin \beta & \cos \beta \end{pmatrix} \begin{pmatrix} h'_1 \\ h'_2 \end{pmatrix}, \\ \begin{pmatrix} g_1 \\ g_2 \end{pmatrix} &= \begin{pmatrix} \cos \beta & \sin \beta \\ -\sin \beta & \cos \beta \end{pmatrix} \begin{pmatrix} g'_1 \\ g'_2 \end{pmatrix}. \end{aligned} \quad (\text{B.11})$$

And the relation between the gauge eigenstates and the mass eigenstates in the fundamental parametrization, becomes particularly simple.

$$\begin{aligned}
\begin{pmatrix} \phi_1^+ \\ \phi_2^+ \end{pmatrix} &= \begin{pmatrix} \cos \beta & \sin \beta \\ -\sin \beta & \cos \beta \end{pmatrix} \begin{pmatrix} \cos \beta & -\sin \beta \\ \sin \beta & \cos \beta \end{pmatrix} \begin{pmatrix} G^+ \\ H^+ \end{pmatrix} = \begin{pmatrix} G^+ \\ H^+ \end{pmatrix}, \\
\begin{pmatrix} g_1 \\ g_2 \end{pmatrix} &= \begin{pmatrix} G^0 \\ A^0 \end{pmatrix}, \\
\begin{pmatrix} h_1 \\ h_2 \end{pmatrix} &= \begin{pmatrix} \cos \beta & \sin \beta \\ -\sin \beta & \cos \beta \end{pmatrix} \begin{pmatrix} h'_1 \\ h'_2 \end{pmatrix} \\
&= \begin{pmatrix} \cos \beta & \sin \beta \\ -\sin \beta & \cos \beta \end{pmatrix} \begin{pmatrix} \cos \alpha' & -\sin \alpha' \\ \sin \alpha' & \cos \alpha' \end{pmatrix} \begin{pmatrix} H^0 \\ h^0 \end{pmatrix} \\
\begin{pmatrix} h_1 \\ h_2 \end{pmatrix} &= \begin{pmatrix} \cos \alpha & -\sin \alpha \\ \sin \alpha & \cos \alpha \end{pmatrix} \begin{pmatrix} H^0 \\ h^0 \end{pmatrix}
\end{aligned} \tag{B.12}$$

where we have defined

$$\alpha \equiv \alpha' - \beta \tag{B.13}$$

On the other hand, from (B.4) and (2.44) we get

$$\eta^{U,0} = \cos \beta \tilde{\eta}^{U,0} + \sin \beta \tilde{\xi}^{U,0} = \cos \beta \tilde{\eta}^{U,0} + \sin \beta \left(\frac{\sqrt{2}}{v_2} T_L^\dagger M_U T_R - \frac{v_1}{v_2} \tilde{\eta}^{U,0} \right)$$

and after applying the unitarity transformations defined in (2.42) we obtain

$$T_L \eta^{U,0} T_R^\dagger = \cos \beta \left(T_L \tilde{\eta}^{U,0} T_R^\dagger \right) + \sin \beta \left[\frac{\sqrt{2}}{v_2} M_U - \frac{v_1}{v_2} \left(T_L \tilde{\eta}^{U,0} T_R^\dagger \right) \right]$$

we should note that the unitary matrices $T_{L,R}$ and $V_{L,R}$ defined in Eq. (2.42) are independent on the basis since they indicate the rotations of the spinors from gauge to mass eigenstates, and rotations (B.3,B.4) do not modify such spinors. Consequently the transformation $T_L X^0 T_R^\dagger$ defines the conversion of the mixing matrices from the gauge eigenstates to the mass eigenstates, therefore

$$\begin{aligned}
T_L \eta^{U,0} T_R^\dagger &= \cos \beta \tilde{\eta}^U + \sin \beta \left(\frac{\sqrt{2}}{v_2} M_U - \frac{v_1}{v_2} \tilde{\eta}^U \right) \\
\eta^U &= \frac{v_1}{v} \tilde{\eta}^U + \frac{\sqrt{2}}{v} M_U - \frac{v_1}{v} \tilde{\eta}^U = \frac{\sqrt{2}}{v} M_U
\end{aligned}$$

so we obtain finally

$$\eta^U = \frac{\sqrt{2}}{v} M_U$$

i.e. the matrix η^U is associated only to the mass of the fermion as expected. Similarly from Eqs. (B.4, 2.47, 2.42)

$$\begin{aligned} \xi^{U,0} &= -\sin \beta \tilde{\eta}^{U,0} + \cos \beta \tilde{\xi}^{U,0} = -\sin \beta \left[\frac{\sqrt{2}}{v_1} T_L^\dagger M_U T_R - \frac{v_2}{v_1} \tilde{\xi}^{U,0} \right] \\ &\quad + \cos \beta \tilde{\xi}^{U,0} \\ T_L \xi^{U,0} T_R^\dagger &= -\tan \beta \frac{\sqrt{2}}{v} M_U + \sin \beta \tan \beta \tilde{\xi}^U + \cos \beta \tilde{\xi}^U \\ \xi^U &= \sec \beta \tilde{\xi}^U - \frac{\sqrt{2} \tan \beta}{v} M_U \end{aligned}$$

furthermore, Eq. (2.47) is also valid for $\eta^{(U,D),0}$ by setting $v_2 = 0$, $v_1 = v$. Using Eq. (2.47) applied to $\eta^{U,0}$ and Eq. (B.4) we get

$$\begin{aligned} \tilde{\xi}^{U,0} &= \sin \beta \left[T_L^\dagger M_U T_R \frac{\sqrt{2}}{v} \right] + \cos \beta \xi^{U,0} \\ \tilde{\xi}^U &= \left[\frac{\sqrt{2} \sin \beta}{v} M_U \right] + \cos \beta \xi^U \end{aligned}$$

similarly

$$\tilde{\eta}^U = M_U \frac{\sqrt{2}}{v} \cos \beta - \sin \beta \xi^U$$

for the down sector is exactly the same. Summarizing, we get the following links among the mixing matrices $(\eta^{U,D}, \xi^{U,D})$ in the fundamental parametrization with the ones in the non trivial basis $(\tilde{\eta}^{U,D}, \tilde{\xi}^{U,D})$:

$$\begin{aligned} \tilde{\eta}^{U,D} &= M_{U,D} \frac{\sqrt{2}}{v} \cos \beta - \sin \beta \xi^{U,D} ; \quad \tilde{\xi}^{U,D} = \frac{\sqrt{2} \sin \beta}{v} M_{U,D} + \cos \beta \xi^{U,D} \\ \eta^{U,D} &= \frac{\sqrt{2}}{v} M_{U,D} ; \quad \xi^{U,D} = \sec \beta \tilde{\xi}^{U,D} - \frac{\sqrt{2} \tan \beta}{v} M_{U,D} \end{aligned} \quad (\text{B.14})$$

and the relations among the gauge Higgs eigenstates and mass Higgs eigenstates in the fundamental parametrization, are given by

$$\begin{aligned}\begin{pmatrix} \phi_1^+ \\ \phi_2^+ \end{pmatrix} &= \begin{pmatrix} G^+ \\ H^+ \end{pmatrix} ; \quad \begin{pmatrix} g_1 \\ g_2 \end{pmatrix} = \begin{pmatrix} G^0 \\ A^0 \end{pmatrix} \\ \begin{pmatrix} h_1 \\ h_2 \end{pmatrix} &= \begin{pmatrix} \cos \alpha & -\sin \alpha \\ \sin \alpha & \cos \alpha \end{pmatrix} \begin{pmatrix} H^0 \\ h^0 \end{pmatrix} \\ \alpha &\equiv \alpha' - \beta\end{aligned}$$

while the analogous relations for the non-trivial bases, are given by Eqs. (2.9).

As a proof of consistency, we shall use the equations B.14 and the Yukawa couplings in the non trivial parametrization Eqs. (2.45, 2.46, 2.48, 2.49) in order to obtain the Yukawa couplings in the fundamental parametrization Eq. (2.39). Let us check first the couplings $\overline{D}DA^0$ in the parametrization in which the model type II becomes apparent, where D refers to the three down fermions. From Lagrangian (2.49) and expressions (B.14)

$$\begin{aligned}\overline{D}DA^0 &: -\frac{ig \tan \beta}{2M_W} \overline{D}M_D \gamma_5 DA^0 + \frac{i}{\sqrt{2} \cos \beta} \overline{D}\tilde{\xi}^D \gamma_5 DA^0 \\ &= -\frac{ig \tan \beta}{2M_W} \overline{D}M_D \gamma_5 DA^0 + \frac{i}{\sqrt{2} \cos \beta} \overline{D} \left[\frac{\sqrt{2} \sin \beta}{v} M_D + \cos \beta \xi^D \right] \gamma_5 DA^0 \\ \overline{D}DA^0 &: \frac{i}{\sqrt{2}} \overline{D}\xi^D \gamma_5 DA^0\end{aligned}$$

now let us examine $\overline{D}DH^0$

$$\begin{aligned}\overline{D}DH^0 &: \frac{g}{2M_W \cos \beta} \overline{D}M_D D \cos \alpha' H^0 + \frac{1}{\sqrt{2} \cos \beta} \overline{D}\tilde{\xi}^D D \sin (\alpha' - \beta) H^0 \\ &= \frac{g}{2M_W \cos \beta} \overline{D}M_D D \cos \alpha' H^0 \\ &\quad + \frac{1}{\sqrt{2} \cos \beta} \overline{D} \left[\frac{\sqrt{2} \sin \beta}{v} M_D + \cos \beta \xi^U \right] D \sin (\alpha' - \beta) H^0 \\ &= \overline{D} \frac{M_D}{v} \cos (\alpha' - \beta) DH^0 + \frac{1}{\sqrt{2}} \overline{D}\xi^U D \sin (\alpha' - \beta) H^0 \\ &= \frac{g}{2M_W} \overline{D}M_D DH^0 \cos \alpha + \frac{1}{\sqrt{2}} \overline{D}\xi^D DH^0 \sin \alpha\end{aligned}$$

now $\overline{D}Dh^0$

$$\begin{aligned}
\overline{D}Dh^0 &: -\frac{g}{2M_W \cos \beta} \overline{D}M_D D \sin \alpha' h^0 + \frac{1}{\sqrt{2} \cos \beta} \overline{D}\tilde{\xi}^D D \cos(\alpha' - \beta) h^0 \\
&= -\frac{g}{2M_W \cos \beta} \overline{D}M_D D \sin \alpha' h^0 \\
&\quad + \frac{1}{\sqrt{2} \cos \beta} \overline{D} \left[\frac{\sqrt{2} \sin \beta}{v} M_D + \cos \beta \xi^D \right] D \cos(\alpha' - \beta) h^0 \\
&= \overline{D} \left[-\frac{g M_D}{2M_W \cos \beta} (\sin \alpha' - \sin \beta \cos(\alpha' - \beta)) \right] D h^0 \\
&\quad + \frac{1}{\sqrt{2}} \overline{D} \xi^D D \cos(\alpha' - \beta) h^0 \\
&= -\frac{g}{2M_W} \overline{D}M_D D \sin(\alpha' - \beta) h^0 + \frac{1}{\sqrt{2}} \overline{D} \xi^D D \cos(\alpha' - \beta) h^0 \\
&= -\frac{g}{2M_W} \overline{D}M_D D h^0 \sin \alpha + \frac{1}{\sqrt{2}} \overline{D} \xi^D D h^0 \cos \alpha
\end{aligned}$$

finally for the charged Higgs, in the Lagrangian where model type II becomes apparent i.e. (2.45) plus (2.49) the Yukawa coupling is given by

$$\begin{aligned}
\overline{U}D H^+ &: -\frac{g \cot \beta}{\sqrt{2} M_W} \overline{U} M_U K P_L D H^+ + \frac{1}{\sin \beta} \overline{U} \tilde{\eta}^U K P_L D H^+ \\
&\quad -\frac{g \tan \beta}{\sqrt{2} M_W} \overline{U} K M_D^d P_R D H^+ + \frac{1}{\cos \beta} \overline{U} K \tilde{\xi}^D P_R D H^+ \\
&= -\frac{g \cot \beta}{\sqrt{2} M_W} \overline{U} M_U K P_L D H^+ - \frac{g \tan \beta}{\sqrt{2} M_W} \overline{U} K M_D^d P_R D H^+ \\
&\quad + \frac{1}{\sin \beta} \overline{U} \left(\frac{\sqrt{2} g}{2M_W} M_U \cos \beta - \sin \beta \xi^U \right) K P_L D H^+ \\
&\quad + \frac{1}{\cos \beta} \overline{U} K \left[\frac{\sqrt{2} g \sin \beta}{2M_W} M_D^d + \cos \beta \xi^D \right] P_R D H^+ \\
&= -\overline{U} \xi^U K P_L D H^+ + \overline{U} K \xi^D P_R D H^+ \\
&= \overline{U} (K \xi^D P_R - \xi^U K P_L) D H^+
\end{aligned}$$

all these couplings coincide with the ones describe in the Lagrangian for the fundamental parametrization, Eq. (2.39). Therefore, with this procedure we can check that all Lagrangians generated from Eqs. (2.45, 2.46, 2.48,

2.49) i.e. $-\mathcal{L}_{Y(U)}^I - \mathcal{L}_{Y(D)}^I$, $-\mathcal{L}_{Y(U)}^I - \mathcal{L}_{Y(D)}^{II}$, $-\mathcal{L}_{Y(U)}^{II} - \mathcal{L}_{Y(D)}^{II}$, $-\mathcal{L}_{Y(U)}^{II} - \mathcal{L}_{Y(D)}^I$, coincides with the Lagrangian (2.39) if we take into account the expressions (B.14).

The results expressed by Eqs. (B.14), show us that the value of the flavor changing vertices is basis dependent, though the value of the couplings are basis independent as it must be. The mixing angles between Higgs gauge eigenstates and Higgs mass eigenstates are also basis dependent as expected. The transformations (B.3, B.4) reveals an $SO(2)$ global symmetry of the model type III. This is like a “*global gauge invariance of the 2HDM type III*” in which $\tan\beta$ fixes the gauge.

In that sense, we can realize that the models type I and II have a remarkable difference respect to the model type III, since it is well known that the former two ones are highly dependent on the $\tan\beta$ parameter while the latter is not. In writing the parametrization \mathcal{L}_Y^{II} we can see easily the reason: $-\mathcal{L}_Y^{II}$ (Type II) clearly depend on $\tan\beta$ but when we add the mixing parameters, they acquire the precise values to cancel such dependence. In other words, the model type II does not have mixing parameters at the tree level to absorb their $\tan\beta$ dependence. We can see the difference from the point of view of symmetries, the 2HDM is constructed in such a way that we make an exact “duplicate” of the SM Higgs doublet.

$$\Phi_1 = \begin{pmatrix} \phi_1^+ \\ \phi_1^0 \end{pmatrix} \quad \Phi_2 = \begin{pmatrix} \phi_2^+ \\ \phi_2^0 \end{pmatrix} \quad Y_1 = Y_2 = 1$$

These doublets have the same quantum numbers and are consequently indistinguishable (at least at this step). Owing to this indistinguishability we can perform the rotation

$$\begin{pmatrix} \Phi'_1 \\ \Phi'_2 \end{pmatrix} = \begin{pmatrix} \cos\theta & \sin\theta \\ -\sin\theta & \cos\theta \end{pmatrix} \begin{pmatrix} \Phi_1 \\ \Phi_2 \end{pmatrix}$$

over an arbitrary angle θ without any physical consequences (it is in fact a change of basis). It means that the model is invariant under a global $SO(2)$ transformation of the “bidoublet” $(\Phi_1 \quad \Phi_2)^T$. However, it is very common to impose a discrete symmetry on the Higgs doublets ($\Phi_1 \rightarrow \Phi_1$, $\Phi_2 \rightarrow -\Phi_2$) or a global $U(1)$ symmetry ($\Phi_1 \rightarrow \Phi_1$, $\Phi_2 \rightarrow e^{i\varphi}\Phi_2$) to prevent dangerous FCNC. In that case, we are introducing a distinguishability between the doublets, because they acquire very different couplings to the fermions (models

type I and II). Of course, we could have defined the symmetry in the opposite way ($\Phi_1 \rightarrow -\Phi_1$, $\Phi_2 \rightarrow \Phi_2$) but once we have chosen one of them, we cannot interchange $\Phi_1 \leftrightarrow \Phi_2$ anymore, without changing the physical content. Such fact breaks explicitly the $SO(2)$ symmetry of the “bidoublet”. On the other hand, it is precisely this symmetry what allows us to absorb the $\tan \beta$ parameter, and since models type I and II do not have that symmetry, we are not able to absorb it properly.

Appendix C

Rotation in the Higgs potential

C.1 Transformation of the parameters in the potential

Let us start from an arbitrary parametrization in which both VEV are in general different from zero. The most general renormalizable and gauge invariant potential read

$$V_g = -\tilde{\mu}_1^2 \hat{A}' - \tilde{\mu}_2^2 \hat{B}' - \tilde{\mu}_3^2 \hat{C}' - \tilde{\mu}_4^2 \hat{D}' + \tilde{\lambda}_1 \hat{A}'^2 + \tilde{\lambda}_2 \hat{B}'^2 + \tilde{\lambda}_3 \hat{C}'^2 + \tilde{\lambda}_4 \hat{D}'^2 + \tilde{\lambda}_5 \hat{A}' \hat{B}' + \tilde{\lambda}_6 \hat{A}' \hat{C}' + \tilde{\lambda}_8 \hat{A}' \hat{D}' + \tilde{\lambda}_7 \hat{B}' \hat{C}' + \tilde{\lambda}_9 \hat{B}' \hat{D}' + \tilde{\lambda}_{10} \hat{C}' \hat{D}' \quad (\text{C.1})$$

where we have defined four independent gauge invariant hermitian operators

$$\begin{aligned} \hat{A}' &\equiv \Phi_1'^\dagger \Phi_1' , \quad \hat{B}' \equiv \Phi_2'^\dagger \Phi_2' , \quad \hat{C}' \equiv \frac{1}{2} \left(\Phi_1'^\dagger \Phi_2' + \Phi_2'^\dagger \Phi_1' \right) = \text{Re} \left(\Phi_1'^\dagger \Phi_2' \right) , \\ \hat{D}' &\equiv -\frac{i}{2} \left(\Phi_1'^\dagger \Phi_2' - \Phi_2'^\dagger \Phi_1' \right) = \text{Im} \left(\Phi_1'^\dagger \Phi_2' \right) \end{aligned}$$

the doublets and the VEV are denoted as

$$\Phi'_{1,2} = \begin{pmatrix} (\phi_{1,2}^+)' \\ (\phi_{1,2}^0)' \end{pmatrix} = \begin{pmatrix} (\phi_{1,2}^+)' \\ \left(\frac{h_{1,2} + v_{1,2} + ig_{1,2}}{\sqrt{2}} \right)' \end{pmatrix} \quad \text{and} \quad \langle \Phi'_{1,2} \rangle = v'_{1,2} \quad (\text{C.2})$$

In appendix B, we have seen that in the Yukawa Lagrangian type III, we are able to make a rotation of the doublets as

$$\begin{pmatrix} \Phi_1 \\ \Phi_2 \end{pmatrix} \equiv \begin{pmatrix} \cos \theta & \sin \theta \\ -\sin \theta & \cos \theta \end{pmatrix} \begin{pmatrix} \Phi'_1 \\ \Phi'_2 \end{pmatrix} \quad (\text{C.3})$$

without changing the physical content of the Lagrangian. However, we must demonstrate that such rotation can be carried out in the potential without changing its physical content either. In order to show it, we shall calculate the way in which $\tilde{\mu}_i$, $\tilde{\lambda}_i$ parameters transform under this rotation. First, we calculate the way in which the operators \hat{A}' , \hat{B}' , \hat{C}' , \hat{D}' transform. Taking into account Eq. (C.3) we get

$$\begin{aligned}
\hat{A}' &\equiv \Phi_1'^\dagger \Phi_1' = \left(\Phi_1^\dagger \cos \theta - \Phi_2^\dagger \sin \theta \right) \left(\Phi_1 \cos \theta - \Phi_2 \sin \theta \right) \\
&= \Phi_1^\dagger \Phi_1 \cos^2 \theta - \Phi_1^\dagger \Phi_2 \cos \theta \sin \theta - \Phi_2^\dagger \Phi_1 \cos \theta \sin \theta + \Phi_2^\dagger \Phi_2 \sin^2 \theta \\
&= \Phi_1^\dagger \Phi_1 \cos^2 \theta - 2 \cos \theta \sin \theta \left(\frac{\Phi_1^\dagger \Phi_2 + \Phi_2^\dagger \Phi_1}{2} \right) + \Phi_2^\dagger \Phi_2 \sin^2 \theta \\
&= \hat{A} \cos^2 \theta + \hat{B} \sin^2 \theta - \sin 2\theta \hat{C}
\end{aligned}$$

similarly, we obtain the transformation for the other operators, the results read

$$\begin{aligned}
\hat{A}' &= \hat{A} \cos^2 \theta + \hat{B} \sin^2 \theta - \hat{C} \sin 2\theta \\
\hat{B}' &= \hat{A} \sin^2 \theta + \hat{B} \cos^2 \theta + \hat{C} \sin 2\theta \\
\hat{C}' &= \frac{1}{2} \hat{A} \sin 2\theta - \frac{1}{2} \hat{B} \sin 2\theta + \hat{C} \cos 2\theta \\
\hat{D}' &= \hat{D}
\end{aligned}$$

$$\begin{aligned}
\hat{A}'^2 &= \hat{A}^2 \cos^4 \theta + \hat{B}^2 \sin^4 \theta + \hat{C}^2 \sin^2 2\theta + \frac{1}{2} \hat{A} \hat{B} \sin^2 2\theta \\
&\quad - 2 \hat{A} \hat{C} \sin 2\theta \cos^2 \theta - 2 \hat{B} \hat{C} \sin^2 \theta \sin 2\theta \\
\hat{B}'^2 &= \hat{A}^2 \sin^4 \theta + \hat{B}^2 \cos^4 \theta + \hat{C}^2 \sin^2 2\theta + \frac{1}{2} \hat{A} \hat{B} \sin^2 2\theta \\
&\quad + 2 \hat{A} \hat{C} \sin 2\theta \sin^2 \theta + 2 \hat{B} \hat{C} \sin 2\theta \cos^2 \theta \\
\hat{C}'^2 &= \frac{1}{4} \left(\hat{A}^2 + \hat{B}^2 \right) \sin^2 2\theta + \hat{C}^2 \cos^2 2\theta - \frac{1}{2} \hat{A} \hat{B} \sin^2 2\theta \\
&\quad + \frac{1}{2} \hat{A} \hat{C} \sin 4\theta - \frac{1}{2} \hat{B} \hat{C} \sin 4\theta \\
\hat{D}'^2 &= \hat{D}^2
\end{aligned}$$

$$\begin{aligned}
\widehat{A}'\widehat{B}' &= \left(\frac{1}{4}\widehat{A}^2 + \frac{1}{4}\widehat{B}^2 - \widehat{C}^2 \right) \sin^2 2\theta + \widehat{A}\widehat{B} (\cos^4 \theta + \sin^4 \theta) \\
&\quad + (\widehat{A}\widehat{C} - \widehat{B}\widehat{C}) \sin 2\theta \cos 2\theta \\
\widehat{A}'\widehat{C}' &= \frac{1}{2}\widehat{A}^2 \sin 2\theta \cos^2 \theta - \frac{1}{2}\widehat{B}^2 \sin^2 \theta \sin 2\theta - \widehat{C}^2 \sin 2\theta \cos 2\theta - \frac{1}{4}\widehat{A}\widehat{B} \sin 4\theta \\
&\quad + \widehat{A}\widehat{C} (4 \cos^2 \theta - 3) \cos^2 \theta + \widehat{B}\widehat{C} (4 \cos^2 \theta - 1) \sin^2 \theta \\
\widehat{A}'\widehat{D}' &= \widehat{A}\widehat{D} \cos^2 \theta + \widehat{B}\widehat{D} \sin^2 \theta - \widehat{C}\widehat{D} \sin 2\theta \\
\widehat{B}'\widehat{C}' &= \frac{1}{2}\widehat{A}^2 \sin 2\theta \sin^2 \theta - \frac{1}{2}\widehat{B}^2 \sin 2\theta \cos^2 \theta + \frac{1}{2}\widehat{C}^2 \sin 4\theta + \frac{1}{4}\widehat{A}\widehat{B} \sin 4\theta \\
&\quad + \widehat{A}\widehat{C} (\cos 2\theta + 2 \cos^2 \theta) \sin^2 \theta + \widehat{B}\widehat{C} (\cos 2\theta - 2 \sin^2 \theta) \cos^2 \theta \\
\widehat{B}'\widehat{D}' &= \widehat{A}\widehat{D} \sin^2 \theta + \widehat{B}\widehat{D} \cos^2 \theta + \widehat{C}\widehat{D} \sin 2\theta \\
\widehat{C}'\widehat{D}' &= \frac{1}{2} (\widehat{A}\widehat{D} - \widehat{B}\widehat{D}) \sin 2\theta + \widehat{C}\widehat{D} \cos 2\theta
\end{aligned} \tag{C.4}$$

Now, we can build up a new parametrization of the potential such that

$$\begin{aligned}
V_g &= -\mu_1^2 \widehat{A} - \mu_2^2 \widehat{B} - \mu_3^2 \widehat{C} - \mu_4^2 \widehat{D} + \lambda_1 \widehat{A}^2 + \lambda_2 \widehat{B}^2 + \lambda_3 \widehat{C}^2 + \lambda_4 \widehat{D}^2 \\
&\quad + \lambda_5 \widehat{A}\widehat{B} + \lambda_6 \widehat{A}\widehat{C} + \lambda_8 \widehat{A}\widehat{D} + \lambda_7 \widehat{B}\widehat{C} + \lambda_9 \widehat{B}\widehat{D} + \lambda_{10} \widehat{C}\widehat{D}
\end{aligned} \tag{C.5}$$

in order to find the values of μ_i , λ_i in terms of $\tilde{\mu}_i$, $\tilde{\lambda}_i$, we use the Eqs. (C.1), and (C.4) to write e.g. the coefficient proportional to the operator \widehat{A} , and these terms are compared with the term proportional to the operator \widehat{A} in Eq. (C.5) obtaining

$$-\mu_1^2 \widehat{A} = (-\tilde{\mu}_1^2 \cos^2 \theta - \tilde{\mu}_2^2 \sin^2 \theta - \tilde{\mu}_3^2 \sin \theta \cos \theta) \widehat{A}$$

therefore, the coefficient μ_1^2 is related to the parameters $\tilde{\mu}_i$, $\tilde{\lambda}_i$ in the following way

$$\mu_1^2 = \left(\tilde{\mu}_1^2 \cos^2 \theta + \tilde{\mu}_2^2 \sin^2 \theta + \frac{1}{2} \tilde{\mu}_3^2 \sin 2\theta \right)$$

by the same token, the other sets of μ_i , λ_i parameters are related to the

$\tilde{\mu}_i, \tilde{\lambda}_i$ parameters in the following way

$$\begin{aligned}
 \mu_1^2 &= \left(\tilde{\mu}_1^2 \cos^2 \theta + \tilde{\mu}_2^2 \sin^2 \theta + \frac{1}{2} \tilde{\mu}_3^2 \sin 2\theta \right) \\
 \mu_2^2 &= \left(\tilde{\mu}_1^2 \sin^2 \theta + \tilde{\mu}_2^2 \cos^2 \theta - \frac{1}{2} \tilde{\mu}_3^2 \sin 2\theta \right) \\
 \mu_3^2 &= (-\tilde{\mu}_1^2 \sin 2\theta + \tilde{\mu}_2^2 \sin 2\theta + \tilde{\mu}_3^2 \cos 2\theta) \\
 \mu_4^2 &= \tilde{\mu}_4^2
 \end{aligned}$$

$$\begin{aligned}
 \lambda_1 &= \left(\tilde{\lambda}_1 \cos^4 \theta + \tilde{\lambda}_2 \sin^4 \theta + \frac{1}{4} (\tilde{\lambda}_3 + \tilde{\lambda}_5) \sin^2 2\theta \right. \\
 &\quad \left. + \frac{1}{2} (\tilde{\lambda}_6 \cos^2 \theta + \tilde{\lambda}_7 \sin^2 \theta) \sin 2\theta \right) \\
 \lambda_2 &= \left(\tilde{\lambda}_1 \sin^4 \theta + \tilde{\lambda}_2 \cos^4 \theta + \frac{1}{4} (\tilde{\lambda}_3 + \tilde{\lambda}_5) \sin^2 2\theta \right. \\
 &\quad \left. - \frac{1}{2} (\tilde{\lambda}_6 \sin^2 \theta + \tilde{\lambda}_7 \cos^2 \theta) \sin 2\theta \right) \\
 \lambda_3 &= \left((\tilde{\lambda}_1 + \tilde{\lambda}_2 - \tilde{\lambda}_5) \sin^2 2\theta + \tilde{\lambda}_3 \cos^2 2\theta + \frac{1}{2} (\tilde{\lambda}_7 - \tilde{\lambda}_6) \sin 4\theta \right) \\
 \lambda_4 &= \tilde{\lambda}_4
 \end{aligned}$$

$$\begin{aligned}
 \lambda_5 &= \left(\frac{1}{2} (\tilde{\lambda}_1 + \tilde{\lambda}_2 - \tilde{\lambda}_3) \sin^2 2\theta + \tilde{\lambda}_5 (\cos^4 \theta + \sin^4 \theta) \right. \\
 &\quad \left. + \frac{1}{4} (\tilde{\lambda}_7 - \tilde{\lambda}_6) \sin 4\theta \right) \\
 \lambda_6 &= 2 (\tilde{\lambda}_2 \sin^2 \theta - \tilde{\lambda}_1 \cos^2 \theta) \sin 2\theta + \frac{1}{2} (\tilde{\lambda}_3 + \tilde{\lambda}_5) \sin 4\theta \\
 &\quad + \tilde{\lambda}_6 (4 \cos^2 \theta - 3) \cos^2 \theta + \tilde{\lambda}_7 (\cos 2\theta + 2 \cos^2 \theta) \sin^2 \theta \\
 \lambda_8 &= \left(\tilde{\lambda}_8 \cos^2 \theta + \tilde{\lambda}_9 \sin^2 \theta + \frac{1}{2} \tilde{\lambda}_{10} \sin 2\theta \right)
 \end{aligned}$$

$$\begin{aligned}
\lambda_7 &= 2 \left(\tilde{\lambda}_2 \cos^2 \theta - \tilde{\lambda}_1 \sin^2 \theta \right) \sin 2\theta - \frac{1}{2} \left(\tilde{\lambda}_3 + \tilde{\lambda}_5 \right) \sin 4\theta \\
&\quad + \tilde{\lambda}_6 (4 \cos^2 \theta - 1) \sin^2 \theta + \tilde{\lambda}_7 (\cos 2\theta - 2 \sin^2 \theta) \cos^2 \theta \\
\lambda_9 &= \left(\tilde{\lambda}_8 \sin^2 \theta + \tilde{\lambda}_9 \cos^2 \theta - \frac{1}{2} \tilde{\lambda}_{10} \sin 2\theta \right) \\
\lambda_{10} &= \left(\left(\tilde{\lambda}_9 - \tilde{\lambda}_8 \right) \sin 2\theta + \tilde{\lambda}_{10} \cos 2\theta \right)
\end{aligned} \tag{C.6}$$

C.1.1 Tadpoles

From now on, we shall consider the potential with invariance under charge conjugation, i.e. $\mu_4 = \lambda_8 = \lambda_9 = \lambda_{10} = 0$ (see section 2.2.1). In that case the tadpoles are given by

$$\begin{aligned}
T &= \left(-\mu_1^2 v_1 - \frac{1}{2} \mu_3^2 v_2 + \lambda_1 v_1^3 + \frac{1}{2} \lambda_3 v_1 v_2^2 + \frac{1}{2} \lambda_5 v_1 v_2^2 + \frac{3}{4} \lambda_6 v_1^2 v_2 \right. \\
&\quad \left. + \frac{1}{4} \lambda_7 v_2^3 \right) h_1 + \left(-\mu_2^2 v_2 - \frac{1}{2} \mu_3^2 v_1 + \lambda_2 v_2^3 + \frac{1}{2} \lambda_3 v_1^2 v_2 \right. \\
&\quad \left. + \frac{1}{2} \lambda_5 v_1^2 v_2 + \frac{1}{4} \lambda_6 v_1^3 + \frac{3}{4} \lambda_7 v_2^2 v_1 \right) h_2 \\
T_3 &= \left(-\mu_1^2 v_1 - \frac{1}{2} \mu_3^2 v_2 + \lambda_1 v_1^3 + \frac{1}{2} \lambda_3 v_1 v_2^2 \right. \\
&\quad \left. + \frac{1}{2} \lambda_5 v_1 v_2^2 + \frac{3}{4} \lambda_6 v_1^2 v_2 + \frac{1}{4} \lambda_7 v_2^3 \right) \\
T_7 &= \left(-\mu_2^2 v_2 - \frac{1}{2} \mu_3^2 v_1 + \lambda_2 v_2^3 + \frac{1}{2} \lambda_3 v_1^2 v_2 \right. \\
&\quad \left. + \frac{1}{2} \lambda_5 v_1^2 v_2 + \frac{1}{4} \lambda_6 v_1^3 + \frac{3}{4} \lambda_7 v_2^2 v_1 \right)
\end{aligned} \tag{C.7}$$

these tadpoles coincide with the minimum conditions as we see from Eq. (A.3) and applying $\mu_4 = \lambda_8 = \lambda_9 = \lambda_{10} = 0$. Now, we find the relation among the tadpoles in both parametrizations by using Eq.(C.7), and the third of Eqs. (B.12).

$$\begin{aligned}
T_3 h_1 + T_7 h_2 &= T_3 (h'_1 \cos \theta + h'_2 \sin \theta) + T_7 (-h'_1 \sin \theta + \cos \theta h'_2) \\
&= (T_3 \cos \theta - T_7 \sin \theta) h'_1 + (T_3 \sin \theta + T_7 \cos \theta) h'_2 \\
&= T'_3 h'_1 + T'_7 h'_2
\end{aligned}$$

from which we see that the tadpoles in both parametrizations are related through the rotation

$$\begin{pmatrix} T'_3 \\ T'_7 \end{pmatrix} \equiv \begin{pmatrix} \cos \theta & -\sin \theta \\ \sin \theta & \cos \theta \end{pmatrix} \begin{pmatrix} T_3 \\ T_7 \end{pmatrix} \quad (C.8)$$

As a proof of consistency, we can check that from (C.7), and from (C.6) the following relation is gotten after a bit of cumbersome algebra

$$\begin{aligned}
T_3 \cos \theta - T_7 \sin \theta &= \left(-\tilde{\mu}_1^2 v'_1 - \frac{1}{2} \tilde{\mu}_3^2 v'_2 + \tilde{\lambda}_1 v'_1{}^3 + \frac{1}{2} \tilde{\lambda}_3 v'_1 v'_2{}^2 \right. \\
&\quad \left. + \frac{1}{2} \tilde{\lambda}_5 v'_1 v'_2{}^2 + \frac{3}{4} \tilde{\lambda}_6 v'_1{}^2 v'_2 + \frac{1}{4} \tilde{\lambda}_7 v'_2{}^3 \right) \\
T_3 \sin \theta + T_7 \cos \theta &= \left(-\tilde{\mu}_2^2 v'_2 - \frac{1}{2} \tilde{\mu}_3^2 v'_1 + \tilde{\lambda}_2 v'_2{}^3 + \frac{1}{2} \tilde{\lambda}_3 v'_1{}^2 v'_2 \right. \\
&\quad \left. + \frac{1}{2} \tilde{\lambda}_5 v'_1{}^2 v'_2 + \frac{1}{4} \tilde{\lambda}_6 v'_1{}^3 + \frac{3}{4} \tilde{\lambda}_7 v'_2{}^2 v'_1 \right) \quad (C.9)
\end{aligned}$$

where

$$\begin{pmatrix} v'_1 \\ v'_2 \end{pmatrix} \equiv \begin{pmatrix} \cos \theta & -\sin \theta \\ \sin \theta & \cos \theta \end{pmatrix} \begin{pmatrix} v_1 \\ v_2 \end{pmatrix}$$

relates the VEV between both parametrizations¹. The terms on right of Eqs. (C.9) are precisely the tadpoles in the “prime parametrization”, then the relations given by Eqs. (C.8) are held as expected. Therefore, tadpoles are preserved by the rotation.

C.1.2 Higgs boson masses

Another important proof of consistency is to verify that both parametrizations predict the same masses for the Higgs bosons. We shall use once again,

¹Observe that, such rotation keeps invariant the quantity $v_1^2 + v_2^2 = v'_1{}^2 + v'_2{}^2 = \frac{2m_w^2}{g^2}$, as it should be.

the potential with C -invariance Eq. (2.4). In a general parametrization, the minimal conditions can be taken from A.3 by using $\mu_4 = \lambda_8 = \lambda_9 = \lambda_{10} = 0$, as it corresponds to the Lagrangian in Eq. (2.4). Those conditions are reduced to

$$\begin{aligned}\mu_1 v_1 &= \left(-\frac{1}{2} \mu_3 v_2 + \lambda_1 v_1^3 + \frac{1}{2} \lambda_3 v_2^2 v_1 + \frac{1}{2} \lambda_5 v_2^2 v_1 + \frac{3}{4} \lambda_6 v_1^2 v_2 + \frac{1}{4} \lambda_7 v_2^3 \right) \\ \mu_2 v_2 &= \left(-\frac{1}{2} \mu_3 v_1 + \lambda_2 v_2^3 + \frac{1}{2} \lambda_3 v_1^2 v_2 + \frac{1}{2} \lambda_5 v_1^2 v_2 + \frac{1}{4} \lambda_6 v_1^3 + \frac{3}{4} \lambda_7 v_1 v_2^2 \right)\end{aligned}$$

the mass matrix is obtained from (A.5), and (A.6) by using once again $\mu_4 = \lambda_8 = \lambda_9 = \lambda_{10} = 0$. Let us start with the matrix elements corresponding to m_{H^0}, m_{h^0} . If we assume that both VEV are different from zero and utilize the minimum conditions, we obtain the following mass matrix

$$\begin{pmatrix} M_{33}^2 & M_{37}^2 \\ M_{37}^2 & M_{77}^2 \end{pmatrix} \quad (\text{C.10})$$

with

$$\begin{aligned}M_{33}^2 &= \frac{1}{4v_1} (2\mu_3^2 v_2 + 8\lambda_1 v_1^3 + 3\lambda_6 v_1^2 v_2 - \lambda_7 v_2^3) \\ M_{37}^2 &= -\frac{1}{2} \mu_3^2 + \frac{3}{4} \lambda_7 v_2^2 + \frac{3}{4} \lambda_6 v_1^2 + \lambda_3 v_1 v_2 + \lambda_5 v_1 v_2 \\ M_{77}^2 &= \frac{1}{4v_2} (2\mu_3^2 v_1 + 8\lambda_2 v_2^3 - \lambda_6 v_1^3 + 3\lambda_7 v_2^2 v_1)\end{aligned} \quad (\text{C.11})$$

For the sake of simplicity, we just show that the determinant of this matrix (i.e. the product of the squared masses), coincides for two parametrizations connected by a transformation like (C.3). The mass matrix in any other parametrization with both VEV different from zero, have the same form as (C.10, C.11) but replacing $\mu_i^2 \rightarrow \tilde{\mu}_i^2$, $\lambda_i \rightarrow \tilde{\lambda}_i$. It is a fact of cumbersome algebra to demonstrate that

$$M_{33}^2 M_{77}^2 - (M_{37}^2)^2 = \widetilde{M}_{33}^2 \widetilde{M}_{77}^2 - (\widetilde{M}_{37}^2)^2$$

this demonstration is carried out by taking into account the relations (C.6) among the parameters in both bases. In a similar fashion, we can show that the eigenvalues coincide in both bases. Therefore, the mass Higgs bosons

are equal in both parametrizations as it must be. Finally, if the angle of rotation is chosen such that one of the VEV is zero, (e.g. $v_2 = 0$) in one of the bases, then the minimum conditions and mass matrix elements become much simpler (see Sec. A.1.1), and the equality is easier to demonstrate.

By the same token, we can check that for the other Higgs mass matrices the determinants and eigenvalues are invariant under the transformation (C.3). Showing that the observables are not altered by this change of basis.

Bibliography

- [1] P. W. Higgs, Phys. Lett. **12** (1964) 132, Phys. Rev. Lett. **13** (1964) 508, Phys. Rev. **145** (1966) 1156; F. Englert and R. Brout, Phys. Rev. Lett. **13** (1964) 321; G. S. Guralnik, C. R. Hagen and T. W. B. Kibble, Phys. Rev. Lett. **13** (1964) 585; T. W. B. Kibble, Phys. Rev. **155** (1967) 1554.
- [2] J. Goldstone, Nuovo Cim. **19** (1961) 154; Y. Nambu, Phys. Rev. Lett. **4** (1962) 380.
- [3] S. Glashow, *Nucl. Phys.* **22** (1961) 579; S. Weinberg, Phys. Rev. Lett. **19** (1967) 1264; A. Salam, in *Elementary Particle Theory* (Nobel Symposium No. 8), edited by N. Svartholm, (Almqvist and Wiksell, Stockholm, 1968).
- [4] M. Sher and Y. Yuan, Phys. Rev. **D44** (1991) 1461
- [5] T. P. Cheng and M. Sher, Phys. Rev. **D35** (1987) 3484
- [6] S. L. Glashow, J. Iliopoulos and L. Maiani, Phys. Rev. **D2** (1977) 1285
- [7] J. L. Diaz-Cruz, et. al., Phys. Rev. **D41** (1990) 891; G. Eilam, J. Hewett and A. Soni, Phys. Rev. **D44** (1991) 1473
- [8] Y. Fukuda *et. al.*, Phys. Rev. Lett. **81** (1998) 1562
- [9] J. Liu and L. Wolfenstein, Nucl. Phys. **B289** (1987) 1
- [10] J. Velhinho, R. Santos and A. Barroso. Phys. Lett. **B322** (1994) 213
- [11] R. Santos, A. Barroso. Phys. Rev. **D56** (1997) 5366, [arXiv: hep-ph/9701257].

- [12] M. Sher. Phys. Rep. **179** (1989) 273.
- [13] N. Cabibbo, *et. al.* Nucl. Phys. **B158** (1976) 295.
- [14] M. Lindner, Z. Phys. **C31** (1986) 295.
- [15] Shuquan Nie, and Marc Sher, Phys. Lett. **B449** (1999) 89, [arXiv: hep-ph/9811234].
- [16] S. Kanemura, T. Kasai, and Y. Okada Phys. Lett **B471** (1999) 182, [arXiv: hep-ph/9903289].
- [17] For a review, see J. Gunion, H. Haber, G. Kane, and S. Dawson, *The Higgs Hunter's Guide* (Addison-Wesley, New York, 1990).
- [18] A. Mendez, A. Pomarol Nucl. Phys. **B349** (1991) 369; M. Capdequi Peyranere *et. al.* Phys. Rev. **D44** (1991) 191.
- [19] Shinya Kanemura, Phys. Rev. **D61** (2000) 095001 [arXiv: hep-ph/9710237].
- [20] J. L. Diaz-Cruz, *et. al.*, Phys. Lett. **B512** (2001) 339 [arXiv: hep-ph/0106001].
- [21] Marc Sher, Phys. Lett. **B487** (2000) 151 [arXiv:hep-ph/0006159]; “*Workshop on Physics at the First Muon Collider and at the Front End of the Muon Collider*”, edited by S. Geer and R. Raja (AIP publishing, Batavia, Il, 1997); D. Atwood, L. Reina, and A. Soni, Phys. Rev. Lett. **75** (1995) 3800; A. G. Akeroyd, A. Arhib, and C. Dove, Phys. Rev. **D61** (2000) 071702, [arXiv: hep-ph/9910287 v2].
- [22] C. Lin, C. Lee and Y-W Yang, Chin. J. Phys. **26** (1988) 180; Phys. Rev **D42**, 2355(1990); [arXiv: hep-ph/9311272].
- [23] H. Georgi and M. Machacek, Nucl. Phys. **B262** (1985) 463; M. S. Chanowitz and M. Golden, Phys. Lett. **B165** (1985) 105; J. F. Gunion, R. Vega and J. Wudka, Phys. Rev. **D42** (1990) 1673; K. Cheung, and D. K. Ghosh, JHEP **0211** (2002) 048; A. G. Akeroyd, Phys. Lett. **B442** (1998) 335.
- [24] D. L. Anderson, C. D. Carone, and M. Sher [arXiv: hep-ph/0303215].

- [25] L. Brücher, R. Santos, Eur. Phys. J. **C12** (2000) 87 [arXiv: hep-ph/9907434]; L. Brücher, R. Santos, Contribution to proceedings of 9th Lomonosov conference [arXiv: hep-ph/0002027]; A. Barroso, L. Brücher, R. Santos, Phys. Rev. **D60** (1999) 035005 [arXiv: hep-ph/9901293].
- [26] G. Abbiendi *et. al.* [OPAL Collaboration], Phys. Lett. **B544** (2002) 44; P. Abreu *et. al.* [DELPHI Collaboration], Phys. Lett. **B507** (2001) 89; A. Heister *et. al.* [ALEPH Collaboration], Phys. Lett. **B544** (2002) 16; P. Achard *et. al.* [L3 Collaboration], Phys. Lett. **B534** (2002) 28.
- [27] B. Abbott *et. al.* [D0 Collaboration], Phys. Rev. Lett. **82** (1999) 2244; T. Affolder *et. al.* [CDF Collaboration], Phys. Rev. **D64** (2001) 092002.
- [28] A. G. Akheroyd, and M. A. Diaz [arXiv: hep-ph/0301203].
- [29] G. C. Branco and M. N. Rebelo, Phys. Lett. **B160** (1985) 117.
- [30] S. Glashow and S. Weinberg, Phys. Rev. **D15** 1958 (1977).
- [31] D. Atwood, L. Reina, and A. Soni, Phys. Rev. **D55** (1997) 3156, [arXiv: hep-ph/9609279].
- [32] C. D. Froggatt, R. G. Moorhouse, and I. G. Knowles, Nucl. Phys. **B386** (1992) 63.
- [33] M.B. Einborn, D. Jones, and M. Veltman, Nucl. Phys. **B191** (1981) 146.
- [34] Rodolfo A. Diaz, and R. Martinez, Revista Mexicana de Física **47** (5) (2001) 489-492. [arXiv: hep-ph/0302058].
- [35] Rodolfo A. Diaz, R. Martinez, and J.-Alexis Rodriguez [arXiv: hep-ph/0103307].
- [36] Rodolfo A. Diaz, R. Martinez, and J. -Alexis Rodriguez, Phys. Rev. **D63** (2001) 095007 [arXiv: hep-ph/0010149]
- [37] Rodolfo A. Diaz, R. Martinez and J.-Alexis Rodriguez, Phys. Rev. **D64** (2001) 033004 [arXiv: hep-ph/0103050];

- [38] Rodolfo A. Diaz, R. Martinez, and J.-Alexis Rodriguez, Phys. Rev. **D67** (2003) 075011, [arXiv: hep-ph/0208117].
- [39] Rodolfo A. Diaz, R. Martinez, and Nicanor Poveda, [arXiv: hep-ph/0209122].
- [40] Rodolfo A. Diaz, R. Martinez, J. Mira, and J. -Alexis Rodriguez, Phys. Lett. **B552** (2003) 287-292, [arXiv: hep-ph/0208176].
- [41] Marcela Carena, Debajyoti Choudhury, Rodolfo A. Diaz, Heather E. Logan, and C.E.M. Wagner, Phys. Rev. **D66** (2002) 115010, [arXiv: hep-ph/0206167].
- [42] G. Cvetic *et. al.*, Phys. Rev. **D66** (2002) 034008 [arXiv: hep-ph/0202212].
- [43] S. Kanemura, T. Kubota, and E. Takasugi, Phys. Lett. **B313** (1993) 155
- [44] A.G. Akeroyd, A. Arhrib, E. Naimi, Phys. Lett. **B490** (2000) 119, [arXiv: hep-ph/0006035].
- [45] S. Kanemura, Eur. Phys. J. **C17** (2000) 473, [arXiv: hep-ph/9911541].
- [46] J. F. Gunion, and H. E. Haber, [arXiv: hep-ph/0207010]; H. E. Haber, [arXiv: hep-ph/9501320].
- [47] H. E. Haber, M. J. Herrero, H. E. Logan, S. Peñaranda, S. Rigolin, and D. Temes, Phys. Rev. **D63** (2001) 055004.
- [48] A. Sirlin, Phys. Rev. **D22** (1980) 971; W. J. Marciano, and A. Sirlin, Phys. Rev. **D22** (1980) 2695 [E: **D31** (1985) 213].
- [49] M. Veltman, Nucl. Phys. **B123** (1977) 89
- [50] A. Denner, R. J. Guth, W. Hollik, J. H. Kühn. Z. Phys. **C51** (1991) 695-705. S. Bertolini, Nucl Phys. **B272** (1986) 77.
- [51] H. E. Logan, Radiative corrections to the $Z \rightarrow b\bar{b}$ vertex and constraints on extended Higgs sectors, Ph. D. Thesis, [arXiv: hep-ph/9906332]; H. E. Haber, and H. E. Logan, Phys. Rev **D62** (2000) 015011

- [52] F. Larios, G. Tavares-Velasco, and C.-P Yuan, Phys. Rev. **D64** (2001) 055004 [arXiv: hep-ph/0103292] and update [arXiv: hep-ph/0205204]..
- [53] T. Plehn, Phys. Rev. **D67** (2003) 014018, [arXiv: hep-ph/0206121]
- [54] E. Eichten et. al., Rev. Mod. Phys. **56** (1984) 579; N. G. Deshpande, X. Tata and D. A. Dicus, Phys. Rev. **D29** (1984) 1527; A. Krause et. al., Nucl. Phys. **B519** (1998) 85; A. A. Barrientos Bendezu and B. A. Kniehl, Nucl. Phys. **B568** (2000) 305; O. Brein and W. Hollik, Eur. Phys. J. **C13** (2000) 175.
- [55] D. A. Dicus, J. L. Hewett, C. Kao and T. G. Rizzo, Phys. Rev. **D40** (1989) 787; O. Brein, W. Hollik and S. Kanemura, Phys. Rev. **D63** (2001) 095001; A. A. Barrientos Bendezu and B. A. Kniehl, Phys. Rev. **D59** (1999) 015009, Phys. Rev. **D63** (2001) 015009.
- [56] Oliver Brein, [arXiv: hep-ph/0209124].
- [57] S. Kanemura, S. Moretti and K. Odagiri, JHEP **02** (2001) 011.
- [58] Stefano Moretti [arXiv: hep-ph/0209210].
- [59] A. Djouadi, W. Kilian, M. Muhlleitner, P. M. Zerwas, Euro. Phys. J. **C10** (1999) 27; A. Djouadi, H. E. Haber, P. M. Zerwas, Phys. Lett. **B375** (1996) 203; J. Kamoshita *et. al.*, [arXiv: hep-ph/9602224].
- [60] M. Battaglia, E. Boos, W. Yao, eConf C010630 (2001) E3016, [arXiv: hep-ph/0111276].
- [61] Shinya Kanemura, Shingo Kiyoura, Yasuhiro Okada, Eibun Senaha, C. -P. Yuan, [arXiv: hep-ph/0209326]. *ibid.* Phys. Lett. **B558** (2003) 157, [arXiv: hep-ph/0211308].
- [62] E. Richter-Was, D. Froidevaux, F. Gianotti, L. Poggioli, D. Cavalli and S. Resconi, Int. J. Mod. Phys. **A13** (1998) 1371; ATLAS Detector and Physics Performance Technical Design Report, CERN/LHCC 99-14/15 (1999).
- [63] C. Kao and N. Stepanov, Phys. Rev. **D52** (1995) 5025; CMS Technical proposal, CERN/LHCC 94-38 (1994).
- [64] Chung Kao, [arXiv: hep-ph/0210001].

- [65] J. Lorenzo Diaz-Cruz [arXiv:hep-ph/0207030].
- [66] A. Sopczak, Int. J. Mod. Phys. **A9** (1994) 1747 and references therein
- [67] P. Gambino and M. Misiak, Nucl. Phys. **B611** (2001) 338 [arXiv:hep-ph/0104034]
- [68] G. W. Bennett *et. al.*[Muon $g - 2$ Collaboration], Phys. Rev. Lett. **89** (2002) 101804; Erratum-ibid. **89** (2002) 129903, [arXiv: hep-ph/0208001].
- [69] M. Knecht, and A. Nyffeler, Phys. Rev. **D65** (2002) 073034; M. Knecht, A. Nyffeler, M. Perrottet, and E. de Rafael Phys. Rev. Lett. **88** (2002) 071802; M. Hayakawa and T. Kinoshita, [arXiv: hep-ph/ 0112102]; J. Bijnens, E. Pallante, and J. Prades, Nucl. Phys **B626** (2002) 410; I. Blokland, A. Czarnecki, and K. Melnikov, Phys. Rev. Lett. **88** (2002) 071803; M. Ramsey-Musolf and M. B. Wise, Phys. Rev. Lett. **89** (2002) 041601; A. Nyffeler [arXiv: hep-ph/0209329].
- [70] F. Jegerlehner, talk at conference on “*Hadronic Contributions to the Anomalous Magnetic Moment of the Muon*”, Marseille, March 2002; M. Davier, S. Eidelman, A. Hocker, and Z. Zhang, Eur. Phys. J. **C27** (2003) 497, [arXiv: hep-ph/0208177]; E. de Rafael [arXiv: hep-ph/0208251]; K. Hagiwara, A. D. Martin, D. Nomura, and T. Teubner, Phys. Lett. **B557** (2003) 69, [arXiv: hep-ph/0209187]. J. F. Troconiz and F. J. Yndurain, Phys. Rev. **D65**, 093001 (2002).
- [71] Athanasios Dedes, Howard Haber [arXiv: hep-ph/0102297].
- [72] Maria Krawczyk, Acta Phys. Polon. **B33** (2002) 2621 [arXiv: hep-ph/0208076]
- [73] M. Krawczyk *et.al.*, Eur. Phys. J. **C8** (1999) 495 [arXiv: hep-ph/9811256]; P. H. Chankowski *et. al.* Eur. Phys. J. **C11** (1999) 661 [arXiv: hep-ph/9905436]; P. H. Chankowski *et. al.*, Phys. Lett. **B496** (2000) 195 [arXiv: hep-ph/0009271].
- [74] G. Abbiendi et. al. [OPAL Coll.], Eur. Phys. J. **C18** (2001) 425 [arXiv: hep-ex/0007040]

[75] P. Bambade et. al. [DELPHI Coll.], DELPHI 2001-070 CONF 498, submitted to ICHEP2002 (preliminary)

[76] G. Abbiendi et. al. [OPAL Coll.], Eur Phys. J. **C23** (2002) 397 [arXiv: hep-ex/0111010]; [DELPHI Coll.], DELPHI 2002-037-CONF-571, submitted to ICHEP02 (preliminary); [ALEPH Coll.], PA 13-027, ICHEP96 (preliminary).

[77] (K) S. M. Keh, “*Tau Physics with the cristal ball detector*”, DESY F31-86-6; (N) M. Narain, UMI-92-05244 “*Inclusive Photon Spektra from Υ decays*”, Ph.D. Thesis, 1991; (L) J. Lee-Franzini, ICHEP88, in proc. p. 1432.

[78] J. Prades, and A. Pich, Phys. Lett. **B245**, 117 (1990); A. Pich, J. Prades, and P. Yepes, Nucl. Phys. **B388**, 31 (1992).

[79] M. Roco [CDF and D0 Coll.], FERMILAB-CONF-00-203-E.

[80] Umberto Coti, Arnulfo Zepeda, Phys. Rev. **D55** (1997) 2998 [arXiv: hep-ph/9611442] and references therein.

[81] Beshtoev Kh. M. [arXiv: hep-ph/0204324] and references therein.

[82] R. Davis, *et. al.*, Phys. Rev. Lett. **20** (1968) 1205.

[83] V. Gribov , B. M. Pontecorvo, Phys. Lett **B28**, (1969) 493.

[84] S. P. Mikheyev , A. Yu. Smirnov, Nuovo Cimento **9** (1986) 17; L. Wolfenstein Phys. Rev. **D17** (1978) 2369.

[85] Hirata K.S. et. al., Phys. Rev. Lett. **63**, (1989) 16

[86] Kameda J., Proceedings of ICRC 2001, August 2001, Hamburg (Germany) p. 1057; Ahmad Q. R. [arXiv: nucl-ex/0106015].

[87] C. Dohmen et. al. Phys. Lett. **B317** (1993) 631.

[88] U. Bellgardt et. al., Nucl. Phys. **B299** (1998) 1.

[89] R. D. Bolton, *et. al.*, Phys. Rev. **D38** (1983) 2077; M. L. Brooks, *et. al.*, Phys. Rev. Lett. **83** (1999) 1521.

[90] Y. Okada, K. Okumura, Y. Shimizu, Phys. Rev. **D61** (2000) 094001.

- [91] K. Arisaka, *et. al.*, Phys. Rev. Lett. **70** (1993) 1049.
- [92] K. Arisaka, *et. al.*, Phys. Lett. **B432** (1993) 230; A. M. Lee, *et. al.*, Phys. Rev. Lett. **64** (1990) 165.
- [93] Marc Sher and Yao Yuan, Phys. Rev. **D44** (1991) 1461; D. Atwood, L. Reina and A. Soni, Phys. Rev. **D55** (1997) 3156; *ibid.* Phys. Rev. Lett. **75** (1995) 3800; G. Lopez Castro, R. Martinez and J. H. Muñoz, Phys. Rev. **D58** (1998) 033003; Rodolfo A. Diaz, R. Martinez and J.-Alexis Rodriguez, Phys. Rev. **D63** (2001) 095007; S.K. Kang, and K.Y. Lee, Phys. Lett. **B521** (2001) 61; E. Ma, and M. Raidal, Phys. Rev. Lett. **87** (2001) 011802; Rodolfo A. Diaz, R. Martinez and J.-Alexis Rodriguez, Phys. Rev. **D64** (2001) 033004; J. E. Kim, B. Kyae, and H. M. Lee, Phys. Lett. **B520** (2001) 298; S. P. Martin, and J. D. Wells, Phys. Rev. **D64** (2001) 035003; H. Baer *et. al.*, Phys. Rev. **D64** (2001) 035004; Wu-Jun Huo *et. al.* [arXiv: hep-ph/0212211]; Wujun Huo, and Tai-Fu Feng [arXiv: hep-ph/0301153]; J. Wu, S. Urano, and R. Arnowitt, Phys. Rev. **D47** (1993) 4006; S. Fajfer, and A. Ilakovac, Phys. Rev. **D57** (1998) 4219; G. Cvetic *et. al.*, Phys. Rev. **D66** (2002) 034008 [arXiv: hep-ph/0202212].
- [94] S. Baek, T. Goto, Y. Okada and K. Okumura, [arXiv: hep-ph/0109015].
- [95] Isabella Masina [arXiv: hep-ph/0210125].
- [96] W. Grimus and L.avoura, Phys. Rev. **D66** (2002) 014016, [arXiv: hep-ph/0204070].
- [97] K.S. Babu, and Sandip Pakvasa [arXiv: hep-ph/0204236].
- [98] M. L. Brooks *et. al.* [MEGA Collaboration], Phys. Rev. Lett. **83** (1999) 1521.
- [99] L. M. Barkov *et. al.*, research proposal to PSI; S. Ritt, in Proceedings of *The 2nd International Workshop on Neutrino Oscillations and their Origin*, edited by Y. Suzuki *et. al.* (World Scientific), p. 245 (2000).
- [100] P. Wintz, in Proceedings of the *First International Symposium on Lepton and Baryon Number Violation*, edited by H. V. Klapdor-Kleingrothaus and I. V. Krivosheina (Institute of Physics, Bristol/Philadelphia), p. 534 (1998).

- [101] M. Bachman *et. al.*, [MECO Collaboration], experimental proposal E940 to BNL AGS (1997).
- [102] Y. Kuno, in proceedings of the *2nd International Workshop on Neutrino Oscillations and their Origin*, edited by Y. Suzuki *et. al.* (World Scientific), p. 253 (2000).
- [103] R. Kitano, M. Koike, and Y. Okada, Phys. Rev. **D66** (2002) 096002, [arXiv: hep-ph/0203110].
- [104] J. E. Kim, P. Ko and D. G. Lee, Phys. Rev. **D56** (1997) 100; K. Huitu, J. Maalampi, M. Raidal and A. Santamaria, Phys. Lett. **B430** (1998) 355; A. Faessler, T. S. Kosmas, S. Kovalenko and J. D. Vergados, Nucl. Phys. **B587** (2000) 25.
- [105] R. Barbieri, *et. al.* Nucl. Phys. **B445** (1995) 219; R. Barbieri and L. J. Hall, Phys. Lett. **B338** (1994) 212; J. Hisano, *et. al.* Phys. Lett. **B391** (1997) 341 [E-ibid: **B397** (1997) 357]; Y. Okada, *et. al.* Phys. Rev. **D58** (1998) 051901; Y. Okada, *et. al.* Phys. Rev. **D61** (2000) 094001; F. Borzumati and A. Masiero, Phys. Rev. Lett. **57** (1986) 961; J. Hisano, *et. al.* Phys. Lett. **B357** (1995) 579; J. Hisano, *et. al.* Phys. Rev. **D53** (1996) 2442; J. Hisano *et. al.* Phys. Lett. **B437** (1998) 351. J. Hisano, *et. al.* Phys. Rev. **D58** (1998) 116010; J. Hisano *et. al.* Phys. Rev. **D59** (1999) 116005; W. Buchmuller, *et. al.* Phys. Lett. **B459** (1999) 171; J. Ellis *et. al.* Eur. Phys. J. **C14** (2000) 319; W. Buchmuller, *et. al.* Nucl. Phys. **B576** (2000) 445; J. Sato, *et. al.* Phys. Lett. **B498** (2001) 189; J. Sato and K. Tobe, Phys. Rev. **D63** (2001) 116010; A. Kageyama, *et. al.* Phys. Lett. **B527** (2002) 206; J. R. Ellis, *et. al.* Nucl. Phys. **B621** (2002) 208.
- [106] S. Weinberg, and G. Feinberg, Phys. Rev. Lett. **3** (1959) 111; W. J. Marciano and A. I. Sanda, Phys. Rev. Lett. **38** (1977) 1512; O. Shanker, Phys. Rev. **D20** (1979) 1608; A. Czarnecki *et. al.* [arXiv: hep-ph/9801218]; H. C. Chiang, *et. al.* Nucl. Phys. **A559** (1993) 526; T. S. Kosmas, *et. al.* Nucl. Phys. **A570** (1994) 637; T. Kosmas and J. D. Vergados, Phys. Rept. **264** (1996) 251; T. Kosmas *et. al.* Phys. Atom. Nucl. **61** (1998) 1161; T. Kosmas, *et. al.* Nucl. Phys. **A665** (2000) 183; T. Siiskonen, *et. al.* Phys. Rev. **C62** (2000) 035502; T. Kosmas, [arXiv: nucl-th/0108045].

[107] J. L. Hewett and T. Rizzo, Phys. Rep. **183** (1989) 193; G. Baremboim, et. al, Phys. Lett. **B422** (1998) 277; V. Barger, M. Berger and R. Phillips, Phys. Rev. **D52** (1995) 1663; R. Martinez, J.-Alexis Rodriguez and M. Vargas, Phys. Rev. **D60** (1999) 077504; F. del Aguila, J. Aguilar Saavedra and R. Miquel, Phys. Rev. Lett. **82** (1999) 1628.

[108] M. Nowakowski and A. Pilaftsis, Nucl. Phys. **B461** (1996) 19; A. Joshipura and M. Nowakowski, Phys. Rev. **D51** (1995) 5271; G. Ross and J. W. F. Valle, Phys. Lett. **B151**, 375 (1985).

[109] A. Kaustubh, M. Graessner Phys. Rev. **D61**, 075008 (2000).

[110] G. Lopez, R. Martinez and G. Muñoz, Phys. Rev. **D58** (1998) 033003

[111] O. Stern, Z. Phys. **7** (1921) 18.

[112] W. Gerlach, and O. Stern, Z. Phys. **8** (1922) 110; Z. Phys. **9** (1922) 349, Z. Phys. **9** (1924) 353; and Ann. Phys. **74** (1924) 45.

[113] J. E. Nafe, et. al., Phys. Rev. **71** (1947) 914, D. E. Nagl, *et. al.*, Phys. Rev. **72** (1947) 971; P. Kusch and H. M. Foley, Phys. Rev. **74** (1948) 250

[114] J. Schwinger, Phys. Rev. **73** (1948) 416; and Phys. Rev. **75** (1949) 898.

[115] J. Bailey, *et. al.*, Nucl. Phys. **B150** (1979) 1.

[116] A. Czarnecki, and W. J. Marciano, Phys. Rev. **D64** (2001) 013014, [arXiv: hep-ph/0102122].

[117] S. J. Brodsky and T. Kinoshita, Phys. Rev. **D3** (1971) 356; T. Kinoshita, et. al., Phys. Rev. **D41** (1990) 593; S. Laporta, Phys. Lett. **B328** (1994) 522; T. Kinoshita, Phys. Rev. Lett. **75** (1995) 4728; V. W. Hughes and T. Kinoshita, Rev. Mod. Phys. **71** (1999) S133.

[118] A. Czarnecki, *et. al.*, Phys. Rev. **D52** (1995) 2619 [arXiv:hep-ph/9506256]; A. Czarnecki, et. al., Phys. Rev. Lett. **76** (1996) 3267 [arXiv: hep-ph/9512369]; M. Knecht, *et. al.*, JHEP 0211 (2002) 003, [arXiv: hep-ph/0205102]

- [119] R. R. Akhmetshin *et. al.*, [CMD-2 Coll.], Phys. Lett. **B527** (2002) 161 [arXiv:hep-ex/0112031]; J. Z. Bai *et. al.* [BES Coll.], Phys. Rev. Lett. **84** (2000) 594 [arXiv: hep-ex/9908046]; Z. G. Zhao, Int. J. Mod. Phys. **A15** (2000) 3739; J. Z. Bai, *et. al.*, [BES Coll.], Phys. Rev. Lett. **88** (2002) 101802 [arXiv: hep-ex/0102003]; M. N. Achasov *et. al.*, [SND Coll.], [arXiv: hep-ex/9809013].
- [120] R. Jackiw and S. Weinberg, Phys. Rev. **D5** (1972) 2396; K. Fujikawa, B. . Lee, and A. I. Sanda, *ibid.* **6** (1972) 2923
- [121] S.K. Kang and K.Y. Lee, Phys. Lett **B521** (2001) 61, [arXiv: hep-ph/0103064]
- [122] K. Hagiwara *et. al.*, Review of Particle Physics, Physical Review **D66** (2002) 010001, and references therein.
- [123] Stephen P. Martin, “*A supersymmetry primer*” [arXiv: hep-ph/9709356].
- [124] M. Carena, R. L. Culbertson, S. Eno, H. J. Frisch, and S. Mrenna, Rev. Mod. Phys. **71** (1999) 937, [arXiv: hep-ex/9712022].
- [125] H. E. Haber and G. L. Kane, Phys. Rept. **117** (1985) 75; H. P. Nilles, Phys. Rept. **110** (1984) 1.
- [126] M. Carena, J. R. Espinosa, M. Quiros and C. E. Wagner, Phys. Lett. **B355** (1995) 209; M. Carena, M. Quiros and C. E. Wagner, Nucl. Phys. **B461** (1996) 407; H. E. Haber, R. Hempfling and A. H. Hoang, Z. Phys. **C75** (1997) 539; R. J. Zhang, Phys. Lett. **B447** (1999) 89; J. R. Espinosa and R. J. Zhang, Nucl. Phys. **B586** (2000) 3; A. Brignole, G. Degrassi, P. Slavich and F. Zwirner, Nucl. Phys. **B631** (2002) 195; S. Heinemeyer, W. Hollik and G. Weiglein, Phys. Rev. **D58** (1998) 091701; Phys. Lett. **B440** (1998) 296; Eur. Phys. J. **C9** (1999) 343.
- [127] P. Fayet, Phys. Lett. **B70** (1977) 461; **B86** (1979) 272; **B175** (1986) 471.
- [128] M. Dine, W. Fischler, and M. Srednicki, Nucl. Phys. **B189** (1981) 575; S. Dimopoulos and S. Raby, Nucl. Phys. **B192** (1981) 353; M. Dine and W. Fischler, Phys. Lett. **B110** (1982) 227; Nucl. Phys. **B204** (1982) 346; M. Dine and M. Srednicki, Nucl. Phys. **B202** (1982) 238;

L. Alvarez-Gaumé, M. Claudson, and M. Wise, Nucl. Phys. **B207** (1982) 96; C.R. Nappi and B.A. Ovrut, Phys. Lett. **B113** (1982) 175; S. Dimopoulos and S. Raby, Nucl. Phys. **B219** (1983) 479.

- [129] M. Dine and A.E. Nelson, Phys. Rev. **D48** (1993) 1277; M. Dine, A. E. Nelson and Y. Shirman, Phys. Rev. **D51** (1995) 1362; M. Dine, A. E. Nelson, Y. Nir and Y. Shirman, Phys. Rev. **D53** (1996) 2658.
- [130] M. Carena, S. Pokorski and C. E. Wagner, Phys. Lett. **B430** (1998) 281.
- [131] R. Culbertson *et al.*, “Low-scale and gauge-mediated supersymmetry breaking at the Fermilab Tevatron Run II”, [arXiv:hep-ph/0008070].
- [132] S. Dimopoulos, M. Dine, S. Raby and S. Thomas, Phys. Rev. Lett. **76** (1996) 3494. S. Dimopoulos, S. Thomas and J. D. Wells, Nucl. Phys. **B488** (1997) 39.
- [133] S. Ambrosanio, G. L. Kane, G. D. Kribs, S. P. Martin and S. Mrenna, Phys. Rev. **D54** (1996) 5395.
- [134] A. Brignole, F. Feruglio, M. L. Mangano and F. Zwirner, Nucl. Phys. **B526** (1998) 136 [Erratum Nucl. Phys. **B582** (2000) 759]; E. Perazzi, G. Ridolfi and F. Zwirner, Nucl. Phys. **B590** (2000) 287.
- [135] H. Komatsu and J. Kubo, Phys. Lett. **B157** (1985) 90; M. Quiros, G. Kane and H.E. Haber, Nucl. Phys. **B273** (1996) 333; H.E. Haber and D. Wyler, Nucl. Phys. **B323** (1989) 267; S. Ambrosanio and B. Mele, Phys. Rev. **D55** (1997) 1399 [Erratum Phys. Rev. D **56**, 3157 (1997)].
- [136] S. Ambrosanio, G.L. Kane, G.D. Kribs, and S.P. Martin, Phys. Rev. Lett. **76** (1996) 3498.
- [137] See, for example, <http://lepsusy.web.cern.ch/lepsusy/>
- [138] M. Carena, M. Quirós and C.E.M. Wagner, Phys. Lett. **B380** (1996) 81; D. Delepine, J.M. Gérard, R. González Felipe and J. Weyers, Phys. Lett. **B386** (1996) 183; J. Cline and K. Kainulainen, Nucl. Phys. **B482** (1996) 73; Nucl. Phys. **B510** (1998) 88; J.R. Espinosa, Nucl. Phys. **B475** (1996) 273; B. de Carlos and J.R. Espinosa, Nucl. Phys. **B503** (1997) 24; D. Bodeker, P. John, M. Laine and

M.G. Schmidt, Nucl. Phys. **B497** (1997) 387; M. Carena, M. Quirós and C.E.M. Wagner, Nucl. Phys. **B524** (1998) 3; M. Laine and K. Rummukainen, Nucl. Phys. **B535** (1998) 423; F. Csikor, Z. Fodor, P. Hegedus, A. Jakovac, S.D. Katz and A. Piroth, Phys. Rev. Lett. **85** (2000) 932; M. Losada, Nucl. Phys. **B537** (1999) 3; Nucl. Phys. **B569** (2000) 125.

[139] T. Moroi, H. Murayama and M. Yamaguchi, Phys. Lett. **B303** (1993) 289.

[140] R. Barbieri and L. Maiani, Nucl. Phys. **B224** (1983) 32.

[141] L. Alvarez-Gaume, J. Polchinski and M. B. Wise, Nucl. Phys. **B221** (1983) 495.

[142] P. H. Chankowski, A. Dabelstein, W. Hollik, W. M. Mosle, S. Pokorski and J. Rosiek, Nucl. Phys. **B417** (1994) 101.

[143] M. Carena, D. Choudhury, S. Raychaudhuri and C. E. Wagner, Phys. Lett. **B414** (1997) 92.

[144] S. P. Martin, Phys. Rev. **D55** (1997) 3177.

[145] C. E. M. Wagner, Nucl. Phys. **B528** (1998) 3.

[146] G. R. Dvali, G. F. Giudice and A. Pomarol, Nucl. Phys. **B478** (1996) 31.

[147] P. R. Harrison and C. H. Llewellyn Smith, Nucl. Phys. **B213** (1983) 223 [Erratum B **223**, 542 (1983)].

[148] S. Dawson, E. Eichten and C. Quigg, Phys. Rev. **D31** (1985) 1581.

[149] W. Beenakker, M. Kramer, T. Plehn, M. Spira and P. M. Zerwas, Nucl. Phys. **B515** (1998) 3.

[150] W. Beenakker, R. Hopker and M. Spira, [arXiv:hep-ph/9611232].

[151] H. L. Lai *et. al.* [CTEQ Collaboration], Eur. Phys. J. **C12** (2000) 375.

[152] H. Baer, M. Drees, R. Godbole, J. F. Gunion and X. Tata, Phys. Rev. **D44** (1991) 725; H. Baer, J. Sender and X. Tata, Phys. Rev. **D50** (1994) 4517.

- [153] R. Demina, J. D. Lykken, K. T. Matchev and A. Nomerotski, Phys. Rev. **D62** (2000) 035011.
- [154] A. Djouadi, M. Guchait and Y. Mambrini, Phys. Rev. **D64** (2001) 095014.
- [155] A. Mafi and S. Raby, Phys. Rev. **D62** (2000) 035003
- [156] M. Carena, S. Heinemeyer, C. E. Wagner and G. Weiglein, Phys. Rev. Lett. **86**, 4463 (2001); E. L. Berger, B. W. Harris, D. E. Kaplan, Z. Sullivan, T. M. Tait and C. E. Wagner, Phys. Rev. Lett. **86** (2001) 4231.
- [157] E. L. Berger, B. W. Harris and Z. Sullivan, Phys. Rev. Lett. **83** (1999) 4472; Phys. Rev. **D63** (2001) 115001.
- [158] C. L. Chou and M. E. Peskin, Phys. Rev. **D61** (2000) 055004.
- [159] C. Boehm, A. Djouadi and Y. Mambrini, Phys. Rev. **D61** (2000) 095006; S. P. Das, A. Datta and M. Guchait, Phys. Rev. **D65** (2002) 095006.
- [160] T. Stelzer and W. F. Long, Comput. Phys. Commun. **81** (1994) 357.
- [161] T. Affolder *et al.* [CDF Collaboration], Phys. Rev. **D65** (2002) 052006.
- [162] F. Abe *et. al.* [CDF Collaboration], Phys. Rev. Lett. **77** (1996) 2616; T. Affolder *et al.* [CDF Collaboration], Phys. Rev. Lett. **87**, (2001) 131802.
- [163] B. Abbot *et al.* [D0 Collaboration], Phys. Rev. Lett. **82** (1998) 29.
- [164] W. Porod, Ph.D. thesis, arXiv:hep-ph/9804208; A. Djouadi and Y. Mambrini, Phys. Rev. **D63** (2001) 115005.
- [165] See, *e.g.*, E. L. Berger and H. Contopanagos, Phys. Rev. **D54** (1996) 3085; S. Catani, M. L. Mangano, P. Nason and L. Trentadue, Phys. Lett. **B378** (1996) 329; N. Kidonakis, Phys. Rev. **D64** (2001) 014009; N. Kidonakis, hep-ph/0110145 and references therein.
- [166] B. Abbot *et al.* [D0 Collaboration], Phys. Rev. Lett. **80** (1998) 442.

[167] J. R. Ellis and D. V. Nanopoulos, Phys. Lett. **B110** (1982) 44; F. Gabiani and A. Masiero, Nucl. Phys. **B322** (1989) 235; S. Bertolini, F. Borzumati, A. Masiero and G. Ridolfi, Nucl. Phys. **B353** (1991) 591; J. S. Hagelin, S. Kelley and T. Tanaka, Nucl. Phys. **B415** (1994) 293; D. Choudhury, F. Eberlein, A. Konig, J. Louis and S. Pokorski, Phys. Lett. **B342** (1995) 180; M. Ciuchini *et al.*, JHEP **9810** (1998) 008.